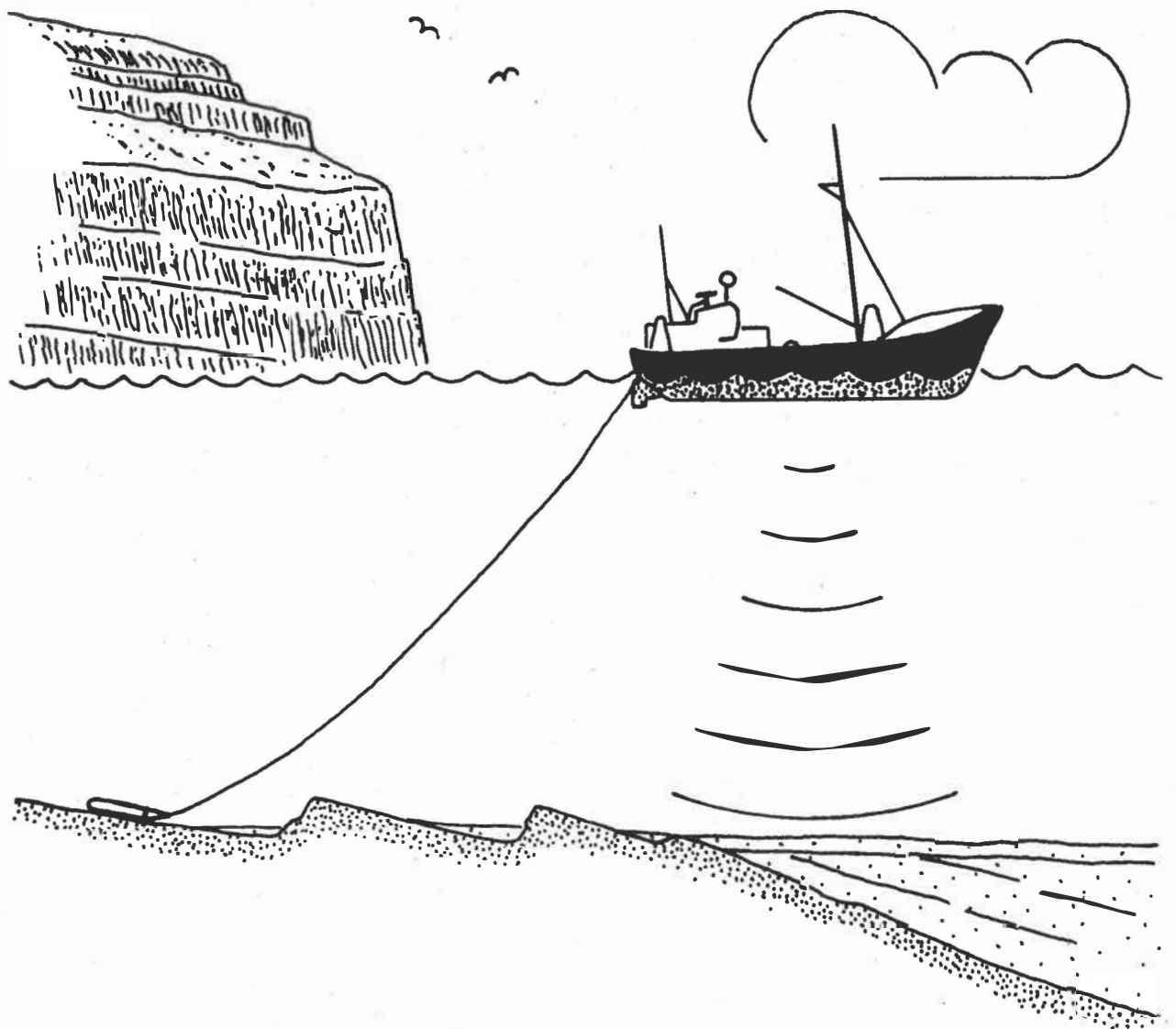# THE GEOLOGY OF
THE FAEROE PLATEAU

R. WAAGSTEIN

PART 1

THE GEOLOGY OF THE FAEROE PLATEAU

BY R. WAAGSTEIN

Regin Waagstein, 25 October 1977

ABSTRACT

The geology of the Faeroe Plateau north and northwest of
Scotland is described. New morphological and petrological
results are provided.

The Faeroe lava pile exceeds 5 kilometres in thickness. It
was poured onto a continental platform slightly before the
opening of the NE Atlantic ocean floor in lower Tertiary. The
3.5 kilometre subarial sequence of the Faeroes ranges from
olivine tholeiites to tholeiites and includes lavas both rich
and depleted in large ionic radii lithophile (LIL) elements.
Systematic changes through the pile in chemistry of the LIL-
-element rich tholeiites reflect steady changes in the P-T-che-
mical conditions of magma formation. Similar subarial basalts
occur on the banks to the southwest (Faeroe Bank, Bill Bailey
Bank and Lousy Bank) and among dredged erratics. However, the
proportion of LIL-element poor tholeiites probably increases
towards the outer oceanic edges of the plateau. The eruption
area seems gradually to have been restricted to the Faeroe Block.

In the waning phase of volcanism the plateau was probably sub-
merged and a "Moberg" series was produced by submarine eruptions.
Dome and basin formation took place on the Faeroe Block before
the end of minor intrusive activity. During continental break-up
at the end of Paleocene the Faeroe Plateau was disintegrated by
crustal thinning and subsidence, and the Faeroe-Shetland, Faeroe
Bank Channel system was formed. Erosion began - and reworked
ashes were deposited in basins on the outer Faeroe shelf - and
the plateau was probably peneplaned in the lower Tertiary. The
Faeroe Block was further uplifted and eroded in late Tertiary,
possibly Pliocene time, and most of the block was repeately
glaciated in Plio-Pleistocene time. Roughly one kilometre of
sediments was deposited in the adjoining channels in the lower
Tertiary, while 0-1.5 kilometres were deposited by vigorous
Norwegian Sea overflow in the upper Tertiary.

ACKNOWLEDGEMENTS

THE GEOLOGY OF THE FAEROE PLATEAU

CONTENTS

FIGURES

TABLES

CHAPTER 1

INTRODUCTION

The Northwest European continental margin has been moulded
through a long period of varying plate-tectonic activity (Laugh-
ton 1975). A particularly complicated area occurs west of the
British Isles (Fig. 1). Here the Rockall Trough and the Faeroe-
-Shetland Channel separate the European shelf from a broad zone
of shoal areas to the west named the Faeroe Rise. The Rockall
Plateau which forms the southern part of the rise has a conti-
nental structure and is considered to be a continental fragment
separated from the European shelf by seafloor spreading in the
Rockall Trough in Mesozoic time. The Faeroe Plateau at the
northern end of the rise is underlain by crust of continental
thickness (Casten 1974; Bott and others 1975; Casten and Nielsen
1975; Nielsen 1976). It is uncertain whether the Faeroe-Shet-
land Channel is underlain by thinned continental crust or oceanic
crust (Bott 1975a). The middle section of the Faeroe Rise is
composed of several banks which are also supposed to be under-
lain by continental crust by inference from gravity measurements
and pre-rifting reconstructions of the N.E. Atlantic (Bott and
Watts 1971; Himsworth 1973). The Iceland-Faeroe Ridge and the
Wyville-Thomson Ridge connect the Faeroe Rise with Iceland and
the European shelf, respectively. The former ridge is underlain
by anomalous thick oceanic crust (Bott and others 1971), whereas
the latter is of debatable origin (Himsworth 1973; Bott 1975a).
At the beginning of the Tertiary, widespread volcanism commenced
on the Faeroe Rise, in the British Isles, in East Greenland and
in intervening shelf areas. Slightly later the N.E. Atlantic
opened west and north of the Faeroe Rise.

The Rockall Plateau has been intensivly studied by geophysical
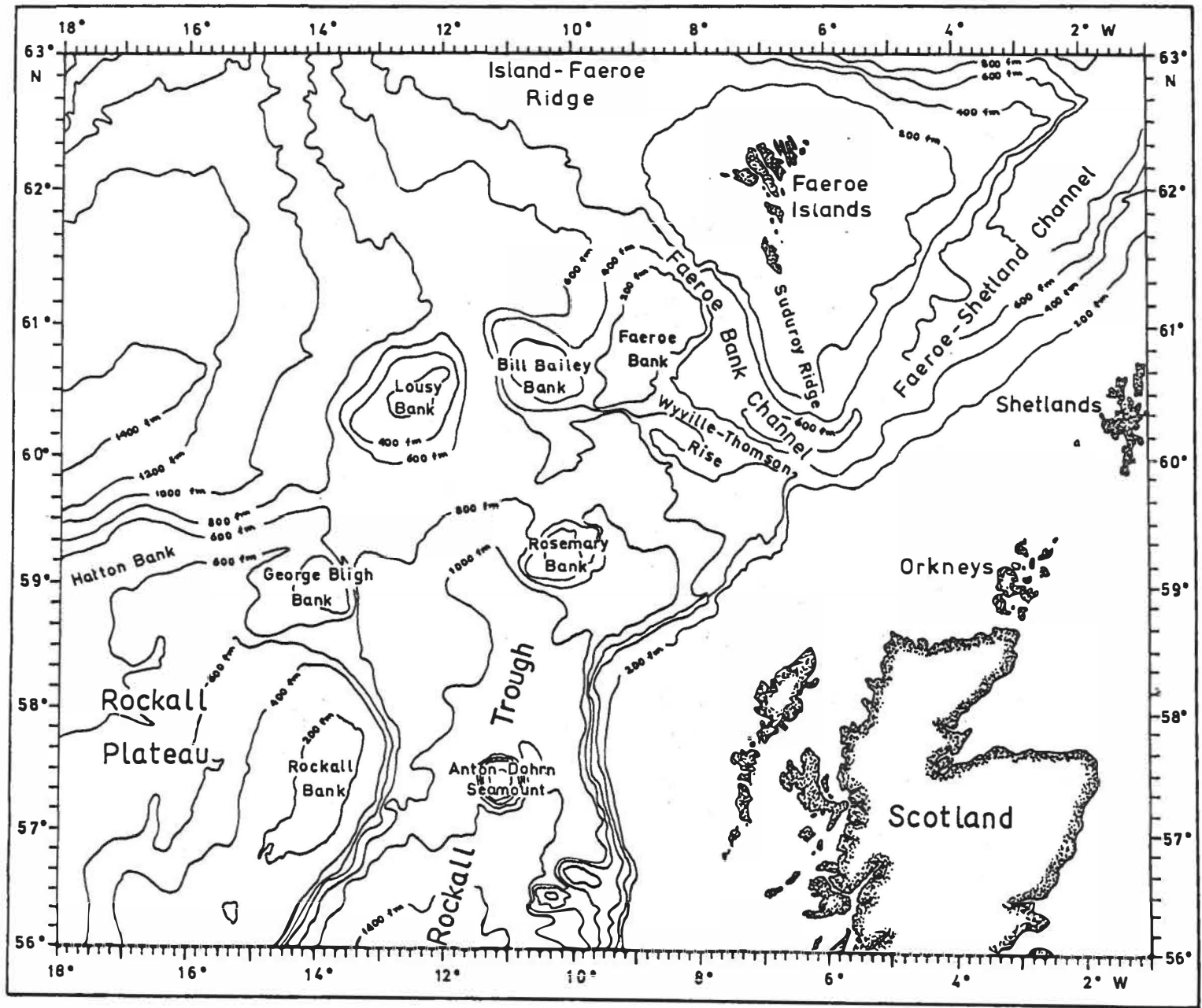
After Himsworth 1973

FIGURE 1
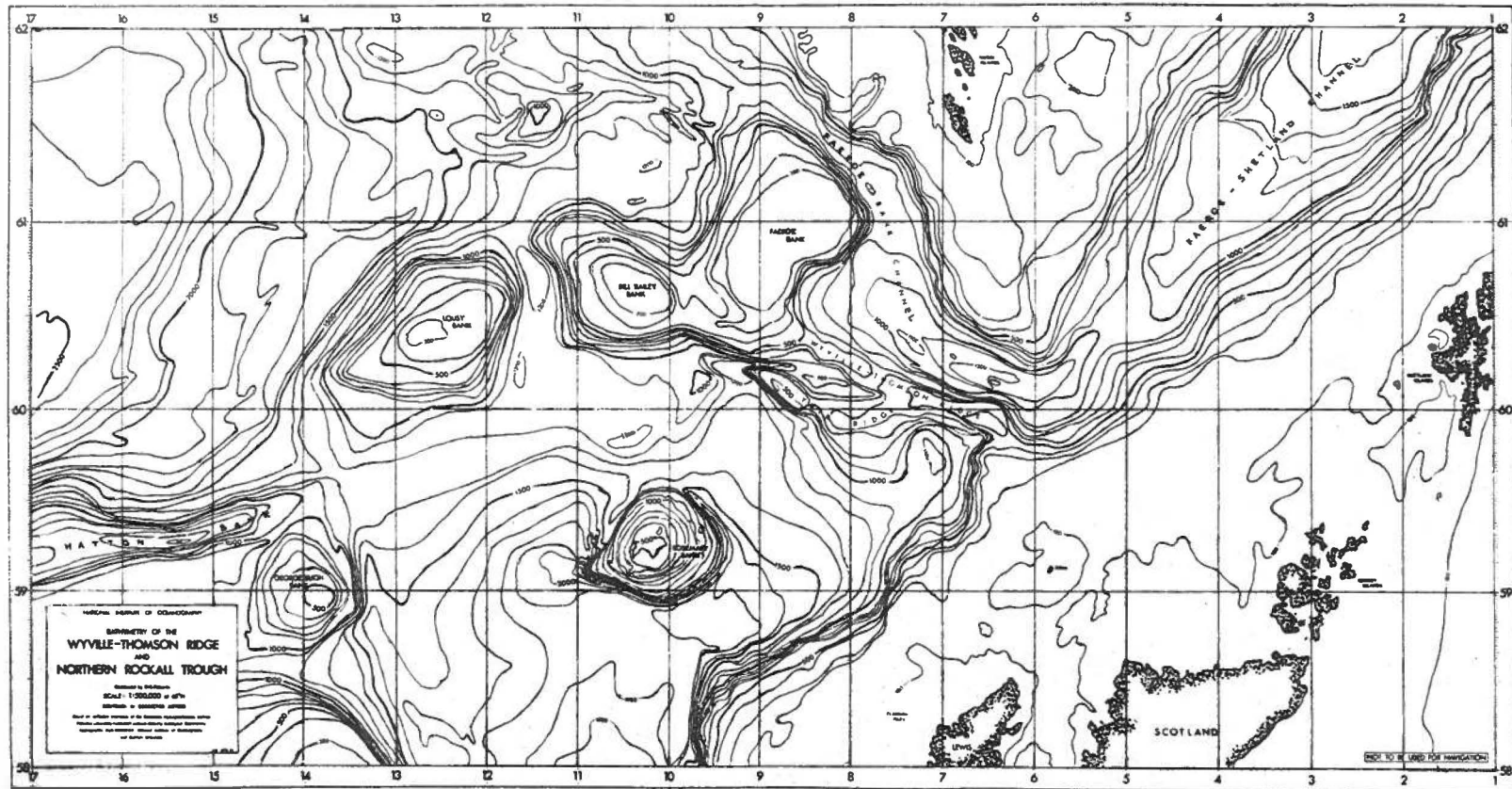
FIGURE 1a. Bathymetry of the southern Faeroe region (unpublished map by D.G. Roberts 1973, with minor corrections, reduced to a scale of 1:4,310 000)

means, deep sea drilling and dredging especially under the auspices of the Institute of Oceanographic Sciences, England; a summary of the geology has recently been published by Roberts (1975a, b). Geophysical studies have been carried out in the northern part of the Faeroe Rise and adjoining areas by scientific groups from several countries and have from time to time been summarized by Bott (1971, 1973, 1975a, b). Very little, however, is known about the rocks immediately below the sea-floor.

In 1971 a dredging programme was initiated by the Geological Department of the Faeroe Islands in order to study the distribution of glacial erratics (Rasmussen 1973; Waagstein and Rasmussen 1975) and possible in situ rocks around the islands. In situ rocks from the sea-floor have been sampled in a few areas, while the erratics at most localities include a small number of rocks clearly derived from the Faeroe shelf.

The aim of the present report is to review the geology of the Faeroe Plateau in the light of some results gained from the study of rocks from this area. Emphasis has been placed on the petrography and geochemistry of basalts from the Faeroe Islands and the banks to the southwest.

CHAPTER 2

STRUCTURAL GEOLOGY

2.1.   The Faeroe Islands

2.1.1. Stratigraphy

The Faeroe Islands are the erosional remnants of a gently warped Lower Tertiary basalt plateau whose base and top are not seen. The lava sequence is divided into the Lower, Middle and Upper Basalt series (Rasmussen and Noe-Nygaard 1969, 1970) (Figs. 2 and 3) and has an exposed thickness of about 3.500 metres. The Lower Basalts consist nearly exclusively of aphyric and slightly plagioclase-phyric, olivine-poor flows with clinkery tops and are averaging about 20 metres in thickness. The flows are separated by tuffaceous beds which are sometimes coal-bearing. The Lower Basalts are capped by a roughly 10 metres thick clay-coal sequence (the A-horizon). The Middle Basalt volcanism started explosively with the eruption of pyroclastics now forming a NW-SE belt of tuff-agglomerates up to 100 metres thick and several kilometres wide. The rest of the Middle Basalts is dominated by amygdaloidal pahoehoe flow units or flows averaging less than 2 metres in thickness. They are occasionally separated by tuffaceous beds. Most flows are plagioclase-phyric, but olivine-phyric and aphyric flows occur at intervals. The base of the Upper Basalts is taken to include some prominent aphyric or olivine-phyric flows called the C-horizon flows. These flows form some very flat shield volcanoes side by side in the northern and northeastern part of the islands. The volcanoes, which are about 10 kilometres in diameter but less than about 60 metres high, were called scutulum volcanoes by Noe-Nygaard (1968). The Upper Basalts are characterized by

Geological map of
the Faeroe Islands

Basalt intrusions
Upper Basalts
Middle Basalts
Tuff agglomerate zone
Coal-bearing sequence
Lower Basalts

I-XI   Sub-profiles of main profile
2.2 Dip of strata in degrees

0   10   20   30 km

After Rasmussen & Noe-Nygaard
1969

Streymoy
Mykines
Vagar
Vidoy
Bordoy
Eysturoy
Nolsoy
Sandoy
Suduroy
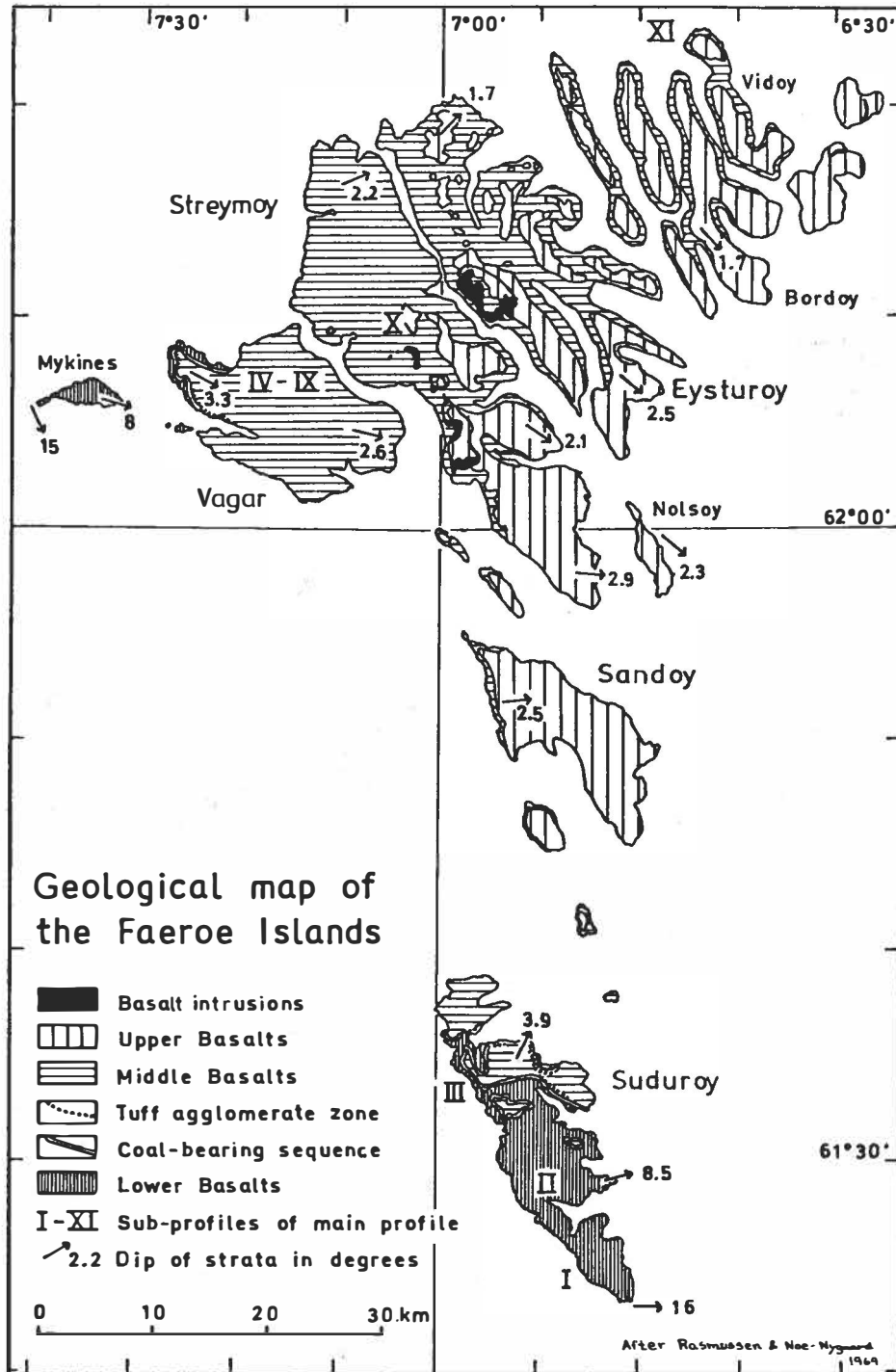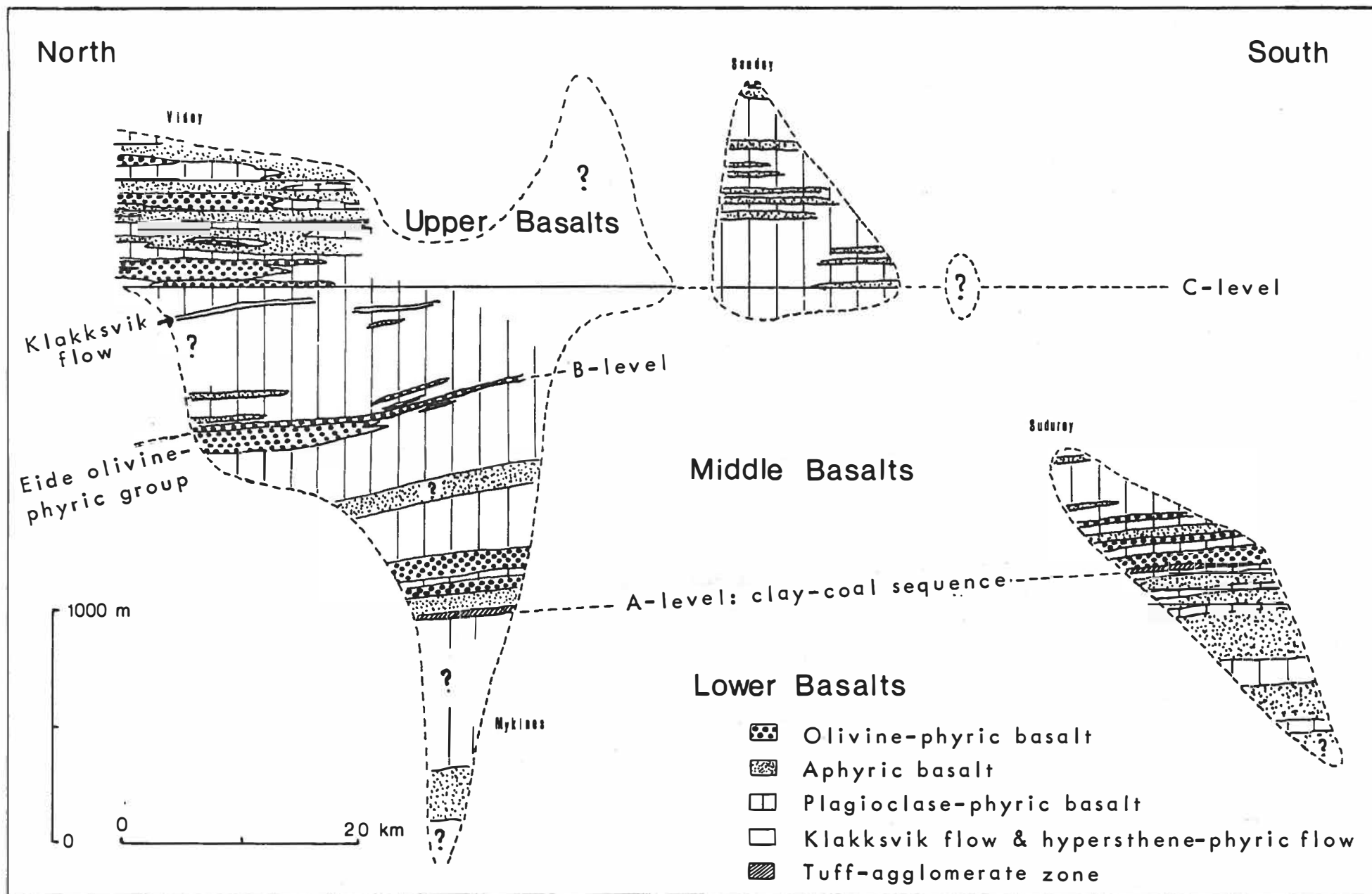
FIGURE 2

Figure 3. Idealized north-south cross section through the Faeroe lava plateau

flows of intermediate thickness separated by thin tuffaceous beds. The flows are mostly aphyric or olivine-phyric in the northernmost and northeasternmost Faeroes, but plagioclase-phyric in the central part of the islands (Fig. 3)[1], and the latter type sometimes shows thin pahoehoe flow units like the Middle Basalts.

---

[1] This north-south cross section through the Faeroe basalt plateau is based on field traverses published by Rasmussen and Noe-Nygaard (1969) and Walker and Davidson (1936) and unpublished field work by N. Hald and the author. It is not a true cross section because the strata get progressively younger towards east across the northern part of the islands (Fig. 2). Except for the main stratigraphic boundaries the strata are not extrapolated beyond their approximate exposure limits on land at different latitudes. The Middle-Upper Basalt boundary (the C-level) is assumed horizontal.

2.1.2. Unconformities

Rasmussen and Noe-Nygaard (1969, 1970) and Noe-Nygaard (1974) suppose that the Faeroe plateau was tilted slightly to the east before the eruption of the Middle Basalts and again before the eruption of the Upper Basalts without giving any conclusive evidence.

The coal-bearing A-horizon represents a prolonged pause in the volcanic activity. At this time vertical adjustments occurred in the plateau as evidenced by a 10 metre high SE striking normal fault on Suduroy affecting the Lower Basalts, but not the Middle Basalts. However, the sequence of lavas close to the A-horizon is similar in the western and southern outcrop areas about 60 kilometres apart. In both areas most of the flows in the uppermost 200 metres of the Lower Basalts contain 5 percent or more olivine mainly in the groundmass in contrast to the flows below which are nearly all olivine-poor. In both areas the A-horizon is partly overlain by tuff-agglomerates, and the lowermost 200-300 metres of the Middle Basalts are dominated by olivine-rich flows (Fig. 3). These long-distance correlations preclude any appreciable component of tilt along the line between the two outcrop areas, though not at right angles to the line. In addition, although the strata just below and above the A-horizon are well exposed for several kilometres along the latter directions, an angular unconformity has only been reported in one place (Rasmussen and Noe-Nygaard 1970, p. 48) and may be of purely volcanic origin. Therefore, if any tilting has occurred between the formation of the Lower and Middle Basalts, it has probably been very slight.

The top of the Middle Basalts is smooth in most places and usually covered by a tuffaceous bed, in turn overlain by the Upper

Basalt C-horizon flows. The tuffaceous bed is about 0.5 metre thick on average and often contains indeterminable plant remains. The vertical distance from the C-horizon flows down to the base of the distinctive Klakksvík flow (Hald and others 1969) decreases irregularly to the south from 120 metres to 70 metres over a distance of about 10 kilometres (Hald and Waagstein, unpublished report 1965). The decreasing distance between the two levels may be accounted for by suggesting that the plateau was tilted about 0.5° to the N or rather NNE and slightly eroded before the eruption of the Upper Basalts. Another stratigraphic level in the Middle Basalts is defined by the olivine-phyric B-horizon flows in the northern and northwestern Faeroes; their base is shown on the geological map (Rasmussen and Noe-Nygaard 1969, 1970). The exposures of the B- and C-horizon show nearly no overlap in the east-west direction, but where they meet, the present component of tilt to the east of the two horizons is very nearly the same according to the above map. In the north-south direction, on the other hand, the vertical distance between the B- and C-level decreases from about 620 metres in the northernmost Faeroes to about 500 metres about 20 kilometres to the south according to the map, again suggesting 0.5° tilt to the north of the Middle Basalts relative to the Upper Basalts. Assuming a constant thickness of the Middle Basalts in the east-west direction, their thickness is about 1465 metres on northern Vágar and approximately 1300 metres half-way between Suduroy and Sandoy; this thinning is consistent with a tilt of the Middle Basalts towards the north of 0.2°. Thus, if the Middle Basalts were tilted before the extrusion of the Upper Basalts, the tilt was probably 0.5° at most, and the direction of tilt was to the north rather than to the east as suggested by Rasmussen and Noe-Nygaard (1969, 1970).

We may conclude that the Lower, Middle and Upper Basalts are approximately concordant, and thus we may expect that these stratigraphic units have a similar thickness where they occur on the surrounding shelf.

2.1.3. Volcanic vents

Several buried volcanic vents are seen in the upper part of the Middle Basalts and the lowermost part of the Upper Basalts. They are filled with agglomerates and tuffs which are sometimes associated with intrusive basalt, and are probably feeders for some of the nearby flows. The vents have only been observed in the sea cliffs, but seem to be elliptical or oblong in cross section. Their apparent diameter varies from about 10 metres to 1.5 kilometres, the latter figure being the length of a 10-50 metres wide NNW-SSE trending fissure along the west coast of Streymoy (Rasmussen 1962). An examination of the basalt types in two vents suggests that they have erupted plagioclase-phyric and aphyric lava respectively. The C-horizon flows must have been erupted from similar short fissures or necks to judge from the shape of the scutulum volcanoes they form (Noe-Nygaard 1968) (section 2.1.1.). A different extrusion form is exemplified by the Klakksvík flow a little below the C-horizon (Hald and others 1969). The Klakksvík flow forms a 5-8 kilometres wide belt from NW to SE across the northeastern Faeroes, and the number of sepa-rate flows or flow units, their total thickness and the amount of overlying slag vary in a manner which suggests that the lava was erupted from several vents along one or several closely spaced NW-SE trending fissures. The distribution of the tuff-agglome-rates at the base of the Middle Basalts likewise seems to indicate that they were erupted from small vents along NW-SE trending fis-sures.

Rasmussen and Noe-Nygaard (1969, 1970) suggest that the thin Middle Basalt flows were erupted from vents of limited extent in-side the present island group, but that the thicker and more ex-

tended Lower and Upper Basalt flows were erupted from large fissures outside the island group. In the present author's opinion, however, most or all Upper Basalt flows were also erupted from local short fissures or necks for the following reasons: 1) The large C-horizon flows, which must have been erupted from central vents (see above), are similar petrographically and chemically to the rest of the aphyric and olivine-phyric Upper Basalt flows; 2) it is difficult to correlate nearby vertical profiles through the Upper Basalts in detail even though different types of basalts alternate in the profiles (Fig. 3); 3) one of the observed vents occurs in the lowermost part of the Upper Basalts, while another one just below the C-level has a block content strongly dominated by aphyric basalt similar to the basalt forming the nearby Upper Basalt flows. The near failure to observe vents in the Upper Basalts may only be a consequence of the supposed small size of the vents relative to the large size of the flows.

2.1.4. Intrusions

Numerous basalt dykes cut the Faeroe plateau. Some saucer-shaped basalt sills up to 100 metres thick intrude the border zone between the Middle and Upper Basalts, and some very irregular sill--like bodies intrude and strongly disturb the clay-coal sequence and the tuff-agglomerates between the Lower and Middle Basalts.

On Suduroy nearly all dykes strike NW-SE, while in the northern Faeroes the dykes scatter all around the compass showing several trend maxima which change in numbers and directions across the islands. The Faeroese dykes do not exceed 20 metres in breadth, though several of them can be traced for more than 10 kilometres. Many dykes clearly intrude former master joints and are often seen fingering out upwards or along the strike of the joints, whereas no dykes seem to be feeders of flows. Most dykes probably belong to a distinct intrusive phase postdating the formation of the plateau. A NE striking sheared dyke on Streymoy intruded into a dextral fault is reported to be younger than three dykes striking between SE and S (Rasmussen and Noe-Nygaard 1970, p. 107). The large Streymoy sill at the Middle-Upper Basalt boundary is fed by an ENE striking dyke (ibid., p. 127), while this sill and the large Eysturoy sill cut several dykes which all but one strike about SE. These few observed age relationships suggest that the intrusive volcanic phase was closed by the emplacement of sills, and dykes striking about NE or E. The irregular intrusions at the Lower-Middle Basalt boundary in the western and southern Faeroes are cut by a N and NW striking dyke , respectively; in both cases the dyke shows clear evidence of cooling against the country rock but not against the intrusions. The intrusions and dykes may be contemporaneous with the above sills as suggested by Rasmussen

and Noe-Nygaard (1969, 1970). A much older age cannot be ruled out, however, as the irregular intrusions and associated dykes have not been traced far above the tuff-agglomerates and chemically show a great resemblance to the early Middle Basalts (section 3.3.5.).

2.1.5. Joints and faults

The plateau is cut by numerous master joints, which are often the locus of minor vertical and horizontal displacements. In the northern islands the large majority of joints occur inside an angle of about 60° and belong to a few indistinct sets of joints whose average direction rotates gradually from about E-W in the western and central northern islands to nearly NE-SW in the north-eastern islands. On Suduroy, on the other hand, nearly all joints trend SE-NW (Fig. 4).

Several strike-slip faults with displacements of 2 to 55 metres occur in the northern Faeroes according to the geological map and show both dextral and sinistral displacements. Most occur on the central island Streymoy, where the average strike of the dextral faults is 65°, and the average strike of the sinistral faults is 96°. The low angle of conjugation of about 31° of the two sets of faults can be directly observed in the few intersections of dextral and sinistral faults which have been mapped.

Normal faults are common in the northern Faeroes and mostly lie inside the acute angle of the strike-slip faults, while all lie between 40° and 135°. On Stremoy they show a pronounced E-W maximum. The normal faults mapped in the northern Faeroes average 8 metres and do not exceed 45 metres. They show a net downthrow towards the north. Normal faults are fairly common too, though generally smaller, on Suduroy where they strike NW-SE like the dykes and joints.

The normal and strike-slip faults displace the dykes and irregular intrusions, while no faults have been reported in or just outside the sills. The master joints, however, cut through all types of intrusions.

north
Vágar

north
Streymoy

north
Eysturoy

north

Northeastern
islands

south

south

south

north

Suduroy

south

The Faeroe Islands
Joint and fault roses
based on Rasmussen and Noe-Nyegaard 1969
Master joints
Dextral faults
Normal faults (also +N)
Sinistral faults
Length of 10 units
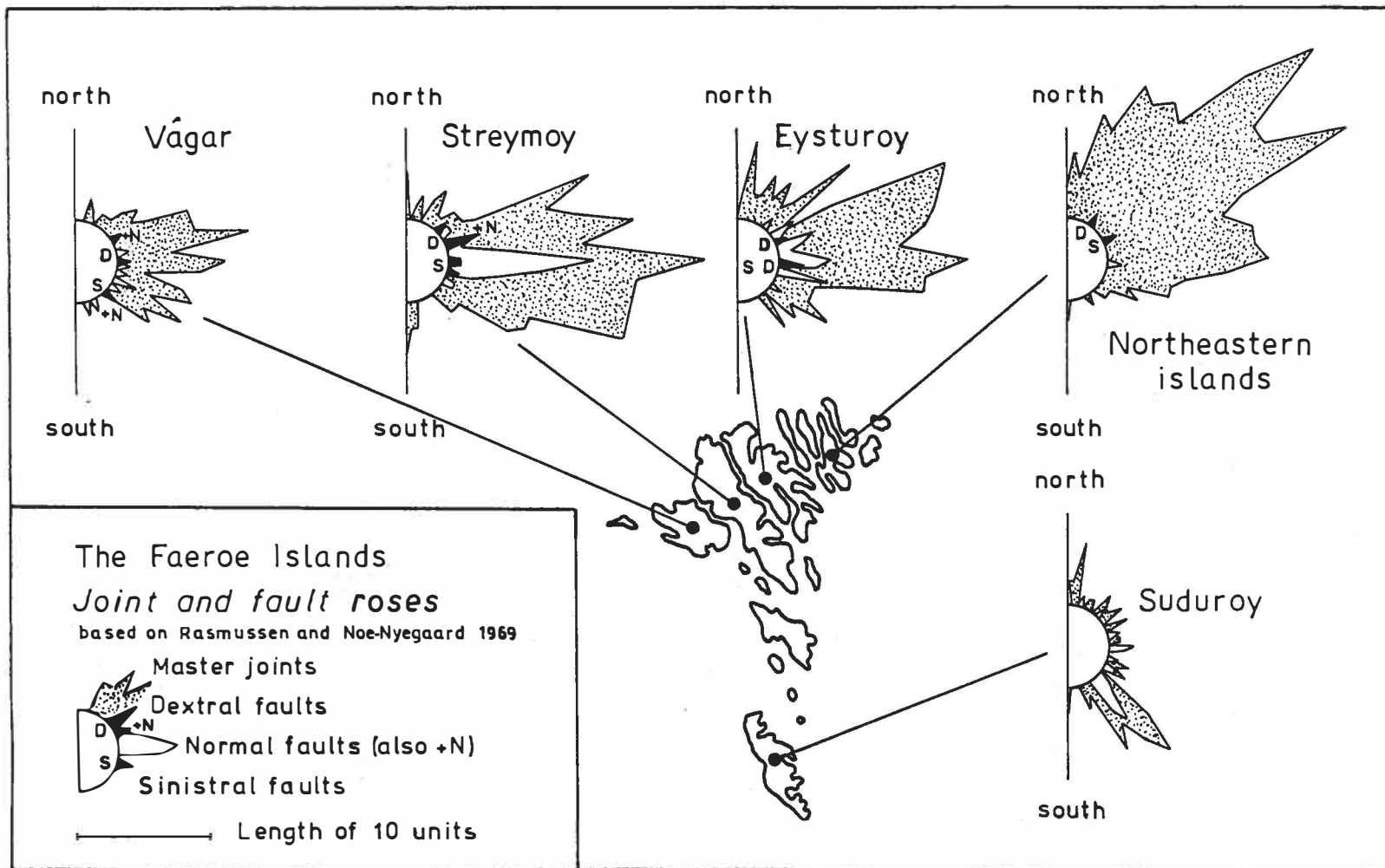
FIGURE 4

2.1.6. Doming

The Faeroe plateau is gently warped into a northern and southern dome which are both centred just west of the islands (Schroeder 1971) (section 2.2.2.). The flank of the northern dome appears on land as a low-amplitude anticline with an easterly plunge (Noe-Nygaard 1966, 1974; Rasmussen and Noe-Nygaard 1969). In most parts of the Faeroes the dip of strata is between 1 and 4°. In the western edge of the Faeroes the dip of strata towards the southeast (Fig. 2) increases upslope from about 3.3^O at the Lower-Middle Basalt boundary in the western Vágar, to about 8° in the central part of Mykines, and to about 15° on Mykines Holmur, the westernmost tip of the Faeroes. This gives the false impression that the older strata have been tilted more than the younger ones. On Suduroy the eastern flank of the southern dome steepens gradually southwards along the strike. At the southern end of the island, Walker and Davidson (1936) report an approximate dip of the lavas of 20° E, while a dip of 16° E is suggested by photo-interpretation of the top of the southern headland Akraberg as a flow top. The map by Rasmussen and Noe-Nygaard (1969) confirms the dip towards east in the southern end of Suduroy, but gives no figures as to the size of the inclination.

2.1.7. Volcanic-tectonic evolution

The few direct and indirect observations made about the elongation or alignment of volcanic vents (section 2.1.3.) all point to an approximate NW-SE trend of these volcanic features, and suggest that the plateau was subject to mild NE-SW tensional forces during its formation, as does a SE striking buried normal fault at the top of the Lower Basalts (section 2.1.2.). Strictly speaking the above observations only apply to the time of extrusion of the Middle Basalts and the preceding volcanically quiet period, but as the three basalt series are essentially concordant, there is no a priori reason to expect any large change in the stress conditions between their formation.

Most dykes and sills were probably injected during a separate intrusive phase succeeding the extrusive phase (section 2.1.4.). In the northern Faeroes, the scatter of dyke trends suggests shifting stress conditions during the intrusive phase. Most simply, this may be explained by a gradual change from the regime of NE-SW tension of the extrusive phase to the regime of NW-SE or N-S tension of the later tectonic phase in accordance with their observed age relationships (section 2.1.4.).

The abundant normal faults in the central northern islands Streymoy and Eysteroy strike above E-W on average, while the acute bisectrix of the conjugated strike-slip faults on the same islands trends about 70° E (section 2.1.5.). Conjugated strike-slip faults are normally taken to indicate compression along the acute bisectrix. However, the low angle of conjugation of about 31° rather suggests tension along the obtuse bisectrix instead (Badgley 1965), and thus both normal and strike-slip faults have probably been

generated by the same approximately N-S tensional forces[1]. Most of the master joints in the area show similar trends as the faults and probably have the same origin.

The average strike of the master joints changes from about E-W to about NE-SW in the northeastern Faeroes as noted earlier, and the very few faults in this area suggest a similar change in the strike of the faults. The northeastern Faeroes therefore seem to have been subject to NW-SE tensional forces rather than N-S tensional forces during the tectonic phase. Suduroy, on the other hand, has probably been subject to NE-SW tension all the time to judge from the strongly dominating NW-SE direction of dykes, joints and faults.

The intrusive and tectonic phases must partly overlap in time, as many faults have been intruded by dykes which have been sheared afterwards. However, most fault movements probably occurred after the emplacement of the intrusions to judge from the fact that dykes cut by the same strike-slip fault always show similar offsets.

The differing tensional axes in the northern, northeastern and southern Faeroes during the tectonic phase strongly suggest that the tension is of secondary origin and therefore probably related to the doming. This easily explains the tension observed on Suduroy which is very nearly at a right angle to the long axis of the southern dome. The northern dome is only slightly elongated,

---

[1] Low angle east and west dipping joints which cut through one or more flows can be seen in the southern headlands of Eysturoy. As low angle joints have not been looked for in other places, it is uncertain whether they are due to regional compression or the thrust of glaciers flowing along the headlands, though the latter alternative is considered most likely.

and the tensional axes varies. On average, the tension axis is nevertheless approximately at a right angle to the dome axis. The above rough parallism between dome axes, faults, and supposed late dykes suggests that the doming started before the extinction of the volcanic activity. Thus, the sills at the Middle-Upper Basalt boundary may well have been intruded in response to the doming explaining why the sills occur close to the crest of the northern dome, but are missing on the small central islands south of the dome.

In conclusion, the succession of Lower Tertiary volcanic and tectonic events on the Faeroes may be summarized as below:

1) Extrusion of the Lower Basalts

2) Deposition of the clay-coal sequence; faulting

3) Extrusion of the Middle Basalts; irregular intrusions?

4) Slight tilting? towards north and subsequent erosion?

5) Extrusion of the Upper Basalts

6) Intrusion of dykes

7) Intrusion of dykes and sills; incipient doming and faulting

8) Continued doming and faulting

2.2.   The basaltic shelf

2.2.1.   Areal extent
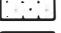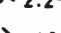
The basalt plateau either outcrops or forms a shallow basement on nearly all the shelf north, west and south of the Faeroes and on the inner shelf east of the Faeroes. The approximate limit of shallow or outcropping basaltic basement is shown in Fig. 5 and is based on various published data including magnetic profiles, seismic reflection profiles and bathymetry supplemented by some echo sounder records obtained during the present marine geological programme. The actual sediment thickness at the limit varies from zero to probably not more than a few hundred metres depending on the evidence available for the drawing of the limit. Some of this evidence will be presented below in different contexts.

2.2.2. Magnetic mapping of the Lower-Middle Basalt boundary

The lower part and the uppermost part of the Lower Basalts on the Faeroes are normally magnetized, while the Middle and Upper Basalts and the middle part of the Lower Basalts are reversely magnetized. Additional, short reversals possibly occur in the Lower Basalts (Saxov and Abrahamsen 1966, Tarling and Gale 1968). Schroeder (1971) has established the boundary between the Lower and Middle Basalts in 10 places close to land from a reconnaissance magnetic survey and concludes that the Faeroe plateau forms two huge dome structures. His survey area does not extend far enough to establish the closure of the northern dome towards the north and west or the southern dome towards the south. The former closure, however, is suggested by the occurrence of a wide, curved belt of negative magnetic anomalies on the outer shelf and slope northwest of the Faeroes shown on the anomaly map of the Iceland--Faeroe Ridge by Fleischer and others (1974). The negative anomaly belt (Fig. 6a) is overprinted by short-waved anomalies and is therefore very probably due to reversely magnetized basalts. Likewise, the closure of the southern lower basalt inlier towards the south is suggested by the work of Himsworth (1973), who notes that the short-waved magnetic anomalies across the ridge are dominantly negative.

The eastern limit of the Lower Basalts on Suduroy runs just east of the islands (Schroeder 1971) conforming to the increase of dips of strata to the east and south observed on land (section 2.1.6.). The base of a Middle Basalt outlier 14 kilometres from the southern end of Suduroy thus dips 4° ENE, while the average dip over the next 2.25 kilometres to the east must be about 9° to fit the same boundary on the sea floor determined magnetically.

Tectonic map of the Faeroe region

FIGURE 5

Legend:
- Outcropping or shallow basaltic basement
- Outcropping metamorphic basement
- Shallow metamorphic basement
- Area of major sediment thickness
- Central portion of sedimentary basin
- Buried basement ridge
- Major fault at surface or depth
- Unconformity in sediments
- -2- Isopachyte in second two-way travel time
- 1000 metre water depth contour
- 2.2° Dip of lavas
- 4° Apparent dip of lavas
- -A,B,C- Marker horizons drawn at sea level
- • Nearly in situ basalt dredged
- + Dredge clinging to rocky sea floor

0   50   100 km
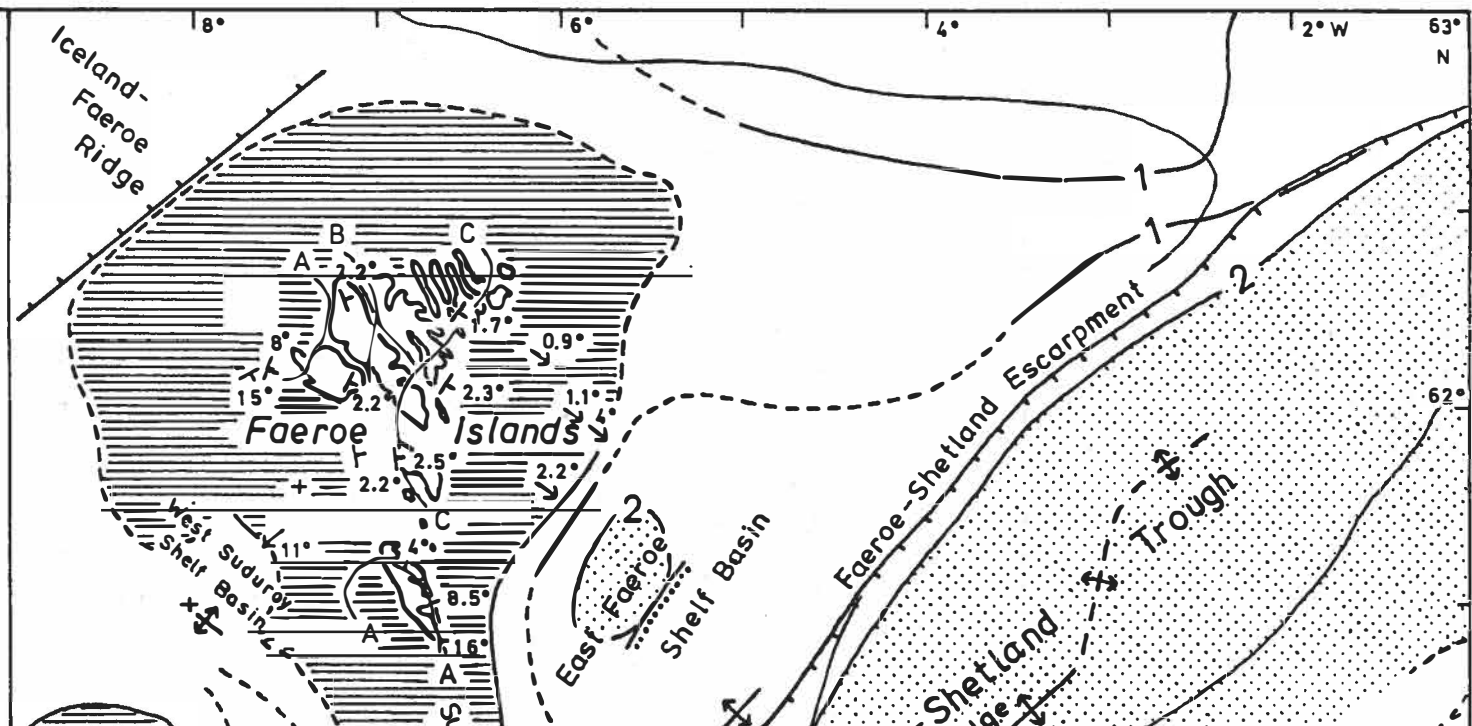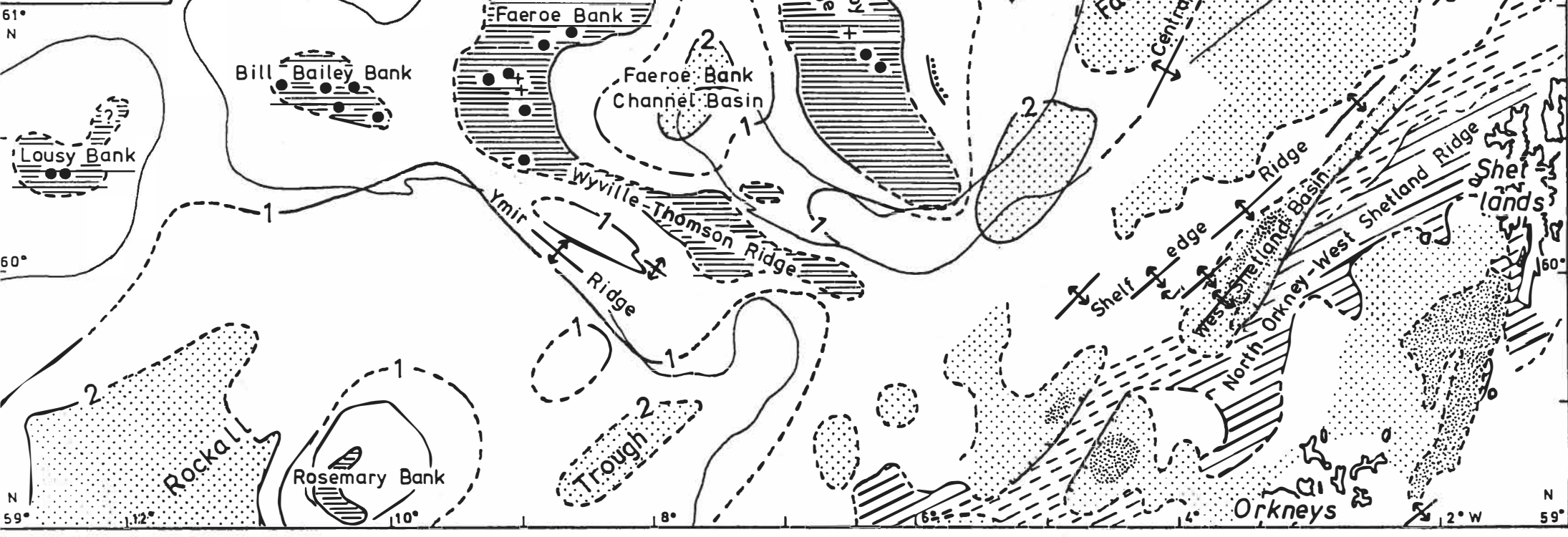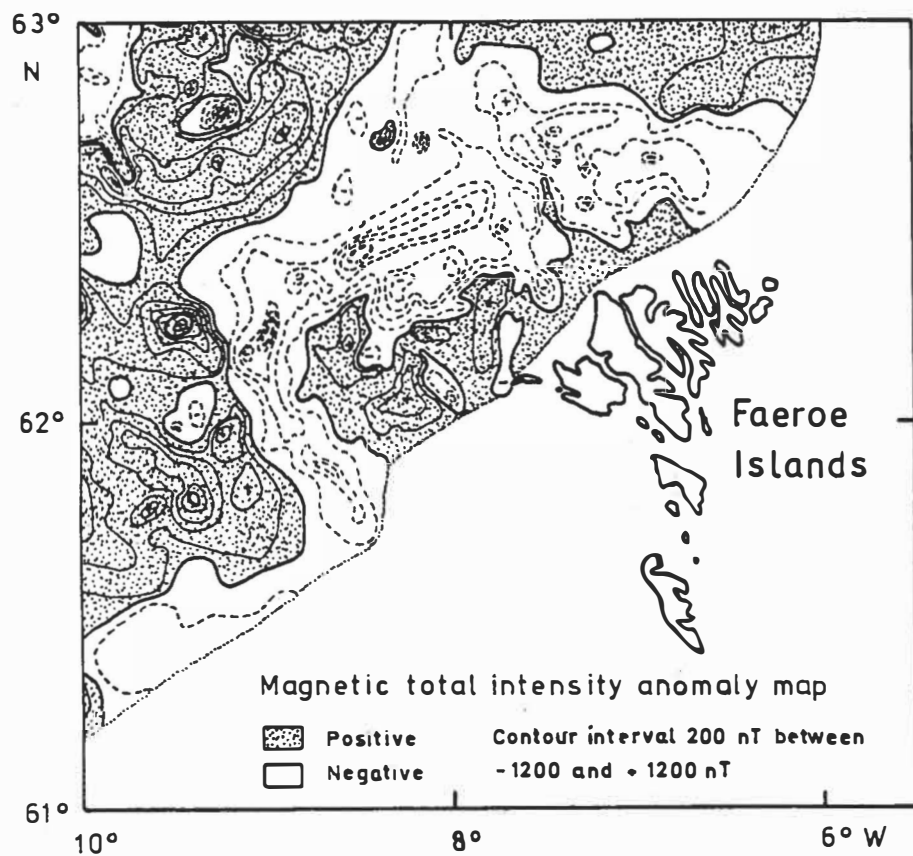
FIGURE 6a. Magnetic total intensity anomaly map of the northwestern Faeroe shelf and adjoining deeper areas.
(Redrawn from Fleischer and others 1974).
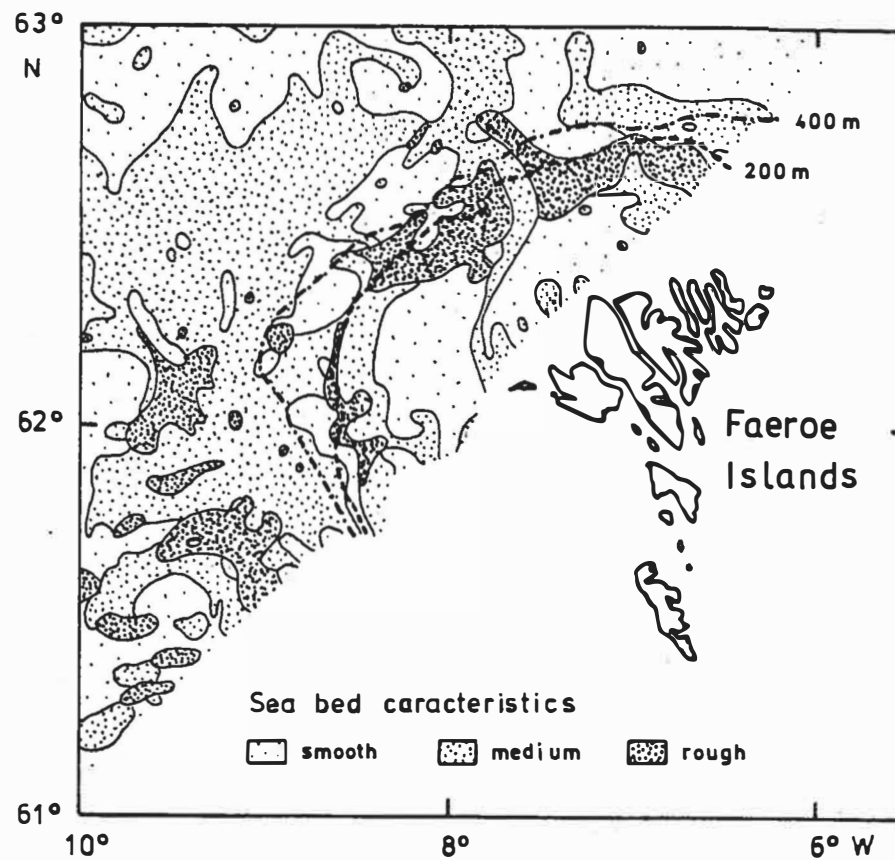
FIGURE 6b. Sea bed characteristics of the northwestern Faeroe shelf and adjoining deeper areas derived from echo sounder records.
(Redrawn from Fleischer and others 1974).
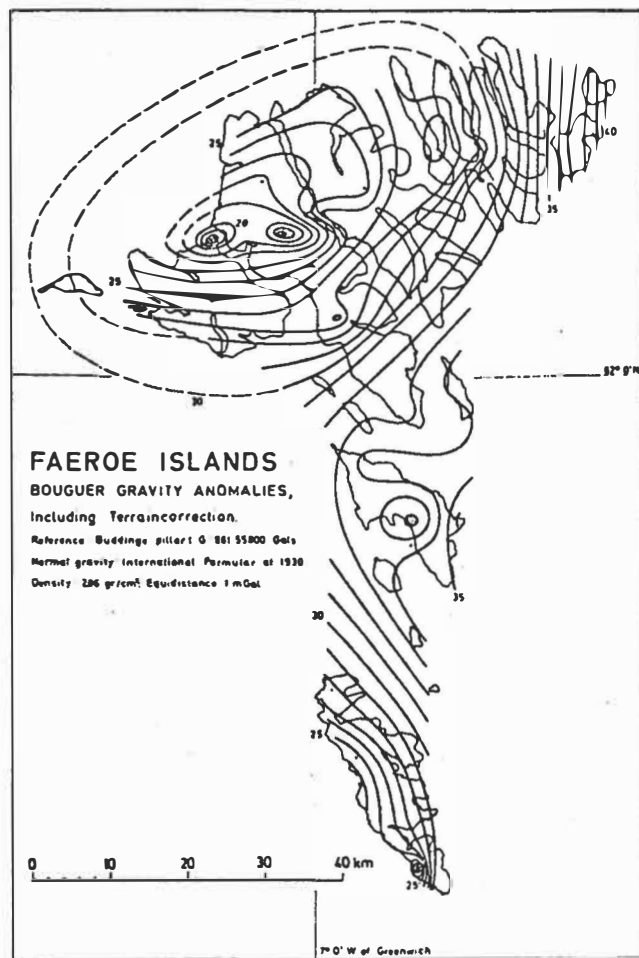
FIGURE 6c. Bouguer gravity anomaly
map of the Faeroe Islands.
(From Saxov and Abrahamsen 1966)
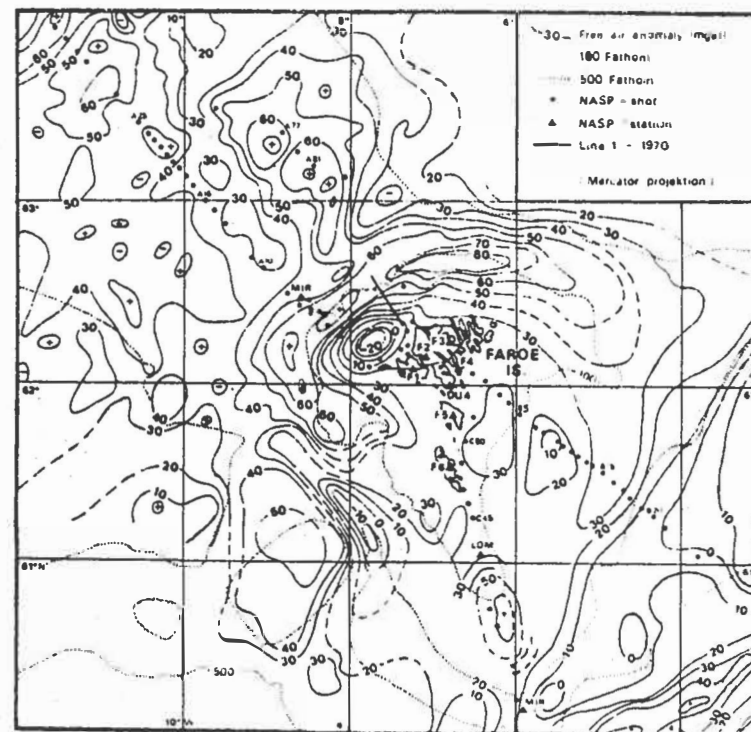
FIGURE 6d. Free air gravity anomaly map
of the Faeroe region based on maps by
Bott and Watts (1971) and Fleischer and
others (1974).
(From Nielsen 1976)

3 kilometres further south on the headland Porkerines a lava top is well exposed from within 2 to 0.5 kilometre from the magnetic boundary on the sea floor and shows an average dip of 8.5° ENE, while a dip of 6.5° is recorded on the geological map at the summit of the headland. The oldest lavas on Suduroy occur on the west coast near the southern end where they strike SSE, and one of these probably forms the islet Sunnböur Holmur west of the southern tip of the island. This islet lies only about 3.5 kilometres west of the magnetically determined Lower-Middle Basalt boundary on the sea floor. The average dip at this latitude therefore must be about 14° E if the thickness of the Lower Basalts is constant; this compares well with the photo-interpreted value of 16° E at Akraberg at the southern end of Suduroy (section 2.1.6.).

The Lower Basalts on the westernmost island Mykines extend only a few kilometres southwards according to Schroeder (1971) who established the boundary from only two crossings. If his interpretation of the magnetic results is correct, the dip of the boundary must increase westwards to roughly 45° south of the islet Mykines Holmur which exposes the oldest lavas (section 2.1.6.), or the boundary must be fault-bounded to the west.

2.2.3. Microtopography and stratigraphy

On land the thick Lower Basalt flows and the somewhat thinner Upper Basalt flows form step-like mountain slopes, while the thin, vesicular Middle Basalt flows form smooth mountain slopes. The same difference in response to erosion of the three series is ob-served on the flat shelf and may be used in stratigraphical map-ping where the sediment cover is too thin to conceal the morpho-logy of the basaltic basement.

Very little is known about the actual sediment distribution on the basaltic shelf, but a continuous sediment cover seems to be present only in small areas for the following reasons: 1) Supposed erosional flow escarpments are commonly observed even close to the edge of the basaltic shelf. 2) Seismic reflection profiles across the Suduroy Ridge (Himsworth 1973) show no sediment cover on the top of the ridge, though it is mostly very smooth. 3) Two out of ten dredge hauls SW and S of the Faeroes inside the limit of shal-low basaltic basement in Fig. 5 were made on sea floor which ap-peared completely smooth over a distance of several kilometres. In both cases (station 15 and 82 in Fig. 10) the ship was firm-ly anchored by the dredge to the sea floor as if the obstacles consisted of solid basalt outcrops.   (Pebbles of local basalt were actually recovered on stations 80 and 81). 4) Finally, though the maximum velocity of the tidal currents in many places probably are within the limits favourable for the formation of sand waves like on the inner shelf west of the British Isles (cf. Kenyon and Stride 1970), no clear examples of wavy sea floor have been observed on the echo sounder records within the basaltic shelf. This suggests that in most places there is insufficient sand for the formation of sand waves.

The description below of the morphology of the basaltic shelf
is primarily based on about 400 kilometres of echo sounding tracks
(south of about 62° N only), navigational charts and a contour
map of the sea floor inside the 100 metres isobath (Rasmussen 1974).

The inner part of the shelf west of Suduroy is very rough with
depth differences up to 20-30 metres similar to the thickness of
the Lower Basalt flows on land. An echo sounding record parallel
to the coast north of 61°26' N shows a step-like topography with
the steps inclined to the north like the flows forming the nearby
sea cliffs. Off the middle part of Suduroy the rough sea floor
extends about 12 kilometres to the west; this is about 4 kilome-
tres east of the only point on the western boundary of the Lower
Basalt inlier established magnetically by Schroeder (1971). The
rough shelf area narrows slowly to the south terminating some 10
kilometres south of the island. This suggests a pear or drop
shape for the inlier with the dome axis running just west of the
island and a steepening of the dome flanks southwards.

The innermost part of the northwestern shelf inside the north-
ern Lower Basalt inlier shows a relief of 20-50 metres. The hilly
topography disappears 10-15 kilometres NW off the islands, probab-
ly not far from the northwestern boundary of the inlier.

The major part of the basaltic shelf west and north of the Fae-
roes is smooth, and is therefore supposed to be underlain by thin,
amygdaloidal pahoehoe flows which, on land, are characteristic for
the Middle Basalts but also occur at intervals in the Upper Basalts.

A set of thicker flows stands out 13 kilometres west of the
northern head of Sandoy (Fig. 7a). The dip of the flows calculated
from their apparent dips on two nearby echo sounder records is
about 2^O ENE or similar to the dip on Sandoy. This means that the
flows lie about 600 metres below the top of the Middle Basalts,
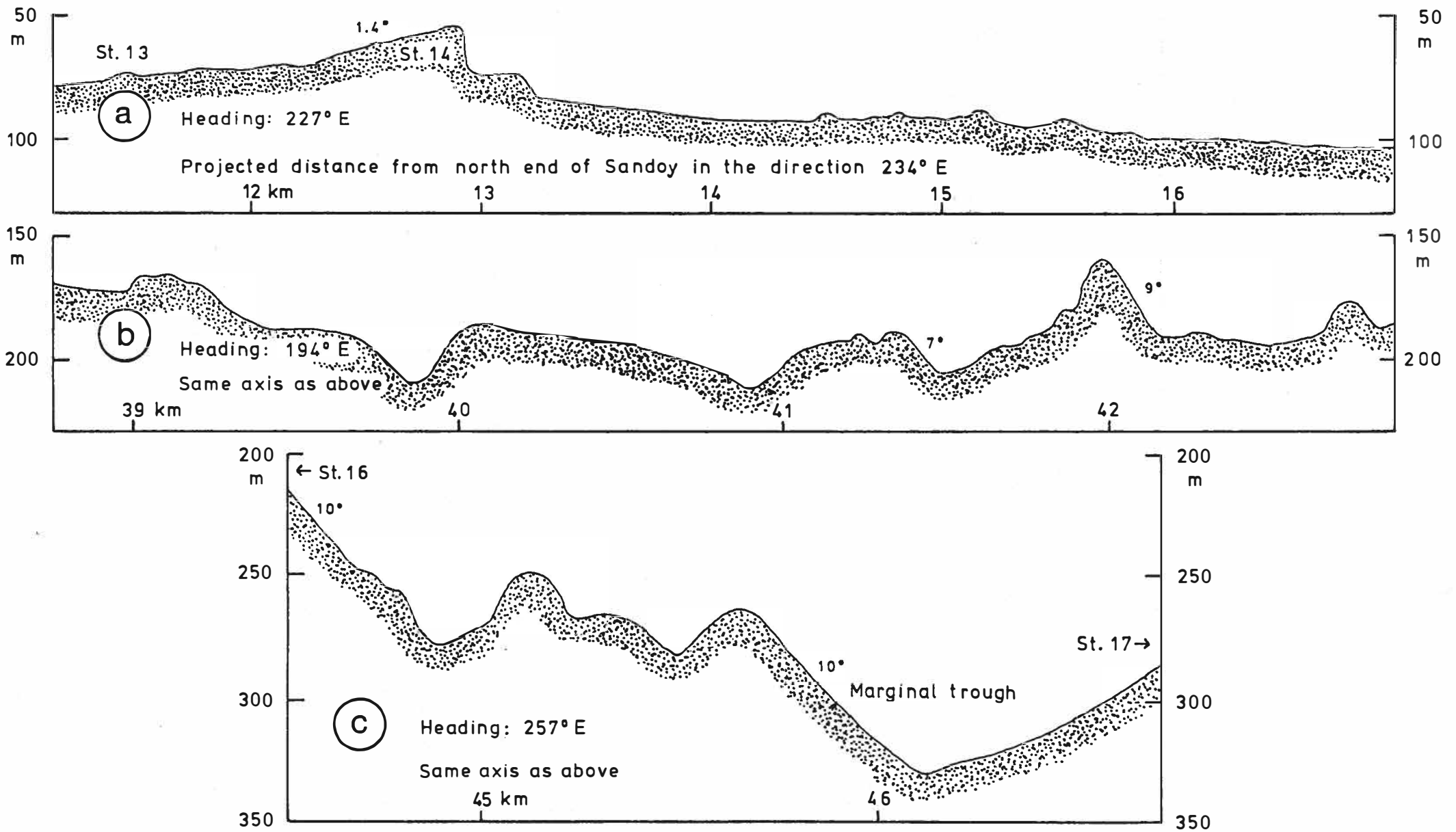
FIGURE 7a–c. Echo sounder profiles across the western basalt shelf
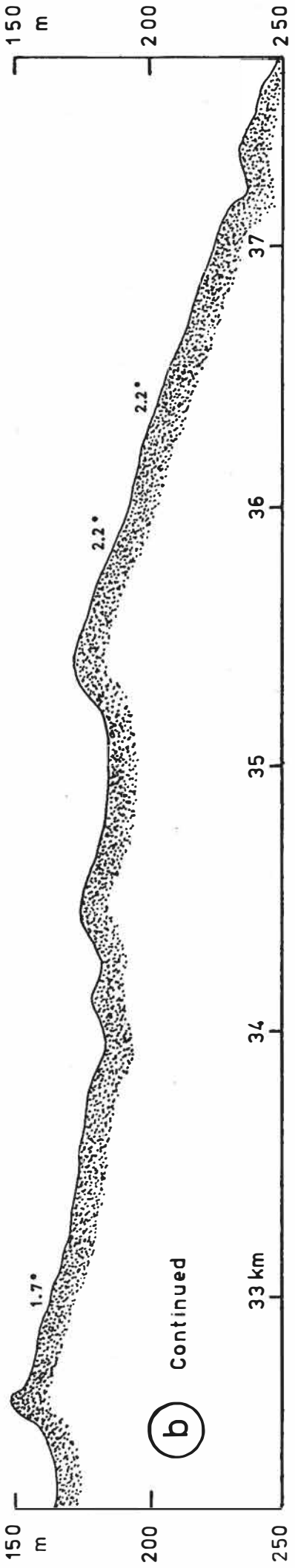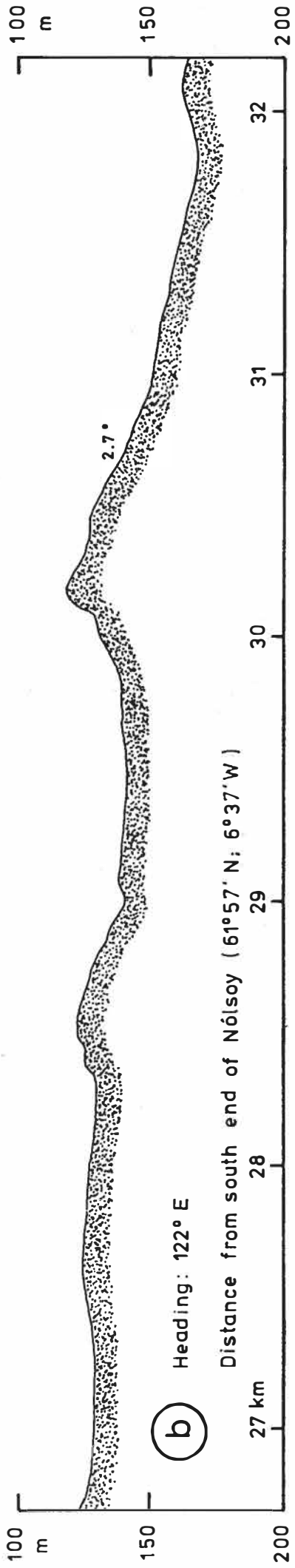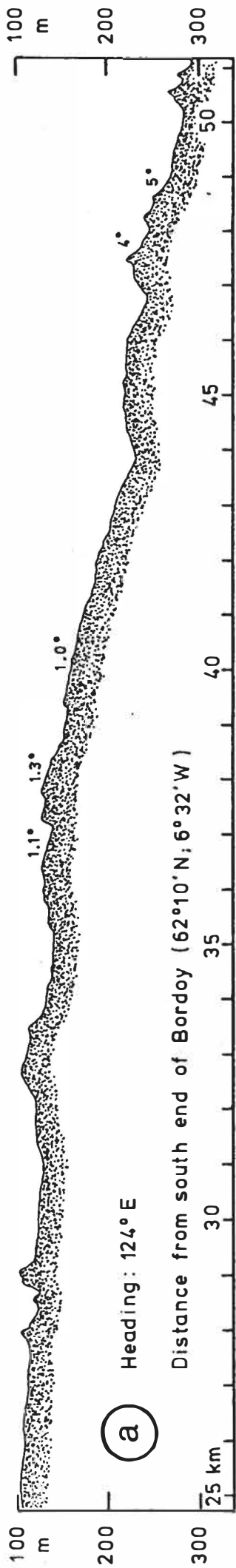
FIGURE 8a–b. Echo sounder profiles across the eastern basalt shelf

and they may therefore be identical to the B-horizon flows further north on land (section 2.1.2.).

The wide northern sector of the eastern basaltic shelf intermittently shows an irregular topography probably due to seaward dipping flows averaging about 10 metres in thickness (Fig. 8a and b). This part of the shelf borders on Upper Basalt flows on land with a similar average thickness, and therefore probably also consists of Upper Basalt flows.

The shelf northwest of the islands, which also borders on Upper Basalts on land, is unexpectedly smooth (cf. Rasmussen 1974). This is one of the least explored of the shelf areas.

A sea floor roughness map by Fleischer and others (1974) shows extensive areas of rough sea floor north and northwest of the Faeroes from the shelf break at a depth close to 200 metres and about 12 kilometres inshore (Fig. 6b). The rough sea floor continues downslope in tongues towards the Iceland-Faeroe Ridge to a depth of 400-500 metres. The shape and size of the irregularities are not described, and they only appear as rare deflections of the 20 metres contours on the bathymetric map by Fleischer and others (1974). The outer shelf is strongly negatively magnetic (Fig. 6a) with short-waved (1 - 1.7 nautical miles) magnetic anomalies exceeding 500 nT (nanno-Tesla = gamma) at sea level according to an amplitude contour map by Fleischer and others (1974). This suggests that reversely magnetized basalts occur at shallow depth. The rough sea floor therefore probably consists of outcropping Upper Basalt flows which are reversely magnetized and respond variably to erosion unlike the thin Middle Basalt flows. In some of the rough areas between 200 and 500 metres depth, on the other hand, the amplitude of the short-waved magnetic anomalies does not exceed 50 nT, and the irregularities here are therefore

perhaps sand waves or iceberg plough marks (Belderson et al. 1973).

The belt of rough sea floor extends southwards along the western shelf border to a shallow depression in the outer shelf facing the Faeroe Bank Channel. This depression coincides with a sediment basin, which will be described later (section 2.4.2.). A roughly 7 kilometres wide belt of rough sea floor occurs along the inner margin of the depression and seems to consist of a series of 5 to 50 metres thick basalt flows dipping towards the depression (Fig. 7b and c). The flows probably belong to the Upper Basalts, because they are fairly thick and apparently overlie the Middle Basalts supposed to form the major, smooth part of the western shelf. The belt of rough sea floor seems to continue along the shelf border south of the above depression, but is much less distinct.

2.2.4. The structure of the basaltic shelf and the thickness of the Upper Basalts

Far the greater part of the Faeroe plateau is submerged. Based on the magnetic and bathymetric surveys and the geology on land the distribution of the three basalt series on the Faeroes and the surrounding shelf is as follows (Fig. 5). The Lower Basalts occur in a northern area which mainly comprises the innermost northwestern shelf, Mykines and the westernmost Vágar, and a southern area which mainly comprises the inner part of the shelf west of Suduroy and Suduroy itself. The Middle Basalts form a large continuous area encompassing the two Lower Basalt inliers. They form the major, smooth part of the western, northwestern and northern shelf, besides most of the Faeroes and the intervening water areas. The Upper Basalts descend eastwards across the northern and central Faeroes from about 650 metres height to sea level. They form the wide, basaltic part of the eastern shelf and probably also the outer fringe of rough sea floor on the shelf north, northwest and west of the Faeroes.

The structure of the basalt plateau thus seems to be a simple one of two partly separated domes. The outline of the basaltic shelf is roughly symmetrical about a NNW-SSE trending line which passes close to the centre of both domes. The wide northern part of the basaltic area is furthermore nearly bisected by the WSW-ENE trending axis of the northern dome. The outline of the basaltic shelf may therefore by and large reflect the combined outer contour of the two domes, that is the Upper Basalts are preserved all the way round. Some structural complexities possibly occur, however, near the western and southern end of the Faeroes, where the largest tilts on land are recorded (section 2.2.2.), and on the narrow Suduroy Ridge.

On some echo sounder records the outcropping lava flows are seen as uniformly inclined steps, from which an apparent dip can be read rather safely. A few records which have been obtained along ship tracks across the middle sector of the eastern shelf show this clearly. These ship tracks run about NW-SE or roughly perpendicular to the supposed strike of the flows, and the dip of the flows read from the echo sounder records is therefore probably close to the true dip. Some of these nearly true dips are shown on Fig. 5 by arrows parallel to the ship track. In the southeastern part of the northwestern island Bordoy the base of the Upper Basalts dip 1.7^O SE. On the shelf about 10 kilometres to the southeast the dip is only about 1^O, however. This dip probably persits to within a few kilometres of the outer limit of the plateau, where it seems to increase rapidly to 4° or so (Fig. 8a). Assuming a dip of 1.7^O on land, a dip of 4° in the outermost 4 kilometres of the shelf, and a dip of 1^O in the intervening part of the shelf SE of Bordoy, the thickness of the Upper Basalts is about 1200 metres. This is only 300 metres more than the exposed thickness of the Upper Basalts on the island Sandoy.

Along a line 10 kilometres further south, the dip is $2.3 - 2.9^O$ on land in the Nolsoy-Tórshavn region and averages about 2.2^O in the outermost 7 kilometres of the basaltic shelf (Fig. 8b). Using these dips and again a dip of 1^O for the intervening part of the shelf the calculated thickness of the Upper Basalts is about the same as along the former line.

The presumed belt of Upper Basalts along the embayment in the plateau SW of the Faeroes has been crossed at a high angle in two places. From the apparent dips on the echo sounder records (Fig. 7b and c) a true dip of 11° in the direction 235° E has been calculated assuming that the dip and strike is constant in the outer

5 kilometres of the belt. In the remaining 2 kilometres of the belt of rough sea floor the dip seems to decrease rapidly. From Fig. 7b and c the stratigraphic thickness of the supposed Upper Basalts is estimated at 900 metres.

2.3.   Deeper structure of the Faroe Block

2.3.1. Crustal layering

The Faeroe Block comprises the Faeroe Islands and the sur-
rounding shelf. Palmason (1965) from seismic refraction measure-
ments on land found a primary wave velocity of 3.9 km/s for the
Upper Basalts, of 4.9 km/s for the Lower and the Middle Basalts
and of 6.4 km/s for an unexposed basement. He equated the base-
ment at a depth of about 2.5-4.5 kilometres with the oceanic
layer 3. Bott and Watts (1971) pointed out that the fit between
the continental margins of Greenland and Northern Europe was con-
siderably improved over the fit of Bullard and others (1965) by
assuming that both the Rockall Plateau and the Faeroe Block were
continental. A steep drop in the Bouguer anomaly of about 80 mgal
between the Iceland-Faeroe Ridge and the Faeroe Block (Fig. 6c)
was attributed to lateral change in crustal density and slight
thickening of crust towards the Faeroes marking the transition
from an anomalous oceanic to a continental type of crust (Bott
and others 1971). This edge anomaly passes into a marked gravity
minimum on the northwestern Faeroe shelf ascribed by Schroeder
(1971) to a concealed, salic (continental) rock body the isosta-
tic movements of which might explain the dome structure of the
basalt plateau. Refraction surveys with recording stations mainly
on land and shot points in the sea in 1970 and 1972 corroborated
the concept of a continental substratum beneath the Faeroese lava
plateau (Casten 1971, 1973, 1974, Bott and others 1974, 1976,
Casten and Nielsen 1975, Nielsen 1976). Time term analyses of the
results from the northwestern part of the Faeroe Block gave an
unreversed velocity of 5.9 km/s which is too low for the oceanic
layer 3 but typical of granites (Casten 1973). Time term analyses

of the results from the North Atlantic Seismic Project (NASP) in
1972 gave a basement velocity of 5.9-6.2 km/s for the northwest-
ern half of the Faeroe Block, i.e. fairly typical of metamorphic
basement rocks of the continental crust. A   basement velocity of
about 5.3-5.5 km/s for the shelf to the southeast could be inter-
preted as a folded series of shales, greywackes, slates and so on
(Bott and others 1974). The primary wave velocity of the mantle
was estimated to be 8.24 ±0.35 km/s and the crustal thickness was
estimated to lie between 27 and 38 kilometres. Bott and others
(1976) demonstrated that primary head waves travelling in the
lower crustal layer and possibly in the topmost mantle beneath
the Iceland-Faeroe Ridge at velocities of about 6.7 and 7.8 km/s
respectively are converted at the intervening margins into a
crustal phase beneath the Faeroe Block. This result adds strong
support to the hypothesis that a true continental margin separates
the anomalously thick (about 27 kilometres) Icelandic type of
oceanic crust beneath the Iceland-Faeroe Ridge from continental
crust beneath the Faeroe Block. The results also suggest an
increase of velocity with depth below the Faeroese basalt plateau
to 6.5 km/s or more.

The crustal layer with a primary wave velocity of about 6 km/s
below the Faeroe Islands extends northwestwards to the continental
margin which occurs approximately beneath the bathymetric scarp
between the Faeroe shelf and the Iceland-Faeroe Ridge. Southeast
of the Faeroes beneath the outer part of the basaltic shelf the
6 km/s basement gives way to a layer with an apparent velocity of
5.3-5.5 km/s (Bott and others 1974, Nielsen 1976) which specula-
tively may mark the transition between areas of crustal and
supracrustal rocks inside a Precambrian shield. Further south the
limit of the 6 km/s basement apparently occurs just east of

Suduroy, and arrivals from more southerly shot points give a poorly reversed velocity of 4.9 km/s reconcilable with a direct wave in the basalts (Nielsen 1976). The 6 km/s basement is probably itself somewhat inhomogeneous. Time term analyses give a well-determined crustal velocity of 5.9 km/s below the Faeroes, where reversal is good, but suggest a velocity of 6.1-6.2 km/s beneath the northwestern shelf region (Bott and others 1974, 1976, Nielsen 1976). A delay of waves travelling between Vágar and Suduroy may indicate an area of lower velocities west of the islands (Nielsen 1976).

2.3.2. Gravity anomalies

Gravity surveys on land show that the Bouguer gravity anomalies form a syncline or bowl in the northern Faeroes and a less pronounced anticline in the central Faeroes and that both/plunge to the east (Saxov and Abrahamsen 1964, 1966). The Bouguer anomalies range from about +16 to +39 mgal (Saxov 1969). The gravity curves are parallel or subparallel to the strike of the basalts in most part of the Faeroes (cf. Figs. 2 and 6c). At sea level the Middle-Upper Basalts boundary approximately coincides with the +30 mgal contour in the northern Faeroes and with the +33 mgal contour along the west coast of Sandoy (Fig. 6c, including corrections by Saxov 1971). The conformity of the Bouguer anomaly pattern with the structure of the basalt plateau suggests that the Bouguer anomalies partly reflect the variations in depth to the base of the basalt plateau. This implies that the basement is distinctively lighter than the basalts which in conjunction with the primary wave velocity of 5.9 km/s points to a granitic composition for the basement.

The gravity minimum of less than +20 mgal in northern Streymoy and Vágar is an offshoot of a sharp gravity minimum of about -20 mgal on the northwestern shelf (Fig. 6d) (Fleischer 1971, Fleischer and others 1974). In the center of this gravity anomaly the time term of the 6 km/s refractor increases abruptly about 0.3 second (Casten 1974, Casten and Nielsen 1975, Bott and others 1976). The gravity anomaly occurs inside an area characterized by short-waved, high-amplitude (>500 nT) magnetic anomalies (Fleischer and others 1974). The gravity anomaly has variously been ascribed to either a thickening of the basalt plateau (Casten 1974), a sediment basin in the basalt plateau (Fleischer

1971, Casten 1974, Casten and Nielsen 1975), a salic rock body, granite intrusion or granite batholith (Schroeder 1971, Fleischer and others 1974, Bott 1975, Nielsen 1976) or a Mesozoic basin (Bott 1975 b).

Casten (1974) computed two crustal models fitting the gravity anomaly and associated high time term of the 6 km/s refractor. He ascribed the geophysical anomalies to an abrupt thickening of the basalt plateau in the first model and to a 0.6 kilometre deep basin with low-density sediments associated with a lesser thickening of the underlying basalt plateau in the second model. The model computations were based on densities of 1.75, 2.55, and 2.75 g/cm^3 for sediments, basalts and supposed granitic basement, respectively. Both models are very speculative as direct density measurements of Faeroese basalts yielded an average density of about 2.86 g/cm^3 (Saxov and Abrahamsen 1964, 1966, Saxov 1969). The second model is also at variance with the character of the magnetic anomalies in the area of the gravity low.

The anomaly may instead reflect the occurrence of a granitic pluton, several kilometres thick, occurring at shallow depth (cf. Schroeder 1971, Fleischer and others 1974). As the gravity anomaly occurs close to the supposed center of the northern dome in the basalt plateau the substratum may be highly elevated in this place (though it probably does not reach the sea floor since non-basaltic rocks have not been reported by Faeroese fishermen). The hypothetical pluton, therefore, does not need to be intruded into the basalt plateau and may be unrelated to the Tertiary volcanism. If a relationship exists, however, the pluton may consist of remelted gneisses as postulated for some Skye granites though it must be noticed that these are associated with a positive gravity anomaly (Bott and Tuson 1973).

It is perhaps more likely that the gravity anomaly reflects a Mesozoic basin (Bott 1975 b) beneath a thin roof of basalts. The gravity anomaly is similar in shape and size to the anomalies above the deep Mesozoic basins west of the Shetlands (Bott and Watts 1970) and a buried basin on the northwestern Faeroe shelf would then, by analogy, be several kilometres thick. Sediments below the basalts would probably form a low-velocity layer not recognizable with the seismic refraction method except as an increase of the time terms (intercept times) of the 6 km/s refractor explaining the high time term in the center of the gravity anomaly.

A positive gravity anomaly with an amplitude of about 20 mgal occurs in the southern corner of the Faeroe shelf. The basement beneath has a time term of about 2/3 s and an apparent velocity of 6.60 km/s similar to the velocity determined, for example, in basement ridges on the shelf west of Shetland (Nielsen 1976).

2.3.3. The hidden part of the basalt plateau and the transition between basalts and basement

The primary wave velocity of the basement refractor averages 5.90 ±0.04 km/s beneath the Faeroe Islands. The corresponding time terms for seven NASP recording stations on the islands range between 0.25 and 0.54 s (Bott and others 1976). The stations range in stratigraphic position from the A-level to about 300 metres above the C-level. They thus lie up to 0.3 kilometre above the main basalt layer with a primary wave velocity of 4.9 km/s which includes the hidden part of the basalt plateau and the Lower and Middle Basalts. Assuming that the intervening crustal section consists of basalts with a primary wave velocity of 4.9 km/s the basement refractor lies 2.2-4.8 kilometres below the stations, the smallest depth being beneath station F6 on central Suduroy and the greatest depth being beneath station DU4 at Tórshavn. The thickness of the 4.9 km/s layer computed from these depths and the stratigraphic distances between the C-level and the stations is given below:

Area	NASP site	Latitude	Longitude	Thickness
Northeastern Eysturoy	F3	$62^O14.6'$ N	$6^O47.6'$ W	3.8 km
Northern Streymoy	F2	$62^O09.7'$	$7^O05.1'$	3.6
Central Vágar	F1	$62^O05.5'$	$7^O14.8'$	4.6
Southern Eysturoy	F4	$62^O05.5'$	$6^O41.6'$	4.2
Southern Streymoy	DU4	$61^O59.9'$	$6^O48.0'$	4.5
Sandoy	F5	$61^O49.9'$	$6^O45.7'$	3.0
Suduroy	F6	$61^O33.0'$	$6^O46.0'$	3.5

The estimated standard error of the time terms is 0.02-0.03 s

(Bott and others 1976) which means that the standard error of the thicknesses is 0.2-0.3 kilometre at best. These few results show that the greatest thicknesses of 4.2-4.6 kilometres occur in a E-W zone around 62° N across Vágar, southern Streymoy and southern Eysturoy. The smallest thickness of 3.0 occurs on Sandoy around $61^O50'$ N. The results from Streymoy agree with the earlier results by Palmason (1965) and Casten (1974) and all indicate an increase of the thickness of the 4.9 km/s layer of roughly one kilometre from the northern to the southern part of Streymoy. The increase occurs abruptly near $62^O06'$ N according to Casten (1974).

In an 18 kilometre unreversed profile from north to south on Suduroy, Palmason (1965) obtained an apparent velocity of 6.58 km/s and a depth of 2.9 kilometres. His results are equally well interpretable in terms of a refractor with, for example, a velocity of 6.4 km/s dipping 1.8^O to the north from a depth of 2.5 to 3.1 kilometres (corresponding to the increase in stratigraphic height) or a refractor with a velocity of 5.9 km/s dipping 7.8^O to the north from a depth of 0.8 to 3.3 kilometres. The latter solution corresponds to a northward increase of the thickness of the 4.9 km/s layer from 2.9 to 4.6 kilometres assuming a constant thickness of the Middle Basalts of 1.3 kilometres on Suduroy (see section 2.1.2.) It gives a thickness of about 3.5 kilometres at site F6 in agreement with the thickness derived from the NASP results above.

Outside the Faeroe Islands, the calculated time terms of the basement refractor become less reliable due to the long distances between shot points and recording stations and the uncertainty about the refractor velocity. The time terms of shot points on the Faeroe shelf have been calculated using a fixed basement

velocity of either 5.9 km/s (Bott and others 1976) or 6.1 km/s (Casten 1974). The time terms are given below as basement depths based on a simple two-layered crustal model involving a 4.9 km/s layer resting upon a uniform basement. Excluding shot point A3 in the center of the gravity low the 11 remaining NASP shot points on the nortwestern shelf indicate an average depth of 2.9 ±0.9 kilometres assuming a basement velocity of 5.9 km/s but 4.2 ±0.9 kilometres assuming a basement velocity of 6.1 km/s. An average depth of 3.3 ±0.7 kilometres is obtained for 6 NASP shot points on the eastern basaltic shelf for a basement velocity of 5.9 km/s. Casten (1974) obtained an average depth of 7.1 kilometres beneath 3 shot points from 1972 northeast of the Faeroes for a refractor velocity of 6.1 km/s, whereas the average depth is about 4.7 ±0.9 kilometres for a velocity of 5.9 km/s.

The average depth of the basement beneath the seven NASP recording stations on the Faeroe Islands is 3.5 ±0.8 kilometres below sea level assuming a refractor velocity of 5.9 km/s. The original thickness of the 4.9 km/s layer averages 3.9 ±0.6 kilometres at the same stations. The stratigraphic position of the shot points on the shelf can be estimated from the supposed structure of the basaltic shelf (section 2.2.4.). The original thickness of the 4.9 km/s layer on the shelf obtained from such estimates and the above average basement depths averages about 3.0 kilometres for the inner eastern shelf and 4.3 kilometres for the northeastern shelf assuming a refractor velocity of 5.9 km/s. On the northwestern shelf the refractor velocity seems rather to be about 6.1 km/s (Casten 1974, Bott and others 1974, 1976) and the average thickness of the 4.9 km/s is estimated to be roughly 5 kilometres. The average thickness of the 4.9 km/s layer thus seems to increase slightly from southeast to north-

west across the Faeroe Block. The thickness of the 4.9 km/s layer beneath the eastern sedimentary shelf cannot be estimated because only apparent velocities have been obtained which suggest that the true velocity is significantly lower than beneath the islands.

There is a fairly good correlation between the structure of the basalt plateau and the Bouguer gravity anomalies as noted earlier which suggests that the gravity anomalies partly reflect the depth to the base of the basalt plateau. However, the well-determined time terms of the recording stations on the Faeroe Islands show little correlation with their structural heights or gravity anomalies. The most simple explanation is that the time terms are locally increased due to sediments occurring in depressions in the basement. Sediments under the basalt plateau would probably form a low-velocity layer which cannot be resolved from the basalts in seismic refraction studies. If the sediments have the same density as the basement and completely fill or conceal the depressions in it, the depressions would not cause any gravity anomalies. Similarly, only minor gravity anomalies would arise if the depressions are partly filled with lighter sediments approximately compensating the excess weight of the basalts above. In both cases, the observed gravity anomalies may arise mainly from the later deformation of the crust affecting the basalt plateau as well as its substratum and thus be correlated with the dome structure of the plateau rather than with basement depth.

The transition between basement and basalts may be somewhat analogous to that observed in the Kangerdlugssuaq area in East Greenland which was probably situated just northwest of the Faeroe Block before the opening of the Northeast Atlantic (Bott and Watts 1971). In the Kangerdlugssuaq area the southernmost and thickest part of the East Greenland Tertiary basalt plateau

overlaps a Precambrian metamorphic basement of predominantly acid gneisses. The basalt plateau rests sometimes directly on the gneissic basement and sometimes on the thin Kangerdlugssuaq series of sediments which mainly consists of shallow marine shales of Upper Creataceous to Paleocene age (Wager 1947, Soper and others 1976 a og b). In the eastern part of the area the Kangerdlugssuaq series is in turn overlain by a thick series of hyaloclastics and bedded volcanogenic sediments suggesting that subsidence roughly kept pace with the build-up of the lowest part of the lava pile (Soper and others 1976 a and b).

The inferred local thickenings of the hidden, lower part of the Faeroese basalt plateau may similarly reflect accumulations of basaltic tuffs and tuff-breccias and perhaps also Upper Cretaceous-Paleocene shales, sandstones etc. Basaltic volcanogenic sediments are usually produced by the interaction of magma and water at shallow depth but large thicknesses of volcanogenic sediments may have formed locally if differential subsidence took place during the formation of the lower, hidden part of the basalt plateau.

The time terms of the individual shot points do not conform with the inferred structure of the basaltic shelf which suggests that sediments also locally underlie the basalts on the shelf. A particularly deep, probably Mesozoic basin may be associated with the sharp, negative gravity anomaly and high time term at shot point A3 on the northwestern shelf as discussed in section 2.3.2.

The postulated sediments are presumably lighter than the basement end since in most cases, they are not associated with any clear, negative gravity anomalies they probably do not fill in completely the depressions in the basement inferred from the

apparent thickness variations of the 4.9 km/s layer. The primary
wave velocity of the sediments is probably lower than in the
basalts but not much so due to the high confining pressure. The
sediments will therefore only cause a small overestimate of the
depth, and this overestimate may be compensated for higher up by
a slight downward increase of the velocity of the basalts from
the velocity of 4.9 km/s determined near sea level. The calculat-
ed thicknesses of the composite layer between the Upper Basalts
and the basement based on a single velocity of 4.9 km/s are thus
probably fairly reasonable, especially when averaged.

The original thickness of the composite 4.9 km/s layer averages
about 3.9 kilometres but ranges between about 3.0 and 4.6 kilo-
metres on the Faeroe Islands according to the limited evidence
given earlier. The exposed thickness of the Lower and Middle
Basalts is about 2.5 kilometres. Assuming no thickness varia-
tions inside the exposed sequence (cf. section 2.1.2.), the un-
exposed sequence varies in thickness from roughly 0.5 to 2 kilo-
metres. The minimum depth of the basement is probably larger
than 0.5 kilometre as the deepest exposures do not necessarily
occur in the thinnest part of the original 4.9 km/s layer. The
thickness variations of the unexposed sequence do not express
themselves clearly on gravity maps and the average density of the
thicker parts of the sequence is therefore probably close to the
density of the basement. This suggests that some part of the
thickness variation is due to sediments lighter than the basement
as argued before. Sediments of the order of thickness of one
kilometre may thus occur locally beneath the Faeroe Islands.
The major part of the sediments may be volcanogenic like in East
Greenland in which case they are an integrated part of the basalt
plateau. These problems can only be resolved by a drilling pro-

gramme.

The Upper Basalts forming the uppermost 3.9 km/s layer are at least 1.2 kilometres thick (section 2.2.4.) and the original thickness of the basalt plateau on the Faeroe Islands therefore probably averages at least 5 kilometres.

2.3.4. Summary

The Faeroe Block is continental and at least 27 kilometres thick. The basalt plateau rests on a 5.9-6.2 km/s layer interpreted as a Precambrian metamorphic basement. This gives way beneath the eastern shelf to a 5.3-5.5 km/s layer tentatively interpreted as Precambrian supracrustal rocks. The original thickness of the basalt plateau is at least 5 kilometres on the Faeroes. The thickness seems to increase from southeast to northwest across the Block. The basalt plateau consists of a 4.9 km/s layer including the Lower and Middle Basalts plus a hidden sequence and a 3.9 km/s layer including the Upper Basalts. The hidden sequence beneath the Faeroes ranges in thickness between about 0.5 and 2 kilometres. The thickest parts of the hidden sequence perhaps includes about 1 kilometre of sediments at the base. The sediments are presumably mainly volcanogenic. A much larger thickness of Mesozoic sediments possibly occurs beneath the plateau in the center of a sharp, negative gravity anomaly on the northwestern shelf.

2.4.   Post-basaltic geology of the Faeroe Block

2.4.1.   The eastern sedimentary shelf

Morphology.   The outer eastern shelf consists of sediments.
The inner margin of the eastern sedimentary shelf is partly
delineated by two troughs which separate Sandoy and Suduroy Banks
from the inner, basaltic shelf. Further south the sediments
border on the Suduroy Ridge, while in the northern part of the
eastern shelf the limit between basalts and sediments possibly
coincides with a shallow north-south running depression in the
shelf.

The inner part of the above two troughs runs parallel to the
basaltic shelf, and the stepped sea floor characteristic of the
basaltic shelf continues in some places eastwards, close to the
floor of this part of the troughs (Figs. 8a and b). The inner
part of the troughs may be classified as marginal troughs which
are characteristic of glaciated shelves and often follow a
stratigraphic boundary (Holtedahl 1970). Both troughs bend more
or less sharply to the southeast and continue as transverse
troughs across the sedimentary shelf. The northern trough exceeds
350 metres in depth between Sandoy Bank and the inner shelf, and
the southern trough exceeds 300 metres in depth between Suduroy
Bank and the inner shelf. The transverse part of the troughs
shallows to the southeast. The northern trough terminates inside
the shelf edge which here occurs at a depth of about 230 metres.

Stratigraphy. A cross section through the eastern sedimentary shelf
and the sediment trough of the Faeroe-Shetland Channel has been
made by Korsakov (1974) from a seismic reflection profile (Fig. 9a).
Korsakov (1974) suggests that the deepest reflector beneath the
Faeroe shelf and the northeastern side of the Faeroe-Shetland
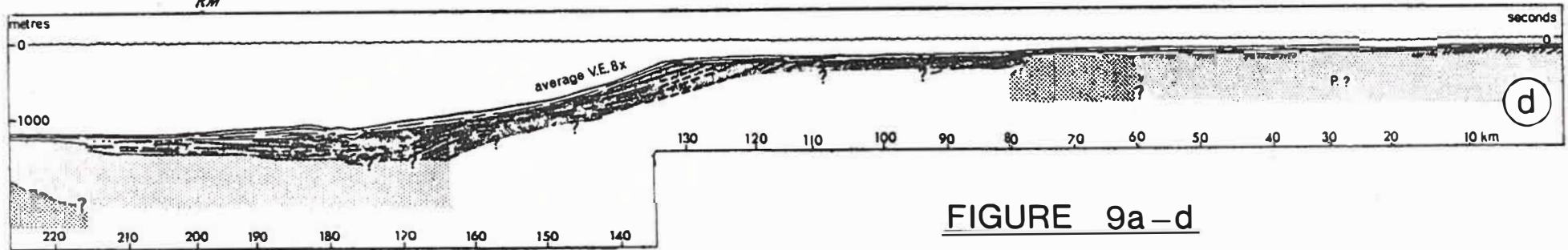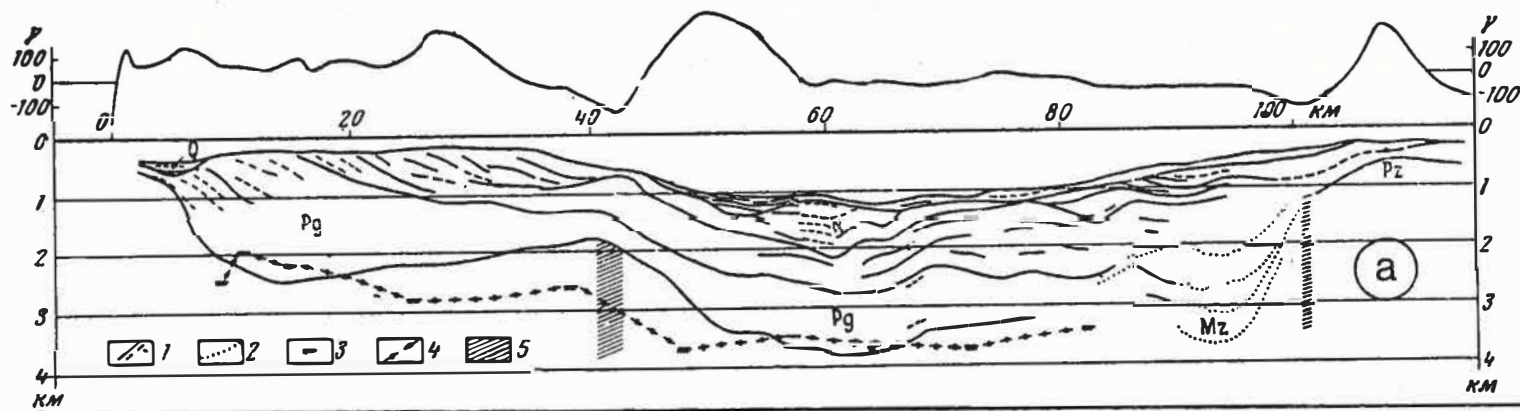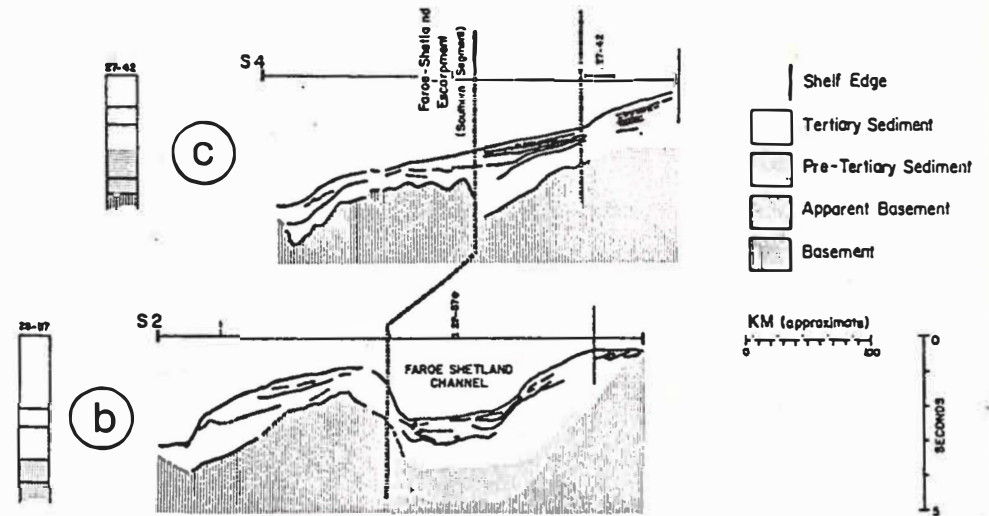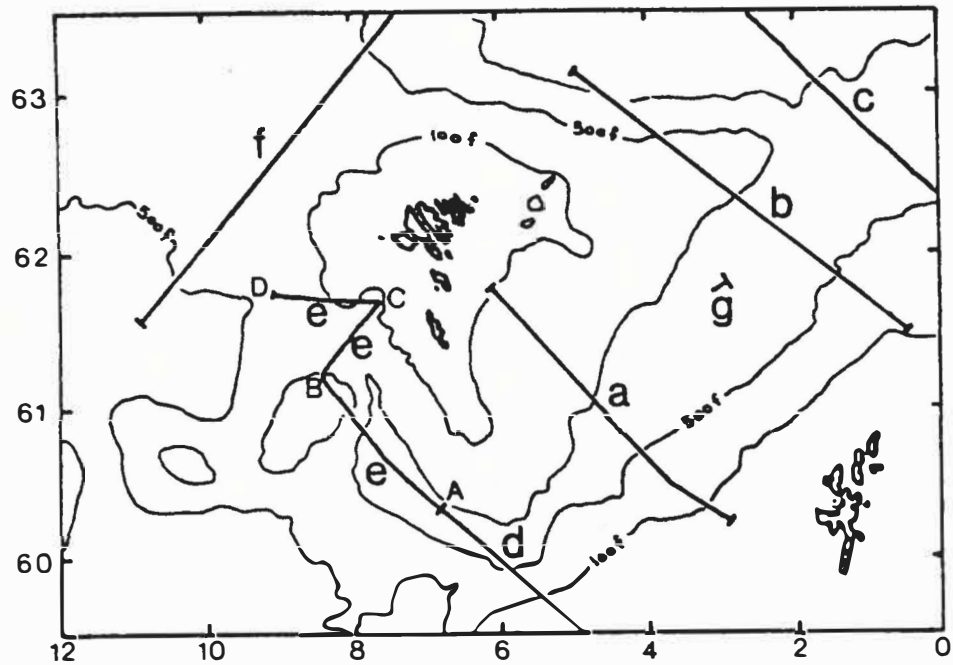
FIGURE 9a–d
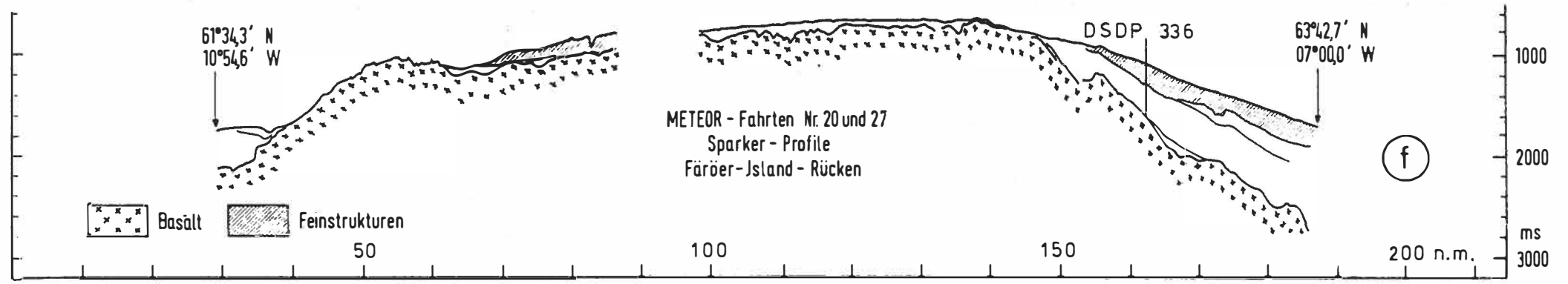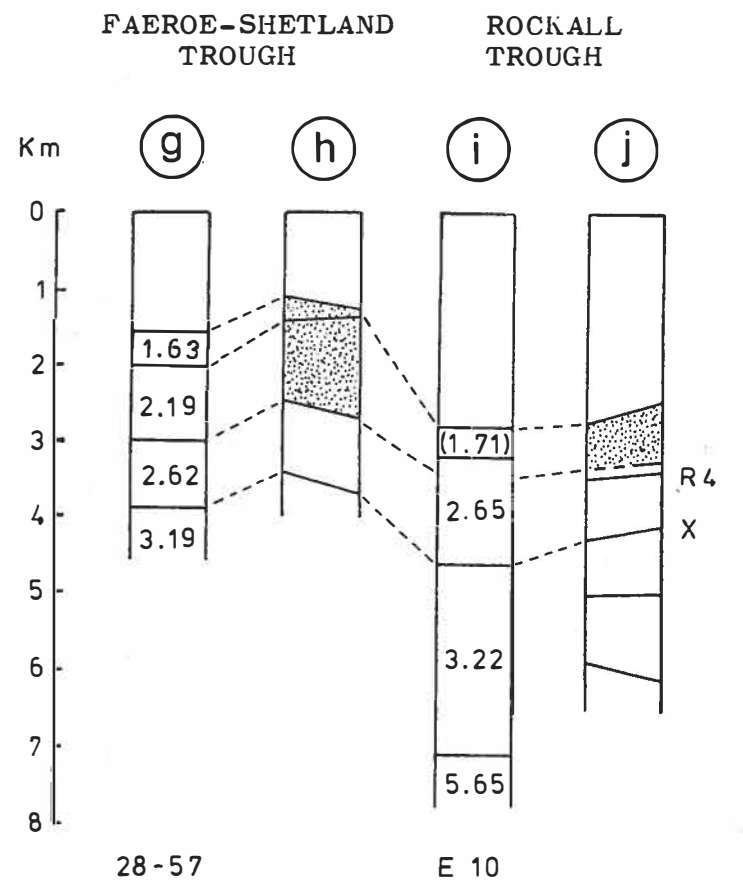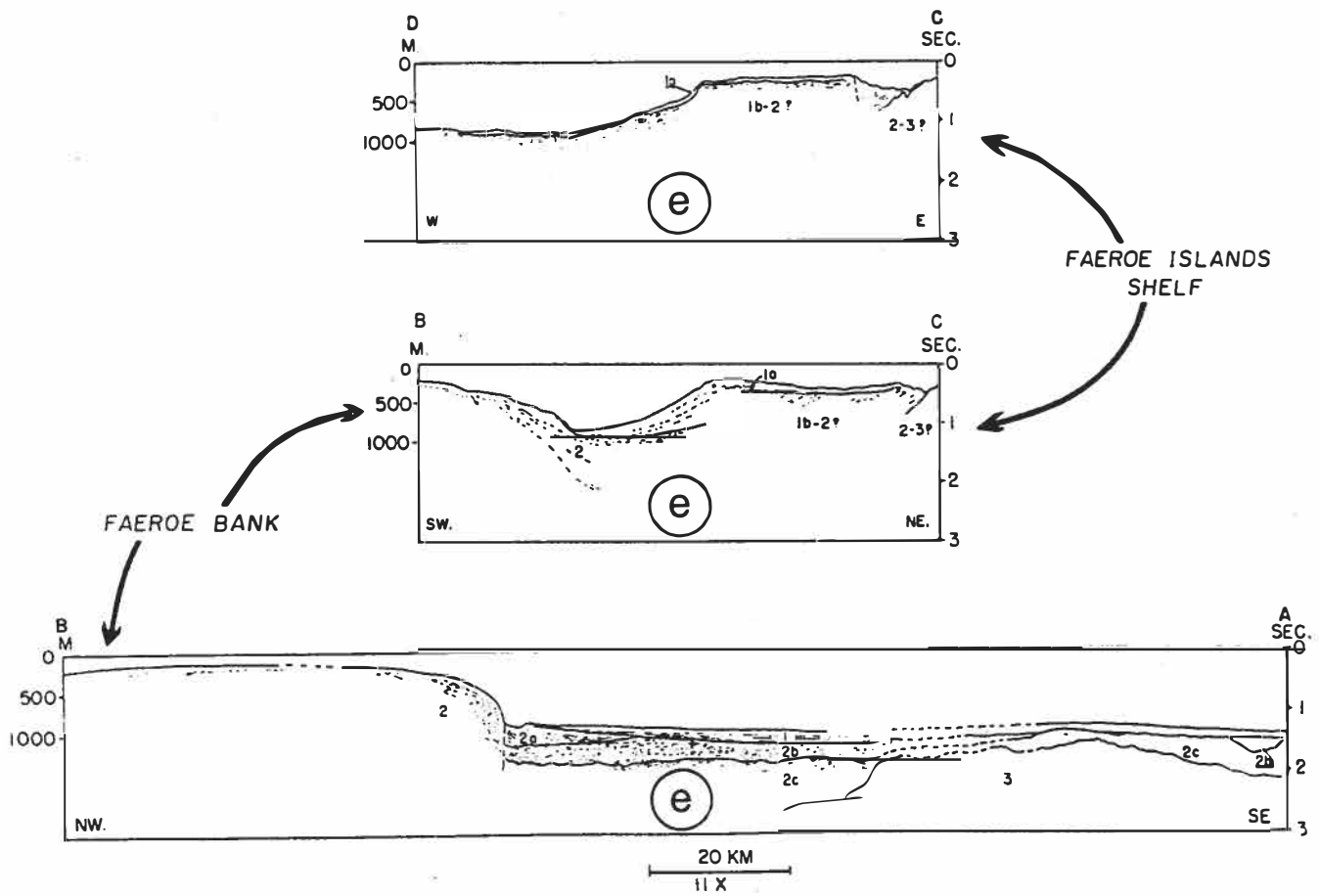
FIGURE 9e-j.

FIGURE 9. Seismic reflection and refraction profiles showing the structure of the sediment basins in and around the Faeroe Block (taken from the literature). An index map is shown besides the profiles. The stratigraphic assignations used in the original papers are indicated. The present authors interpretations appear in the text.

a. Cross section through the East Faeroe Shelf Basin and the Faeroe-Shetland Trough. 1) Seismic reflectors; 2) hypothetical geological boundaries; 3) calculated upper limit of the magnetic basement; 4) boundary based on 3); Pz = Paleozoic; Mz = Mesozoic; Pg = Paleogene; N = Neogene; Q = Quaternary. (Note that the horizontal scale is about 2.1 times larger than indicated. (From Korsakov 1974).

b-c. Line drawings of seismic reflection profiles across the northeastern end of the Faeroe-Shetland Trough inside and outside the entrance to the Faeroe-Shetland Channel. Control from nearby seismic refraction profiles (left) is indicated. Vertical scale is given in seconds of two way travel time. A primary wave velocity of 2.50 km/s is used to distinguish between Cenozoic (blank) and Mesozoic (dots) sediments. Thicker patterned lines indicate structural lineaments. (From Talwani and Eldholm 1972).

d. Line drawing of a seismic reflection profile across the southwest end of the Faeroe-Shetland Trough and the Shetland--Hebridean shelf. Vertical scale is given in seconds of two way travel time and also in metres at a velocity of sound in sea water. Blank = Quaternary; gray = Tertiary; light dots = Mesozoic or Paleozoic (P); heavy dots = basement. (From Stride and others 1969).

e. Line drawings of seismic reflection profiles in the vicinity of the Faeroe Bank Channel. Unconformities and major contacts are emphasized by heavy solid or dashed lines. All other lines are traced from selected reflecting layers as they are actually shown on the original records. Tentative correlations between the profiles are shown by number and letter symbols (3 is basement). Vertical scale as in Fig. 9d. (From Stride and others 1967).

f. Line drawing of a seismic reflection profile across the Iceland-Faeroe Ridge about 40 kilometres northwest of the Faeroe shelf. Vertical scale in milliseconds; horizontal scale in nautical miles (1.854 kilometres). Crosses = basalt; ruled = fine structures. (From Fleischer and others 1974).

g-j. Vertical profiles through the Faeroe-Shetland Trough and the Rockall Trough. Profiles g and i are unreversed seismic refraction profiles from Talwani and Eldholm (1972) and Ewing and Ewing (1959). Profile h and j show the depth to the main horizons in nearby reflection profiles. Left and right sides of profile h are lines through the uppermost northwestern channel filling and the middle of the Faeroe-Shetland Trough in Fig. 9a, respectively. Left and right sides of profile j are lines through the deepest part of the Rockall Trough in Fig. 30 and 32 of Roberts (1975 a), respectively; the travel times are converted into depths using the interval velocities and depths in Fig. 9i. Differentially deposited sediments are dotted.

Trough consists of basalts or metamorphic Precambrian rocks since the reflections are very strong and lie at a depth corresponding reasonably well to that estimated for the magnetic basement. The profile passes southeastwards across the northern trough and the northernmost Suduroy Bank close to a gravity minimum which is supposed to mark the center of a sedimentary basin (Bott and Watts 1971). The 1.5 and 2 kilometre contours of the basin, henceforth called the East Faeroe Shelf Basin, are tentatively shown on Fig. 5 based on the above seismic profile and the free air anomaly contours in Bott and Watts (1971).

The oldest series of sediments in the East Faeroe Shelf Basin is exposed near the inner margin. The sediments occur beneath a distinct reflector which can be traced into the Faeroe-Shetland Trough (Fig. 9a). The oldest beds dip to the southeast near the inner margin of the shelf basin and thicken down dip. The series of old sediments thins above a basement high below the slope towards the Faeroe-Shetland Channel and then merges into a thick lower series of sediments in the Faeroe-Shetland Trough.

An intermediate series of irregularly bedded sediments occurs above the distinct reflector in the East Faeroe Shelf Basin and the Faeroe-Shetland Trough. The intermediate series is thin on the shelf. The beds dip to the southeast and thin down dip. Near the edge further southeast the series increases slowly in thickness again and it attains a maximum thickness in the southeastern side of the Faeroe-Shetland Trough.

A late series of sediments occurs above an unconformity at a depth of about 600 metres in the outer half of the sedimentary shelf. The beds dip to the southeast and seem to have been built out into deep water. It can be seen that each successive younger bed spreads somewhat further southeast. The uppermost beds con-

tinue over a threshold into the Faeroe-Shetland Trough.

The latest series of sediments partly fills the troughs on the shelf and forms a continuous top layer in the Faeroe-Shetland Trough. On the shelf the sediments exceed 200 metres in thickness in the trough north of Suduroy Bank (Fig. 9a). The troughs on the shelf appear to be glacially overdeepened which strongly suggests a Quaternary age for the sediment fillings.

A seismic reflection profile tracing by Himsworth (1973) shows the layering beneath the southeastern slope of the Faeroe shelf just east of the Suduroy Ridge. The profile which trends about ENE shows that the sediments near the ridge have an easterly dip. About 20 kilometres from the ridge some younger sediments occur above an unconformity. The younger sediments are apparently flat-lying, but probably dip towards the Faeroe-Shetland Channel at a right angle to the profile. The unconformity is supposed to be the same one observed below the young sediments built out towards the Faeroe-Shetland Channel further northeast (Fig. 9a). Both unconformities are shown on the map in Fig. 5.

Talwani and Eldholm (1972) have published a seismic reflection profile tracing which runs in the direction northwest-southeast across the northeastern slope of the Faeroe shelf and the Faeroe-Shetland Trough (Fig. 5 and 9b). The sediments in the corner of the Faeroe shelf have an order of thickness of one kilometre. The basement suddenly disappears towards the Faeroe-Shetland Trough and the northwestern side of the trough is supposed to be fault bounded. The basement escarpment is termed the Faeroe-Shetland Escarpment (Talwani and Eldholm 1972).

2.4.2. The West Suduroy Shelf Basin

Another sedimentary shelf area occurs in a small embayment in the western border of the basalt plateau off Suduroy and will here be called the West Suduroy Shelf Basin (Fig. 5). The basin is bounded landwards by a marginal trough. The northwestern and southeastern boundaries of the basin are not known exactly.

The marginal trough is more than 350 metres deep at the northern end. The eastern side of the trough consists of basalts (Figs. 7a and 9e, leg B-C). The marginal trough is connected with two wide transverse troughs which seem to shallow outwards. The high ground between the troughs forms a curved bank with the long axis in the direction northeast-southwest.

The structure of the West Suduroy Shelf Basin is known from a combined seismic reflection, magnetic and gravity profile (Stride and others 1967, Bott and Stacey 1967). One leg of the profile runs southwest-northeast from Faeroe Bank over the Faeroe Bank Channel and the middle of the shelf basin to the basaltic shelf (Fig. 9e, B-C). The profile then turns west passing over the northern part of the shelf basin (Fig. 9e, C-D).

The gravity and magnetic data suggest that the shelf basin is deepest close to the inner margin which may be fault bounded and that the basin is separated by a low threshold from another depression delineated by the Faeroe Bank Channel. Assuming a density contrast of 0.4 g/cm^3 between sediments and basement the shelf basin is about one kilometre deep (Bott and Stacey 1967). The basement near the inner margin of the basin is strongly magnetic suggesting that it consists of basic igneous rocks.

The oldest beds in the basin apparently occur at the inner margin where they dip to the southwest (Fig. 9e, B-C). They are overlain by successively younger beds towards the southwest with

a similar dip. The youngest beds in the succession form the slope of the Faeroe Bank Channel and rest unconformably on some older sediments in the channel. The top of the older sediments forms a strong reflector in the middle of the channel but the reflector weakens to the northeast and disappears below the shelf edge where the slope sediments exceed 500 metres in thickness. The present author tentatively correlates the reflector in the channel with one of the inclined bedding planes in the middle of the shelf basin which lie nearly on continuation of the slightly upwardly concave reflector. If this extrapolation is correct the older sediments on the shelf are probably of the same age as the sediments on the northeastern slope of Faeroe Bank and the sediments below the strong reflector in the Faeroe Bank Channel.

The youngest sediments on the shelf rest unconformably on the inclined beds and have a thickness of roughly 100 metres. The present marginal trough postdates these sediments (Fig. 9e, C-D) which are supposed, at least partly, to be Quaternary (Stride and others 1967).

2.4.3. Discussion of the post-basaltic geology

Basement-sediment contact. The oldest shelf sediments are found at the margin of the sediments areas (Figs. 9a and 9e, B-C) adjacent to the youngest parts of the basalt plateau (section 2.2.4.). The shelf sediments are therefore probably all younger than the basalt flows. The basalt beds seem to increase in dip close to the sediment areas (Figs. 7a and 8b) so that they approximate the dip of the basin margin. This suggests that they continue for some distance under the sediments. The oldest sediments are likewise approximately parallel to the basin margin and may therefore only slightly post-date the basalts. This suggestion is supported by the discovery of erratics of tuff-carbonate sediments inside the sedimentary shelf areas (section 3.5.)

Dome and basin formation. The basin formation must have started early since the oldest series of sediments forms a major part of the shelf basins. The doming of the basalt plateau began before the end of intrusive activity on the Faeroe (section 2.1.7.) which also suggests an early date for the doming. The dome and basin formations were therefore probably more or less synchronous.

Erosion. The oldest series of sediments in the East Faeroe Shelf Basin thickens towards the center of the basin and then thins quickly towards the threshold beneath the slope of the shelf (Fig. 9a). A substantial part of the oldest series therefore probably consists of clastic sediments derived from the Faeroe Plateau, the erosion of which was probably initiated or accelerated by the process of doming.

Peneplanation. The thin, intermediate series in the middle of the East Faeroe Shelf Basin which corresponds to a much thicker series in the Faeroe-Shetland Trough (Fig. 9a) gives evidence for a strongly diminished supply of sediments from the Faeroe Plateau.

This could be a consequence of either subsidence or peneplanation of the plateau. There is no other evidence of subsidence, whereas the second explanation finds some support in the morphology of the Faeroes. The altitude of the highest mountain peaks on the islands is fairly constant inside smaller areas and shows a smooth regional variation unrelated to stratigraphy. The highest peaks occur in the northern fringe of the Faeroes where 15 peaks inside a 10 kilometres wide belt are between 751 and 882 metres high. The peak height decreases slowly to the south to the central island Sandoy where the eight highest peaks are 351-479 metres high. On Suduroy 13 peaks are between 459 and 610 metres high. A smoothed surface through the highest peaks on the Faeroes (a so-called gipfelflur) is supposed to define the approximate position of an old, deformed peneplain. The corresponding mature stage of erosion is tentatively correlated with the thin, intermediate series in the East Faeroe Shelf Basin.

Uplift and renewed peneplanation. The young beds which have been build out into deep water both southeast and southwest of the Faeroes indicate a strongly increased supply of clastic sediments from the Faeroe Plateau. This new cycle of sedimentation is tentatively correlated with the uplift of the old peneplain towards its present position.

The net uplift of the old peneplain in relation to the present sea level averages about 600-700 metres on the Faeroes. The uplift seems only to have been 400-500 metres in the central part of the islands but about twice that amount in the northernmost part of the islands. The basement ridge beneath the southeastern slope of the Faeroe shelf seems to have been uplifted about 300 metres relative to the East Faeroe Shelf Basin since the deposition of the intermediate shelf series (Fig. 9a).

The new cycle of erosion and deposition initiated by the uplift has now progressed nearly to a conclusion. The emerged part of the plateau after the uplift is estimated to be of about the same size as the area inside the 200 metres depth contour around the Faeroes or about 24,000 square kilometres. Now only 1,400 square kilometres or 6 per cent of this area is above sea level.

The erosion west and north of the islands has mainly been due to wave action to judge from the high sea cliffs which face open water in these directions.

Glaciation and sea level changes. The system of troughs associated with the sedimentary shelf are apparently glacially over-deepened which means that they were at least partly formed by glacial erosion during the Pleistocene. The troughs on the eastern shelf have been filled with sediments of supposed glacial origin, while the trough along the inner margin of the West Suduroy Shelf Basin cuts through a cover of sediments probably at least in part Pleistocene in age (Figs. 9a and 9e, B-C).

During the last glacial epoch the Faeroe Islands were covered by an ice-sheet up to an altitude of about 500 metres (Geikie 1880). The ice-sheet reached the shelf edge southeast and probably also southwest of the islands to judge from dredged erratics (Waagstein and Rasmussen 1975 and section 3.4.1.). It probably also reached the shelf edge north and west of the islands; this shelf edge lies at a shorter distance from land than the southeastern shelf edge. The ice-sheet may not have covered the southern end of the Suduroy Ridge, however, as the ridge would tend to divert the flow of ice.

The sea level during the last glacial epoch seems to have been at least 180 metres lower than now as supposed beach gravels have been dredged from about this depth on the Suduroy Ridge and are only slightly weathered (section 3.4.3.). A Flandrian beach

conglomerate has been dredged from the same depth on the Rockall Bank (Roberts and others 1972). Isostatic movements due to the weight of ice thus seem to have been negligible, which suggests that the ice-sheet on the shelf was not much thicker than the present water depth. The thickness of the ice-sheet on the open shelf was probably mainly a function of the distance to the edge of the sheet, and as the last ice-sheet seems to have covered most of the shelf, it is also unlikely that the ice-sheet of any of the preceeding glacial epochs were voluminous enough to cause isostatic movements.

2.5.   The Faeroe-Shetland and Faeroe Bank Channel system

2.5.1. Topography and present environment

Bathymetry. The Faeroe-Shetland Channel runs northeast-south-
west between the Faeroe shelf and the shelf west of the Shetland
Isles shallowing southwestwards from about 1700 to 1000 metres.
At the southern end of the Suduroy Ridge it is linked to the
Faeroe Bank Channel which runs southeast-northwest between the
Faeroe shelf and the rise to the southwest formed by the Wyville-
Thomson Ridge and Faeroe Bank (Fig. 1a). The Faeroe Bank Channel
(or south-western Faeroe Channel, cf. Harvey 1965) has a sill
depth of about 830 metres in the narrow part between Faeroe Bank
and the Faeroe shelf (Harvey 1965) but is about 900 to 1200 metres
deep between the Wyville-Thomson Ridge and the Suduroy Ridge.
The sill depth of the Wyville-Thomson Ridge is 644 metres (Ellett
and Roberts 1973).

Norwegian Sea overflow. Warm, saline Atlantic surface water
flows northwestwards into the Norwegian Sea, mainly between the
Faeroes and Scotland. Here the water cools and sinks to ultimate-
ly overflow back between Greenland, Iceland, the Faeroes and Scot-
land into the North Atlantic (see e.g. Worthington 1970). The
overflowing water approximates the temperature and salinity of the
large homogeneous mass of Norwegian Sea Deep Water and has gener-
ally been considered to have been derived from this body of water.
It appears, however, on basis of analyses of tritium (released
during the atmospheric nuclear bomb tests in the early 1960's),
that the formation and exchange of deep water in the Greenland
and Norwegian seas are essentially isolated from the formation
of the dense overflow waters (Peterson and Rooth 1976). This
suggests that the overflow waters are formed above the permanent

pycnocline of the Norwegian Sea.

The overflow through the Faeroe Bank Channel is probably continuous and has a magnitude of 10^6 m^3/sec. The overflows over the other shallower sills are probably intermittent, but are of a similar magnitude. The dense overflow waters entering the Atlantic are converted into Northeast Atlantic deep water by entrainment with the overlying Atlantic water. The circulation of the Northeast Atlantic deep water is to a large extent controlled by the basin morphology and the Coriolis force (which diverts a flow to the right in the northern hemisphere).

The strong bottom flow debouching from the Faeroe Bank Channel runs westwards along the southern flank of the Iceland-Faeroe Ridge and adjoins the overflow from this ridge. The deep flow continues southwestwards along the flank of the Reykjanes Ridge to about 53° N. Here it curves to the west through the gap formed by the Charlie-Gibbs Fracture Zone and then to the north along the other flank of the Reykjanes Ridge in response to the Coriolis force. The flow is deflected to the southwest again by the sill between Iceland and Greenland and continues along the continental slope of southeast Greenland where it meets the overflow from the Denmark Strait.

An intermittent overflow from the Faeroe-Shetland Channel spills over the Wyville-Thomson Ridge into the Rockall Trough (Ellett and Roberts 1973). The bottom flow in the Rockall Trough runs southwestwards in the western side of the trough and curves around the southern corner of the Rockall Plateau.

The dense overflowing waters carry sediments in suspension and are the sources of some important sediment drifts in the Northeast Atlantic basins, e.g. the Gardar Ridge on the southeastern flank of the Reykjanes Ridge, the Eirik Ridge at the southern tip of Greenland and the Feni Ridge along the western side of the Rockall

Trough (Johnson and Schneider 1969, Jones and others 1970).

The deeper part of the Rockall Plateau is swept by a subsurface flow of Labrador Sea water involved in the deposition of drift sediments in the Rockall-Hatton Basin and along the western side of Hatton Bank (Roberts 1975 a).

Channel topography and present bottom current regime. Too little information exists about the deep currents in the Faeroe-Shetland and Faeroe Bank Channels to assess their influence on the sedimentary processes taking place here. It is possible however to have some idea about the processes from the bottom topography.

The topographical details given below are extracted from bathymetric maps issued by the National Institute of Oceanography (Fig. 1a) and Institute Scientifique et Tecnique des Peches Maritimes, maps published by Harvey (1965), Talwani and Eldholm (1972), Ellett and Roberts (1973), Flinn (1973), bathymetric profiles from Harvey (1965) and Berthois (1969), and seismic reflection profiles from Stride and others (1967, 1969), Talwani and Eldholm (1972), Himsworth (1973) and Korsakov (1974).

Near the northeastern entrance of the Faeroe-Shetland Channel the channel floor is about 70 kilometres wide and reaches a depth of about 1600 metres close to the Faeroe slope. The floor is inclined about 0.2° to the northwest and exhibits shallow marginal channels along the slopes of the channel bounded inwards by shallow ridges (Fig. 9b). The smooth ridge and channel topography adjoining the slopes of the channel is characteristic of a flow-conditioned differential deposition regime as observed for example in the Rockall-Hatton Basin (Roberts 1975a). It is not known if this topography is continuous in the northern part of the channel.

The Faeroe-Shetland Channel becomes nearly symmetrical in cross section in the middle segment. From about $3^{\circ}30'$ to $3^{\circ}45'W$ the

central part of the channel floor shallows from about 1300 to 1100 metres forming a broad arch in cross section suggestive of a sediment drift. In a bathymetric profile by Berthois (1969) the crest of the arch is about 12 kilometres wide and delineates two smooth marginal channels, about 30 kilometres wide, extending to a depth of 100-130 metres below the central arch. Over the next 25 kilometres to the southwest the median ridge and southeastern channel roughly retain their form, whereas the northwestern channel shallows. The channel floor narrows farther southwestwards and a median channel takes the position of the median ridge (Fig. 9a).

Near $5^O15'$ W the channel is only about 15 kilometres wide at 1000 metres depth. According to a profile by Berthois (1969) the middle of the channel floor consists of a 4 kilometre wide flat-topped ridge at 1000 metres depth separating two marginal channels with maximum depths of 1100-1120 metres. The angular shape of the ridge suggests that it is of erosional origin. The ridge soon disappears and southeast and south of the southern end of the Suduroy Ridge the smooth channel floor is inclined about $0.5-0.8^O$ towards the foot of the Suduroy Ridge to a maximum depth of 1150-1250 metres. The closed deep at the foot of the Suduroy Ridge may be due to non-deposition or slight erosion, but the major part of the channnel floor to the southeast and south is subject to differential deposition as evidenced by the sparker profile in Fig. 9d across the Shetland-Hebridean shelf and the southern end of the Faeroe-Shetland Channel by Stride and others (1969). The profile exhibits a depositional ridge, about 60 metres high, which delineates a roughly 10 kilometre wide double marginal channel along the foot of the Shetland-Hebridean slope. The sediment drift thins gradually northwestwards but the uppermost thin beds on the channel floor seem to continue to the northwestern end of

the profile at about 60°20' N and 6°50' W at the easternmost end of the Faeroe Bank Channel. In the narrow passage between the two channels, the channel floor is about 18 kilometres wide and exhibits a shallow ridge about 6 kilometres from the foot of the Wyville-Thomson Ridge suggesting a thickening of the sediment drift in this place.

Near 6°40' W, at the entrance to the Faeroe Bank Channel, the channel floor widens to about 27 kilometres and the inclination of the floor shifts from north to south. The ridge and associated marginal channel at the foot of the Wyville-Thomson Ridge disappear and a new ridge and channel appear instead at the foot of the Suduroy Ridge (cf. profiles 12/71 and 15/71 in Himsworth 1973). This suggests that the area of maximum deposition shifts from south to north when approaching the leeward side of the Suduroy Ridge. Farther to the west the channel floor becomes slightly irregular and seismic profile 17+21 by Himsworth (1973) shows that the sediments in the channel are strongly eroded, though the resolution of the profile is too coarse to show if a thin surface layer is present.

West of about longitude 7° W the floor of the Faeroe Bank channel shallows from about 1100 to 1000 metres and begins to widen towards the north. The channel floor becomes smooth, horizontal and conformable with the sub-bottom reflectors (profile 30/70 in Himsworth 1973; Fig. 9e, profile section A-B).

These changes take place approximately off the lowest point on the crest of the Wyville-Thomson Ridge. Here the Norwegian Sea water probably intermittently spills over into the basin between the Wyville-Thomson Ridge and the Ymir Ridge (Fig. 1a). The saline, cold water is probably diverted westwards via a marginal channel along the southwestern side of the Wyville-Thomson Ridge to drop down through the narrow passage between the Ymir Ridge

and Faeroe Bank onto the floor of the Rockall Trough, while mixing with the water above. The marginal channel is interpreted by Ellett and Roberts (1973) as a non-depositional channel bounded to the southwest by a depositional ridge, but a seismic reflection profile by Himsworth (1973) shows that the channel and associated ridge are of erosional origin. The upper part of the channel is about 7 kilometres wide and 75 metres deep. The smooth walls and floor of the narrow deep between the Ymir Ridge and Faeroe Bank are strongly reflective to the signals of the echo sounder and may consist of rock outcrops (Ellett and Roberts 1973), although three dredge hauls at about 600-1000 metres depth on the northern wall, conducted by the present author, only revealed colonial corals. The deep debouches into the Feni sediment drift which has no clear topographical expression in the northernmost part of the Rockall Trough.

The Faeroe Bank Channel narrows towards the northwest between Faeroe Bank and the Faeroe shelf and the smooth channel floor acquires a small inclination to the southwest. The topography of this part of the channel has been studied in several bathymetric profiles by Harvey (1965). He found a sill depth of about 830 metres near $8^{\circ}06'$ W. The channel is narrowest 5-20 kilometres farther to the northwest. At this place the channel is about 30 kilometres wide in cross section at a depth of 200 metres. The channel floor is about 6 kilometres wide and inclined nearly 0.4° to the southwest to a depth of about 850 metres.

The eastern corner of Faeroe Bank is very steep with slopes of up to 12° or more at 600-900 metres depth. A small erosional channel occurs here at the foot of the bank. The erosional channel is seen in leg A-B of the seismic reflection profile in Fig.9e taken from Stride and others (1967). It has also been inferred by Harvey (1965) from bathymetry some kilometres farther to the

north, but seems to be restricted to the steep eastern corner of the bank. The northeastern slope of Faeroe Bank has an inclination of about 3° and is slightly irregular in some places. The reflection profile section B-C in Fig. 9e across the narrowest part of the channel seems to show that the northeastern slope of the bank has also been eroded. The floor and northeastern side of the channel is very smooth and shows no indications of either erosion or deposition of sediments by deep sea currents. However, Harvey (1965) found a difference of up to 30 metres between the maximum depth determined by him and those obtained from a 20 years older survey for the middle section of the narrow channel and this might reflect the growth of a sediment drift at this place.

Immediately to the northwest of the Faeroe Bank Channel the sea bed becomes irregular (Fig. 1a) and profile section C-D in Fig. 9e just inside the entrance reveals a top layer of variable thickness which suggests that it has formed by differential deposition.

A neutrally buoyant float experiment by Crease (1965) gave a current speed of 109 cm/s at 760 metres depth in the northwestern end of the channel well above the threshold velocity of sand movements (Inman 1963), but also demonstrated a rapid decrease of the current speed to 26 cm/s 20 kilometres farther to the west.

Bottom sediments. The floor of the channels has not been sampled yet. Berthois and Du Buit (1971) have investigated two tube samples from about 500 and 600 metres depth on the northwestern side of the Faeroe-Shetland Channel. 33 and 78 percent of the samples are finer than 0.08 millimetre and rich in calcite but poor in clay minerals. This suggests that they are calcareous oozes. Tube samples taken during the present work show a fairly regularly decrease in grain size down the southeastern Faeroe slope, and most samples from about 600 metres depth have been

classified macroscopically as muds (Table 1). The mud layer is too thin at this depth to completely cover the ice-rafted erratics deposited during the last glacial epoch and probably moves a little from time to time to judge the surface appearance of the erratics.

It is reasonable to suppose that the recent sediments on the channel floor are also mostly very fine-grained and therefore easily moved by currents. It is noticeable that submarine canyons are absent on both sides of the channels and the supply of terri-geneous sands must therefore be small, except possibly in places where glacio-marine deposits are being eroded in the channels.

2.5.2. Sediment distribution

The Faeroe-Shetland Channel and Faeroe Bank Channel form two separate sediment basins which will here be called the Faeroe-Shetland Trough and the Faeroe Bank Channel Basin. The forms of the basins are shown in Fig. 5. The isopachytes are based on the line drawings of seismic reflection profiles by Stride and others (1967, 1969), Talwani and Eldholm (1972) and Himsworth (1973) and an iso-pachyte map contoured by Korsakov (1974). A uniform velocity of 2 km/s has been used to convert the two-way travel times of the seismic reflection records into sediment thicknesses. Compared to the interval velocities of an unreversed seismic refraction profile in the Faeroe-Shetland Channel (Talwani and Eldholm 1972), a constant velocity of 2 km/s gives only from 0.1 kilometre too high to 0.2 kilometre too low depths down to a depth of 2.3 kilo-metres. The map by Korsakov (1974) is based on five seismic reflection profiles across the channels. He only indicates the position of one of these profiles (Fig. 9a) and does not state how travel times have been converted into thicknesses.

According to Korsakov the lowermost reflector in the Faeroe-Shetland Trough is in contact with the basement reflector beneath the Faeroe shelf, but gradually disappears eastwards, and has no counterpart beneath the Shetland-Hebridean slope. The reflector forms an anticline in the middle of the channel which is clearly observed in the southern half of the channel (Fig. 9a), whereas the reflector is only clearly observed close to the Faeroe slope in the northern end of the channel. Korsakov has tentatively drawn isopachytes also in the eastern side of the trough, but in Fig. 5 they have here been replaced by the dot signature used by Watts (1971) for the areas of major sediment thicknesses on the Shetland-Hebridean shelf.

The acoustic basement in the Faeroe-Shetland Trough approximately coincides with the magnetic basement according to calculations made by Korsakov (Fig. 9a) and Himsworth (1973, p. 63). Himsworth has used a magnetic profile along the axis of the trough to estimate the depth of the magnetic basement at about $61^O20'$ N and 4° W using the power spectral analysis method. He obtained a basement depth of 3.5 kilometres equivalent to a sediment thickness of about 2.3 kilometres in this place which lies just inside the 2.5 kilometre isopachyte of Korsakov. The deepest reflector mapped by Korsakov in the Faeroe-Shetland Trough is therefore probably in most places either true basement or a sedimentary horizon just above the crystalline basement.

The Faeroe-Shetland Trough has a sediment thickness of 2-3 kilometres in the middle. The trough is bounded to the northwest by the Faeroe-Shetland Escarpment beneath the Faeroe slope (Talwani and Eldholm (1972) and to the southeast by a buried basement ridge along the edge of the Shetland-Hebridean shelf (Watts 1971). The trough and the Faeroe-Shetland Escarpment continue as buried structures beneath the North Sea slope northeast of the entrance of the Faeroe-Shetland Channel. Near $62^O45'$ N the buried escarpment is about 1.1 kilometres high and the total sediment thickness just east of the escarpment is about 2.0 kilometres (Fig. 9c), but both structures have disappeared at 63° N (Talwani and Eldholm 1972). In the southwestern end, the Faeroe-Shetland Trough is separated from the Rockall Trough by the Wyville-Thomson Ridge and from the Faeroe Bank Channel Basin by a buried basement threshold which occurs at the eastern end of the Faeroe Bank Channel near 7° W. The reflection profile section A-B in Fig. 9e by Stride and others (1967) between the southeastern end of the Faeroe Bank Channel and Faeroe Bank shows a minimum sediment thickness above the threshold

of about 300 metres. A reflection profile by Himsworth (1973) at
a right angle to the above one shows that the threshold rises
southwestwards and nearly reaches the channel floor in a small
area along the foot of the Wyville-Thomson Ridge at about 1100
metres depth. The map by Korsakov (1974) indicates a large area
devoid of sediments above the middle of the threshold, and this
area has been reduced in Fig. 5 to a small area south and immedi-
ately east of the two above reflection profiles.

The Faeroe Bank Channel Basin between the Faeroe shelf, the
Wyville-Thomson Ridge and Faeroe Bank contains some 2 kilometres
of sediments. The acoustic basement has been observed continous-
ly or nearly so across the deep part of the basin between the
Suduroy Ridge and the Wyville-Thomson Ridge by Himsworth (1973)
and Korsakov (1974) and there is little doubt that it is a true
basement reflection. Between Faeroe Bank and
the Faeroe shelf the lowermost weak reflector about one kilometre
beneath the floor of the channel is possibly a basement reflection
as it seems to be continuous with the highly magnetic basement of
Faeroe Bank (Fig. 9e, B-C).

2.5.3. <u>Stratigraphy</u>

<u>The Faeroe-Shetland Trough.</u> The cross section through the Faeroe-Shetland Trough in Fig. 9a made by Korsakov (1974) from a seismic reflection profile shows that the sediments above the acoustic basement in the trough form two contrasted series separated by a basin wide reflector. The lower series is acoustically transparent and about one kilometre thick in the middle of the trough. The top of the lower series is conformable with the slightly deformed acoustic basement. The upper series is irregularly bedded and about 1.5 kilometres thick in the middle of the trough. The bedding planes are mostly impersistent and exhibit internal unconformities. They are also unconformable with the top of the lower series and the present sea bed. Numerous cut-offs are seen near the top of the upper series. Since the upper series rests on a relatively undeformed surface, it is unlikely that the unconformities are due to deformation and subaerial erosion as Korsakov (1974) seems to suggest. The unconformities rather result from differential deposition and erosion by underwater currents.

The upper, bedded series in Fig. 9a indicates an ever-changing current regime. The lowermost 200-300 metres seems to be essentially concordant with the top of the lower, transparent series. Subsequently, a sediment ridge was built-up in the southeastern side of the trough, and a wide marginal channel at the same time evolved in the northwestern side due to non-deposition. The bedding on the other side of the ridge is unknown since seismic penetration is poor in this part of the trough. During the following period, deposition was rather uniform in the trough. The ridge and channel morphology was retained, but the channel axis migrated to the northwest while becomming more accentuated.

Thereafter, the marginal channel was gradually silted up in its new position, perhaps due to an increased sediment supply from the Faeroe shelf resulting from a new period of uplift and erosion of the Faeroe Block (section 2.4.3.) Later, a new, smaller channel was created about 15 kilometres farther to the northwest by erosion. A similar channel in the southeastern side of the trough probably originates from the same stage of erosion. The channels were silted up again, basin wide erosion then took place, and finally a 100-200 metres thick top layer was deposited on the floor and the southwestern slope of the trough.

A reflection profile by Talwani and Eldholm (1972) about 185 kilometres farther to the northeast in the Faeroe-Shetland Channel shows that similar sedimentary processes occurred here (Fig.9b). Marginal channels are clearly seen extending downwards from the sea bed on both sides of the trough, though the scale of the line drawing is too small to allow any detailed correlations with Korsakov's profile. The lowermost reflector lies at a depth of about 0.75 kilometres below the sea bed and is possibly an internal bedding plane in the upper series.

Northeast of the entrance of the channel, in a profile by Talwani and Eldholm (1972) crossing the northeastern end of the Faeroe-Shetland Trough, the upper bedded series and the acoustically transparent lower series attain a maximum thickness of about one kilometre each, and the upper series only exhibits minor unconformities (Fig 9c).

In the profile by Stride and others (1969) across the southeastern end of the Faeroe-Shetland Trough it is not quite clear if the upper series has been fully penetrated beneath the southeastern slope, but if so, the maximum thickness is here about 0.75 kilometre (Fig. 9d). The upper series apparently thins northwestwards to a

trifling thickness above the threshold separating the Faeroe-Shetland Trough from the Faeroe Bank Channel Basin.

A profile by Stride and others (1967) lying on the continuation of the above one shows that the sediments above the threshold consist of an upper 100-150 metres thick unit resting unconformably on two older units (Fig. 9e, A-B). A profile by Himsworth (1973, profile 17+21) cutting the channel and the above profile at a right angle near the crestal line of the threshold shows only a few impersistent reflectors and indicates that the older beds are parallel with the sloping basement. The beds do not thin upwards but are truncated by the present sea bed. The younger sediments in the middle of the channel lack visible bedding and are probably equivalent to the upper unit in the former profile. Stride and others (1967) correlate this unit across a data gap? in their profile with the uppermost sediments in the Faeroe Bank Channel Basin which they consider, at least partly, to be Quaternary in age. The present author would rather suggest that all sediments above the threshold predate the upper, bedded series in the Faeroe-Shetland Trough since this series in Fig. 9d apparently wedges out towards the threshold and the sediments above the threshold appear relatively transparent.

The Faeroe Bank Channel Basin. A distinct reflector occurs about 0.5 kilometres beneath the sea bed in the Faeroe Bank Channel Basin. The overlying sediments are irregularly bedded and exhibit internal unconformities (Fig. 9e, A-B). They no doubt belong to the upper, current deposited series in the channels. The underlying horizon is taken as the base of the upper series because it is a good reflector and because most of the underlying sequence appears acoustically transparent.

Himsworth (1973) shows a seismic reflection profile between

the Suduroy Ridge and the Wyville-Thomson Ridge across the south-
eastern part of the basin, a profile across the southeastern mar-
gin of the basin, close to Faeroe Bank, and two profiles across
the southeastern flank of Faeroe Bank. The first three profiles
yielded nearly continuous basement reflections but showed a poor
resolution for the sediments, while the last profile showed very
little penetration. The only internal reflector traceable across
the basin in the first profile lies at the same depth as the re-
flector in the crossing profile A-B by Stride and others (1967)
used above to define the base of the upper series, and must be
the same one. Himsworth (1973) suggests that it may be equivalent
to reflector R in the Northeast Atlantic basins (Jones and others
1970) without discussing this. The beds of the lower series are
exposed in a 5-10 kilometres wide belt along the Wyville-Thomson
Ridge. They thicken down dip and appear on this side of the basin
to be conformably overlain by the upper series beds. The south-
eastern flank of Faeroe Bank consists of 300-400 metres of sedi-
ments forming regular beds which thicken slightly down dip, being
conformable with the basement and the slope but eroded at the top
of the bank. All, or the major part, of these sediments probably
also belong to the lower series. At the basin margin along the
Suduroy Ridge the oldest sediments are approximately conformable
to the basement and possibly belong to the lower series, but they
are here overlapped above a slight unconformity by upper series
sediments which seem to be conformable to the sea bed.

The slope sediments on the northeastern side of Faeroe Bank
consist of slightly irregular beds which thicken down dip and ap-
pear to have been eroded after their deposition (Fig. 9e, B-C).
These sediments probably belong to the lower series. They are
unconformably overlain beneath the channel floor by sediments of

the Faeroe slope. The latter sediments form a conformable sequence of fore-set beds and show that the sediments of the adjoining West Suduroy Shelf Basin (see section 2.4.2.) were built out into the Faeroe Bank Channel. Each successive bed spreads somewhat further to the southwest on the channel floor, and there is thus no true bottom-set sequence. This suggests that the depth and width of the narrow channel were kept roughly constant by concurrent erosion of the southwestern side of the channel by bottom currents. This impression gains support from the steepness of the lower part of the southwestern slope and from the presence of an erosional channel at the foot of the eastern corner of Faeroe Bank (Fig. 9e, A-B).

The deposition of the slope sediments above the unconformity in the narrow part of the Faeroe Bank Channel is supposed to have begun simultaneously with the deposition of slope sediments above an unconformity at a similar depth in the outer part of the East Faeroe Shelf Basin, the deposition in both places being greatly enhanced by renewed uplift and erosion of the Faeroe Block (section 2.4.3). The latter unconformity can be followed into the Faeroe-Shetland Trough as an internal bedding plane in the upper series, 0.5-1.2 kilometres above the lower series (Fig. 9a). Hence, if the above correlations are correct, the unconformity in the narrow part of the Faeroe Bank Channel probably spans half or more of the time elapsed after the formation of the lower series. Since the top of the lower series does not appear to be eroded beneath the unconformity, the bottom current in this part of the Faeroe Bank Channel was probably strong enough during this long period to prevent deposition, but too weak to cause appreciable erosion.

The same unconformity is probably shown on the east-west profile C-D in Fig. 9e which terminates just inside the north-

western entrance of the Faeroe Bank Channel. The unconformity is
rather poorly revealed because the younger sediments are thin and
the traverse is apparently along the strike of the underlying
strata (Stride and others 1967). The top of the supposed lower
series beneath the unconformity is irregular and may have been
scoured by bottom currents. The layer above consists probably
mainly of glacial sediments redistributed by bottom currents be-
cause it only averages about 50 metres in thickness and exhibits
an undulating surface.

According to Fig. 9e, assuming two-way travel times of 1.48 km/s
in water and 1.60 km/s in the uppermost sediments, the top of the
lower series attains a maximum depth of about 930 metres below sea
level both near the entrance of the channel and about 60 kilometres
further to the souteast. The channel is about 840 metres deep at
the northwestern entrance according to a bathymetric map by
Fleischer and others (1974), while Harvey (1965) obtained a maxi-
mum depth of about 920 metres in the northwesternmost profile
made by him about 25 kilometres to the southeast of the entrance.
This may suggest that the lower series is partly exposed also on
the floor of the channel.

Strong bottom currents also prevail northwest of the channel
as evidenced by the large basement exposure on the southern flank
of the Iceland-Faeroe Ridge in Fig 9f.

Summary. The sediments in the Faeroe-Shetland Trough and the
Faeroe Bank Channel Basin form two series separated by a more or
less distinct unconformity. The upper series has an irregular
bedding indicating differential deposition by bottom currents and
varies widely in thickness. The lower series exhibits few bedding
planes in the middle of the basins and is approximately conformable
with the underlying basement.

The upper series is about 0.75-1.5 kilometres thick along the

axis of the Faeroe-Shetland Trough and about 0.5 kilometre thick
in the middle of the Faeroe Bank Channel Basin but less than about
0.2 kilometres thick or missing beneath the axis of the narrow
channel sections between the southern end of the Suduroy Ridge and
the Wyville-Thomson Ridge and between the Faeroe Shelf and Faeroe
Bank.

The lower series attains a thickness of between about 0.5 and
1.5 kilometres in the channel way. The maximum thickness is recor-
ded in the middle of the Faeroe Bank Channel Basin and the minimum
thickness is recorded between the southern end of the Suduroy Ridge
and the Wyville-Thomson Ridge. The lower series is exposed or
nearly so in the latter place and also in a belt along the north-
eastern side of the Wyville-Thomson Ridge and the southeastern
and northeastern sides of Faeroe Bank.

The lower series also includes the old series of sediments
partly exposed along the inner margin of the sediment basins in
the Faeroe Shelf.

2.5.4. <u>The age of the sediments in the channels</u>

<u>The onset of vigorous overflow of Norwegian Sea water.</u> The pre-
dominance of differential deposition in the upper series indicates
a strong bottom current regime undoubtedly caused by the exchange
of water between the Atlantic and the Norwegian Sea through the
channels. Wheather the owerflow of Norwegian Sea water began or
became more vigorous at the onset of differential deposition in
the upper series, either event would probably have a marked influ-
ence on the bottom current regime in the Northeast Atlantic. This
event should therefore also be detectable in the sedimentological
record to the south and west of the channels.

An important marker horizon (R), west of the Rockall Plateau
and in the Rockall Trough (Jones and others 1970, Ruddiman 1972,
Himsworth 1973), has been shown from intersecting reflection profiles
to be identical with reflector 4 in the intervening Rockall-Hatton
Basin (Roberts and others 1970), and has been renamed R4 (Roberts
1975a). R4 marks a period of downwarping coupled with an important
change in the sedimentary regime, and defines a major unconformity
at the basin margins. R4 is overlain by a series of strong, imper-
sistent reflectors identifiable with beds of cherts in the Deep
Sea Drilling Project (DSDP) holes 116 and 117 in the Rockall-Hat-
ton Basin. This strongly reflecting sequence is between about
0.1 and 0.4 kilometres thick in the middle of the basins in and
around the Rockall Plateau, but pinches out at the basin margins.
The weaker reflectors above the cherts are in many places irregular,
discontinuous and unconformable, and are reminiscent of a ridge
and channel sea bed morphology characteristic of a differential
depositional regime. The ridges and channels have changed their
form and position in time but differential deposition has prevai-
led inside the same areas on and around the Rockall Plateau since

the formation of the chert sequence.

R4 has been interpreted as an intra-Oligocene unconformity by Laughton, Berggren and others (1972), whereas Roberts (1975a) suggests that R4 lies at the base of the Oligocene and has an age of about 37 milion years in accordance with the results of Ruddiman (1972). The chert sequence is essentially Oligocene in age and represents a period of reduced sedimentation. According to Roberts (1975a), the onset of differential deposition roughly dates back to the beginning of Miocene time about 23 million years ago. He suggests from the stability of the sediment drifts and their relationship with the regional bottom flow that the present day circulation in the Northeast Atlantic is essentially post-Oligocene in age. There is a thickening of the pre-R4 sequence between the Rockall Plateau and the Reykjanes Ridge which may indicate an earlier phase of differential deposition initiated about 45 million years ago (Ruddiman 1972).

Vogt (1972) links the Miocene increase of bottom currents noted in the western North Atlantic to the submergeance of a postulated land bridge from Greenland, via Iceland and the Faeroes, to Scotland as a result of thermal contraction of the cooling lithosphere. Vogt suggests that differential deposition may have begun south of Iceland in late Eocene in response to the formation of the first open water between Greenland and the Faeroes. He suggests that the Miocene increase in current activity reflects the point at which sill depths were great enough ot admit subsurface water from the Norwegian Sea. Vogt imagines that the aseismic ridges west and east of Iceland were kept at a shallow level due to the deposition of shelf sediments up to that point, but that the initial overflow of Norwegian Sea deep water reinforced itself quickly by generating erosional channels which were cut deeper and

deeper into the sediments.

The Faeroe Bank Channel has a sill depth which is about 350 metres greater than the sill depth of the Iceland-Faeroe Ridge. Vogt (1972) suggests that this channel has also been deepened abruptly by current erosion, though there is no evidence of this as discussed earlier.

Roberts (1975a) suggests instead that the early Miocene overflow came through the Faeroe Bank, Faeroe-Shetland Channel system and that the overflow across the Iceland-Faeroe Ridge began in late Miocene resulting in a more vigorous circulation, perhaps indicated by some major changes in the position of the crests and marginal channels of some of the sediment drifts. In support of this the sill depth of the Iceland-Faeroe Ridge was less than 150 metres 10 million years ago according to computations by Vogt (1972) based on the assumption that the ridge during the last 10 million years has subsided at the normal rate of oceanic lithosphere of a similar age. It is thus not necessary to invoke a lower thermal subsidence rate than normal for the ridge, as done by Vogt (1972).

According to the preliminary report of DSDP Leg 38 by the shipboard party (Talwani and others 1975), basaltic basement was drilled at site 336 on the northeastern flank of the Iceland-Faeroe Ridge about 80 kilometres from the Faeroe Shelf, and is covered by rubble probably derived from the basalt by subaerial erosion. Nearly 300 metres of marine middle Eocene to late middle Oligocene sediments follow above and are in turn overlain by 168 metres of Plio-Pleistocene glacial sediments. At site 352 on the southwestern flank of the Iceland-Faroe Ridge and about 55 kilometres from the Icelandic shelf, late middle Oligocene sediments were recovered beneath a cover of glacial sediments. Unlike north of the ridge, the microfauna and microflora of the Oligocene sediments south of

the ridge are rich and typical North Atlantic. The nature of the
sediments is also quite different. This suggests that there was
still no direct connection across the Iceland-Faeroe Ridge in
late middle Oligocene time (Talwani and others 1975).

Fleischer and others (1974) have published line drawings of
four sparker profiles across the Iceland-Faeroe Ridge. The south-
easternmost profile bypasses the DSDP site 336 on the northeastern
flank of the ridge/a distance of about 5 kilometres. The uppermost,
fine bedded layer in this profile undoubtly correlates with the
glacial sediments in hole 336 (Fig. 9f). The glacial sediments
rest unconformably on the Tertiary sequence beneath. The top of
this sequence is somewhat irregular probably due to erosion by
bottom currents and consists of progressively younger sediments
downslope. Hole 336 was drilled at a water depth af about 811
metres. Further downslope, at a water depth of about 920 metres,
a reflector subcrops beneath the glacial cover. This reflector
closely parallels the sloping basement,and the thickness of the
intervening sediments is roughly 100 metres larger than the thick-
ness of the sediments cored beneath the unconformity at site 336.
The marine Tertiary sediments at site 336 seem to have been de-
posited at a fairly constant rate, averaging about 14 m/mill.
years. By extrapolation, the above reflector is roughly 7 million
years younger than the late middle Oligocene sediments subcropping
at site 336 and therefore probably defines the Oligocene-Miocene
boundary or a horizon very close to it. Over the next 13 kilo-
metres to the northeast the supposed Miocene sequence grows to a
thickness of about 150 metres (0.15 s two-way travel time) and the
water depth increases to 1050 metres. The age of the uppermost
Miocene sediments is estimated to be 10-15 million years assuming
a similar sedimentation rate as for the Eocene-Oligocene sediments

further upslope. In the last 20 kilometres of the profile, down to a water depth of about 1300 metres, the boundary between the Miocene and glacial sediments is smooth and both sequences increase slightly in thickness downslope. The supposed hiatus in this place is therefore probably mainly due to non-deposition rather than erosion.

DSDP site 336 is situated off the two deepest passages across the Iceland-Faeroe Ridge with sill depths between 480 and 490 metres and the erosional unconformity is not observed farther to the northwest on the northeastern flank of the ridge. This suggests that the unconformity is due to erosion and non-deposition by upslope currents of water flowing across the deepest parts of the ridge into the East Reykjanes Basin, rather than by contour currents flowing along the northeastern ridge flank. The overflow of Norwegian Sea water across the Iceland-Faeroe Ridge therefore probably began or became vigorous at a date between 10 and 15 million years ago (about middle Miocene) and was probably restricted to the oldest and deepest parts of the ridge near the Faeroe shelf.

The glacial sediments which cover most of the ridge flanks indicate a strong decrease of the current activity coupled with an increased sediment supply. The overflow across the ridge probably decreased drastically during the glacial epochs since the oceanic circulation pattern was quite different from the present one during these epochs with little or no flow of Atlantic surface water into the Norwegian Sea (cf. Flinn 1971, Ruddiman and McIntyre 1973). The increased sedimentation rate undoubtedly reflects the greatly increased supply of terrigeneous sediments due to ice-rafting.

The lack of sediments on most of the ridge crest suggests that the overflow occurred intermittently over all sections of the ridge, at least during the short interglacial times, so that earlier deposited glacial sediments could be removed, except for the sparse glacial erratics.

Most of the above problems are no doubt dealt with in Vol. 38 of the Initial Reports of the Deep Sea Drilling Project which is still in the press (Oct. 1977). In the present context we only need to say that, contrary to the belief of Vogt (1972), the overflow across the Iceland-Faeroe Ridge probably became vigorous at too late a date to explain the early Miocene increase in the bottom current activity in the North Atlantic.

Montadert, Roberts and others (1976, 1977) using paleobathymetric data derived from micropaleontological criteria infer that the passive continental margins of the Northeast Atlantic have subsided thermally with a time constant similar to the 50 million year exponential time constant deduced for the oceanic crust. The thermal subsidence first begins at the date of actual plate separation and the rate of subsidence after the submergence seems to be independent of the initial altitude of the passive margin. This work was based on deep sea drillings in the southwestern corner of the Rockall Plateau and the northeastern side of the Bay of Biscay.

The northwesternmost part of the Faeroe Bank Channel may have subsided in a similar manner. The continental margin northwest of the Faeroes approximately coincides with the bathymetric scarp between the Faeroe shelf and the Iceland-Faeroe Ridge (Bott and others 1971 and 1976). The bathymetric map by Fleischer and others (1974) shows that the scarp forms a long straight line close to the 400 metre depth contour which may reflect the very

margin. The entrance to the Faeroe Bank Channel lies about 40 kilometres from the southwestern continuation of this line. This is probably a maximum estimate of the distance from the channel to oceanic crust, since the oceanic crust may well extend into the bight between the Faeroe Block and Bill Bailey Bank as it does between the Lousy Bank and Hatton Bank to the south (Feather-stone and others 1976).

The top of the lower series lies at a depth of about 930 metres below sea level beneath the northwesternmost part of the channel and does not appear to have been appreciably eroded (profiles B-C and C-D in Fig. 9e).

The paleobathymetric data obtained from DSDP sites 403 and 404 in the southwestern corner of the Rockall Plateau 60-70 kilometres from the oldest oceanic crust magnetic anomaly to the west (anomaly 24) fits a theoretical subsidence curve for 56 million years old oceanic crust (Montadert and others 1977). Using this curve, the top of the lower series lay at a depth of about 240 metres below sea level in the early Miocene 23 million years ago. This may have been the critical depth of continuous overflow of dense subsurface water from the Miocene Norwegian Sea.

According to Roberts (1975 a) the overflow across the Wyville-Thomson Ridge also began in the early Miocene, though the ridge has a sill depth lying between the sill depths of the Faeroe Bank Channel and the Iceland-Faeroe Ridge. The inferred lower subsidence rate for the Wyville-Thomson Ridge since Oligocene perhaps reflects the remoteness of this ridge from Tertiary oceanic crust.

The above considerations about subsidence rates support the hypothesis of Roberts (1975 a) that the early Miocene onset of differential deposition in the Northeast Atlantic was related to

the overflow of Norwegian Sea water through the Faeroe-Shetland
and Faeroe Bank Channels. The onset of differential deposition
in the Rockall-Hatton Basin was probably due to an influx of
Labrador Sea water at intermediate depths coming from the south-
west, and Roberts (1975 a) suggests that this flow was also re-
lated to the overflow of Norwegian Sea water. However, we cannot
exclude a purely climatic cause for the increased bottom current
activity in the Northeast Atlantic Basins in early Miocene
(Montadert and others 1976).

   The age of the upper series. The above indirect evidence points
to the earliest Miocene, about 23 million years ago, as the most
likely date of onset of differential deposition in the upper
series in the Faeroe-Shetland and Faeroe Bank Channels. If the
hypothesis of Robert (1975 a) is correct this date is probably
accurate to within a few million years. The final dating of the
sediments must await direct sampling. This sampling could be
done in part by taking cores of the sea bed since the older stata
are laid bare in many places due to erosion and non-deposition.
However, until such samples are made available we must rely on
the indirect dating and keep in mind that this dating could be
seriously in error and may invalidate some of the conclusions
below.

   The lower age of the upper series of about 23 million years
indicates an average post-Oligocene depositional rate of about
65 m/mill. years for the middle of the Faeroe-Shetland Trough.
Such a high rate is fairly typical of drift deposits. The sedi-
ment drifts in the Atlantic show exceptionally high sedimentation
rates during Plio-Pleistocene time due to ice-rafting and high
biogenic production rates. The uppermost channel fillings in
Fig. 9a are therefore probably glacial; this implies a thickness

variation from about 0 to 700 metres for the glacial layer in the
Faeroe-Shetland Channel. The reflector forming the base of the
outer prograding sequence in the East Faeroe Shelf Basin can be
traced in Fig. 9a into the Faeroe-Shetland Trough. Here it de-
scends to a depth of about one kilometre below the sea floor in
the northwestern marginal channel but rises again in the broad
median ridge and subcrops beneath a roughly 200 metres thick top
layer. The uplift of the Faeroe Block supposed to be associated
with the outer prograding sediments on the shelf is therefore
possibly Pliocene in age, and the thin intermediate series in the
East Faeroe Shelf Basin may span all the Miocene (see section
2.4.3).

The age of the lower series. A part of the cross section
through the Faeroe-Shetland Trough in Fig. 9a is reproduced
schematically in Fig. 9h. The left side of Fig. 9h represents
a line through the uppermost northwestern channel filling, the
right side represents a line through the deepest part of the
trough. Fig. 9g to the left of Fig. 9h shows the unreversed re-
fraction profile by Talwani and Eldholm (1972) from the north
central part of the trough. Talwani and Eldholm interpret the
1.6 km/s layer as glacial sediments, the 2.2 km/s layer as Terti-
ary sediments and the 2.6 and 3.2 km/s layers as Mesozoic sedi-
ments, the interpretations being based on the velocities them-
selves. The top layer is about 0.45 kilometre thick and may be
a channel filling. The base of the 2.2 km/s layer lies about
1.4 kilometres below the sea floor which is similar to the depth
of the distinct reflector further to the southwest in Fig. 9a
forming the base of the upper series. This suggests that the
2.2 km/s layer encompasses the Miocene and the major part of the
Pliocene.

The base of the 2.6 km/s layer lies about 2.3 kilometres below the sea bed which is similar to the depth of the basement reflector mapped by Korsakov (1974). The present author assumes that the lower series approximately coincides with the 2.6 km/s layer and reinterprets the age of the layer as lower Tertiary. The smooth acoustic basement of the Faeroe-Shetland Trough, the rather constant thickness of the lower series in the middle of the trough and the lack of internal acoustic horizons suggest that no major tectonic events or other changes of the environment took place during the deposition of the lower series. The lower series thus seems to postdate the volcanic activity and the major phase of doming on the Faeroes. As discussed later on (chapter 4) the doming is presumably related to the initiation of sea floor spreading close to the Paleocene/Eocene boundary. The lower series is roughly one kilometre thick and therefore probably covers in time nearly all the period between doming and the onset of differential deposition, i.e. Eocene and Oligocene.

A similar layering occurs in the Rockall Trough and adds some support to the indirect dating of the lower series. Fig. 9i shows refraction profile E 10 by Ewing and Ewing (1959) in the centre of the Rockall Trough. Fig. 9j shows the depths to the main horizons in the two nearest reflection profiles by Roberts (1975 a) south and north of E 10 (left and right side of Fig. 9j, respectively). The travel times were converted to depths by using the interval velocities and associated thicknesses of E 10. Roberts (1975 a) suggests that reflector X in the Rockall Trough dates back to the onset of sea floor spreading between the Rockall Plateau and East Greenland (which he assumes began in Paleocene about 60 million years ago). The sequence in the Rockall Trough between the base of the post-Oligocene Feni drift (dotted) and

reflector X is roughly one kilometre thick like the lower series in the Faeroe-Shetland Trough and appears to have a similar primary wave velocity of about 2.6 km/s. The strongly reflective Oligocene cherts are apparently missing north of the Wyville-Thomson Ridge while only a few reflections have been noted lower down at these two localities.

2.5.5. The deeper structure of the Faeroe-Shetland Trough

The acoustic basement. The seismic refraction profile by Talwani and Eldholm (1972) in the Faeroe-Shetland Trough is located near 61°48' N, 3°00' W. The 3.2 km/s refractor occurs at a depth of about 2.3 kilometres below the sea floor which is similar to the depth of the acoustic basement recorded by Korsakov (1974). The velocity of the 3.2 km/s layer is too low for crystalline rocks but is appropriate for semi-consolidated sediments. No distinct reflections have been recorded just above the acoustic basement to the southwest or northeast of the refraction profile and this suggests that the refractor forms a part of the acoustic basement. The strong basement reflection indicates a large increase in the acoustic impedance (= primary wave velocity x density) at the interface which could be due to a major change in the type of sediment. Considering the geological setting it is possible for example that the acoustic basement in some places forms the top of a sequence of turbidites of basaltic sand overlain by pelagic sediments. Pleistocene turbidites of basaltic sand have been drilled west of the Rockall Plateau and probably originate from the Icelandic shelf. The turbidites form hard sandstone beds which are highly reflective with primary wave velocities in the range of 2.3 to 3.8 km/s and are strongly magnetic (Laughton and others 1972, p. 370). If turbidites of basalt sand occur at the base of the lower series in the Faeroe-Shetland Trough, this might explain the smoothness of the acoustic basement and the disappearance of the basement reflection towards the southeastern side of the trough.

However, the present author believes that the crystalline basement in most places either corresponds to or lies at a fairly shallow depth beneath the acoustic basement recorded by Korsakov (1974).

The central ridge. According to Korsakov (1974) the acoustic basement forms an anticline plunging to the NNE near 4° W in the southern part of the trough. The basement reflection disappears to the southeast beneath the Shetland-Hebridean slope and Korsakov hypothesizes that Mesozoic sediments have accumulated to the southeast of this anticline or basement ridge (Fig. 9a).

The basement ridge is associated with a positive magnetic anomaly with an amplitude of about 50 nT in Fig. 9a. Korsakov (1974) indicates the position of the ridge diagrammatically on his isopachyte map. A linear magnetic high occurs in the same position on the aeromagnetic total intensity map by Avery and others (1968) and extends further in both directions. The direction of the magnetic anomaly changes from NNE to NE at roughly $61^O05'$ N, $3^O45'$ W and then again to about NNE at roughly $61^O20'$ N, $3^O10'$ W before the anomaly ends near $61^O40'$ N, 3° W in the middle of the channel. In the opposite direction the positive magnetic anomaly extends to the SSW beneath the lower part of the Shetland-Hebridean slope to a position of about $60^O35'$ N, $4^O15'$ W. It probably then bends to the SW along the slope but is absent on the next flight line near $60^O23'$ N. The magnetic anomaly has a total length of about 160 kilometres and increases in width from about 15 to 35 kilometres towards northeast. The amplitude varies between about 50 and 350 nT.

The basement ridge is also associated with a positive gravity anomaly. The largest gravity anomaly is observed beneath the lower part of the Shetland-Hebridean slope just SSW of the position of the ridge in Fig. 9a. The free-air anomaly shows a maximum of about +34 mgal above the lower slope as against minima of about +12 mgal above the upper slope and of about -15 mgal above the middle of the channel (see Fig. 37 in Himsworth 1973) The

free-air anomaly is affected by intra-crustal density differences, the water depth and the Moho depth. The Moho depth probably decreases towards the middle of the channel and partly offsets the decrease of the anomaly due to increasing water depth. The above gravity high shows a local maximum with an amplitude of about 15 mgal and a width of about 10 kilometres which is presumably, at least partly, caused by the basement relief, though the maximum may also reflect intra-basement density contrasts associated with the basement high. At the position of Fig. 9a the ridge is seen as a small gravity high on the Bouguer anomaly map by Watts (1971). The free-air gravity anomaly associated with the ridge decreases northeastwards as the water depth increases and is seen on the free-air gravity anomaly map of Bott and Watts (1971) as small deflections of the +10, 0 and -10 mgal contours. At about $61^{\circ}40'$ N, 3° W, where the magnetic anomaly stops, the ridge possibly changes direction again from NNE to NE and forms the edges of two gravity lows on either side of the middle of the channel. These lows occur between about 3° and 2° W and have amplitudes of 20-30 mgal according to the free-air gravity anomaly map by Talwani and Eldholm (1972).

The coincidence of the above magnetic and gravity anomaly ridges with the clear acoustic basement ridge near 4° W suggests that the central basement ridge extends over half or more of the length of the Faeroe-Shetland Trough.

The central ridge is parallel with the shelf edge ridge and the West Orkney-North Shetland Ridge to the southeast which are also associated with gravity and magnetic highs (Fig. 5). The West Orkney-North Shetland Ridge is partly exposed on the sea floor at the southwestern end. It probably consists of strongly magnetic, highly dense metamorphic rocks whick are most likely

Lewisian (Precambrian) granulites of Scourian type (Watts 1971).
This suggests that the ridge is separated from the Caledonian
metamorphic rocks on the Shetland Isles by the Moine Thrust which
runs along the northwestern side of Scotland. A major normal
fault separates the West Orkney-North Shetland Ridge from the
West Shetland Basin. The fault zone varies in strike between
about NE and NNE and extends to the continental slope north of
the Shetland Isles.

The shelf edge ridge on the northwestern side of the West
Shetland Basin shows similar trends. In the southern end it con-
sists of two or three parallel ridges and is presumably bounded
by a complex system of faults. The shelf edge ridge lies on the
continuation of North Rona and the Outer Hebrides to the south-
west which consist of Lewisian metamorphic rocks. Watt (1971)
also interprets this ridge as a Precambrian basement ridge.

The central ridge in the Faeroe-Shetland Trough is similar in
dimensions to the shelf edge ridge and the West Orkney-North
Shetland Ridge and allowing for its greater depth it has a simi-
lar magnetic and gravity imprint. Like the latter ridges it
plunges to the NE or NNE and forms an angle of about 20° with
the edge of the Shetland-Hebridean shelf. Due to the oblique
trend compared to the Faeroe-Shetland Channel and the similarity
to the other two ridges the present author suggests that the cen-
tral ridge is also a Precambrian metamorphic basement ridge.

The Mesozoic Shetland slope basin. A Mesozoic basin probably
occurs beneath the wedge of Tertiary sediments on the slope west
of the Shetland Isles. The basin is separated from the West
Shetland Basin by the shelf edge ridge. Several exploration
wells have been drilled on either flank of this ridge and large
thicknesses of Mesozoic sediments presumably occur on both sides

beneath a Tertiary cover (Whitbread 1975, Kent 1975).

The Shetland slope basin is associated with a residual gravity low with an amplitude of about 20-30 mgal (after the assumed regional field is removed) and also with a magnetic low (Watts 1971). Watts (1971) has interpreted a gravity profile about 50 kilometres northeast of the section in Fig. 9a. He assumes an inclined regional field parallel to the edges of the anomaly and a density contrast between sediments and basement of either -0.3 or -0.4 g/cm^3 and arrives at a maximum sediment thickness of 2.5 or 1.9 kilometres, respectively. However, to these figures should be added the sediment thickness above the upper and lower edges of the anomaly, i.e. above the shelf edge ridge and the central ridge. The former ridge lies about 2.1 kilometres below sea level according to an interpretation of a magnetic profile along the same line (Watts 1971) and the central ridge occurs 2-2.5 kilometres below the channel floor according to the iso-pachyte map by Korsakov (1974). Assuming a constant inclination of the regional gravity field between the ridges the sediment thickness beneath the slope is therefore rather 4-5 kilometres. An interpretation by Himsworth (1973) of a gravity profile just southwest of the section in Fig. 9a suggests only slightly smaller sediment thicknesses in this place when the 1.5-2 kilometres of sediments above the enclosing ridges are added. The basin possibly attains its largest thickness further to the northeast in a local gravity low between about 3° and 2° W associated with negative magnetic anomalies southeast of the supposed extention of the central ridge.

Other Mesozoic basins (?) A narrow gravity low also occurs along the Faeroe slope between about 3° and 2° W close to the Faeroe-Shetland Escarpment (Talwani and Eldholm 1972). The

free-air anomaly exceeds -30 mgal like south of the central
ridge. The isostatically corrected anomaly has an amplitude of
about 25 mgal and a width of about 50 kilometres (Fig. 5 in
Talwani and Eldholm 1972). Talwani and Eldholm suggest that
the gravity low is due to a large thickness of low-density Terti-
ary sediments. They indicate on their isopachyte map of Tertiary
sediments a thickness of about 2 kilometres in this gravity low
as against 1-1.5 kilometres in the remaining part of the trough.
However, the present author suggests that the reflections used
to construct this map differ in age. The acoustic basement in
the northernmost profile close to the above gravity minimum is
probably the base of the lower Tertiary lower series (Fig. 9c),
whereas the lowest reflections obtained by Talwani and Eldholm
further to the southwest come instead from a horizon above the
acoustically transparent lower series. The total thickness of
the Tertiary sediments in the gravity low is therefore probably
not much different from the thickness southwest of the gravity
low. This suggests that the gravity low at least in part may be
due to low-density Mesozoic sediments at a greater depth. The
gravity low is associated with a sharp linear magnetic low along
the Faeroe-Shetland Escarpment. This magnetic anomaly is proba-
bly partly an edge effect of the escarpment and can be traced
with varying but smaller amplitudes for most of the length of the
southeastern Faeroe slope.

2.5.6. The origin of the Faeroe-Shetland and Faeroe Bank Channels

Crustal thickness. The channels show a high background Bouguer anomaly in relation to the surrounding high areas probably due to crustal thinning. Bott and Watts (1971) have interpreted a gravity profile across the southern part of the Faeroe-Shetland Channel in terms of a decrease of the Moho depth from about 27 to 21 kilometres between the Orkneys and the middle of the channel. Himsworth (1973) estimates the Moho depth at 16 kilometres in the same place of the channel using a gravity profile with a more easterly trend. Himsworth bases all his gravity interpretations on a Moho depth of 25 kilometres beneath the Shetland-Hebridean shelf. The main reason for his lower estimate of the Moho depth in the channel is that he assumes a thickness of about 3 kilometres and a density of 2.1-2.25 g/cm^3 of the sediments in the channel whereas Bott and Watts (1971) assume a thickness of about 0.5 kilometres and a density of 2.53 g/cm^3. Himsworth (1973) in a similar way estimates the Moho depth at 15-18 kilometres in the southwestern end of the Faeroe-Shetland Channel and the southeastern end of the Faeroe Bank Channel. The crustal thinning in the Faeroe-Shetland Channel is confirmed by the results of the North Atlantic Seismic Project (Bott 1975 b).

Type of crusts. Talwani and Eldholm (1972, 1977) identify an escarpment beneath the North Sea slope, which separates shallow basement to the northwest from deep sediment-covered basement on the southeast side, with the continental boundary. They suggest that the escarpment is displaced to the northwest near the entrance of the Faeroe-Shetland Channel so that it forms the northwestern margin of the channel, and they call both segments the Faeroe-Shetland Escarpment. Talwani and Eldholm thus interpret the crust beneath the Faeroe-Shetland Channel as continental and

the crust beneath the Faeroes and the surrounding shelf as oceanic.

Himsworth (1973), on the other hand, suggests that not only the Faeroe-Shetland Channel but also the outer southeastern part of the Faeroe shelf, the Suduroy Ridge, the Wyville-Thomson, Ymir Ridges and the intervening part of the Faeroe Bank Channel like the Rockall Trough are underlain by Mesozoic oceanic crust. This interpretation is mainly based on the reduced Moho depths beneath the low-lying areas inferred from gravity measurements and on the fit between the northwest and southeast margins of the Rockall Trough.

Roberts (1975 a) has identified with some confidence the continental boundaries beneath the southern part of the Rockall Trough and the position of the boundaries suggests that the Mesozoic spreading axis extends northeastwards into the Faeroe-Shetland Trough.

According to Bott (1975 b) the crust beneath the Faeroe-Shetland Channel may be thinned, subsided continental crust, or it may be anomalous, thick oceanic crust produced during a Mesozoic episode of sea-floor spreading. He favours the latter hypothesis because of the strongly magnetic character of the basement beneath the sediments in the channel and the assumed plate geometry of the opening of the Rockall Trough, and he believes that the spreading axis continues northeastwards beneath the North Sea slope and the Vøring Plateau off Norway. Bott (1975 b) supposes that the Faeroe Bank Channel formed by either subsidence, erosion during Tertiary uplift or incipient sea-floor spreading.

Korsakov (1974) suggests that the basement in the Faeroe-Shetland Channel consists of Precambrian metamorphic rocks or one of the Faeroese basalt series.

The present author believes that both channels are underlain

by continental crust and has interpreted an oblique basement ridge in the Faeroe-Shetland Trough associated with positive magnetic and gravity anomalies as a Precambrian metamorphic ridge (section 2.5.5.)

The origin of the channels. The supposed Precambrian basement ridge is directly overlain by the so-called lower series of sediments which have been indirectly dated as lower Tertiary (section 2.5.4.) If the interpretation of the ridge and sediments is correct this implies that the Faeroe-Shetland Channel formed in the early Tertiary by subsidence of continental crust. The Faeroe Bank Channel probably formed at the same time since the same series of lower Tertiary sediments seems to overlie the basement in this area.

The present author hypothesizes that both channels formed by thinning and subsidence of the crust in connection with the early Tertiary continental break-up between Greenland and Europe.

2.6.   The Wyville-Thomson Rise, Faeroe Bank, Bill Bailey Bank
        and Lousy Bank

Topography.   A number of shoal areas which form the middle
section of the Faeroe Rise and the northern margin of the Rockall
Trough are considered to be a part of the Faeroe Plateau.   They
are (from east to west) the Wyville-Thomson Rise, Faeroe Bank,
Bill Bailey Bank and Lousy Bank.   The latter bank is separated
by a wide gap from Hatton and George Bligh Banks of the Rockall
Plateau (Fig. 1).

The Wyville-Thomson Rise consists of the Wyville-Thomson Ridge
proper and the Ymir Ridge (Ellett and Roberts 1973).   The Wyville-
Thomson Ridge trends WNW-ESE and connects the southern end of
Faeroe Bank to the Shetland-Hebridean shelf.   The crest of the
ridge comprises a row of knolls and depressions varying in depth
between about 384 and 644 metres (Ellett and Roberts 1973).   The
Ymir ridge lies just southwest of the Wyville-Thomson Ridge. The
northwest end of the Ymir ridge is separated from Faeroe Bank by
a narrow deep; the southeast end is attached to the Wyville-
Thomson Ridge (Fig. 1a).

Faeroe Bank is flat-topped with a minimum depth of about 87
metres.   The bank is roughly rectangular in shape with the long
axis in the direction SW-NE; inside the 200 metre depth contour
the length is about 87 kilometres and the width about 47 kilo-
metres.   The steep northeast and southwest flanks exhibit a clear
"shelf" break between 160 and 240 metres depth.

Bill Bailey Bank lies just west of the southern end of Faeroe
Bank; the sill depth between the two banks is about 517 metres
according to the bathymetric map of the Institut Scientifique et
Technique des Pêches Maritimes (Map sheet No. 19). Bill Bailey
Bank has a minimum depth of about 115 metres on the Decca map;

a minimum depth of 132 metres was observed near station 31 during dredging. Inside the 200 metre depth contour the bank measures about 43 kilometres in the direction WNW-ESE.

Lousy Bank lies WSW of Bill Bailey Bank and is separated from the latter by a 1200 metres deep channel. A minimum depth of 258 metres was recorded during dredging on Lousy Bank, and the smaller depths of 173-201 metres shown on the Decca map near stations 38 and 39 could not be confirmed.

<u>The continuation of the Faeroe basalt plateau to the southwest.</u> Bott and Stacey (1967) and Dobinson (1970) reported short-waved, high amplitude magnetic anomalies over Faeroe Bank and suggested that it consisted of basalt. Himsworth (1973) showed that the Wyville-Thomson Ridge was associated with strong magnetic anomalies which were mainly negative and he concluded that reversely magnetized basalts occurred on the ridge. He observed weaker magnetic anomalies over Bill Baily Bank than over Faeroe Bank. He attributed this difference to the absence of basalt on Bill Bailey Bank.

The present work shows that subaerial basalt lavas outcrop not only on Faeroe Bank, but also on Bill Bailey Bank and Lousy Bank. The basalts belong petrographically and geochemically to the Faeroe basalt plateau (Chapter 3). To date, only erratics have been recovered from the Wyville-Thomson Ridge (Murray and Philippi 1925, Berthois 1969).

<u>Areas of basalt outcrops.</u> The areas of outcropping and shallow basaltic basement are outlined in Fig. 5.

The supposed basaltic basement of the Wyville-Thomson Ridge is exposed on the ridge crest and partly also on the upper ridge flanks according to the seismic reflection profiles of Himsworth (1973) and the isopachyte map of Korsakov (1974). The lack of

sediments is probably due to the Norwegian Sea overflow. The Ymir Ridge is draped with sediments.

The dredge hauls on Faeroe Bank indicate frequent basalt out-crops. The outlined area shows where local basalt was recovered and/or the dredge clung to the bottom. The limit of the area is also based on the seismic reflection profiles by Stride and others (1967) (Fig. 9e) and Himsworth (1973) across the northeast and southeast margins of the bank, the magnetic anomaly profiles of Dobinson (1970) and the sea bed morphology.

On Bill Bailey Bank outcropping basement is seen on a seismic reflection profile by Himsworth (1973). Five out of the six shallowest dredge hauls (135-280 metres) recovered local basalt and indicate that outcrops of basalt are widespread at shallow depth although the sea bed is mostly smooth.

On Lousy Bank only two out of the five shallowest dredge hauls (283-355 metres) recovered local basalt. However, on the Decca map shells and stones are indicated on three sites and fine sand on only one site inside the 200 fathoom (365 metre) depth con-tour. Since the former signatures are usually associated with rocky sea bed, basalts may outcrop over much of the top of this bank also.

On all three banks the basalt outcrops are interspersed with shell sand to judge from tube samples taken during some of the dredge hauls and the alternating hard and soft movements of the dredge observed during many hauls.

Sea bed morphology and thickness of the basalt beds. According to Dobinson (1970) the southwestern half of Faeroe Bank is rug-ged with a relief of up to 30 metres, whereas the northeastern half is far more smooth. Since basalt outcrops are frequent in both areas the different aspects of the sea bed probably partly

reflect variations in the thickness of the basalt beds, as earlier inferred for the Faeroe shelf (section 2.2.3). Continuous echo sounder records were obtained during the later dredge cruises; the aspect of the sea bed on echo sounder records is also shown schematically on the bathymetric map of the Institut Scientifique et Technique des Pêches Maritimes. These observations suggest that the lava thickness is commonly 5-10 metres on the southern part of Faeroe Bank and may exceed 20 metres, but that it is generally much smaller on the northern part of the bank. A belt of thick flows possibly occurs along the southeastern margin of the outcrop area outlined in Fig. 5.

Similar observations on Bill Bailey Bank suggest that 5-10 metres thick flows are uncommon but that thin flows are very common like in the Middle Basalts on the Faeroes.

On Lousy Bank a gentle scarp, about 38 metres high, was recorded just below station 36 and may be the edge of a lava bed as local basalt was recovered on station 36 and on the near-by station 37. Most of the flows near the two stations are probably less than 10 metres thick, however.

Structure of the basalt plateau. Too few echo sounder records have been available to have an idea of the strike and inclination of the basalt beds which probably form some of the rugged sea floor on the banks. However, unpublished asdic records obtained along with the continuous reflection profile by Stride and others (1967) in the vicinity of the Faeroe Bank Channel showed low-relief outcrops up to 0.5 kilometre long with a definite arcuate structure concentric with the northeast edge of the bank (R.H. Belderson, personal communication to Dobinson (1970, II, p. 28)). This might suggest that the basalt plateau forms a dome on Faeroe Bank. Two escarpments can be traced for a distance of 40 kilo-

metres along the northwest edge of Faeroe Bank and are probably fault scarps (Dobinson 1970). The vertical distance between them is 25-35 metres and the scarps increase in depth from the northeast to the southwest from about 170 to 200 metres and from about 200 to 230 metres, respectively.

A NNW trending linear magnetic anomaly has been traced over a distance of 20 kilometres from the northwest edge to the middle of Faeroe Bank; here it is truncated by a NE trending anomaly. The former anomaly is positive, about one kilometre wide, with a maximum amplitude of 1200nT. This anomaly is probably caused by a normally magnetized basalt dyke, about 80 metres wide (Dobinson 1970). Less prominent short-waved anomalies mainly trend NE or N and may reflect the strike of dykes, faults or lavas.

Deeper structure of the banks and ridges. Gravity interpretations by Himsworth (1973) suggest that the Wyville-Thomson Rise, Faeroe Bank and Bill Bailey Bank are underlain by crust with a thickness of roughly 25 kilometres. Lousy Bank presumably has a similar crustal thickness though no gravity measurements are available from this bank. The present author believes that all the high-lying areas are underlain by continental crust, although opinions differ as to the origin of the crust beneath the Wyville-Thomson Ridge (cf. section 2.5.6).

The magnetic mapping of Faeroe Bank by Dobinson (1970) shows that the short-waved anomalies are superimposed on anomalies with a longer wave length which are probably of a more deep-seated origin. These first order anomalies mainly trend ENE-WSW. The largest one occurs near the southeast and northeast edges of the bank. It is about 30 kilometres long and 10 kilometres wide, positive, with an amplitude of about 1200 nT. Dobinson (1970) suggests that it may be caused by one or more basic plutonic

centres. Himsworth (1973) found a gravity low with an amplitude of about 15 mgal approximately beneath the magnetic high and suggests instead that a granitic intrusion occurs at a shallow depth. However, Bott (1974 b) prefers to attribute the anomalies to an underlying metamorphic basement.

Sediments. The sediments on the northeast and southeast margins of Faeroe Bank and the northeast margin of the Wyville-Thomson Ridge have been decribed in a previous section about the Faeroe Bank Channel Basin (section 2.5.3.) and are interpreted as lower Tertiary (section 2.5.4.).

According to Himsworth (1973) the sediments southwest of the Wyville-Thomson Ridge attain a maximum thickness of about 1.5 kilometres in the narrow trough between this ridge and the Ymir ridge. The sediments thin above the Ymir Ridge but thicken to 2-3 kilometres in the northernmost part of the Rockall Trough. Nearly one kilometre of sediments occurs on the southern margin of Bill Bailey Bank.

The reflection profiles by Himsworth indicate that the sediments of Bill Bailey Bank and the sediments on the southwestern flank of the Ymir Ridge pre-date reflector R4 in the Rockall Trough; R4 is Eocene-Oligocene in age according to Roberts (1975 a) (section 2.5.4). Himsworth tentatively identifies some cuspate reflections in the trough between the Wyville-Thomson Ridge and the Ymir Ridge as R4. The acoustically transparent series beneath has a maximum thickness of 0.5 kilometre or more, and Himsworth speculates that it may be partly pre-Tertiary. The transparent series apparently lies below the magnetic basement and therefore probably includes some kind of basaltic sediments of local provenance. The upper sediments between the two ridges appear to be differentially deposited; the top of the

sequence is eroded.

The pre-R4 sediments on Bill Bailey Bank are probably all Tertiary since they overlap the basalt plateau.

According to Roberts (1975 a) the deep basement sill between Lousy Bank and the northern end of the Rockall Plateau is only covered with a few hundred metres of lower Tertiary (pre-R4) sediments.

Summary. The Faeroe basalt plateau extends to the southwest across the Faeroe Bank Channel and forms the top of the Wyville-Thomson Ridge, Faeroe Bank, Bill Bailey Bank and Lousy Bank. Very limited evidence on Faeroe Bank suggests that the bank is formed by doming and faulting of the basalt plateau. The basalt beds are generally thinner on the northern part of Faeroe Bank and on Bill Bailey Bank than on the southern part of Faeroe Bank and probably on Lousy Bank. The banks and ridges are probably flanked by lower Tertiary sediments, although the occurrence of pre-Tertiary sediments on the southwestern side of the Wyville-Thomson Ridge cannot be ruled out. The present evidence is re-concilable with the hypothesis that all the high-lying areas are underlain by continental crust of normal thickness.

THE GEOLOGY OF
THE FAEROE PLATEAU

R. WAAGSTEIN
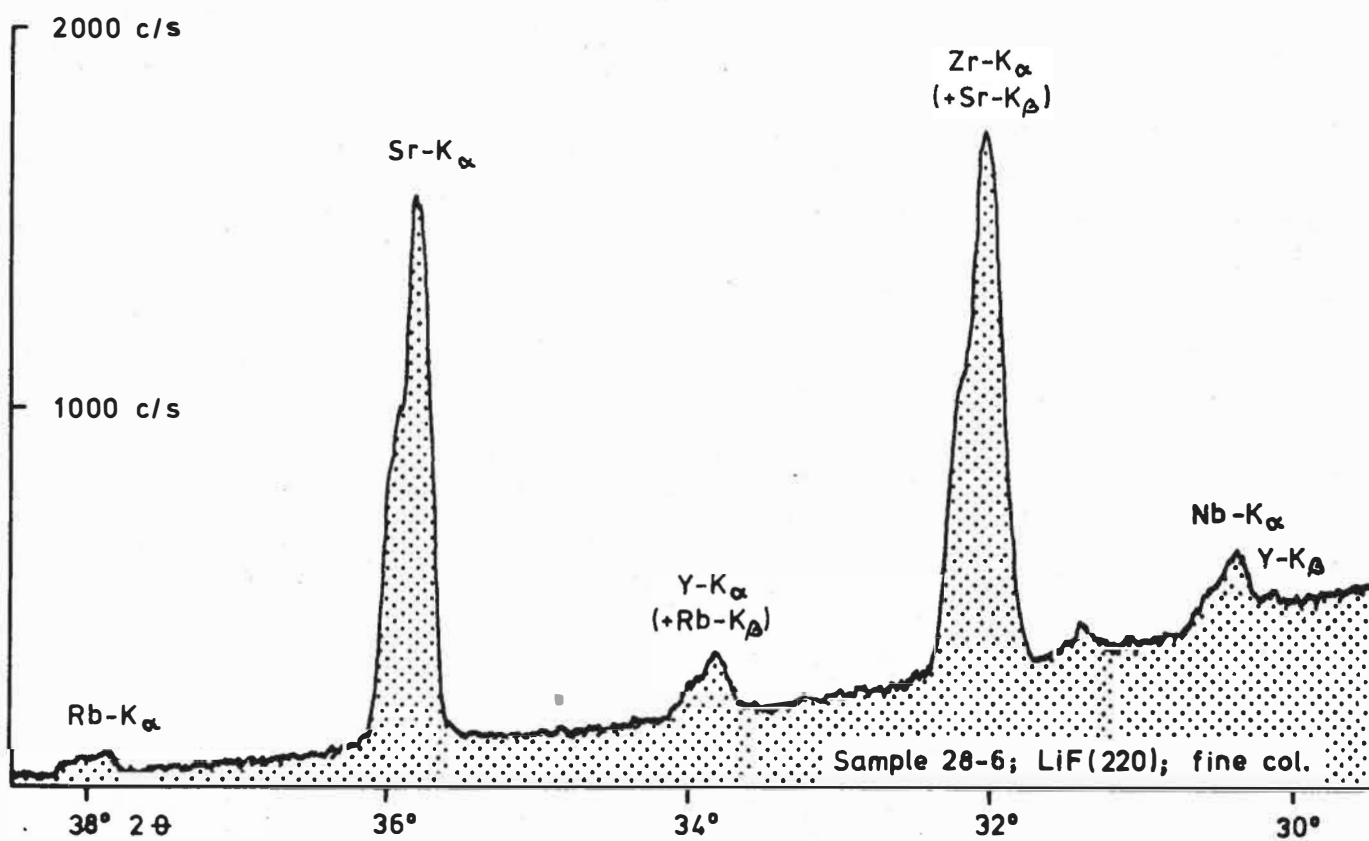
PART 2

CHAPTER 3

PETROLOGY

3.1.   Introduction

The aim of the present chapter is to give a review of the pe-
trology of the Faeroe region. The petrology of the south-western
banks is presented for the first time based on basalts from 13
dredge hauls. The petrology of the Faeroe shelf is inferred from
petrographical studies of glacial erratics and a few nearly in
situ rocks dredged east, west and south of the islands. The pe-
trology of the Faeroe Islands is already well-known from work
done by A. Noe-Nygaard, J. Rasmussen and several others. Some
additional sampling has been made in a single profile, however.
These samples have been analysed for major elements and partly
for trace elements, while most of the earlier samples from the
main profile through the lava pile (Rasmussen and Noe-Nygaard
1969) have been reanalysed for selected elements.

The Faeroe Islands are the only part of the area where the
stratigraphy of the basalts is known, and the basalts from here
will therefore be dealt with first. A large survey of thin sec-
tions was made in an attempt to correlate the basaltic erratics
on the shelf with the stratigraphic divisions on land, and this
work is summarized. The geochemistry of the Faeroese basalts is
likewise described from a stratigraphic viewpoint. The basalts
from the southwestern banks are described petrographically and
geochemically, and their modifications by different types of al-
teration are dealt with. They are compared with the Faeroese ba-
salts, and some long-distance litho-stratigraphical correlations
are suggested. Finally, basalts and tuff-carbonate sediments
from the Faeroe shelf are dealt with. A morphological study of
the basalts, which are dominantly glacial erratics, is summarized

and is used in a discussion of which types of basalts are mainly derived from land and which are mainly derived from the shelf.

3.2.   Methods of investigation

3.2.1.   Sampling of rocks

The upper part of the Middle Basalts above the B-level was re-sampled in 1971 and 1974 at the mountain Sneis on Streymoy. The Sneis profile is part of the main profile through the lava plateau and is represented by 9 basalt samples in the memoir by Rasmussen and Noe-Nygaard (1969, 1970). The profile comprises more than 100 flows and flow units, however, from which about 85 samples were collected for a study of the magmatic evolution.

The sea floor around the Faeroes has been sampled by dredge hauling since 1971 using the Faeroese fishing research vessel "J.C. Svabo" (138 gross register tons). Two types of dredges are used: 4 foot and 6 foot Pecten dredges with front openings of the indicated breadth and an effective mesh width of 5 centimetres. The front opening of the smaller one is only 12 centimetres high and is provided with rake teeth below; they seem useful in digging out small erratics from a soft sea floor, but impede sampling on a rocky sea floor. The large dredge, on the other hand, which is much heavier and has no rake teeth gives good results on the latter type of sea floor. It also strains the wire more, however, because the heavy dredge often clings to the rocks instead of bouncing across them. The 6 foot dredge was therefore only used on the southwestern banks, where it proved nearly impossible to get any rocks with the 4 foot dredge. During the later cruises a tube sampler was mounted below the dredge in order to collect the finer sediment fraction. The tube sampler consists of a 40 centimetres long, 2 inches diameter, steel tube closed at one end. On rocky sea floor the tube sampler was occasionally filled with pebbles, while the dredge gave no or a few rocks.

The dredge was usually hauled 1 to 2 kilometres at a speed be-

tween 2 and 5 knots, and on slopes the direction was preferably parallel to the isobaths. The position of the ship was read on Decca at the beginning and usually also at the end of each haul, while the depth was read from the digital display unit of a Simrad scientific echo sounder system. The depth was also recorded continuously on a Simrad analogue paper recorder. The Decca coordinates have been converted to latitude and longitude by means of a computer programme. The variable error of position is less than 0.5 kilometres to judge from readings of all three Decca coordinates on Bill Bailey Bank and Lousy Bank, where the Decca lines cross at an angle of 15-25° at most. The fixed or systematic error, on the other hand, may possibly reach 2 kilometres, particularly in coastal regions (Himsworth 1973). No corrections were made for the roughly 300 to 1000 metres lag of the dredge behind the ship.

About 90 dredge hauls have been made east, west and south of the Faeroes and on the southwestern banks, and two thirds of these gave between 1 and 150 rock fragments of cobble and boulder size (Fig. 10 and Table 1 and 2).The rock fragments are numbered with the number of the dredge station followed by a hyphen and a serial number, which starts over again with No. 1 at each station. The total number of cobbles and boulders recovered is about 1200, and most of these are glacial erratics (Waagstein and Rasmussen 1975). Local basalts were recovered, however, on the southwestern banks and the Suduroy Ridge.

On the southwestern banks the dredge hauls gave either more than 90 per cent or roughly 50 per cent basalts, the remaining fragments being varied sedimentary, metamorphic and plutonic rocks (Table 2). The fragments from dredge hauls with roughly 50 per cent basalts, except dredge haul No. 29, have the typical appearance of glacial erratics with occasional glacial striae, and they
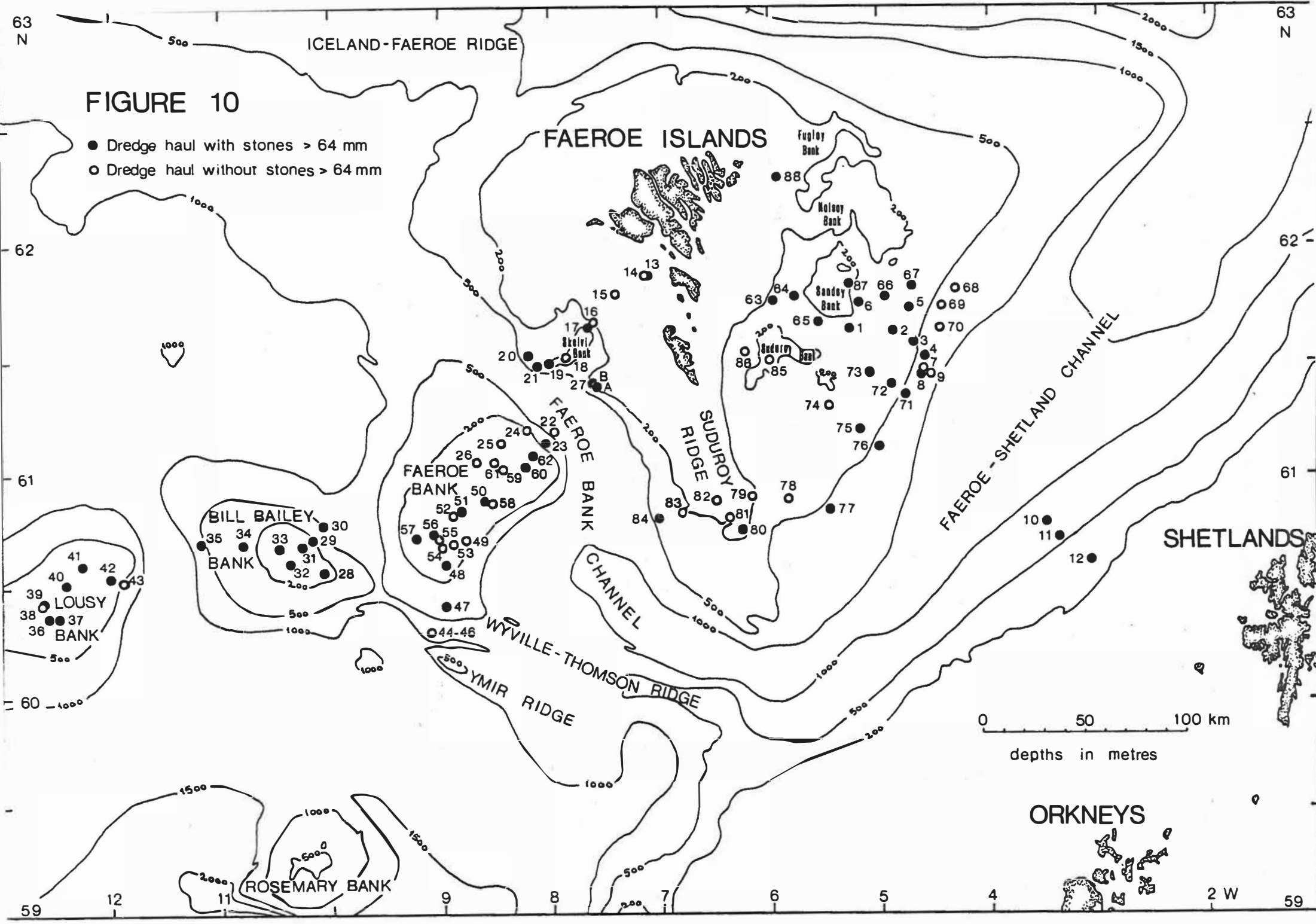
FIGURE 10

TABLE 1 . ABUNDANCE OF ROCKS DREDGED AROUND THE FAEROES AND CHARACTERISTICS OF BASALT COBBLES AND FINES

St. No. (1)	Depth meters (2)	Dist. km (3)	No. of cobbles (4)				Size cm (5)	Roundness (6)			Stria. (7)		% Exp. (8)	Tube sample (9)	Wire movements (10)
			Bas	Tuf	Sed	Met		Mean	SD	SDM	A	B			
A. South-east of the Faeroes															
63	250	+ 69	14		1		12	1.9	1.2	0.3			55	sand	moderate
86	264-270	+ 65												sand	
64	246-248	+ 60	1				(9)	(1.5)					(20)	sand	moderate
85	170	+ 53												shell sand	hard
65	255	+ 47	5	2			13	2.9	1.3	0.6		3	25	mud	moderate
87	182-201	+ 38		1											
1	229	+ 32	5			1	14	3.1	0.6	0.3	1	1	90		
6	201-210	+ 31	2				(20)	(3.0)					(60)		
66	ca. 220	+ 19	1			1	(8)	(2.5)					(60)	sand	
74	200	+ 18												sh. & 1 pebble	slight
73	250	+ 15	7				13	2.6	0.9	0.3			60	mud	moderate
2	234-238	+ 11	7				15	2.8	0.5	0.2	1	3	65		
67	230	+ 9	8				17	2.8	1.2	0.4	2	2	80	empty	hard
78	350-353	+ 7												sand	hard
5	219-258	+ 5	29	11	1		13	2.9	0.7	0.1	1	5	70		
72	270-290	+ 4	5				16	2.9	0.6	0.3		1	65	sandy mud	rather hard
75	400	0	2				(14)	(2.5)					(55)	sand	hard
3	422	- 1	15	2	7	6	16	2.8	1.0	0.3	2	1	75		
71	590-602	- 4	8	3	9	4	11	2.1	0.7	0.3	1		55	sandy mud	moderate
4	571-622	- 6	75	7	36	21	12	2.2	1.2	0.1	11	15			
8	677-719	- 7	60	4	40	22	12	2.1	1.0	0.1	14	8	60		
7	677-732	- 8													
69	580-590	- 8												mud	slight
70	610-615	- 11												mud	slight
68	600-606	- 11												mud	slight
77	590-610	- 11	5		7	4	12	2.1	1.3	0.6		1	60	sand	slight
9	896-909	- 12													
76	590-600	- 12	11	2	7	2	12	2.5	1.2	0.4	4	2	55	mud	very lively
10	713-732	- 95	6		40	12	13						55		
11	549	-105	2		40	11	(11)	1.4	1.3	0.4	1	1	(65)		
12	307	-123	1		17	6	(16)						(100)		

TABLE 1 . (Continued)

St. No. (1)	Depth meters (2)	Dist. km (3)	No. of cobbles (4)				Size cm (5)	Roundness (6)			Stria. (7)		% Exp. (8)	Tube sample (9)	Wire movements (10)
			Bas	Tuf	Sed	Met		Mean	SD	SDM	A	B			
B.	**South-west of the Faeroes**														
13	82	+ 59	2				(13)	(4.0)					(100)		hard +
14	ca. 70	+ 59													lively
15	128-130	+ 45													hard +
16	190-214	+ 27													
17	154-262	+ 24			3										
18	174-187	+ 8													hard
19	194-201	+ 5	13			1	16	2.4	0.8	0.2	1		95		very liv. +
20	260-264	+ 4	128	3	5	4	13	2.8	0.8	0.1		6	85		rather liv.
27A	199-208	+ 3	4				}12	}3.0	1.6	0.7			}90	pebbles & sh.	
27B	207-225	+ 3	2		1									pebbles	
21	232-307	+ 2	49	2	1		12	3.0	1.0	0.1	1		95		
22	622-633	- 27												mud	slight
23	271-344	- 33	7		1		12	2.2	1.1	0.4			80	shell sand	slight
C.	**Suduroy Ridge**														
82	154-160													shell sand	hard +
80	172-180		3				(9)	(3.2)					(80)	sh. & pebbles	hard
81	180													sh. & pebbles	
79	190													sh. & pebbles	hard
83	212-214													shell sand	
84	390-450				1	1								empty	slight

1. Station number. 2. Depth interval dredged. 3. Distance in km to the 400 meters isobath around the Faeroes reckoned positive landwards. 4. Number of dredged fragments >64 mm of basalt (Bas), tuff-carbonate sediments (Tuf), other sediments (Sed) and metamorphic and plutonic rocks (Met). 5. Mean length of basalt fragments >64 mm. 6. Roundness of basalt fragments >64 mm in rho grades (Powers 1953) ranging from 0 to 6 with increasing roundness. SD = standard deviation, SDM = SD of mean. 7. Number of basalt fragments >64 mm with A: clear and B: faint glacial striae. 8. Mean percentage exposure on the sea floor of basalt fragments >64 mm 9. Preliminary description of the wet sediment collected in the tube sampler (if used) or found in a thin tube in the frame of the dredge (St. 22 and 23). sh = shell sand. 10. The captain's description of the wire movements during some of the hauls. liv. = lively, +: the dredge were clinging to the sea floor for some time.

TABLE 2. ABUNDANCE OF ROCKS DREDGED FROM THE SOUTHWESTERN BANKS

Station number		Lati- tude	Longi- tude	Depth interval	Number of rock fragments		
New	Old	North	West	Metres	Bas	Sed	Met

Faeroe Bank

Station number New	Old	Latitude North	Longitude West	Depth interval Metres	Bas	Sed	Met
23	XXIII	61°09.2' 61°08.6'	8°02.1' 8°02.7'	271–344	7	1	
44		60°18.0' 60°18.2'	9°05.1' 9°04.8'	591–?		4	
47		60°24.8' 60°25.3'	8°58.1' 8°58.7'	371–?	1		
48		60°35.1' 60°35.9'	8°57.5' 8°57.5'	181–187	20	3	
50	F1599	60°52.9' 60°53.6'	8°37.6' 8°35.7'	135	2		
51	F1600	60°50.3'	8°49.2'	110	1		
56	F1605	60°44.8'	9°03.6'	126–128	1		
57	F1606	60°43.3'	9°13.0'	141–146	36		
60	F1609	61°02.0'	8°14.0'	110	18		
61	"Poppy"	61°03.6'	8°30.5'	?		1	

TABLE 2 (Continued)

Station number		Lati-tude	Longi-tude	Depth interval	Number of rock fragments		
New	Old	North	West	Metres	Bas	Sed	Met

Bill Bailey Bank

New	Old	North	West	Metres	Bas	Sed	Met
28		60°34.3' 60°34.6'	10°03.8' 10°04.7'	150-155	48	1	2
29		60°43.2' 60°42.8'	10°09.4' 10°10.8'	183-229	21	19	9
30		60°47.0' 60°47.0'	10°04.0' 10°05.0'	461-514	5	4	2
31		60°40.9' 60°41.1'	10°15.7' 10°15.8'	135	1		
32		60°35.6' 60°36.3'	10°22.6' 10°23.1'	150-157	1		
33		60°40.2' 60°40.3'	10°29.7' 10°28.8'	152-155	15	1	1
34		60°41.5' 60°41.5'	10°49.0' 10°48.4'	265-280	8		
35		60°42.1' 60°42.3'	11°12.1' 11°10.9'	596-664	2	2	2

Lousy Bank

New	Old	North	West	Metres	Bas	Sed	Met
36		60°21.4' 60°22.1'	12°34.1' 12°35.6'	283-287	31	3	1
37		60°22.1' 60°22.3'	12°29.2' 12°28.3'	307-316	16	1	
39		60°25.5' 60°26.3'	12°38.0' 12°38.8'	293-304	10	4	3
40		60°31.2' 60°30.8'	12°25.6' 12°22.8'	355	0	2	
41		60°35.8' 60°35.9'	12°17.0' 12°15.0'	353	4	5	1
42		60°32.3' 60°33.1'	11°59.0' 12°01.9'	415	6	3	4

Note: Bas = basalt; Sed = sediments (no tuff-carbonate sediments);
Met = metamorphic and plutonic rocks.

are probably all ice-rafted. Most of the basalt fragments from dredge hauls dominated by basalts, on the other hand, are no doubt locally derived. They consist of only one or a few different types of basalts which vary with the dredge site. The fragments of local basalt may be angular and are sometimes free of epifaunal over-growths, as if they have been detached from rock outcrops along pre-existing fractures by the dredge (specimen numbers 33-2, -4; 50-1; 57-3,-16, -19, -29, -32; 60-7, -18). Most of the basalt fragments are subangular or subrounded, however, and very probably represent coarse beach gravels. They differ from the ice-rafted basalts by being more uniformly worn on all surfaces, by a slightly higher degree of roundness and a better roundness sorting (disregarding the above angular fragments) and by the lack of glacial striae (Table 4). The rock fragments from station 29 on Bill Bailey Bank also look like beach gravel though they include a large proportion of non-basaltic rocks; they are considered to be reworked erratics. The beach gravels occur down to a depth of at least 180 metres on Faeroe Bank, at least 264 m on Bill Bailey Bank and at least 306 metres on Lousy Bank. On some sites, as for example station 28, the boulders and cobbles of local basalt show a tendency to spall off the outermost one millimetre or so of the weathering crust when tumbled during the haul; this feature has never been observed with the erratic basalts.

The nature of the sea floor can be partly inferred from the the wire movements during dredging. On sites where local basalts were recovered the wire movements were always lively or hard at least part of the time, and on several sites the dredge clung to the sea floor with great risk of breaking the wire. In these places coarse gravels or solid outcrops of basalt very likely occur. On sites on the southwestern banks where only erratics were

recovered, only slight movements were observed, and here most of the sea floor probably consists of fine sand or mud similar to that recovered in the tube sampler. On the few stations from which only one or two basalt fragments were recovered, the character of the haul suggested that the basalts might be local, and this suggestion is supported by the geochemical studies.

3.2.2. Morphologic investigations of the dredged basalts

A detailed study of the morphology of the dredged basalts has
been carried out in an attempt to classify the rudaceous deposits
which may consist of lodgement tills, ablation tills, glacio-ma-
rine deposits or beach gravels. The classification is hampered
by the lack of matrix in the glacial deposits which has probably
been swept out by bottom currents, and by the strong selectivity
of the dredges, especially the small dredge, as to the size of
the dredged fragments. The ultimate aim of the morphological in-
vestigations was to investigate further those dredge hauls which
probably have a high content of basalts derived from the Faeroe
shelf itself.

The morphological investigations encompass the size, surface
and roundness of the fragments. The basalt fragments like the
fragments of other rock types were measured along their longest
axis and usually also along the other two principal axes. The
surface of the basal fragments from the Faeroe shelf and the sur-
rounding deeper areas was investigated systematically in two ways:
glacial striae were looked for on all fragments and characterized
as either clear or faint, and the degree of exposure on the sea
floor of the fragments was estimated (using 10 per cent intervals)
from their epifauna, weathering colour and iron-manganese coatings.
The same basalt fragments and the basalt fragments from a few
dredge hauls on the southwestern banks were also studied systemati-
cally as to the degree of roundness (Table 1 and 4).

Roundness is defined as the description of the relative sharp-
ness of the corners of the fragments. The roundness of the basalt
fragments was determined quantitatively by using a five times pho-
tographic enlargement of a visual comparator prepared by Krumbein

(1941) (Fig. 11). This consists of maximum projection silhouettes of actual pebbles (16-32 mm) measured according to the formula of Wadell (1933):

$$P_d = \frac{\Sigma(r/R)}{N}$$

where r is the curvature of individual corners, N is the number of corner radii including corners whose radii are zero, and R is the radius of maximum inscribed circle. The silhouettes are grouped by Krumbein in 9 roundness classes from P_d (degree of roundness) 0.1 to 0.9. During the present work they were remeasured and regrouped in 6 roundness classes based on class intervals that are multiples of $\sqrt{2}$ as shown in Table 3. This class division, which is nearly identical to that proposed by Powers (1953), is favoured because roundness distribution of fragmental deposits tends to be log-normal whether they are sands (Folk 1955, Sahu and Petro 1970) or gravels (Table 4). Furthermore, a conversion proposed by Folk (1955) of the P_d scale to a rho scale (Table 3) comparable to the phi scale of grain size was adopted to facilitate computation of mean roundness and roundness sorting (1 standard deviation of the mean). The rho values can be computed directly from P_d values by the formula: rho = k x $\log_{10}P_d$ + 6, where k = 2/$\log_{10}2$ = 6.644. The comparative classification of the basalt fragments was supported by a large number of direct measurements of P_d to reduce the subjective errors of the comparative method. Duplicate roundness determinations of series of about 25 fragments on different days generally agree within 0.1 - 0.2 rho values.

Contrary to the opinion of Powers (1953), it is more difficult to classify angular than rounded fragments when logarithmic roundness grades are used. All fragments with P_d less than 0.177 were
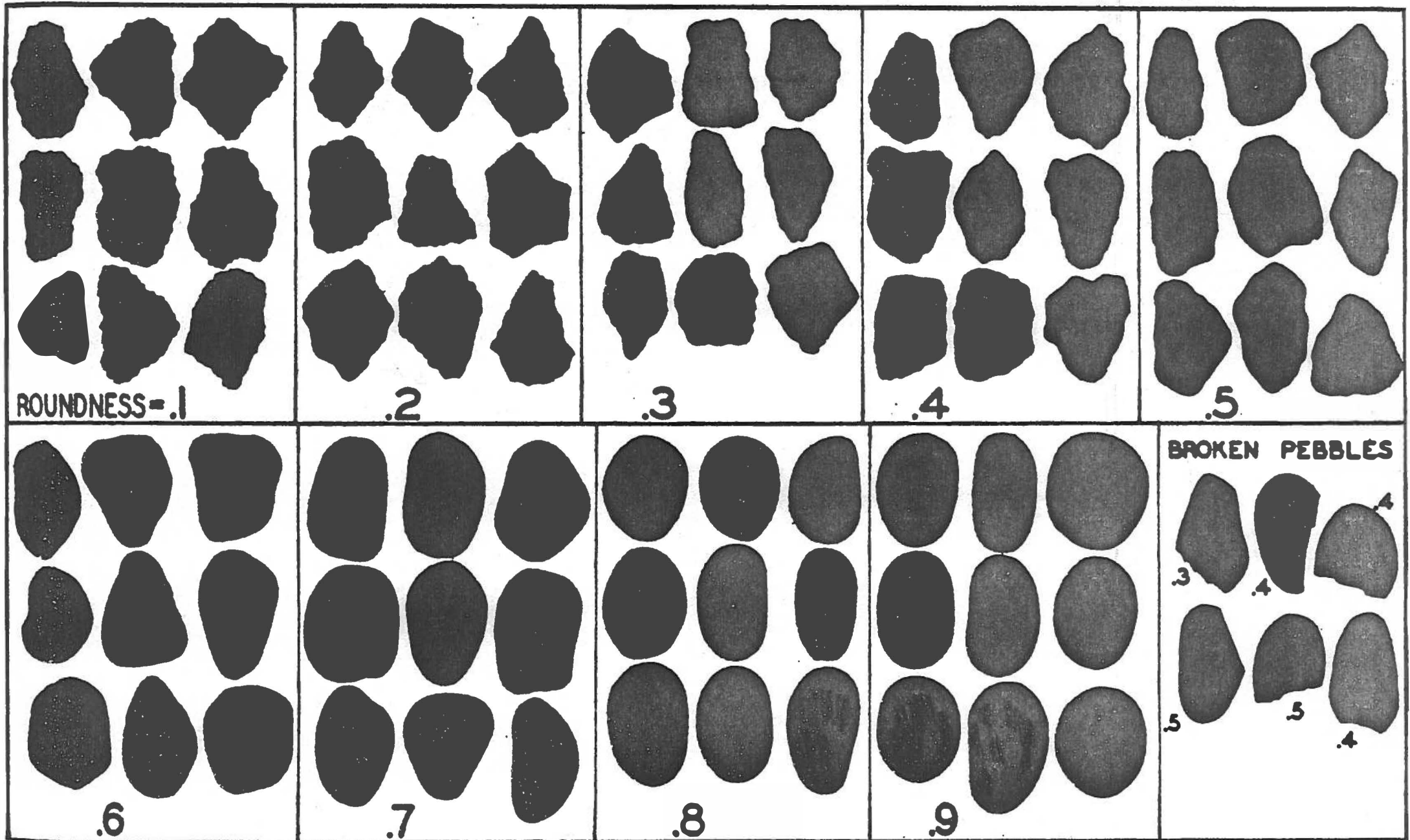
FIGURE 11. Pebble images for visual roundness (from Krumbein 1941)

TABLE 3   ROUNDNESS CLASSES

Class name	Abbrevation	P_d scale	rho scale
Very angular	VA	0.125 - 0.177	0 - 1
Angular	A	0.177 - 0.250	1 - 2
Subangular	SA	0.250 - 0.354	2 - 3
Subrounded	SR	0.354 - 0.500	3 - 4
Rounded	R	0.500 - 0.707	4 - 5
Well rounded	WR	0.707 - 1.000	5 - 6

TABLE 4.   EXAMPLES OF ROUNDNESS DISTRIBUTION OF DREDGED BASALTS

Station No.	Number of basalt fragments								Rho roundness		Mean size cm
	All	With Striae	VA	A	SA	SR	R	WR	Mean	STD	
4	75	26	14	20	21	16	4		2.18	1.16	12.0
8	60	22	9	19	20	10	2		2.12	1.04	12.0
5	29	6		2	14	12	1		2.91	0.68	13.4
20	128	6	1	19	55	50	2	1	2.78	0.79	12.8
21	49	1	2	3	17	22	4	1	3.03	0.96	12.3
28	48	0		3	25	19	1		2.88	0.64	18.5
36	31	0	1	7	14	7	2		2.56	0.93	19.0
37	16	0		4	8	4			2.50	0.73	23.9

Note: The fragments from stations 4 and 8 on the SE slope of the Faeroe shelf are probably ice-rafted erratics, those from station 5 at the southeastern shelf border and stations 20 and 21 at the western shelf border are supposed to be derived from lodgement tills whereas those from station 28 on Bill Bailey Bank and stations 36 and 37 on Lousy Bank probably are derived from beach gravel.

therefore placed in the 0-1 rho class, though a few of them pro-
bably fall below the lower limit of the class. The computations
of the statistical parameters were based on the assumption that
all classes are of equal size on the rho scale, however. This
assumption greatly simplifies the computations, and the resulting
error is small compared to the errors of the roundness determina-
tions.

Scores of publications deal with the roundness of rock frag-
ments from various kinds of gravels and morainic deposits, but in
most the roundness estimates are relative only, and the remaining
publications show little agreement about exactly how to quantify
roundness. Thus no other investigations exist with which the
present roundness determinations can be closely compared.

3.2.3. Petrographic investigations

The dredged rocks have been classified according to rock type (Table 1 and 2) (Waagstein and Rasmussen 1975). The basalts were divided into olivine-phyric, plagioclase-phyric and aphyric basalt with the porphyritic types named after the sole or most abundant phenocryst mineral. The classification of the basalts was mostly based on an examination under a stereo microscope of both fresh fracture surfaces and surfaces cut by a diamond saw. Few basalts are strictly aphyric, but for practical reasons near-aphyric and microphyric basalts were grouped with the aphyric ones. A near-aphyric basalt was defined as a basalt with no phenocryst minerals exceeding 1 per cent of the volume of the rock, while a microphyric basalt was defined as a basalt with smaller than 1 millimetre sized crystals of the principal phenocryst mineral (> 1 vol. %). Such basalts are likely to be classified as aphyric in the field.

About 500 of the basalt fragments from the Faeroe shelf, the Faeroe-Shetland Channel and the Faeroe Bank Channel were further subdivided according to the volume and maximum crystal size of the principal phenocryst mineral (Table 11). The following classes of volume and maximum size were used: less than 1%, 1-5%, 5-15% and more than 15%; and less than 1 mm, 2-5 mm and more than 5 mm. The abundance of the phenocrysts was estimated by using a visual comparator, while the maximum crystal size was measured with a ruler. In all, except the most sparsely porphyritic samples, several crystals are close to the maximum size, and this parameter is therefore easy to determine accurately in contrast to the mean crystal size. The latter measure is furthermore ambiguous because most phenocrysts are likely to be cut obliquely to their longest axis, and because small phenocrysts are more numerous than large

ones. Most basalts are glomerocrystic, but the individual crystals can easily be discerned by their partial outline and, in the case of plagioclase, by their cleavage and twinning. Some plagioclase tablets may be much longer than the others and in most cases consist of two crystals intergrown end to end, but in several basalts two different size populations of plagioclase phenocrysts are clearly present. In this case the classification by maximum crystal size was based on the dominant population. Most basalts contain phenocrysts of both olivine and plagioclase, and the abundance and crystal size of the subsidiary phenocryst mineral were noted too. Many basalts also carry subordinate phenocrysts of pyroxene,which are difficult to recognize, however, owing to their small number and size.

In the near-aphyric and microphyric basalts the two-fold division according to the principal phenocryst mineral becomes impracticable, and has to be supplemented by classes of near-aphyric and microphyric basalts, in which phenocrysts of olivine and plagioclase are both present and occur in roughly equal amounts. The estimates of the relative or absolute abundance of microphenocrysts in hand specimens cannot be very accurate, but as they were done with great care, the results from different dredge hauls are probably comparable. Pyroxene microphenocrysts are present in many basalts, but are easily confused with the ore minerals, and so have not been looked for systematically. Ophitic pyroxene texture, on the other hand, has a distinctive appearance in hand specimens, and therefore probably has been noticed in most cases.

The alteration of the basalts has been characterized by noting the presence of fresh olivine and white amygdales. The white amygdales mostly consist of zeolites, but probably also included analcite, calcite and silica minerals.

The abundance and size of plagioclase phenocrysts in the basalts from the Sneis profile on the Faeroes were estimated and measured in a similar way, but instead of using class intervals the approximate values were notes (Fig. 12 and Table 17).

The macro- and mesoscopic examinations of the basalts were supplemented by the examination of a large number of thin sections. These include sections from about 100 basalts from the southwestern banks which are nearly all local, about 100 basalts from the Faeroe shelf, the Faeroe Shetland Channel and the Faeroe Bank Channel which are nearly all erratics, and about 70 basalts from the Sneis profile. In addition, most of the thin sections in Professor A. Noe-Nygaard's collection of Faeroese basalts were cursorily examined for comparison with the dredged basalts, and to get an impression of the relations between petrography, stratigraphy and chemistry. The observations were mainly aimed at the phenocrysts, the olivine content and the pyroxene texture. To this end point counts were made of either the phenocrysts or the whole rock of most of the chemically analysed specimens from the southwestern banks and of a few Faeroese basalts (Table 8, 13 and 18).

The petrographical work also includes a study of erratics of varied tuff-carbonate sediments in hand specimen and thin sections.

3.2.4. Selection and preparation of rocks for chemical analysis

62 out of 87 basalt samples collected from the Sneis profile on the Faeroes and 48 out of nearly 200 cobbles and boulders of presumed local basalt dredged from the southwestern banks were carefully selected for geochemical studies together with 2 weathering crusts and some vesicle fillings.

On average a few hundred grammes, occasionally less than hundred grammes, of each sample were crushed. The Faeroese basalts were cut into slices by a diamond saw, and weathering crusts and larger amygdales were removed if present. Any contaminations from the saw blade were removed by wet grinding with carborundum powder, and the sample was cleaned in an ultrasonic bath. The sample was crushed in a hydraulic rock crushing machine, then crushed by hand in a steel percussion mortar, and finally a split sample was ground for about half an hour in an automatic agate mortar. The basalts from the southwestern banks were broken into pieces by a hammer and/or a hydraulic splitter. After the removal of any weathering crusts and larger amygdales the small fragments were crushed in a wolfram carbide jaw crusher. A roughly 100 grammes split of the sample was then ground in a wolfram carbide ball mill for 10 minutes, and a third of this portion was finally ground in a smaller wolfram carbide ball mill for another 10 minutes. 10 samples were crushed instead in a steel percussion mortar and then ground in 4-7 portions in an agate swing mill for about 5 minutes (samples No. 33-2, 33-4, 47-1, 48-1, 51-1, 56-1, 57-1, 57-4, 60-3, 60-9). All grinding methods resulted in a rock powder generally finer than 300 mesh.

The ball mills plus jaw crusher add about 50 ppm wolfram to the rock powder according to the neutron activation analyses. The wolfram carbide contains some cobalt, the concentration of which

is not stated by the manufacturers. However, a comparison of 9 samples ground in the agate mill with the 9 most similar samples ground in the wolfram carbide mills does not show any enrichment at all in Co in the last group, so the contamination by Co seems to be negligible. The same set of samples does not reveal any SiO_2 contamination during the short runs in the agate mill.

3.2.5. Geochemical procedures

Major elements. Major elements have been determined essential-
ly by the X-ray fluorescence technique. 50 analyses of the basalts
from the southwestern banks have been made by G. Hornung at the
University of Leeds. These analyses were performed on glass discs
prepared from rock powder diluted 1 to 4 by a lithium tetraborate-
-lithium metaborate flux (Spectroflux 110 from Johnson Matthey).
Ag X-ray tube and a TlAP analysing crystal were used throughout;
this gives the highest possible precision for the light elements
Na and Mg (Hornung, pers. comm. 1975). Other operational condi-
tions and the method of calibration against a synthetic standard
and corrections for differences in mass-absorption are essentially
as described for this laboratory by Padfield and Gray (1971). The
volatiles were determined by the loss of ignition method.

62 basalts from the Sneis profile on the Faeroes and 5 samples
of earthy amygdales from the basalts dredged on the southwestern
banks have been analysed by Ib Sørensen at the Geological Survey
of Greenland (GGU). The GGU laboratory uses the same fusion mix-
ture based on a sodium tetraborate flux as Patfield and Gray (1971)
and a similar analytical method except for Na and Mg, which are
analysed by the atomic absorption method. A Cr X-ray tube is used
throughout. At the time of analysis (autumn 1974) some elements
were calibrated against rock standards and others against synthetic
standards and corrected for differences in mass-absorption. The
GGU analytical procedure gave results which, except for phosphorus,
compared closely with those from other laboratories, including the
laboratory in Leeds.

The Cr K_α radiation (2.291 Å) strongly excitates the Ca K_α line
(3.089 Å) whose second order reflection line interferes with the
first order line P K_α line (6.155 Å). A correction for this inter-

ference was first made at the end of 1974, and therefore the phosphorus content in the basalts low in phosphorus but high in calcium was greatly overestimated. Only a few analyses of the basalts and the analyses of the amygdale samples are corrected for Ca interference.

In 1976 the author reanalysed all the Sneis samples for phosphorus in the XRF laboratory at the Institute for Petrology using a germanium analysing crystal which gives no second order reflections. The analyses were made on powder pellets instead of on the old glass discs, some of which had acquired a dull surface since they were analysed in 1974. Though the precision was better than 0.01 per cent P_2O_5 the accuracy of the powder analyses was poor. The analyses were calibrated against the international rock standards W-1, BCR-1, GSP-1, AGV-1 and CRPG-GA for which an average concentration versus net XRF intensity factor was computed neglecting the few per cent differences in the mass absorption at the P K_α wave-length. The results based on this factor and normalized against the recommended values (Flanagan 1973) used for the computation of the factor have a coefficient of variation (C.V.) of 14 per cent. The inclusion of the results for the standards JB-1 and ZGI-BM does not change this figure. The results for 7 basalts normalized against results on glass discs corrected for Ca interference average 0.96 with a C.V. of 14 per cent (Table 7). The results for 10 basalts from the southwestern banks analysed in Leeds show a similar spread around a regression line y = 0.73x + 0.086, where x and y are the P_2O_5 contents in per cent measured on powder pellets and glass discs, respectively. Thus the two methods give comparable results at concentrations near 0.30 per cent P_2O_5, whereas at x about 0.05 per cent P_2O_5 y is about 0.12 per cent as directly shown by two of the samples. This bias may

possibly be due to Ca interference in the analyses from Leeds.
These are calibrated against a synthetic standard with twice as
much CaO and much more P_2O_5 than the basalts, however, and a fall
out of the impulse discrimination circuit should therefore result
in an overestimate of the P_2O_5 content in basalts both low and
high in phosphorus. Most of the scatter of the results on powder
pellets with similar P_2O_5 contents is probably due to microabsorp-
tion effects. These are most serious at long wave-lengths of
elements occurring in high concentrations in a minor phase such
as phosphorus in apatite. It is therefore perhaps more likely
that the results on the powder pellets are biased by some obscure
mineralogical differences between the basalts with a low phospho-
rus content and the basalts with a high phosphorus content. It
must be concluded that there is some uncertainty about the real
P_2O_5 content in the basalts low in phosphorus, especially in
those only analysed on powder pellets.

Most of the analyses of Faeroese basalts published by Rasmus-
sen and Noe-Nygaard (1969) are XRF analyses on rock powder. These
were made about 1965 by Ib Sørensen. The XRF results were cali-
brated against chemical analyses of basalts from the Faeroe Islands
and other parts of the world, while no corrections were made for
differences in mass-absorption. About 80 of the Faeroese basalts
have been reanalysed by Ib Sørensen for SiO_2, Al_2O_3, FeO^* and CaO,
and partly for K_2O and TiO_2, on glass discs. The new analyses
were made in 1974 at the same time as the analyses of the basalts
from the Sneis profile. Earlier partial and complete chemical
analyses partly used for calibration of the XRF results on powder
pellets agree within a few per cent relative with these new re-
sults except for potassium which is difficult to analyse accurately
with chemical methods at the low concentrations considered (Table

7). The chemical results for SiO_2 are about 0.5 per cent absolute too low compared to the new XRF results, while a similar difference in the Al_2O_3 results disappears when the old chemical analyses are corrected for the influence of iron on the titration factor, which correction was first used at a later date in the chemical laboratory (Ib Sørensen, pers. comm.).

The old XRF results for Si, Al, Ca, K and Ti are similar to the new ones, while the old XRF results for Fe are 10 per cent too high (Table 7). The large difference between the old and new Fe results can only be explained as a calibration error, and the old results may perhaps erroneously have been read as FeO on a calibration curve based on total iron as Fe_2O_3. The quotients between old and new XRF results for Si, Al, Fe, Ca and K show a coefficient of variation of 3.5-8 per cent, which is 4-6 times higher than for the quotients between the chemical results and the new XRF results, except for potassium (Table 7). The larger variation must be due to the influence of total chemistry and mineralogy on the analyses on powder pellets. The uncertainty is higher for the analyses of titanium than for the analyses of the other elements because the mineralogical effect is particularly high for titanium as it is for phosphorus. Titanium mainly occurs in the oxide minerals, and differences in the composition, exolution and grain size of these minerals may cause large differences in the intensity of the Ti K_{α} radiation due to micro-absorption effects, which can be avoided only by extremely fine grinding or by melting of the samples.

The magnesium analyses were at the limit of the capacity of the old XRF apparatus used for the analyses on rock powder (Ib Sørensen, pers. comm.). 29 samples were reanalysed for MgO and Na_2O by the atomic absorption method in the GGU laboratory in 1977, while the 3 year-old glass discs were analysed by the author in

the XRF laboratory at the Institute for Petrology. The XRF analyses were made as an experiment because the effects of aging on the glass discs were unknown. The discs of the chemically analysed samples were used for calibration, and no mass-absorption corrections were made. Acceptable results were obtained for the many discs with no or very slight signs of alteration, while the dull discs gave too low results. The hydration layer was removed from these discs by grinding with steel wool. The Mg K_{α} radiation intensity versus concentration ratio was thereby raised about 16 per cent above that for the unground, clear discs, which suggests that the latter discs were also hydrated. The accuracy of the analyses of ground discs and unground, clear discs was about the same or about 4 per cent relative assuming an imprecision of 2 per cent relative, but no systematic error, on the chemical analyses whether made conventionally or by the atomic absorption method.

Revised analyses of the basalts from the Faeroese main profile are not presented in this report, but are available from Professor A. Noe-Nygaard on request. During the compilation of these results the XRF analyses on glass discs were ranked above the chemical analyses except for MgO, the chemical analyses were ranked above the XRF analyses on rock powder except for K_2O, and the new atomic absorption analyses of Na_2O were ranked above the old flame photometrical analyses. The old analyses of SiO_2, Al_2O_3, FeO^* and CaO were multiplied with the average quotients between new and old XRF results for samples of similar compositions from the same stratigraphic interval (as defined in Table 10). Such corrected concentrations are used for 22 samples, most of which are now being reanalysed in the GGU laboratory. For 7 samples too little or no rock powder and no glass discs were available for the re-

vision of the MgO analyses on powder pellets, and these were re-adjusted in a similar way.

Trace element analyses. The 50 basalts from the southwestern banks were analysed by emission spectrography for Ba, Zr, Sr, Ga, Cu, V, Co, Ni, Cr and partly for Sc, and by XRF spectrography for Rb, Ba, La, Nb, Zr, Sr and Y. Ten of the samples were also analysed by the neutron activation method for rare earth elements, Sc, Cr, Co, Hf, Ta and Th. A few samples of amygdales in the basalts were analysed for 9 trace elements by the first two methods. 10 basalts from the Sneis profile and 12 other basalts from the Faeroe Islands were analysed for trace elements with emission spectrography only.

XRF spectrography. The XRF analyses were made by the author on pressed powder pellets in the laboratory at the Institute for Petrology using a Philips PW 1410 spectrometer. The operating conditions are listed in Table 5. A standard discriminator setting was used throughout with a lower limit of 20 per cent and an upper limit of 70 per cent. The XRF intensity of the L_α line of Ba and La and the K_α line of Ti, Rb, Sr, Y, Zr and Nb was measured together with the background intensity on both sides of the line. Background factors were determined experimentally using quartz powder and international peridotite standards as blanks. The following interferences were corrected for: Ti K_α with Ba L_α (0.27%) and La L_α; Sc K_β with Ba L_α; Rb K_β with Y K_α (30%); Sr K_β with Zr K_α (6.0%); and Y K_β with Nb K_α (0.26%). The approximate size of the interference is given in parentheses in per cent of the intensity of the K_α line of the interfering element measured under the same instrumental conditions as the analytical line. The in-

TABLE 5 — INSTRUMENTAL CONDITIONS AND SENSITIVITY FOR XRF ANALYSES OF PRESSED POWDER PELLETS

Element	Analytical line	Interfering lines[1]	X-ray tube target	voltage (KV)	current (mA)	Vacuum	Collimator[2]	Analysing crystal	Counter[3]	Counting time in seconds at peak position, 2 cycles[4]	Standard deviation in ppm 2 cycles[5]
Ba	La	Ti Ka, Sc Kb	Cr	60	20 (7)[6]	yes	fine	LiF 200	gas	2 x 100	1.6 (2.8)[7]
Ti	Ka	no	Cr	60	20 (7)[6]	yes	fine	LiF 200	gas	2 x 20	
La	La	Ti Ka	W	80	30	yes	coarse	LiF 200	gas	2 x 200 (100)[8]	0.39[9]
Rb	Ka	no	Mo	80	30	no	fine	LiF 200	scint.	2 x 100	0.14
Sr	Ka[10]	no	Mo	80	30	no	fine	LiF 200	scint.	2 x 100 (40)[8]	0.37 (0.64)[10]
Y	Ka	Rb Kb	W	80	30	no	fine	LiF 220	scint.	2 x 100	0.64
Zr	Ka	Sr Kb	W	80	30	no	fine	LiF 220	scint.	2 x 40	1.05
Nb	Ka	Y Kb	W	80	30	no	fine	LiF 220	scint.	2 x 200	0.50

1) Interference corrections have been applied using intensities of Ka lines of Ti, Rb, Sr and Y, emission spectrography analyses of Sc and major elememt analyses (Ti correction of La La line).

2) 150 μm (fine) or 550 μm (coarse) primary collimator. 3) Gas flow proportional counter (gas) or scintillation counter (scint.). 4) Background measurements add 80 - 200 % to the above figures. 5) Standard deviation s calculated from the formula $s^2 = 1/4k(d_1^2 + d_2^2 + \ldots + d_k^2)$, where k is the number of analysed samples and d_i is the difference between the two results calculated from the two counting cycles of sample i. 6) 7 mA tube current was used for samples with more than 1.7% TiO_2 to avoid dead time problems. 7) 7 mA tube current. 8) Reduced counting time used at higher concentrations. 9) Error in Ti correction not included. 10) Counting time 2 x 40 seconds.

terference measurements were made on quartz powder spiked with the element of interest. Actually, Rb and Sr were measured before Y, Zr and Nb and at other instrumental conditions (Table 5), and the Rb and Sr interference factors were therefore changed in proportion to the change of the Rb and Sr K_α net intensities on the standards between the two runs. The interference of Ti K_α with La L_α and the interference of Sc K_β with Ba L_α was related to the concentrations instead of the K_α intensities of Ti and Sc. The former interference equalled about - 3.4 ppm La/ % TiO_2, the latter one about + 0.2 ppm Ba / ppm Sc. The former interference is negative because the two background measurements were made on the same side of the interfering line. The concentrations of Ti and Sc were taken from the major element and emission spectrography analyses, respectively. Sc concentrations were guessed in the basalts not analysed for this element.

The XRF analyses were calibrated against several international rock standards. These were measured at the beginning and end of the analytical run, and sometimes also in between. The count time on the line and background positions was divided into two sessions so instrument stability could be checked. A sample giving a high count rate on one of the analytical lines was chosen as an instrument drift monitor and counted once on this line during each session.

The count rate of analytical and interfering lines was corrected for the background computed for the line, then if necessary for the instrument drift revealed by the count on the drift sample, and finally for any interference from other lines. The resulting count rate is the net count rate or net intensity of the line. A conversion factor k was found from the standards by dividing the known concentration of the element with the net count

rate and the mass-absorption coefficient at the wave-length of the analytical line. The mass-absorption coefficients of standards and samples were computed beforehand from their major element composition using the absorption data of Heinrich (1966). An average k factor for each element was computed from either all standards or only those which gave the most similar results. The net intensity on the sample was finally converted into a concentration by multiplication with the mass-absorption coefficient of the sample and the average k factor. The correction for Sc interference with Ba was first made at this step, while the TiO_2 concentrations used for the interference correction of the La analyses were converted into XRF intensities. All computations were made separately for the two count sessions on each sample, and thus in effect two independent results were obtained. These duplicate results were used to compute the precision of the total analysis (Table 5). The precision of the TiO_2 and Sc analyses made by other methods is not included in these figures.

The standards ultimately used for calibration are listed in Table 6 . The La analyses were calibrated against BCR-1 only, while the background factor was extrapolated from the Faeroese basalt X.16 with 2.2 ppm La (Schilling and Noe-Nygaard 1974). The concentrations used for the international rock standards were taken from Flanagan (1973) except for the concentrations of Nb, Zr and Y, which were XRF analyses taken from Erlank and Kable (1976). The calibration method used gives, over a wide range of concentrations, results in agreement with the recommended values for some of the best analysed international standards as shown in Table 6 . It must be remembered, however, that the present results for the standards in this table partly rely on the recommended values for these standards which were compiled from a variety of

TABLE 6 . TRACE ELEMENT RESULTS FOR THREE INTERNATIONAL ROCK STANDARDS

	W-1			BCR-1			GSP-1		XRF standards used
	Spec	XRF	Rec	Spec	XRF	Rec	XRF	Rec	
					ppm				
Rb	..	21.2	21	..	46.8	46.6	254	254	1,2,4
Ba	126	170	160	550	684	675	1221	1300	1 - 6
La	..	10.0	9.8	..	26	26	..	..	2
Nb	..	6.8	6.8	..	11.3	11.3	25.7	25.4	1 - 3
Zr	106	97.6	95.1	190	190	192	533	543	1 - 3
Sr	169	191	190	300	328	330	234	233	1,2,4
Y	..	20.8	20.3	..	33.9	33.4	24.4	25.4	1 - 3
Ga	20	..	16	16	..	(20)	..	..	
Cu	110	..	110	17	..	18.4	..	..	
V	240	..	264	360	..	399	..	..	
Sc	33	..	35.1	..	..	..	..	..	
Co	42	..	47	33	..	(38)	..	..	
Ni	74	..	76	10	..	15.8	..	..	
Cr	130	..	114	10	..	17.6	..	..	

Comments: Emission spectrography analyses (Spec) by H. Bollingberg of W-1 (1976 and 1977) and BCR-1 (1976). XRF analyses by R. Waagstein (1976) calibrated against international rock standards using the recommended (Rec) values in Flanagan (1973) except for Nb, Zr and Y which are XRF analyses from Erlank and Käble (1976). The international standards used for calibration are identified by numbers in the last column as follows: 1) W-1, 2) BCR-1, 3) GSP-1, 4) AGV-1, 5) G-2, 6) CRPG-BR. The precision (1 standard deviation) is about 10 % relative of the spectrography analyses and better than 1 ppm and/or 1 % relative of the XRF analyses.

analytical techniques including XRF.

Neutron activation analysis (NAA). Ten basalts from the south-
western banks were analysed in 1974 by the neutron activation me-
thod at the Atom Research Centre at Risø by R. Gwozdz (Table 15).
The samples were irradiated together with a synthetic standard.
The iron contents of the samples, which were known from the major
element analyses, were used to relate the measured gamma-ray in-
tensities in the standards and samples to each other. The preci-
sion estimated from counting statistics is less than about 2 per
cent (1 st.d.) for Fe, Sc, Co, Cr and Sm, averages 3-6 per cent
for Eu, La and Ce, 8-12 per cent for Lu, Yb and Hf and 20 per
cent for Th. The accuracy of the analyses is not known, but the
rare earth element concentrations compare well with the concen-
trations measured by Schilling (Schilling and Noe-Nygaard 1974)
in Faeroese basalts with similar major element compositions. The
NAA results for La seem, however, to be slightly too low compared
to the XRF results for the same samples, while the XRF results
for Faeroese basalts previously analysed by Schilling do not dif-
fer much from the results obtained by Schilling (Table 7).

Emission spectrography analysis. These analyses have been
made by H. Bollingberg at the Institute for Petrology using a
Large Hilger Quartz Spectrograph. The estimated precision of ana-
lyses made at different times averages about 10 per cent (1 st.d.)
for all analysed elements except Ba. When the analyses are made
in one series, as is the case of the basalts from the southwestern
banks, the estimated precision for the same elements is 5 per cent
or better. The results for Ba are somewhat erratic at concentra-
tions below 30 ppm.

TABLE 7 .   COMPARISON OF ANALYTICAL METHODS

	Analytical methods compared	Sample loca-lity	Quotients of concentrations[4]			Concen-tration range
			No.	Mean	C.V.%	
						%
SiO_2	$Chem^1/XRF_{gl}^1$	A	19	0.988	0.8	47 - 50
Al_2O_3	-	-	19	1.001	1.4	11 - 17
FeO	-	-	21	1.005	0.9	10 - 15
CaO	-	-	11	1.018	1.1	9 - 11
K_2O	-	-	8	0.85	16	0.2 - 0.8
TiO_2	-	-	10	0.977	1.6	2 - 3
MgO	$Chem^{1,2}/XRF_{gl}^3$	-	39	1.000	4.4	5 - 11
Na_2O	$Chem^3/Chem^2$	-	29	0.979	7.1	1 - 3
SiO_2	XRF_p^1/XRF_{gl}^1	-	66	0.992	3.5	46 - 53
Al_2O_3	-	-	66	0.993	7.9	10 - 17
FeO	-	-	66	1.099	6.3	9 - 15
CaO	-	-	66	1.009	4.2	9 - 12
K_2O	-	-	8	1.01	7	0.2 - 0.8
MgO	XRF_p^1/XRF_{gl}^3	-	64	0.96	18	5 - 15
TiO_2	$XRF_p^1/Chem^1$	-	28	0.96	13	1 - 3
P_2O_5	XRF_p^2/XRF_{gl}^1	B	7	0.99	18	0.3 - 0.3
P_2O_5	XRF_p^2/XRF_{gl}^2	C	10	0.84	33	0.1 - 0.6
						ppm
Ba	$Spec/XRF_p^2$	-	46	0.71	15	30 - 350[5]
Zr	-	-	34	0.96	6.7	100 - 350[6]
Sr	-	-	50	0.90	8.6	70 - 460
Sc	$Spec/NAA^1$	-	10	0.84	12	35 - 52
Cr	-	-	10	1.10	14	22 - 260
Co	-	-	10	0.89	4	49 - 58
La	XRF_p^2/NAA^1	-	7	1.25	12	6 - 33
La	XRF_p^2/NAA^2	A	4	1.08	11	8 - 15

Comments on next page.

COMMENTS TO TABLE 7

Chem[1,2,3]   Chemical analyses by Ib Sørensen 1) about 1965
                  (partly published in Rasmussen and Noe-Nygaard
                  1969), 2) in 1977; 3) Na_2O analyses by Me Mou-
                  ritsen (flame photometry).

XRF$_{gl}$[1,2,3] XRF analyses on glass discs by 1) Ib Sørensen
                  1974 - 1975, 2) G. Hornung 1975, 3) R. Waagstein
                  1977.

XRF$_p$[1,2]   XRF analyses on rock powder by 1) Ib Sørensen
                  about 1965 (in Rasmussen and Noe-Nygaard 1969),
                  2) R. Waagstein in 1976.

Spec   Emission spectrography analyses by H. Bolling-
                  berg in 1975.

NAA[1,2]   Neutron activation analyses by 1) R. Gwozdz in
                  1975, 2) J.-G. Schilling (Schilling and Noe-
                  Nygaard 1974).

A   Basalts from the Faeroe Islands (Rasmussen and
                  Noe-Nygaard 1969).

B   Basalts from the Sneis profile, the Faeroe Islands.

C   Basalts from Faeroe Bank, Bill Bailey Bank and
                  Lousy Bank.

4   Number, mean and coefficient of variation of
                  quotients of results obtained with two different
                  analytical methods.

5   Less samples with < 30 ppm Ba.

6   Less samples with < 100 ppm Zr. Linear regression
                  analysis of all results gives $y = 1.19x - 25$, where
                  x and y are the XRF and spec. results in ppm.

The emission spectrography analyses are calibrated against synthetic mixtures using Pd as an internal standard. The results obtained for the international rock standards W-1 and BCR-1 of elements with concentrations above 30 ppm agree within limits of ± 15 per cent with the recommended values except for Ba (Table 6). The Ba results are systematically about 20 per cent too low compared to the recommended values. Several elements have been analysed with both emission spectrography and either XRF spectrography or NAA. The emission spectrography analyses give on average 30 per cent too low results for Ba and 10 per cent too low results for Sr compared to the XRF analyses, while the emission spectrography results for Co are about 10 per cent too low compared to the NAA results (Table 7). The emission spectrography and XRF results for Ba, Zr and Sr seem to be linearly dependent over the considered concentration ranges. Linear regression with the method of least squares gives $y = 1.27x + 6$ ($s_b = 0.03$) for Ba, $y = 1.19x - 25$ ($s_b = 0.02$) for Zr, and $y = 1.23x - 17$ ($s_b = 0.04$) for Sr, where x and y are the emission spectrography and XRF results, respectively, in ppm, and s_b is the standard deviation of the inclination factor. The regression lines clearly do not pass through the origin; the reason for this is not known. The emission spectrography analyses underestimate the total range of Sr and Zr concentrations in the basalts compared to the XRF analyses.

3.3.   Petrology of the Faeroes Islands

3.3.1. Earlier work

The first detailed petrological investigation of the Faeroese lava succession was made by Walker and Davidson (1936). They described the stratigraphy in a general way in terms of 5 main petrographic types of basalts which they compared with similar types of basalts from the Hebridean province. Litho-stratigraphically they divided the Faeroese lava sequence from below and upwards into a Suduroy group of mainly olivine-poor tholeiitic basalts, a Tórshavn group of mainly plagioclase-phyric and aphyric tholeiitic basalts, and an olivine-rich group with abundant olivine-basalt flows. They also found olivine-basalt flows in the two lower groups. According to Walker and Davidson (1936) many of these, apart from a paler colour of the pyroxene, were identical in thin sections to the Plateau Type of basalt flows of Bailey and others (1924). This suggested that alkali-olivine basalts were present on the islands (cf. Turner and Verhoogen 1960, p. 223), though none of the few chemically analysed basalts were nepheline normative.

The geological mapping of the Faeroes by Rasmussen and Noe-Nygaard (1969, 1970) has greatly extended the knowledge about the lava stratigraphy. They divided the lava pile into the Lower, Middle and Upper Basalt Series on a purely stratigraphic basis. The lava succession was investigated in all parts of the islands in a large number of profiles, from which they composed an arbitrary main or type profile through the basalt plateau. Most of the detailed petrographic studies and all geochemical studies were restricted to samples from this main profile (Noe-Nygaard and Rasmussen 1968). The lithological division by Walker and Davidson (1936) broadly coincides with the stratigraphic division in the

main profile. In the central part of the islands, however, the Tórshavn group included extensive Upper Basalt areas (cf. Fig. 3), and the type localities referred to by Walker and Davidson (1936) are Upper Basalts.

According to Noe-Nygaard and Rasmussen (1968) the Lower and Middle Basalts mainly consist of quartz tholeiites and the Upper Basalts mainly of olivine tholeiites. Only a couple of basalts were nepheline normative, probably due to zeolitization. They found that the Middle Basalts were chemically intermediate to the Lower and Upper Basalts in most respects. The average TiO_2 content of the basalts shows a large decrease upwards (Noe-Nygaard 1967). Noe-Nygaard (1966) demonstrated that the Tertiary basalts from the Faeroe Islands are similar to the Tertiary basalts in Iceland and East and West Greenland. He noted that the quartz tholeiites from this trans-atlantic belt are distinctly higher in FeO^*, TiO_2, P_2O_5 and K_2O, but lower in MgO and Al_2O_3 than the basalts now being erupted from the Mid-Atlantic ridge south of Iceland.

Schilling and Noe-Nygaard (1974) found that most Faeroese basalts were enriched in the light rare earth elements relative to the heavy ones. More surprisingly, however, they found that the olivine tholeiites in the Upper Basalts and a predecessor in the Middle Basalts were depleted in the light rare earth elements like ocean ridge basalts. They postulated that the latter basalts were derived from the low velocity zone of the upper mantle, while the light rare earth element enriched basalts were derived from hot mantle upwelling from deeper levels. To explain the fluctuations between the two magma types they suggested that the upwelling of hot mantle occurred in blobs rather than in a continuous flow as visualized for other supposed areas of rising mantle plumes by

Morgan (1971), Schilling (1973) and many others. Schilling and
Noe-Nygaard (1974) suggested that the basalts on the Faeroe Is-
lands and in East Greenland were erupted during a period of high
plume discharge 50-60 million years ago in the opening phase of
the Northeast Atlantic. They suggested that the plume activity
in this proto-Icelandic plume was similar to the activity of the
present Icelandic plume, and that the plume activity was much smaller
during most of the intervening period. It never completely ceased,
however, to judge from the high elevation of the sea floor between
the Faeroe Islands, Iceland and Greenland, and to judge from the
presence of both light rare earth element enriched and depleted
basalts in a DSDP borehole on the northern flank of the Iceland-
-Faeroe Ridge (Schilling, in press). The variation of other
trace elements in the Faeroe plateau confirms the occurrence of
both basalts enriched in LIL (large ionic radius lithophile) ele-
ments such as K, Ba, Sr and La and akin to the basalts from sup-
posed plume centres and LIL-element depleted basalts akin to
ocean ridge basalts (Bollingberg and others 1975).

3.3.2. Petrography

Classification on olivine content. The Faeroese basalts range from olivine tholeiites to quartz tholeiites. No andesitic or more evolved lavas have been observed. Olivine tholeiites are usually classified as basalts with normative olivine and hypersthene and quartz tholeiites as basalts with normative quartz and hypersthene (Yoder and Tilley 1962).

In Tertiary and older basalts, which have nearly always passed through a stage of low-temperature alteration, the effect of alteration on the norm must be considered. It is common practice to correct the norms for low-temperature oxidation by adjusting either the Fe_2O_3 content or the ratio between Fe_2O_3 and FeO to some low fixed value similar to that found in fresh basalts. It is thereby assumed that the alteration process has been isochemical apart from the uptake of oxygen and water. This is clearly not always the case, however, as will be demonstrated later (sections 3.3.4. and 3.6.2.)

Macdonald and Katsura (1964) have proposed a limit of 5 per cent modal olivine to differentiate between tholeiitic olivine basalt and tholeiitic basalt from Hawaii. This petrographic criterion was also adopted for the basalts from the Faeroe region, but following Carmichael (1964) the shorter terms olivine thole-iite and tholeiite were preferred. The terms tholeiite or tholeiitic basalts is sometimes used to denote both types of basalts, but in case of ambiguity the prefix olivine-poor or olivine-free can be used.

Nearly all Faeroese basalts carry groundmass olivine. Macdonald and Katsura (1964) claim that the Hawaiian basalts of the tholeiitic suite do not contain proper groundmass olivine, and that the phenocrysts or microphenocrysts of olivine usually show signs of resorption. However, Moore and Evans (1967) have detected

groundmass olivine with the electron microprobe in the uppermost part of the prehistoric Makapuhi lava lake. Only below 6 metres depth in this tholeiitic lava lake was the cooling rate slow enough to allow complete reaction of the small groundmass olivine crystals with the residual liquid.

Phenocrysts. The plagioclase phenocrysts tend to be subequant in the olivine tholeiites but tabular in the tholeiites. The composition of the plagioclase phenocrysts averages An_{84} in the Upper Basalt olivine tholeiites and An_{66} in the Middle Basalt tholeiites (Noe-Nygaard and Rasmussen 1968). The subequant plagioclase crystals are mostly between 0.2 and 2 millimetres in diameter and are often intergrown in small, compact glomerocrysts, in which smaller crystals are partly or completely enclosed by larger ones. The crystals seem commonly to have grown together in a twin position as so-called synneusis twins (Vance 1969). The phenocrysts and glomerocrysts are mantled by a thin rim of more albitic plagioclase. The core-rim transition is often sharp and the cores in rare cases show slight signs of resorption.

The tabular plagioclase phenocrysts usually range in size from 1 to 20 millimetres, but may be even larger. They also usually form glomerocrysts, but the crystals are more loosely grown together and often at oblique angles to each other. Sometimes the plagioclase tablets radiate out from a common nucleation centre occupied by one or a few small olivine crystals. In thin section most glomerocrysts show less than 10 individuals, but in some basalts they show 50 or more individuals. The tabular plagioclase is usually unzoned apart from a narrow zonal rim , and shows no signs of resorption.

The subequant plagioclase occurring in compact glomerocrysts

has probably crystallized slowly in a magma chamber to judge from the interlocking crystal boundaries and the common occurrence of synneusis twins. Similar glomerocrysts are very common in ocean ridge basalts, and were first noted in these rocks by Muir and Tilley (1964). The tabular plagioclase occurring in loose glomerocrysts has probably crystallized much more rapidly to judge from the larger surface/volume ratio of the crystals, the loose form of the glomerocrysts, the apparent stellar growth of some glomerocrysts and the lack of zoning. The large tabular crystals have often settled a few centimetres or decimetres after the extrusion of the lava, and in a magma chamber they would soon have settled out of the magma. The rapid growth of the large tabular crystals is therefore probably the result of a sudden rise of the plagioclase liquidus due to the formation of a gas phase by pressure release during the ascent of the magma.

In many of the Faeroese basalts the plagioclase phenocrysts are of some intermediate type and can only with difficulty be grouped with either of the above two phenocryst types.

In some basalts, especially in the upper part of the Middle Basalts, two distinct sizes of tabular phenocrysts are found (Fig. 12 and Table 17). The phenocrysts belonging to the larger size class are always few, and it is suggested that they have been derived from non-consolidated cumulates incorporated into the magma on the way up.

The olivine phenocrysts are mostly of the polyhedral type in the terminology of Donaldson (1976), that is equant or tabular with well-formed crystal faces. However, they grade into the granular type with rounded edges and rounded groundmass inclusions or the skeletal (hopper) type with smooth curvilinear lobes and re-entrants. The form is mostly equant or subequant and the size 0.2-2

millimetres. Thin, tabular crystals are also present in many basalts, however, and may exceed 5 millimetres in length. In several olivine-rich basalts the crystals are all thin, tabular and sometimes strongly skeletal. In cross section they may be filled with holes and look like a straight chain, or nearby olivine plates may be parallel as if they were part of the same crystal (cf. Donaldson 1976). The olivine phenocrysts are completely altered in most of the tholeiites, but fresh or at least partly preserved in most olivine tholeiites. The alteration products are varied sheet silicates or more rarely mineraloids, calcite, zeolites or opaque minerals.

Tiny inclusions of a brown, translucent spinel often occur in the subequant, fresh olivine, especially in the olivine-rich basalts, but are rare in the thin, tabular crystals. Spinel inclusions are not observed in altered olivine.

The clinopyroxene phenocrysts are equant, sub- or euhedral, with a diameter of 0.5-2 millimetres and some show simple twinning. A thin rim with a slightly different extinction is sometimes seen and belongs to the microphenocryst stage of crystallization. Orthopyroxene phenocrysts occur in a small group of chemically anomalous flows in the Sneis profile (Table 17).

The most olivine-rich basalts are picritic with 15-30 per cent olivine mainly as phenocrysts (cf. Fig. 14a). The olivine is usually equant and therefore possible cumulate, but a few samples with tabular, skeletal olivine and no phenocrysts of other minerals probably represent true picritic liquids. These supposed liquids include both LIL-element enriched and depleted magma types. Most of the strongly olivine-phyric basalts also carry some plagioclase phenocrysts, however, whether the olivine is equant or thin, tabular, while clinopyroxene phenocrysts occur in addition

to the olivine and plagioclase phenocrysts in some of the LIL-element enriched types.

The olivine tholeiites with about 5-15 per cent olivine are usually only weakly porphyritic, microphyric or even aphyric. Olivine tends to be the dominant or only phenocryst mineral in the more olivine-rich types, while plagioclase tends to be the dominant or only phenocryst phase in the more olivine-poor types. Clinopyroxene phenocrysts often occur subordinately to the olivine and/or plagioclase phenocrysts in the LIL-element enriched olivine tholeiites, while in the LIL-element depleted olivine tholeiites they are only seen in samples fairly rich in plagioclase phenocrysts.

Tholeiites with about 1-5 per cent olivine are nearly all plagioclase-phyric. The amount of phenocrysts is very variable, but averages about 10 per cent. Olivine phenocrysts are subordinately present in all, except the most sparsely porphyritic, tholeiites, but usually only as pseudomorphs. A minor part of the olivine-bearing tholeiites also carries clinopyroxene phenocrysts.

The tholeiites with no or less than about 1 per cent olivine are again mostly weakly porphyritic, microphyric or aphyric. Plagioclase is the dominant phenocryst mineral, but olivine or clinopyroxene phenocrysts are occasionally seen too.

Microphenocrysts. Most of the Faeroese basalts contain microphenocrysts either in addition to the true phenocrysts or as the only type of phenocryst. The plagioclase microphenocrysts are typically thin, tabular and less than 1 millimetre long. They are unzoned apart from a narrow normally zoned rim. The clinopyroxene microphenocrysts are typically equant, 0.2-0.5 millimetre in diameter and are commonly optically strained. Most of the

optically strained crystals consist of domains with slightly different extinctions (rarely forming an hourglass-structure), but in some basalts there is a complete gradation into small glomerocrysts consisting of discrete pyroxene grains of widely differing orientations. The olivine microphenocrysts are typically equant, sub-euhedral and 0.1-0.5 millimetre in diameter. They sometimes show embayments in their crystal outline, which are probably relicts of initial skeletal growth of the olivine.

It is sometimes difficult to distinguish between phenocrysts and microphenocrysts, but the presence of a particular type can often be seen from bi- or poly-mineralic glomerocrysts. The pyroxene microphenocrysts are easy to identify due to their anhedral form and lattice distortions. This type of pyroxene is never grown together with large plagioclase or olivine phenocrysts. The microphenocrysts of pyroxene often form small bi-mineralic glomerocrysts together with the plagioclase microphenocrysts, on the other hand, and in case of doubt the presence of plagioclase microphenocrysts can be established by finding such micro-glomerocrysts. Sometimes a pyroxene microphenocryst encloses the plagioclase subophitically, and the plagioclase microphenocrysts then often get thinner or wedge out near the centre of the pyroxene grain indicating that the two minerals have grown simultaneously. The phenocrysts and microphenocrysts of olivine are less commonly grown together with the other two minerals, and it is therefore sometimes impossible to be sure whether the olivine has started to crystallize early or late in comparison to other phenocryst minerals.

In the most fine-grained basalts the microphenocrysts are easily discernible from the groundmass minerals, but in the less fine-grained basalts the plagioclase and olivine microphenocrysts

often show a complete size gradation into the groundmass. The pyroxene microphenocrysts are easier to identify in the latter cases, because most basalts have an intergranular texture, which means that the groundmass pyroxene forms fine aggregates between the network of plagioclase crystals. Again, the presence of microphenocrysts of the other two minerals may be confirmed in those cases where some of them occur in glomerocrysts together with the pyroxene.

During the hand specimen classification of basalts from the Faeroe region a pure size criterion had to be used to distinguish between porphyritic and microphyric basalts using a maximum size of one millimetre of the crystals as a limiting value (section 3.2.3. and Table 11 and 12). During the microscopy of thin sections an attempt was made to differentiate between crystals of the phenocryst, microphenocryst and groundmass stage of crystallization not only from their size, but also from their appearance and relationships with other minerals (Table 8 , 17 and 18). Many basalts contain phenocrysts of plagioclase and olivine, while the pyroxene has crystallized later as microphenocrysts. Microphenocrysts of plagioclase and olivine are usually present in this case too, and show that these minerals started to nucleate again simultaneously with the pyroxene. The more albitic rims around the plagioclase phenocrysts with a thickness similar to the half-width of the microphenocrysts likewise indicate an accelerated growth of this mineral. Similarly, more fayalitic rims have probably been deposited on the olivine phenocrysts, but are only occasionally seen as an increase in the birefringence. In basalts with only a few pyroxene microphenocrysts the plagioclase and olivine often do not form clear microphenocrysts, however, and it is not clear whether this is due to a delay in the nucleation of plagio-

clase and olivine or whether the growth of early formed crystals of these minerals have been restrained by a continued growth of new crystals.

The typical microphenocrysts have probably crystallized at a rather high degree of undercooling. This is suggested by the slenderness of the plagioclase crystals and their higher albite content compared to the phenocrysts. The albite content of the crystallizing plagioclase is highly temperature-dependent, and the difference between the albite content in the phenocrysts and microphenocrysts appears directly as a difference in the extinction angle between the core and thin mantle of the plagioclase phenocrysts. The lattice distortions and anhedral form of the pyroxene are probably also a result of undercooling. This undercooling is easily explained as an effect of the rapid cooling of the basalts after the extrusion, but may also be a consequence of a rise in the liquidus temperature due to degassing during extrusion. Though the microphenocrysts have probably not crystallized in equilibrium with the basalt magma the presence of microphenocrysts of olivine, plagioclase and clinopyroxene is supposed to indicate that these minerals are either on or close to the liquidus of the magma at a pressure of one atmosphere.

Groundmass minerals. The plagioclase is lath-shaped in thin section, twinned, with an ill-defined crystal outline and usually normally zoned in the outermost part. The plagioclase crystals rarely exceed 1 millimetre in length.

Most of the pyroxene is augite or ferroaugite, but pigeonite is subordinately present in the tholeiites (Noe-Nygaard and Rasmussen 1968). The vast majority of basalts have an intergranular pyroxene texture. The average grain size of the intergranular

pyroxene is generally between 0.02 and 0.07 millimetres and tends to increase with decreasing olivine content. Subophitic texture has been observed in all types of basalts but is uncommon. According to Walker and Davidson (1936) and Noe-Nygaard and Rasmussen (1968), the olivine tholeiites typically have an ophitic texture. The present author has observed ophitic texture in almost all the LIL-element depleted olivine tholeiites just around the B-level in the Middle Basalts, but only in a few olivine tholeiites from higher stratigraphic levels and in none of the LIL-element enriched olivine tholeiites in the lower part of the Middle Basalts. The maximum size of the ophitic crystals averages 0.5 to 2 millimetres in diameter.

The Fe-Ti oxides consist of equant magnetite and tabular ilmenite. The magnetite grades in form between fine cubes, fine dendritic crystals, small, irregular, subhedral crystals, subpoikilitic, subhedral crystals and large, poikilitic crystals with a more or less cubic outline. The average grain size is between 0.01 and 0.2 millimetres. The small, irregular crystals partly bounded by crystal faces are most abundant and are often intergrown. The fine cubes and dendritic crystals mainly occur in basalts poor in mesostasis, while the subpoikilitic and poikilitic crystals, which partly or fully enclose crystals of the other groundmass minerals, are mostly found in basalts with more than a few per cent mesostasis. The poikilitic crystals exceed 0.5 millimetres in maximum size in some tholeiites, especially in the Lower Basalts, and contain many inclusions of the other groundmass minerals. The large poikilitic crystals are microphenocrystic in size and are considered by Noe-Nygaard and Rasmussen (1968) as true phenocrysts which have resided for a long time in the melt. However, the present author has not observed any clear examples

of magnetite grown together with microphenocrysts or phenocrysts of plagioclase, pyroxene or olivine and believes that the magnetite in most or all cases has started to nucleate later than these minerals. Magnetite crystals of a similar size are sometimes seen in patches of residual melt and range in form from intricate skeletons to nearly perfect cubes.

Tabular ilmenite is almost always present in addition to the magnetite. The tabular ore occurs in small amounts in most basalts, but is the major type of ore in many of the plagioclase--phyric basalts and often the only type in the segregation veins or patches regardless of the composition of the host basalt. The tabular ilmenites range in form from small, thick tablets to thin, platy skeletons. The skeletons appear in thin section as discontinuous laths or needles which sometimes occur in pairs side by side. The skeletons are generally less than one millimetre in length, but may attain a length of several millimetres in segregation veins and patches. In most basalts the ilmenite is of some intermediate form.

The groundmass olivine is typically equant, sub- or anhedral with an average diameter between 0.05 and 0.15 millimetres. The olivine shows no reaction relationship with the residual liquid and may be found even in segregation veins or patches. The groundmass olivine is predominantly fresh in olivine-rich basalts with a zeolitic mesostasis and fairly often is partly preserved in other olivine tholeiites. It is nearly always completely altered in the tholeiites. Most commonly, olivine is replaced by sheet silicates and mineraloids which have a greenish colour when they are non-weathered. In basalts poor in interstitial alteration products the partly or completely altered olivine is more easy to see than fresh olivine. In the basalts rich in intersti-

tial alteration products the altered olivine is more difficult to recognize but its pseudomorphs can usually be distinguished from altered mesostasis by their outline, relict cracks, textural relationships and/or by differences in the colour, birefringence or orientation of the alteration products (cf. Baker and Haggerty 1967, p. 260-263). In some olivine-poor basalts it is impossible, however, to estimate the former olivine content accurately.

Mesostasis. The abundance of mesostasis in the Faeroese basalts averages about 5 per cent, but varies from less than 1 per cent to more than 15 per cent (cf. Rasmussen and Noe-Nygaard 1969, p. 75-80). The olivine tholeiites with intergranular pyroxene texture generally are much poorer in mesostasis than the tholeiites. In the intergranular and subophitic basalts the mesostasis predominantly represents the residual liquid, but it now consists mainly of mineraloids or fine aggregates of sheet silicates with greenish, yellowish or brownish colours. For the want of a common name these earthy microcrystalline or amorphous substances will be called coloured alteration products. The difference in colour probably reflects a difference in the degree of oxidation rather than in the overall chemistry. In many basalts the mesostasis contains quench crystals which nearly exclusively occur in narrow interstitial spaces, but not in the large interstitial areas. At low degrees of crystallization the quench crystals consist of tiny cubes or skeletons of magnetite, while at higher degrees of crystallization fibrous pyroxene occurs in abundance together with the magnetite. The areas rich in fibrous pyroxene have a turbid, pale brownish colour and do not appear to be appreciably altered. In some rocks the anisotropic pyroxene-rich areas alternate with small isotropic areas of a similar colour

which are supposedly fresh or slightly hydrated glass.

The mesostasis in the intergranular basalts is more or less concentrated into diffuse patches or bands with an order of thickness of 1 millimetre. The mesostasis occurs in these areas in a framework of plagioclase mainly at the expense of pyroxene and Fe-Ti oxides. Areas moderately enriched in mesostasis have an intersertal texture with only some pyroxene and ore replaced by mesostasis, while areas strongly enriched in mesostasis have a hyalo-ophitic texture with little or no pyroxene and ore between the plagioclase laths. The inverse relationship between mesostasis and pyroxene plus ore suggests that the mesostasis in the intersertal and hyalo-ophitic areas represents in situ residual melt rather than residual melt drained from the intergranular, mesostasis-poor parts of the groundmass. In larger interstitial areas the mesostasis rarely contains any quench crystals as mentioned above, and sometimes consists of zeolites. Thus, in some cases, the mesostasis probably does not replace glass, but fills in irregular cavities in the groundmass formed by crystallization shrinkage of the lava. Such cavities may, in form and size, grade into gas vesicles filled with coloured alteration products and/or zeolites.

The ophitic olivine tholeiites contain similar amounts of mesostasis to the tholeiites. The mesostasis is concentrated in areas between the ophitic pyroxene crystals. In smaller areas the mesostasis occurs in an open network of plagioclase crystals, whereas in larger areas plagioclase crystals project into the mesostasis. This minor texture is sometimes named diktytaxitic (cf. Wilkinson 1967, p. 200). Small olivine crystals sometimes adhere to the plagioclase, while ore minerals are uncommon in the mesostasis-rich areas. The mesostasis often consists only of

zeolites and never contains skeletal quench minerals. It is therefore difficult to tell how much of the mesostasis replaces glass and how much fills cavities.

Segregation patches and veins. A small proportion of the inter-granular basalts contain segregation patches or veins. The patches are mostly about 1 millimetre in diameter, and rarely more than 5 millimetres. The patches in rare cases fill former gas vesicles. The small segregation patches consist of the same minerals as the surrounding groundmass but are more coarse-grained and generally richer in mesostasis which often contains quench crystals of ilmenite or magnetite and sometimes also of pyroxene and plagioclase. The veins are typically horizontal, 1 to 10 centimetres thick, more fine-grained than the host basalt and have fewer or no phenocrysts. They are similar in mineralogy to the host basalt, but the ore mainly or exclusively consists of thin, platy ilmenite which may reach several millimetres in length and looks like small, shiny hairs in hand specimen.

3.3.3. Petrographic stratigraphy

Lower Basalts. Most of the Lower Basalt flows in the main pro-
file on Suduroy are slightly microphyric or aphyric tholeiites.
They have an estimated average olivine content of 1-2 per cent.
The olivine mostly occurs in the groundmass and is nearly always
completely altered. The pseudomorphed olivine grains are often
difficult to recognize, but only a few flows seem to have been de-
void of olivine. The microphenocrysts consist of plagioclase,
pyroxene and occasionally olivine. The groundmass magnetite forms
large poikilitic crystals in several flows, most of which have
less than 1 per cent olivine. A small number of the Lower Basalt
tholeiites on Suduroy are weakly porphyritic with true phenocrysts
of plagioclase and sometimes also pyroxene and olivine. Some oli-
vine-tholeiitic flows occur in the uppermost part of the Lower Ba-
salts on both Suduroy and Vagar. In the former place the olivine
occurs in the groundmass and is completely altered (Table 8),
whereas a couple of flows in the latter place carry fresh olivine
partly as phenocrysts (cf. Rasmussen and Noe-Nygaard 1969, p. 93).

Early Middle Basalts. In the lowermost 200-300 metres of the
Middle Basalts on both Suduroy and Vágar olivine-phyric, olivine-
-microphyric and aphyric olivine tholeiites alternate. A few of
the olivine-phyric flows are picritic with more than 15 per cent
olivine. A flow in the main profile (No. IV.11) contains nearly
30 per cent olivine mainly as phenocrysts, which are thin, tabular
and partly skeletal, but there are no phenocrysts of other mine-
rals. This flow probably represents a true picritic liquid. Most
other olivine-phyric basalts also contain some small phenocrysts
of plagioclase and pyroxene. A single flow in the main profile
is plagioclase-phyric. Some of the olivine-microphyric basalts
contain a few microphenocrysts of plagioclase and pyroxene.

TABLE 8 . MODAL COMPOSITION OF BASALTS FROM THE FAEROE ISLANDS

	Late Lower Basalts			Late Middle Basalts				
	III.2	III.6	III.7	15586 B-horizon	15507	15522	15539	15559

Whole rock modal composition (%)

	III.2	III.6	III.7	15586 B-horizon	15507	15522	15539	15559
Olivine	7.5^c	5.8^c	7.8^c	14.2	26.1	4.2^a	1.2^c	1.8^c
Plagioclase	37.7^a	39.5	49.2	47.9^a	37.8^a	54.3	47.9	47.1
Clinopyroxene	39.7	43.6	34.0	30.6	25.9	26.5	32.3	33.2
Ore	5.3	5.9	4.1	2.2	3.1^e	5.8	5.1	7.6
Mesostasis^d	9.8^c	5.2^b	4.9^b	5.1^c	7.1^c	9.2^b	13.5^b	10.3^c
Total	100.0	100.0	100.0	100.0	100.0	100.0	100.0	100.0

Modal % phenocrysts and microphenocrysts

	III.2	III.6	III.7	15586 B-horizon	15507	15522	15539	15559
Olivine		< 1		3.7^f	13.1^f	3.9	$\pm$	$\pm$
Plagioclase	1.0	0.8	15.5	6.8^f		32.7	18.9^f	6.5^f
Clinopyroxene	~ 3	< 1	~ 3			0.4^f	0.4^f	0.4^f

Maximum size of phenocrysts and microphenocrysts (mm)

	III.2	III.6	III.7	15586 B-horizon	15507	15522	15539	15559
Olivine				1.0	2.8	1.3	0.9	1.4
Plagioclase	1.5	0.8	2.2	1.2	0.4	10	4	3
Clinopyroxene	0.6	0.8	1.0	Ophitic	Ophitic	0.5	0.5	1.6

Comments: 1000 or 2000 (III.7) counts inside 1.8 sq.cm at 80 x magnification.
a) >10 % altered, b) >90 % altered, c) completely altered, d) including amygdales,
e) including 0.2 % spinel in olivine, f) grades into the groundmass minerals.

The next 600 metres of the Middle Basalts up to the B-horizon are poorly sampled (profiles VII-IX in the main profile), but plagioclase-phyric tholeiites clearly dominate. Most of them also carry phenocrysts or microphenocrysts of olivine and pyroxene. The uppermost sample (No. IX.2) is olivine-tholeiitic with fresh olivine occurring in the groundmass. This sample shows a large, strongly resorbed phenocryst of (?)albite-rich plagioclase together with a few microphenocrysts of plagioclase, olivine and pyroxene.

Late Middle Basalts. The uppermost 600 metres of the Middle Basalts have been closely sampled by the author in the Sneis profile on northern Streymoy in the same place as profile X in the main profile. The profile starts with the B-horizon which here consists of 3 flows with a total thickness of about 15 metres (Fig. 12). These flows are the earliest flows in the main profile with ophitic texture. They carry a few per cent of phenocrysts of plagioclase and olivine with a maximum size of about 1 milli-metre and contain about 14 per cent fresh olivine (Table 17 and 8). The B-horizon flows in the Sneis profile are the only repre-sentatives of the Eide group of olivine-tholeiitic flows which attain a total thickness of about 100 metres in northernmost Streymoy and Eysturoy (Fig. 3) (Rasmussen and Noe-Nygaard 1969). Most of these flows have an ophitic texture and some are strongly olivine-phyric. 80 metres above the base of the B-horizon in the Sneis profile occurs another olivine-tholeiitic horizon. This 7 metre thick horizon is picritic with about 26 per cent olivine partly occurring as up to 2-3 millimetres sized, equant phenocrysts in an ophitic groundmass (Table 8 and 17); it can be followed over a distance of at least 7 kilometres. The next olivine t[ole]-iites in the profile are the C-horizon flows about 500 metres

FIGURE 12. The Sneis profile, Faeroe Islands.
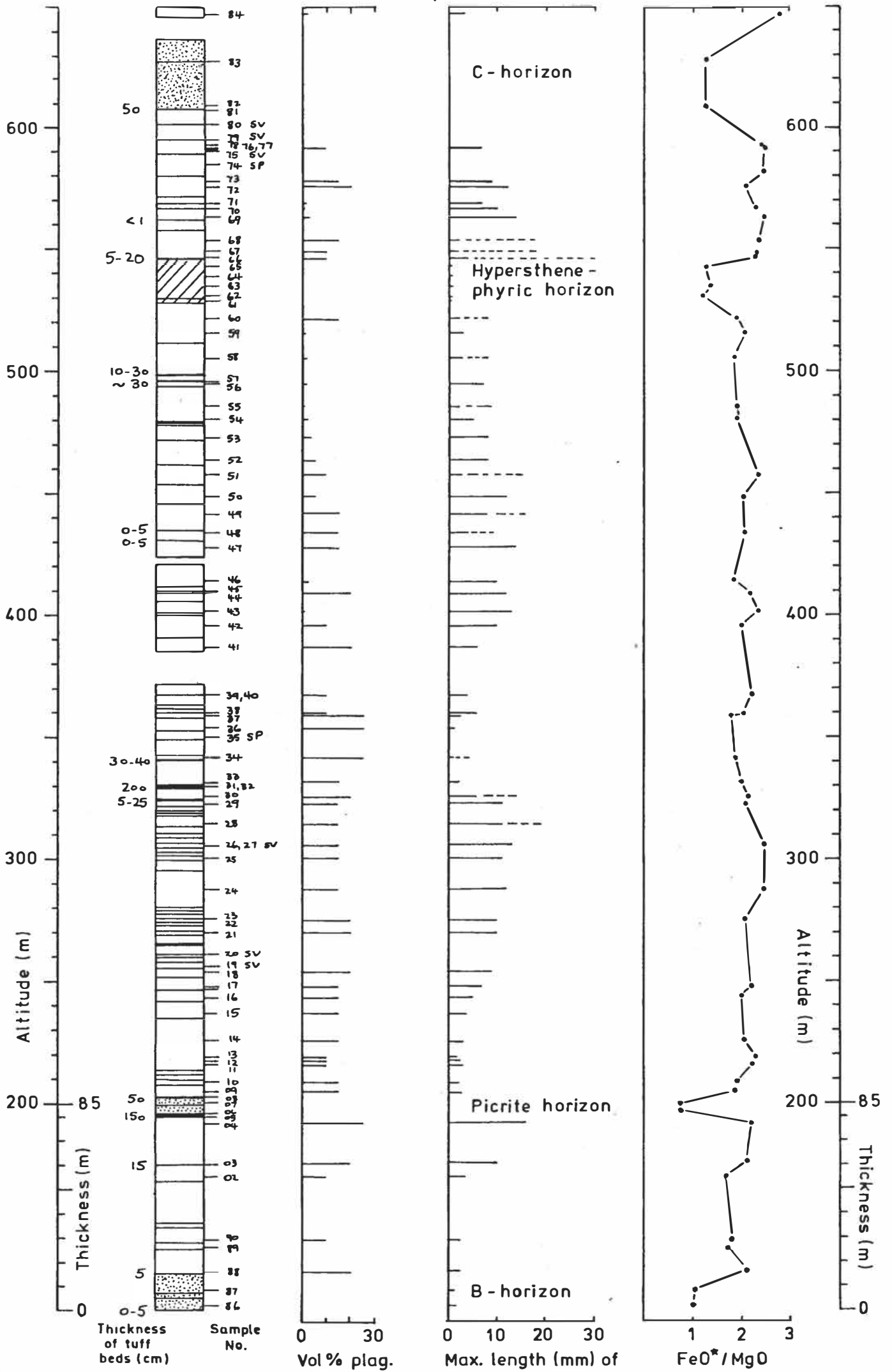
higher up in the lava sequence (section 2.1.1.). The C-horizon here consists of two flows or flow units, each about 10 metres thick, which are slightly microphyric in plagioclase and olivine with a very fine-grained intergranular groundmass poor in meso-stasis.

About 80 metres below the C-horizon occurs the only lava on the Faeroes in which orthopyroxene phenocrysts have been observed. The lava is about 9 metres thick and consists of 3-4 flow units with sparse phenocrysts of orthopyroxene, olivine (sometimes mantled by orthopyroxene), clinopyroxene and plagioclase.

The major part of the late Middle Basalts consists of plagio-clase-phyric tholeiites. Nearly all of them also carry a few small olivine phenocrysts which are sometimes partly fresh, while clinopyroxene almost exclusively occurs in the groundmass and as sparse microphenocrysts (Table 17). The groundmass is typically rather coarse-grained and mesostasis-rich. Almost all basalts seem to contain a little, altered groundmass olivine which is some-times difficult to distinguish from the interstitial alteration products.

Most of the lava succession is completely exposed in a stream bed. The well exposed tholeiitic flows are of the typical pahoe-hoe type described by Macdonald (1967). The lava beds are rarely more than 4 metres thick with abundant round vesicles and smooth or exceptionally ropy tops. Lava beds more than one metre thick often appear as more or less distinct benches in the stream. The bed partings are seen as a red line or surface. Below this often occurs a 5-50 centimetres thick zone almost devoid of phenocrysts, while a corresponding cumulus zone occurs in the bottom of the flow. The lower crust appears as a few centimetres thick zone with a similar amount of phenocrysts to the middle of the bed,

while the upper crust contains sporadic phenocrysts. The thinner beds are vesicular throughout, but beds more than about 2 metres thick may be almost compact in the lower part except for a thin bottom zone. The most clear partings are shown in Fig. 12. Some of the beds consist of several thin sub-units, which are mostly very indistinct.

The many beds in which the phenocrysts have settled are likely to have cooled slowly, and this suggests that they were formed in quick succession during a single eruption. Other factors remaining constant, the last flow unit during this eruption should show the least settling of the plagioclase, but in practice the thicknesses of the phenocryst-poor top zones can only be roughly estimated because they form the flat parts of the stream bed and are crowded with amygdales. Besides, the settling velocity clearly depends on the size of the plagioclase phenocrysts. It is thus impossible in the field to tell how many flow units have formed during a single eruption. Tuffaceous beds, which are generally supposed to indicate a longer pause in the volcanic activity, are infrequent, but place a lower and upper limit of the thickness of basalts poured out during a single eruption at 3 and 120 metres, respectively.

The abundance and size of the plagioclase phenocrysts seem to vary in a cyclic manner at intervals of 100-200 metres (Fig. 12). The variation of these two parameters is not in harmony and is difficult to understand. Besides, as explained earlier, several beds show two distinct size classes of plagioclase phenocrysts.

The three flows below the C-horizon are composite and consist of a lower, strongly plagioclase-phyric part and an upper aphyric part. The transition between the two parts is sharp as to the phenocrysts whereas no boundary is visible in the groundmass even

in thin section. All three composite flows show aphyric segregation veins about 0.5 metre above the base. Several similar composite flows occur above the C-horizon, but have not been investigated in detail.

Upper Basalts. The Upper Basalts are the most inhomogenous part of the Faeroese lava sequence. Olivine tholeiites are abundant in the northeastern and northern part of the islands, but much less common in the central part of the islands. In addition, there is an increase in the abundance of olivine tholeiites from west to east across the northern part of the islands (Rasmussen and Noe-Nygaard 1969). The macroscopic olivine-phyric types mainly occur in a roughly 15 kilometres wide E-W belt in the northernmost part of the islands (Fig. 3) in which profile XI of the main profile is situated (Fig. 2). The olivine tholeiites in the main profile show a crude variation upward from strongly olivine-phyric basalts near the base of the Upper Basalts, through nearly aphyric basalts with a few small phenocrysts or microphenocrysts of olivine and plagioclase in the middle of the profile to plagioclase-phyric basalts with additional phenocrysts of both olivine and clinopyroxene in the highest exposures[1]. Several forerunners for the Upper Basalt olivine tholeiites occur in the uppermost part of the Middle Basalts in the northern and northeastern part of the islands. A prominent group of olivine-rich basalts occurs

---

[1] The present author has only seen microphotographs of the thin sections of the samples from profile XI and some of the uppermost samples are possibly tholeiites in a petrographic sense with less than 5 per cent olivine. However, geochemically they are very similar to those richer in olivine. These uppermost samples were also classified as olivine tholeiites by Noe-Nygaard and Rasmussen (1968).

about 100 metres below the top of the Middle Basalts in the south-
western part of Eysturoy but seems to thin out quickly in all di-
rections except possibly towards the north (cf. profiles 18, 21,
22 and 23 in Rasmussen and Noe-Nygaard 1969). One of these flows
(No. 21.6) contains roughly 25 per cent fresh olivine phenocrysts
and a little groundmass olivine in an intergranular groundmass.
The olivine phenocrysts are dominently thin, tabular with a maxi-
mum length of 3.5 millimetres and partly skeletal. As no other
phenocrysts are observed this basalt may well represent a picritic
magma.

The tholeiites within the Upper Basalts are dominantly porphy-
ritic like the tholeiites from the Middle Basalts, but generally
form thicker flows. A few samples of plagioclase-phyric thole-
iite have been collected from the lower part of the Upper Basalt
main profile and these are petrographically similar to tholeiites
from the Middle Basalts.

Intrusions. The petrography of the dykes, sills and irregular
intrusions has been described by Rasmussen and Noe-Nygaard (1969,
1970) and Walker and Davidson (1936). They seem to represent
the same type of basalt as the flows, though the former authors
note that the dykes are generally more rich in olivine.

3.3.4. Chemistry

Low-temperature alterations. The alteration of the residual glass presents itself chemically as a scatter in the granitic components SiO_2, Na_2O and K_2O of the basalts. The tholeiites from the Sneis profile are all fairly similar chemically (Table 17). Their SiO_2 contents taken from analyses recalculated to 100 per cent without H_2O^+ decrease at a H_2O^+ content near 1 per cent and then keep roughly constant with increasing H_2O^+ (Fig. 13). SiO_2 averages 49.9 per cent on a water-free basis in 10 basalts with H_2O^+ less than 1 per cent but 49.2 per cent in 35 basalts with H_2O^+ more than 1 per cent, whereas the differences for other elements are small (Table 9). The average compositions of the basalts at four incremental steps of H_2O^+ are also very similar considering the small number of samples they are based on (Table 9). The 10 basalts with H_2O^+ less than 1 per cent are evenly distributed in the profile among similar basalts lower in SiO_2. The variation of SiO_2 with H_2O^+ may be explained as a leaching effect. The basalts with H_2O^+ less than 1 per cent appear generally to have a less altered mesostasis and are more often fine--grained, mesostasis-poor than basalts higher in H_2O^+. The composition of the original residual liquids is not known. However, the estimated average mesostasis content in the Sneis tholeiites is only about 10 per cent and the residual liquid may therefore well have been rhyolitic. Rhyolitic residual glass has been reported by Wilkinson and Duggan (1973) in a tholeiite with a similar composition and a similar content of residual glass as the Sneis tholeiites. The end products of the alteration of the residual glass seem to be chlorites which are generally low in silica (cf. Deer and others 1962). Assuming an original content of residual glass of 10 per cent and a difference of 20 per cent
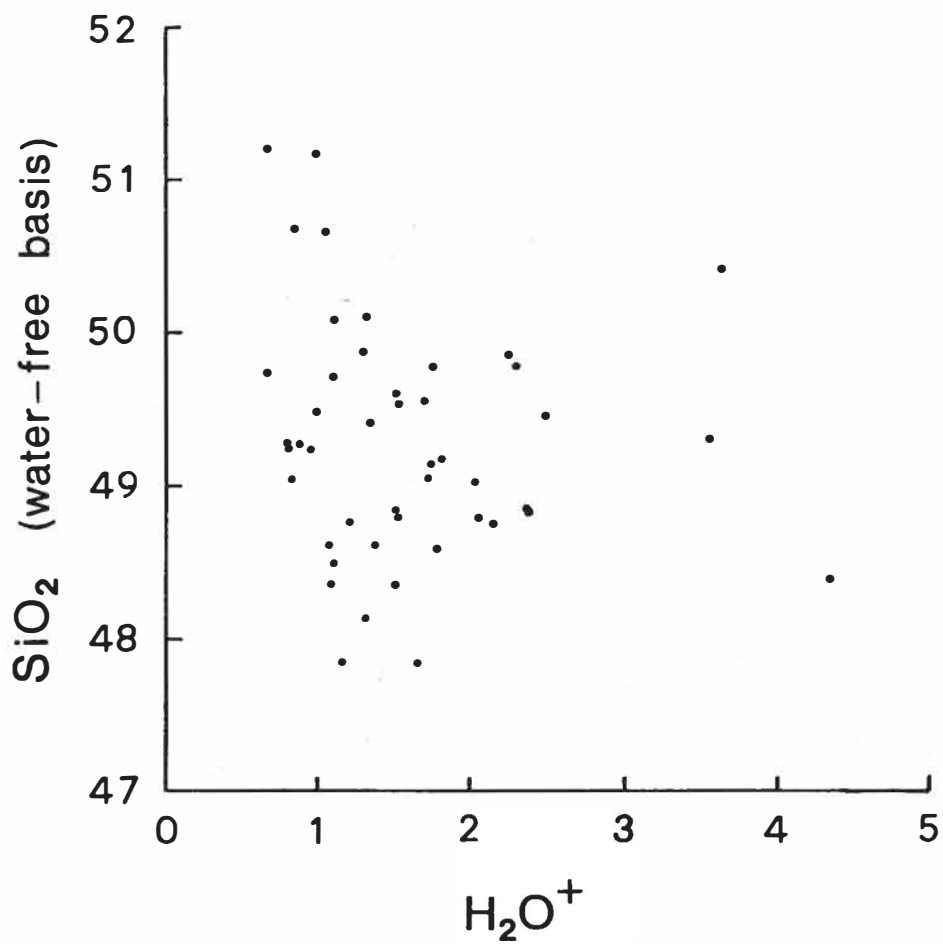
FIGURE 13. SiO$_2$ on a waterfree basis versus H$_2$O$^+$ for tholeiites from the Sneis profile, Faeroe Islands. (excluding hypersthene-phyric basalts and segregation veins and patches).

TABLE 9. AVERAGE COMPOSITION OF THOLEIITES FROM THE SNEIS
PROFILE AT INCREMENTAL STEPS OF H_2O^+

H_2O^+	0-1.00	1.01-1.51	1.51-2.00	2.01-4.00	1.01-4.00
No. of samples	10	14	10	11	35
SiO_2	49.91	49.04	49.22	49.26	49.17
TiO_2	2.83	3.09	2.92	2.84	2.96
Al_2O_3	15.02	14.76	15.12	15.64	15.14
Fe_2O_3	4.32	4.80	4.97	4.34	4.70
FeO	8.28	8.51	7.76	7.82	8.08
MnO	0.20	0.20	0.20	0.20	0.20
MgO	5.56	5.81	5.92	5.84	5.85
CaO	10.64	10.76	10.84	10.50	10.70
Na_2O	2.57	2.40	2.39	2.93	2.56
K_2O	0.36	0.29	0.32	0.32	0.31
P_2O_5	0.31	0.34	0.34	0.31	0.33
Total	100.00	100.00	100.00	100.00	100.00
H_2O^+	0.83	1.22	1.67	2.68	1.81
FeO*	12.17	12.83	12.23	11.73	12.31
FeO*/MgO	2.19	2.21	2.07	2.01	2.10
Plagioclase phenocrysts					
Modal %	8.7	11.0	12.0	13.7	12.1
Max. length[1]	8.1	6.1	4.7	6.9	6.0

[1] Note that the figures for the maximum length of the plagio-
clase phenocrysts are averages weighed according to the abundance
of phenocrysts.

SiO_2 between the residual glass and its final alteration products, this implies that up to 2 per cent of the SiO_2 content of the basalts may have been leached out of the residual glass and deposited somewhere else. All or some of this silica now almost certainly resides in the abundant amygdales which were deliberately avoided during sampling. Fig. 13 suggests that leaching of SiO_2 begins when H_2O^+ attains a level of 0.5-1 per cent in the basalts (or 5-10 per cent in the glass) and comes to an end rapidly with increasing uptake of water.

The low-temperature oxidation of iron seems mostly to occur in an initial phase of alteration not represented among the basalts as they all have a rather high Fe_2O_3/FeO ratio which does not increase much with increasing H_2O^+ contents (Table 9).

The Na_2O and K_2O contents of the tholeiites vary in an irregular manner through the lava sequence (Table 17) showing little correlation with other elements. The variation of Na_2O and K_2O may in part be due to migration of late stage residual melts in the crystallizing flows as suggested for an Icelandic basalt flow by Hart and others (1971). However, some redistribution of these elements during alteration processes is suggested by the occurrence of rocks strongly enriched in K_2O but low in Na_2O. The rocks which show this most clearly are mesostasis-rich segregation veins or patches in the tholeiitic flows, the most extreme example being sample No. 35 with 1.48 per cent Na_2O and 1.77 per cent K_2O (Table 17). It is notable that Na_2O and K_2O do not show any correlation with H_2O^+ and thus may be concentrated into as well as leached out of the mesostasis.

The supposed chemical alteration of the residual glasses throws suspicion on the use of SiO_2 and alkalis in differentiation indices and also on the CIPW norms of the many tholeiites from the Faeroe

Islands which contain more than 1 per cent H_2O^+. Since the losses
or redistribution of SiO_2 and alkalis in individual samples cannot
be corrected for in any reliable way, little emphasis has been
placed on the use of these elements or normative values for cor-
relation purposes. In the case of Na_2O and K_2O, which seem to
vary in a largely random manner, it is likely that average values
for groups of samples are reasonably close to the primary average
values.

Chemistry. Fig. 18b shows the alkalis - SiO_2 diagram for sub-
-profile averages from the Faeroe Islands (Table 10). Before
plotting, the averages were recalculated on a water-free basis.
The small number of averages, with a fairly uniform range of alte-
ration, fall in the field of tholeiitic basalts according to the
Hawaiian division line (Macdonald and Katsura 1964) and tend to
plot parallel to this line, as already noted by Noe-Nygaard and
Rasmussen (1968). Since many of the Faeroese tholeiites are con-
sidered to have lost some SiO_2, the unaltered tholeiites probably
lay even further away from the division line.

Histograms for the Faeroe Islands samples, showing their petro-
graphic type and the FeO^*/MgO ratios, reveal a bimodal distribu-
tion. This bimodal distribution is apparent for the early Middle
Basalts, late Middle Basalts and Upper Basalts, but not for the
Lower Basalts (Fig. 14b). The low FeO^*/MgO population has ratios
ranging from about 0.75 to 1.5 and the other group has ratios
ranging from about 1.75 to 2.5. The small number of samples lying
between these two groups coincides roughly with the petrographic
boundary between olivine tholeiites and tholeiites (5% modal oli-
vine) (Fig. 14a).

The hypersthene-phyric flows and the segregation veins and
patches in the late Middle Basalts and flow XI.6 in the Upper
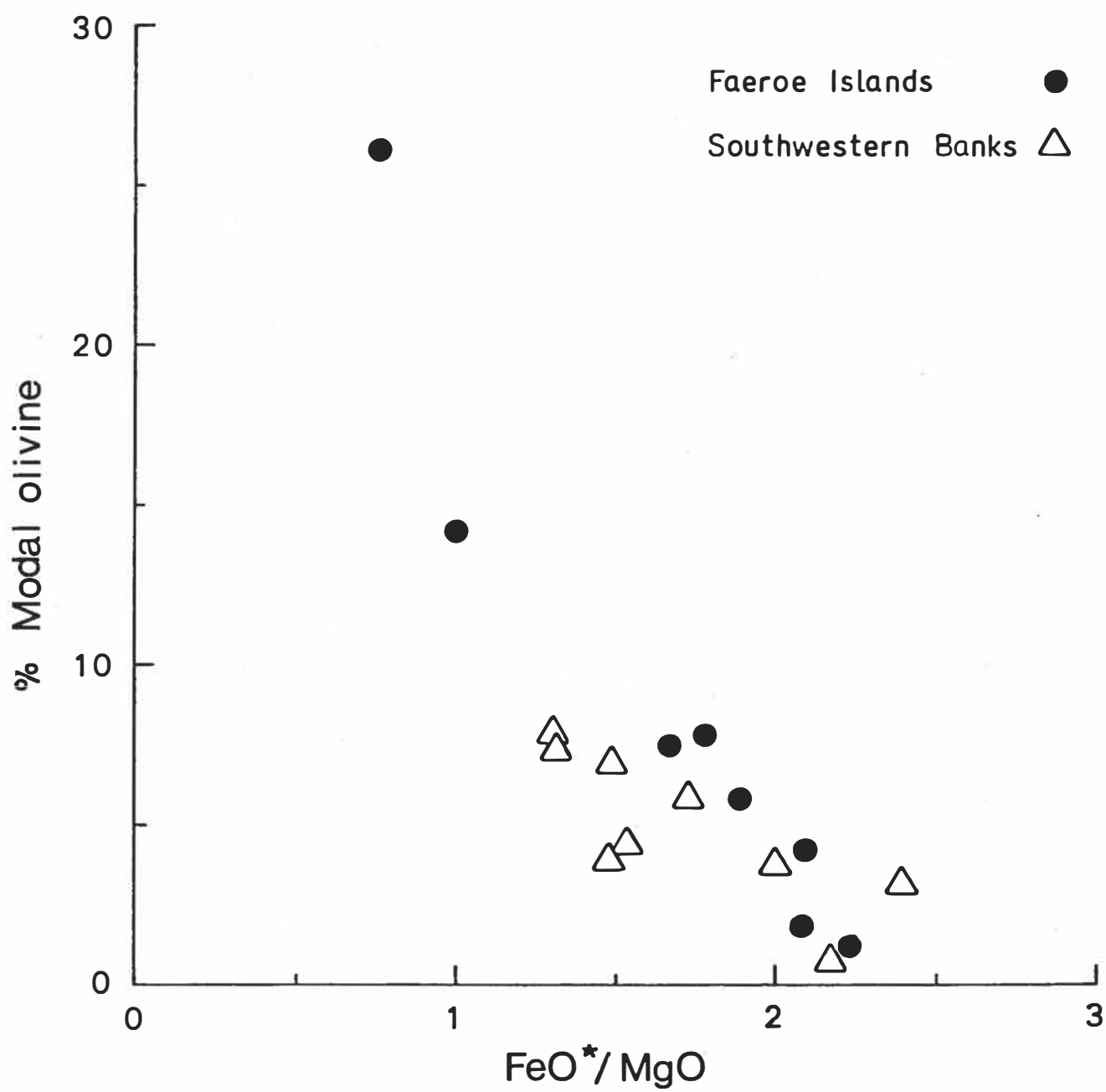
FIGURE 14a. Modal % olivine versus FeO*/MgO diagram for basalts from the Faeroe region.

Upper Basalts

Faeroe Bank, Bill Bailey Bank, Lousy Bank

late Middle Basalts

early Middle Basalts

Faeroe Islands

Lower Basalts

East Greenland

No.

30

20

10

0

1   2   3

FeO*/MgO

1   2   3

FeO*/MgO

Plagioclase-phyric basalt (>1 % plagioclase phenocrysts)

Microphyric, near-aphyric and aphyric basalt

Olivine-phyric basalt (1-10 % olivine phenocrysts)

Olivine-phyric basalt (>10 % olivine phenocrysts)
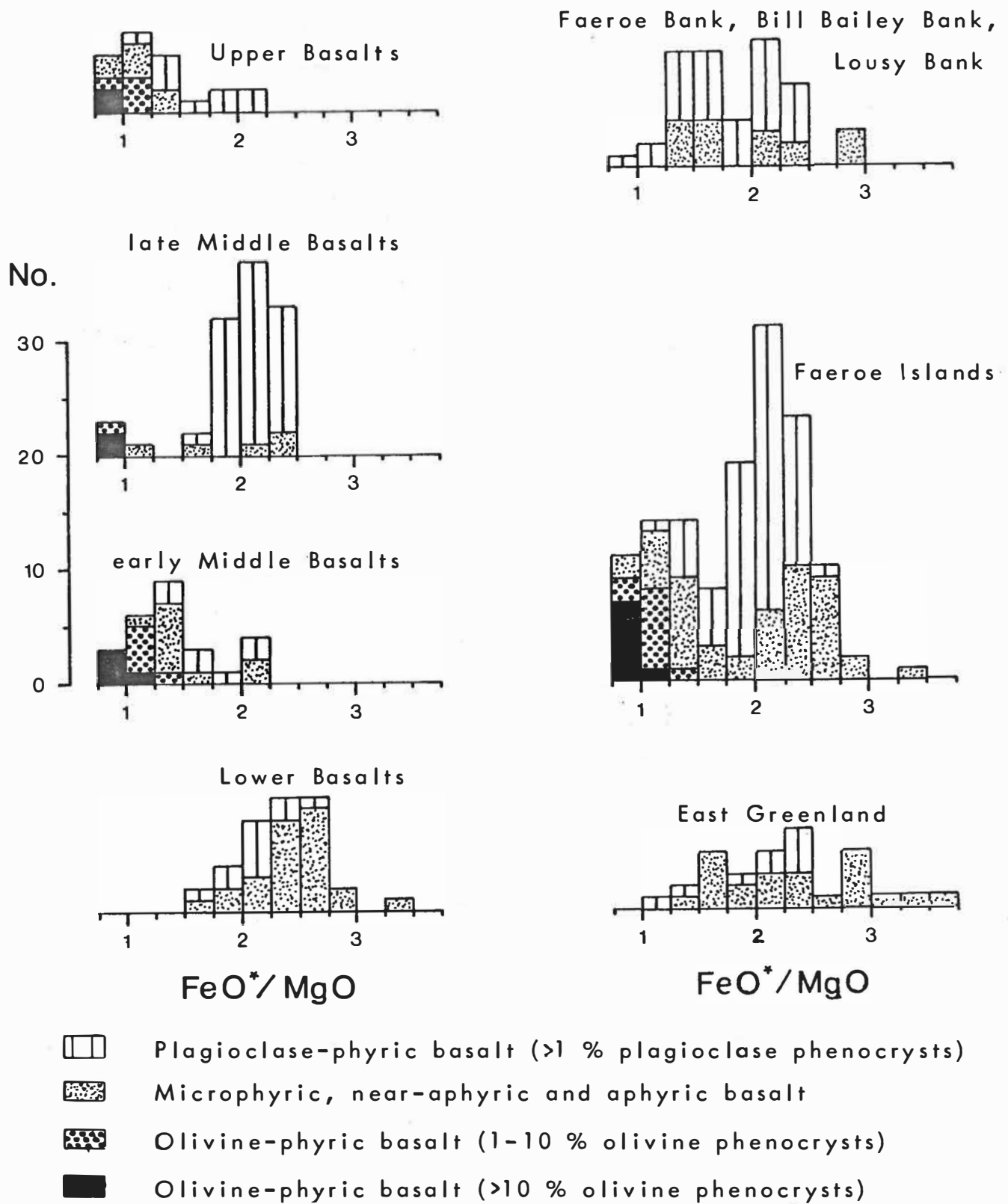
Figure 14b. Histograms of FeO*/MgO ratios for basalts from the early Tertiary North Atlantic basalt province.

Basalts have been excluded from all averages and diagrams.

The anomalous petrography and chemistry of the hypersthene-
-phyric flows in the Sneis profile (Table 17) are considered to
reflect crustal contamination. The Klakksvík flow which occurs in
the northeastern part of the Faeroes at a similar depth (about
100 metres) below the base of the Upper Basalts, and XI.6 in the
lowest part of the Upper Basalts, are likewise high in SiO_2 (53-54%),
rather high in MgO (6.4-8.6%), but low in TiO_2 (1.15-1.70%) and
do not fit into the chemical spectrum of the Faeroese basalts.

The segregation veins and patches in the Sneis lavas (marked
SV and SP in Table 17) are all basaltic but are more rich in FeO*
and TiO_2 than their hosts (e.g. sample No. 20 contains 15.64% FeO* and
4.17% TiO_2).

3.3.5. Chemical stratigraphy

The TiO_2/FeO^* versus FeO^*/MgO plot (Fig. 15) separates well the various stratigraphic subdivisions of the Faeroe Islands basalts. The Lower Basalts are relatively high in FeO^*/MgO ratios (1.5-3.5) and exhibit comparatively low TiO_2/FeO^* ratios. In contrast, the earliest Middle Basalts are mostly olivine tholeiites with FeO^*/MgO ratios below 1.5 and they are relatively high in TiO_2/FeO^* ratios. The overlying tholeiites from the Middle Basalts lie on a similar trend in this diagram but generally show higher FeO^*/MgO ratios. There is virtually no overlap with the Lower Basalts. The olivine tholeiites of the late Middle Basalts are low in TiO_2/FeO^* and FeO^*/MgO ratios, and show distinctly lower TiO_2/FeO^* ratios compared with olivine tholeiites in the early Middle Basalts. The subsequent olivine tholeiites of the Upper Basalts take up a similar position in the diagram while the tholeiites in the Upper Basalts can be grouped together with the tholeiites of the late Middle Basalts.

The same plot is presented in Fig. 16, but only averaged sub--profile values are employed. Excluding the LIL-element depleted tholeiites which plot independently, this figure reveals a fairly systematic sequence of changes for the Faeroese lava pile. These systematic trends imply that the pressure-thermal-chemical conditions of magma formation in the upper mantle were also undergoing steady changes. Such fundamental changes should be reflected over wide areas of the Faeroe Plateau. It is thus possible that well-sampled areas on the shelf close to the Faeroe Islands, and perhaps even on the more distant banks to the southwest, could be integrated with some confidence into the sequence of events on the Faeroe Islands, and thereby located within the Faeroes basaltic column.
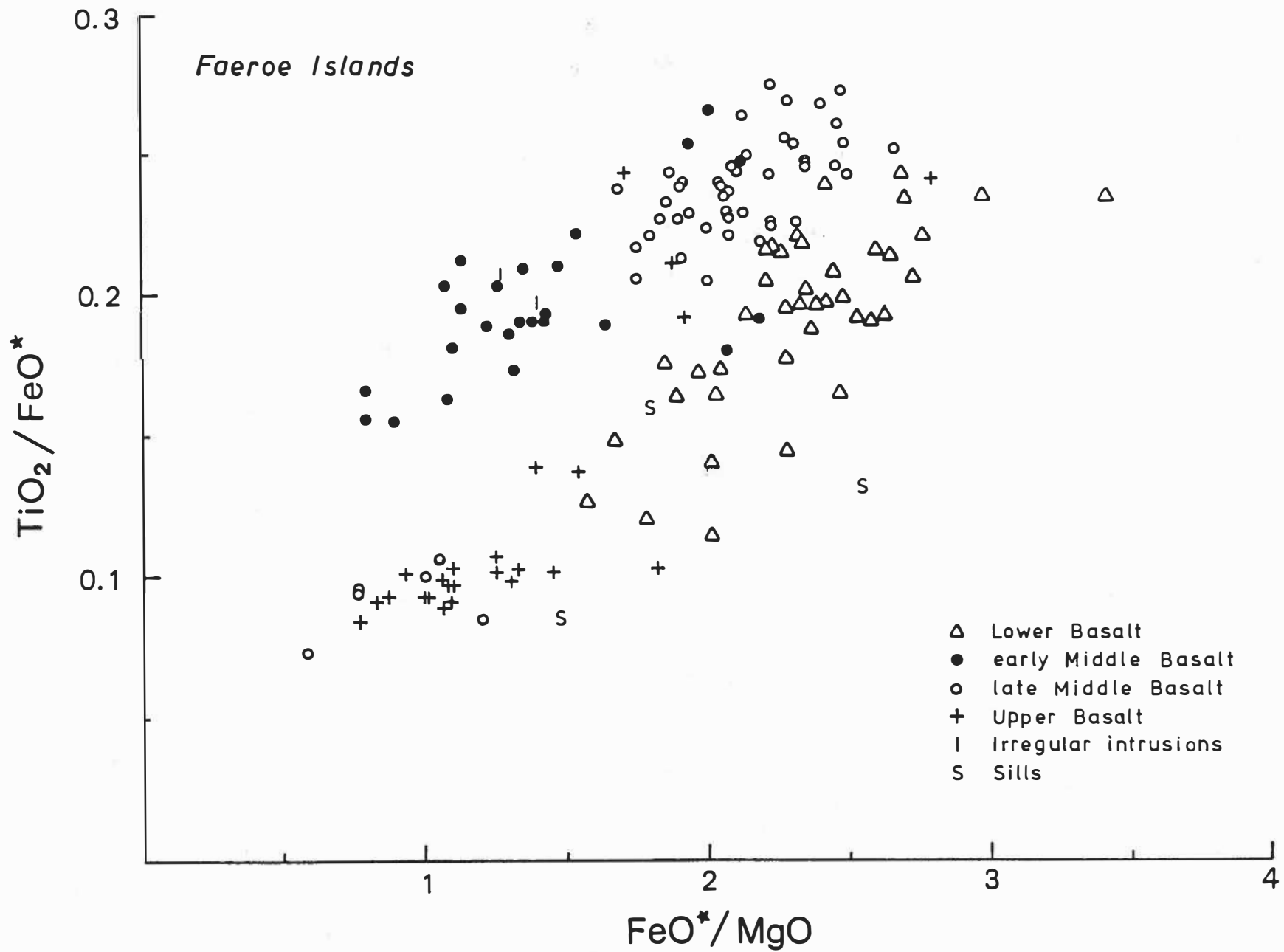
FIGURE 15. TiO_2/FeO^* versus FeO^*/MgO diagram for Faeroes lavas
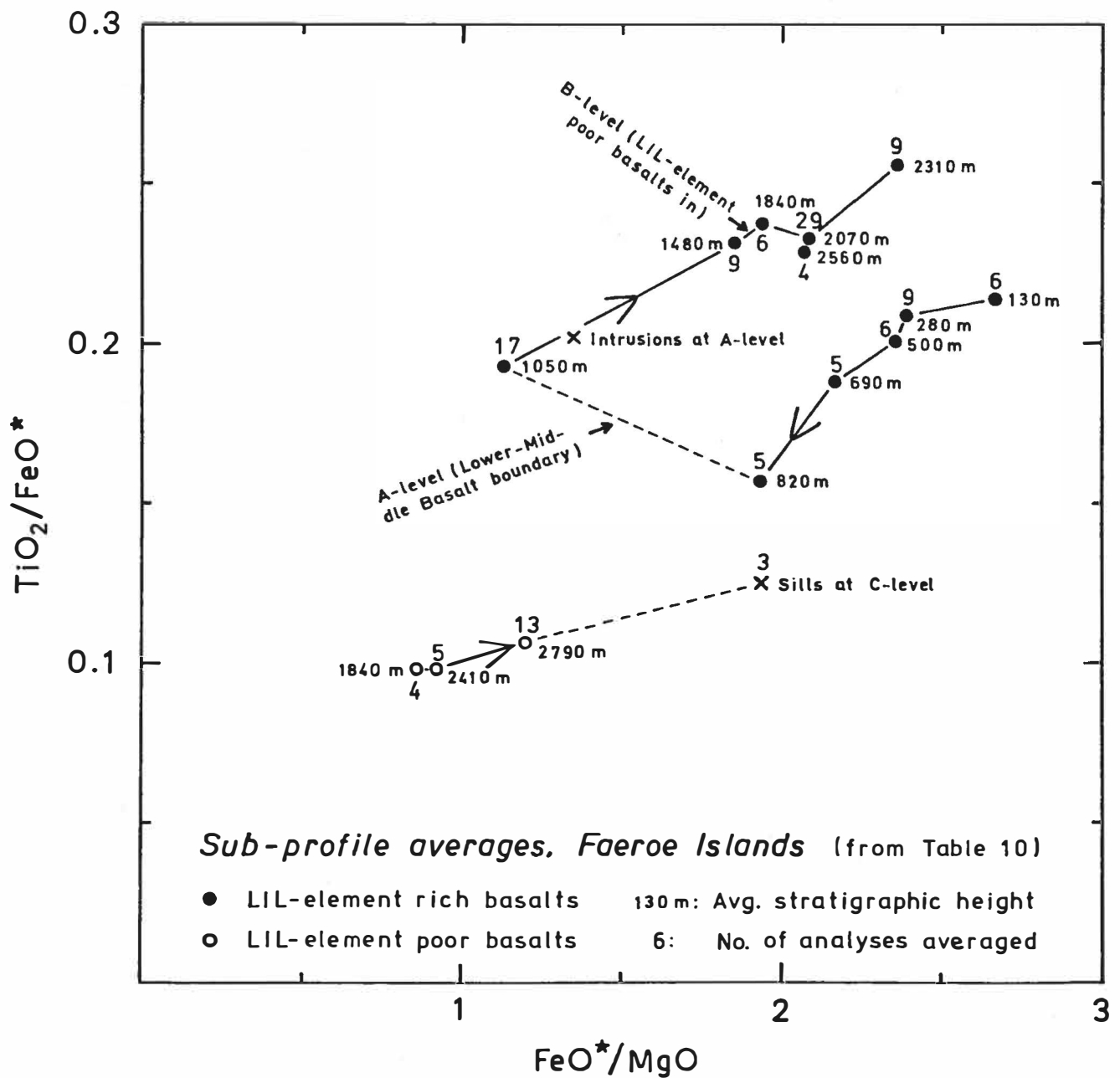
FIGURE 16. Progressive variation of the average composition
of LIL-element rich (closed circles) and LIL-element poor
(open circles) tholeiitic basalts with stratigraphic height
in the main profile through the Faeroese lava pile. The
average stratigraphic height of successive height intervals
considered (see Table 10) and the number of analyses (in
brackets) on which the average compositions of the intervals
are based are shown beside the circles.

TABLE 10   AVERAGE COMPOSITIONS OF FAEROESE BASALTS

| | Normal tholeiitic basalt | | | | | | |
| | Lower Basalts | | | | | Middle Basalts | |
Profile No.	I	IIa	IIb	III	III	IV-VI	VII-IX
Stratigraphic height (m)	50-205	205-355	355-645	645-740	740-890	920-1170	1170-1795
No. of anal.	6	12	9	5	5	17	9
SiO_2	48.15	47.95	47.77	46.99	48.43	46.98	48.13
TiO_2	3.01	2.86	2.70	2.55	1.95	2.03	2.45
Al_2O_3	13.06	13.23	13.66	13.81	14.16	12.98	14.83
Fe_2O_3	6.17	7.34	6.27	7.36	4.23	3.21	4.06
FeO	8.47	7.20	7.81	6.90	8.46	8.08	7.40
MnO	0.21					0.19	0.18
MgO	5.30	5.75	5.72	6.28	6.45	9.73	5.99
CaO	10.19	9.70	10.41	10.88	11.54	11.00	11.16
Na_2O	2.61	2.63	2.41	2.30	2.10	1.95	2.38
K_2O	0.51	0.40	0.47	0.39	0.33	0.40	0.36
P_2O_5	0.32	(0.34)	(0.32)				(0.27)
H_2O^+	2.20						
Total	100.20	(97.40)	(97.54)	(97.46)	(97.65)	(96.55)	(97.21)
FeO^*	14.02	13.81	13.45	13.52	12.27	10.97	11.05
FeO^*/MgO	2.65	2.40	2.35	2.15	1.90	1.13	1.85
TiO_2/FeO^*	0.215	0.207	0.201	0.189	0.159	0.185	0.222
No. of anal.	6	12	9	3[§]	4[§]	10	3
Ba	99	97	100	120	69	68	90
Zr	240	230	230	170	130	175	195
Sr	260	305	305	220	190	250	300
Cu	285	290	240	180	140	140	155
V	480	390	400	340	300	235	245
Co	51	57	56	49	47	65	48
Ni	94	91	105	67	76	280	130
Cr	115	110	140	87	180	710	265
Sc	(33)	(38)	(44)	39	36		
No. of anal.		1		3[§]	4[§]	2	2
La		17.4		14.9	9.4	7.4	14.1
Sm		7.6		6.5	4.8	4.7	7.5
$La/Sm_{E.F.}$		1.6		1.6	1.4	1.1	1.3

Comments: Major element averages for profile X are calculated from the analyses in this report (Table 17).   Rare-earth element averages are based on the analyses in Schilling and Noe-Nygaard (1974).   All other averages are based on unpublished analyses (see Section 3.2.5.)

TABLE 10   (Continued)

	Normal tholeiitic basalt				LIL-element poor basalt		
	Middle Basalts			Upper Bas.	Mid. Bas.	Upper Basalts	
Profile No.	X	X	X	XI	X	XI	XI
Stratigraphic height (m)	1810-1875	1880-2255	2275-2355	2495-2630	1795-1880	2355-2465	2525-3065
No. of anal.	6	29	9	4	4	5	13
SiO_2	47.65	48.62	48.31	47.63	45.78	47.13	47.79
TiO_2	2.62	2.77	3.35	2.77	1.00	0.95	1.15
Al_2O_3	15.67	14.95	14.14	14.24	14.07	14.34	14.42
Fe_2O_3	4.32	4.18	5.65	3.24	2.02	2.46	2.44
FeO	7.12	8.11	7.99	9.68	8.36	7.76	8.55
MnO	0.19	0.20	0.20	0.19	0.20	0.18	0.19
MgO	5.71	5.72	5.57	6.12	11.82	10.86	8.99
CaO	10.79	10.59	10.06	10.40	11.40	12.00	12.02
Na_2O	2.62	2.53	2.42	2.34	1.78	1.72	1.95
K_2O	0.26	0.34	0.32	0.49	0.19	0.28	0.28
P_2O_5	0.29	0.31	0.38		0.07		
H_2O^+	2.47	1.51	1.37		2.73		
Total	99.71	99.83	99.76	(97.10)	99.42	(97.68)	(97.78)
FeO^*	11.01	11.87	13.08	12.60	10.18	9.97	10.75
FeO^*/MgO	1.93	2.08	2.35	2.06	0.86	0.92	1.20
TiO_2/FeO^*	0.238	0.233	0.256	0.220	0.098	0.095	0.107
No. of anal.		5	4	4	4	5	13
Ba		64	51	31	< 10	< 10	< 30
Zr		180	230	215	83	73	96
Sr		265	235	240	97	115	125
Cu		165	225	275	125	205	215
V		275	365	400	230	285	330
Co		44	47	52	57	63	59
Ni		110	83	88	270	295	195
Cr		185	125	120	575	480	360
Sc		(33)	34		36	(39)	
No. of anal	1	3		2	2	2	5
La	14.6	12.9		11.2	1.8	2.0	3.5
Sm	7.2	7.0		6.3	2.5	2.6	3.0
$La/Sm_{E.F.}$	1.4	1.3		1.2	0.50	0.57	0.79

§ denotes that one sample have been given double weight to remove a bias in major element composition between the set of samples on which the major and trace element averages are based, respectively. Sc values in parenteses represent one or two analyses only.

Table 10 presents average major and trace element analyses for single or grouped sub-profiles with the main basalt profile of the Faeroe Islands. Averages for the Lower Basalts show a steady decrease in the FeO^*/MgO ratio and sympathetic variations for other elements, e.g. TiO_2, Na_2O, K_2O, Zr, Cu and V generally decrease whereas levels of Al_2O_3 and CaO increase. These variations are comparable to the changes observed at Kap Stosch in East Greenland (Noe-Nygaard and Pedersen 1974) but they occur in reverse order. According to the available normalized La/Sm ratios (1.3-1.7) (Schilling and Noe-Nygaard 1974), the Lower Basalts are relatively enriched in the light REE and have been assigned to a LIL-element enriched ("plume") type of basalt.

When the few LIL-element depleted tholeiites are eliminated from the Middle Basalt series, the remaining LIL-element enriched basalt, on average, pass from olivine tholeiites to tholeiites and show a trend of increasing FeO^*/MgO ratios with increasing stratigraphic height. This trend is most pronounced in the lowermost and in the uppermost parts of the sequence. Coincident with this trend are increase in TiO_2, Zr, Cu and V but decreases in CaO, Ni and Cr. It is notable, and unexpected, that levels of Na_2O, K_2O, Ba and Sr remain roughly constant. The earliest olivine tholeiites are poor in Al_2O_3 and distinctly high in MgO, Co, Ni and Cr. These features may reflect partly the accumulation of olivine crystals and also the presence of some picritic liquids among these flows. The overlying tholeiites are rather high and scattered in Al_2O_3 due to the varying abundance of plagioclase phenocrysts.

Only a few analyses exist for the Upper Basalts. The average is chemically close to the Middle Basalts at the 1880-2255 metre stratigraphic level, except for its low Ba content.

LIL-element depleted basalts occur at intervals from the base of the Eide group to two-thirds of the way above the base of the Middle Basalts, and also within the Upper Basalts. They are characterized by low contents of TiO_2, Na_2O, K_2O, Ba, Zr, Sr, La and a normalized La/Sm ratio less than 1. The most MgO-rich samples, on average, occur in the Eide group while the samples at higher levels possess lower and lower MgO contents.

A number of small intrusions cut the lava pile (section 2.1.4.) and analyses for some of them were presented by Rasmussen and Noe-Nygaard (1969). Two analyses (op. cit., p. 303) of the irregular intrusions which were emplaced between the Lower and Middle ∧ Basalts show that they are olivine tholeiites very similar to the overlying lavas, i.e. LIL-element enriched. This type of composition is not represented at higher stratigraphic levels or among the other intrusions. It is likely that they are roughly coeval with the overlying lavas of similar chemistry (see also section 2.1.4.).

Three sills have been analysed (op. cit., p. 325). The analysis of the Streymoy sill is very similar to the LIL-element depleted lavas in the uppermost part of the Upper Basalts. The other two sills lie on the continuation of the chemical trends established for the LIL-element depleted Upper Basalts. Trace element analyses of the Eysturoy sill reveal only 38 ppm Ba and 96 ppm Sr. It appears that these three sills are related to the latest basalts in the Faeroese sequence.

Four dyke analyses (op. cit., p. 252) can also be equated chemically with the Upper Basalts and were presumably emplaced shortly after the eruption of the basalts (see section 2.1.7.).

Thus, the available analyses of dykes and sills, when plotted on the TiO_2/FeO^* versus FeO^*/MgO grid, show no indication of a reversal to magma types occurring below the late Middle Basalts.

3.4.   Petrography of the basaltic shelf

3.4.1. Method of transport of the basaltic erratics

The basaltic erratics dredged from the Faeroe shelf and from the slopes of the Faeroe-Shetland Channel and the Faeroe Bank Channel were examined in several ways (see sections 3.2.2. and 3.2.3.) to assess their method and distance of transport.

Fig. 17 based on data on cobble-sized (64-256 millimetres) erratics presented in Table 1 shows that the rock types probably derived from the Faeroes and the surrounding shelf, i.e. basalts and subordinate tuff-carbonate sediments, are strongly dominant on the shelf and the slope to a depth of roughly 400 metres. Southeast of the Faeroes there is a sudden increase downslope in the abundance of other rock types which are mainly sandstones and gneisses. Waagstein and Rasmussen (1975) interpreted the sandstones and gneisses as ice-rafted erratics derived from outside the Faeroes and the Faeroe shelf. They suggested that an ice--front was standing along the shelf edge southeast of the Faeroes during nearly all the last glacial epoch preventing ice-rafting over the southeastern sector of the shelf. The abundance of basaltic erratics on the shelf edge along the Faeroe Bank Channel southwest of the islands suggests that the ice-sheet also reached deep water in this sector of the shelf.

Fig. 17 shows that basaltic erratics from the outer part of the shelf are generally more rounded than the erratics from more than 400 metres depth outside the shelf. This difference suggests that the erratics from the shelf were mostly derived from lodgement tills whereas the ice-rafted erratics from outside the supposed ice-front include a large proportion of fragments derived from the surface and the interior of the ice-sheet.

Ignoring dredge haul 63, all dredge hauls inside the 400 metres
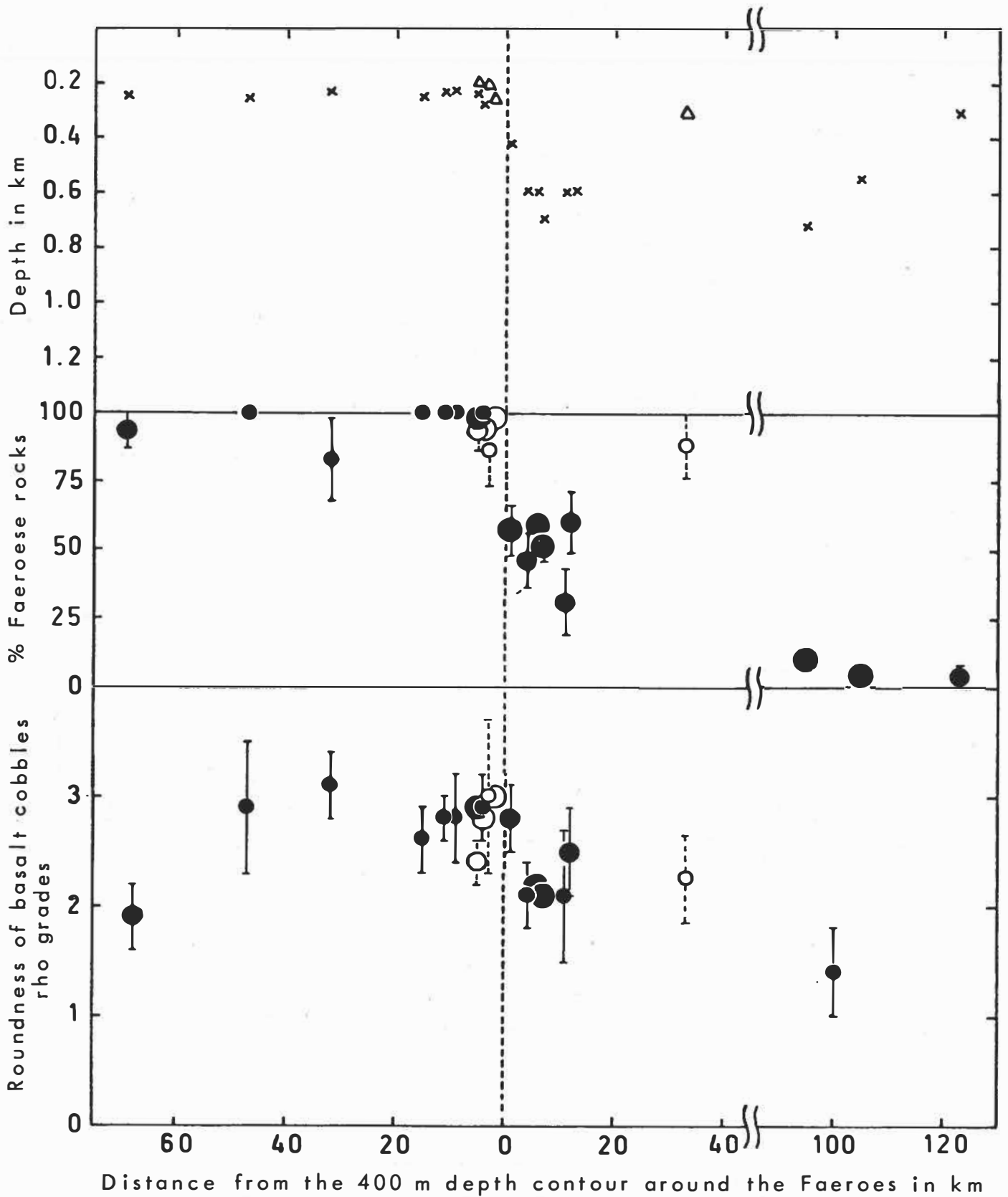
Figure 17. Variation with distance in km from the 400 m depth contour around the Faeroes of depth of dredge stations, abundance of Faeroese rocks among dredged cobbles, and mean roundness of basalt cobbles. ●○ 5-9 cobbles, ●○ 10-24 cobbles, ●○ ≥ 25 cobbles. Error bars based on counting statistics indicate 1 st.d. of mean but are not shown when shorter than the diameter of the circles. Filled circles and crosses indicate dredge hauls SE of the Faeroes, open circles and triangles indicate dredge hauls SW of the Faeroes.

depth contour which gave five or more basalt cobbles were recovered
from at least 25 kilometres outside the limit of the basaltic
part of the shelf southeast and southwest of the islands. The
mean roundness of basalt cobbles from these dredge hauls only
varies between 2.4 and 3.1 rho roundness grades (see definition
in section 3.2.2.), i.e. it falls into the upper part of the sub-
angular class and the lowermost part of the subrounded class.
The mean roundness shows no correlation with distance from the
basaltic shelf and most of the spread in mean roundness values
is no doubt a consequence of the small numbers of fragments they
are based on. Thus the basaltic erratics carried in the base of
the ice for a distance of 25 kilometres across the sedimentary
shelf probably acquired a mature form.

The basaltic erratics from 570-720 metres depth on the south-
eastern slope show a mean roundness of about 2.2, which is in the
lower part of the subangular class. A single station at 423 me-
tres depth (No. 3) shows a mean roundness of 2.8 while 7 basaltic
erratics dredged from the southeastern side of the Faeroe-Shetland
Channel (stations 10-12) show a mean roundness as low as 1.4.

The basaltic erratics also differ as to the frequency of gla-
cial striae (Table 1). On the southeastern slope of the Faeroe
shelf at 570-720 metres depth, 19 per cent of the basalt cobbles
on average show clear glacial striae and 16 per cent on average
show faint glacial striae. Inside the 400 metres depth contour
southeast of the islands, only 8 per cent of the basalt cobbles
are clearly striated while 23 per cent are faintly striated (again
ignoring dredge haul 63 close to the basaltic shelf and dredge
hauls which recovered less than 5 basalt cobbles). The basaltic
cobbles from the southwestern shelf edge, inside the small sedi-
mentary basin facing the Faeroe Bank Channel, rarely show any gla-
cial striae (stations 19-21). The rarity of clear glacial striae

on cobbles from supposed lodgement tills on the sedimentary parts of the shelf possibly indicates that a large proportion of the underlying Tertiary sediments (see section 3.5.) were admixed with the basalt fragments carried in the base of the flowing ice. This should result in considerable grinding but little crushing and scouring of the fragments. The matrix of the lodgement tills has not been recovered and has probably been swept away by bottom currents.

3.4.2. Origin of the basaltic erratics

According to Geikie (1880) no marks of glaciation are found above a height of about 500 metres on the Faeroes. The flow of ice during the last glacial epoch was strongly controlled by the morphology of the islands, and the islands Sandoy and Suduroy forming the southern part of the island group constituted individual flow centres. The morphology of the islands and the observations of glacial striae and roches moutonnées suggest that the southern parts of the northeastern islands and the main island Eysturoy, the southeastern part of the main island Streymoy, the eastern part of Sandoy and most part of Suduroy were drained by glaciers flowing towards the eastern shelf. A substantial part of the ice-rafted basaltic erratics in the Faeroe-Shetland Channel has probably been carried on the surface or in the interior of the ice as argued earlier from roundness data and has presumably been derived from the upper reaches of the above areas. The basaltic erratics from the eastern shelf, on the other hand, which are supposed from their mature form to have been carried mostly in the base of the ice are likely to include a substantial proportion of fragments eroded from the eastern basaltic shelf. The average size of the fragments is about 14 centimetres. Since the fragments carried in the base of the ice are abraded and sometimes break into pieces during the transport the latest over-ridden basalt areas will be overrepresented among such large clasts compared to the smaller clasts. The basaltic erratics from the small sedimentary shelf area southwest of the Faeroes are likewise suspected from their mature form to have been carried in the base of the ice and to include basalt fragments eroded from the western shelf.

3.4.3. Petrography of basaltic erratics and implications about the petrography of the basaltic shelf

The basaltic erratics dredged from the Faeroe shelf and from the Faeroe-Shetland Channel and the Faeroe Bank Channel show the same range of basaltic types as the Faeroe Islands. Significantly, no more evolved lava types and no plutonic rocks were found indicating the presence of central volcanic complexes on the shelf, and no basalt tuff breccias or pillow fragments were found indicating a marine environment close the Faeroes during the building of the plateau. The erratics were studied petrographically by the unaided eye, under stereo microscope and sometimes also in thin sections and classified according to the phenocryst contents as described in section 3.2.3. The results of this study are summarized in Tables 11 and 12.

In Table 11, the basaltic erratics from three regions are compared. The first group of erratics are from stations at 580 to 720 metres depth on the southeastern slope of the Faeroe shelf (stations 4, 8, 71, 76 and 77). The second group includes all dredge hauls southeast of the Faeroes at less than 290 metres depth which recovered five or more basalt cobbles with the exception of station 63 closest to the basaltic shelf (i.e. stations 1, 2, 5, 65, 72 and 73). The third group consists of basalts from station 21 inside the small sedimentary shelf area southwest of the islands. The basalts from the nearby station 20 appear very similar to the basalts from station 21 but, because of the great number of samples, they have not been classified.

Table 11 suggests that the southeast shelf is poorer in erratics of olivine-phyric basalts and macroscopic aphyric (i.e. near--aphyric, microphyric and aphyric basalts) basalts but is richer in plagioclase-phyric basalt erratics than the southeast slope.

A closer inspection of the macroscopic aphyric basalts from the southeastern shelf reveals that olivine phenocrysts or microphenocrysts are subordinate to plagioclase phenocrysts or microphenocrysts, whereas most of the microphyric basaltic erratics from the southeast slope have olivine as the dominant phenocryst phase. Aphyric basalts are also more abundant on the southeast slope than on the southeast shelf.

A substantial part of the erratics from the southeast slope were probably derived from the higher levels of the mountains on the Faeroe Islands, i.e. that part of the Faeroes facing the southeast shelf and dominantly consisting of Upper Basalts and late Middle Basalts. Drainage from this part of the Faeroes is towards the southeast.

A substantial part of the erratics on the southeast shelf were probably eroded from the southeast basaltic shelf which consists of Upper Basalts (section 2.2.4.).

Comparing the southeast slope and shelf, it can be seen that there is a decrease in the abundance of olivine-phyric and microphyric basalts (olivine tholeiites) towards the southeast. This decrease is not consistent with the suggestions of Noe-Nygaard and Rasmussen (1968) and Noe-Nygaard (1974) that the Upper Basalt olivine tholeiites have been erupted from fissures east of the islands. It rather appears that the abundance of olivine tholeiites in the Upper Basalts decreases towards the centre of the Faeroe block (i.e. the Faeroes and the surrounding basaltic and sedimentary shelf) (cf. Fig. 3).

On the southwest shelf, there is a higher percentage of olivine-phyric basalts (Table 11). Table 12 shows the abundance of olivine-phyric basaltic erratics plus microphyric and near-aphyric basaltic erratics with olivine as the dominant microphenocryst

TABLE 11. TYPES OF BASALTS DREDGED SOUTHEAST AND SOUTHWEST OF THE FAEROE ISLANDS

Estimated vol. % phenocrysts	Max. size mm	Phenocryst minerals	Number of basalts SE-slope	Number of basalts SE-shelf	Number of basalts SW-shelf	Percentage of basalts SE-slope	Percentage of basalts SE-shelf	Percentage of basalts SW-shelf	Percentage of basalts SE-slope	Percentage of basalts SE-shelf	Percentage of basalts SW-shelf	Percentage of basalts SE-slope	Percentage of basalts SE-shelf	Percentage of basalts SW-shelf
Olivine-phyric basalts														
> 15	2-5		4	0	1	2.5	0	2.0	3.8	0	2.0			
	1-2		2	0	0	1.3	0	0						
5-15	2-5		3	1	4	1.9	1.5	8.2	3.2	4.5	8.2	8.9	6.0	16.3
	1-2		2	2	0	1.3	3.0	0						
1-5	2-5		0	0	2	0	0	4.1	1.9	1.5	6.1			
	1-2		3	1	1	1.9	1.5	2.0						
Plagioclase-phyric basalts														
> 15	> 5		2	3	2	1.3	4.5	4.1	7.6	13.5	22.4			
	2-5		7	3	6	4.4	4.5	12.2						
	1-2		3	3	3	1.9	4.5	6.1						
5-15	> 5		2	1	2	1.3	1.5	4.1	17.8	30.5	10.2	40.6	56.1	51.0
	2-5		12	9	3	7.6	13.7	6.1						
	1-2		14	10	0	8.9	15.3	0						
1-5	> 5		2	0	1	1.3	0	2.0	15.2	12.1	18.4			
	2-5		7	0	4	4.4	0	8.2						
	1-2		15	8	4	9.5	12.1	8.2						
Near-aphyric basalts														
< 1	> 1	Olivine	4	0	2	2.5	0	4.1	17.7	21.3	20.5			
	> 1	Ol. + plag.	19	12	7	12.0	18.3	14.4						
	> 1	Plagioclase	5	2	1	3.2	3.0	2.0						
Microphyric basalts														
> 1	< 1	Olivine	20	0	0	12.6	0	0	20.2	12.1	10.2	50.5	37.9	32.7
	< 1	Ol. + plag.	4	6	0	2.5	9.1	0						
	< 1	Plagioclase	8	2	5	5.1	3.0	10.2						
Aphyric basalts														
Aphyric basalts			20	3	1	12.6	4.5	2.0	12.6	4.5	2.0			
Total			158	66	49	100.0	100.0	100.0	100.0	100.0	100.0	100.0	100.0	100.0

TABLE 12.   COBBLES AND PEBBLES DREDGED ON THE SHELF AND SLOPE SOUTH-WEST AND SOUTH OF THE FAEROE ISLANDS

	19	20	21	27A	27B	79	80	81	84	SE-Slope	SE-Shelf
Station No.	19	20	21	27A	27B	79	80	81	84	1)	2)
Mean depth in metres	198	262	269	203	215	190	176	180	420	1)	2)
Basalt	13	127	49	6	41	25	31	22	1	159	66
Tuff & agglomerate		1			1						
Tuff carbonate sediments		3	2						1	16	13
Other sediments		5	1		2	6		1	1	99	1
Metamorphic & plutonic rocks	1	4			1	2	1	2	1	53	1
Total number of stones	14	140	52	6	45	33	32	25	4	327	81
% foreign rocks[3]	7	6	2	0	7	24	3	12	50	46	2
% pebbles (less than 64 mm)	0	0	0	33	93[4]	100[4]	91[4]	100[4]	50	0	0
Minimum size in millimetres	–	–	–	37	18	7	9	13	9	–	–
% olivine-phyric basalt	15		16	17	13	0	0	14	0	9	6
% plagioclase-phyric basalt	39		50	50	18	20	12	18	100	41	56
% aphyric basalt[5]	46		34	33	69	80	88	68	0	50	38
% "olivine basalt"[6]	46		22	17	29	0	0	27		24	6
Mean roundness of basalt[7]	2.4	2.8	3.0	2.3	2.9	3.2	3.0[8]	3.2		2.17	2.86
Spread of roundness values[9]	0.8	0.8	1.0	0.8	1.2	0.6	0.8	0.7		1.10	0.78
% striated basaltic cobbles	8	5	2	0	0	–	0	–	–	35	30

Comments on next page

COMMENTS TO TABLE 12

1) Stations 4, 8, 71, 76 and 77 at a depth of 580-720 m on the slope southeast of the Faeroes.

2) Stations 1, 2, 5, 65, 67, 72 and 73 at a depth of 200-290 m on the shelf and slope southeast of the Faeroes.

3) Metamorphic, plutonic and sedimentary rocks, except tuff--carbonate sediments.

4) Excluding numerous pebbles smaller than the indicated minimum size.

5) Including basalts with phenocrysts smaller than 1 mm and/or fewer than 1%.

6) Basalts with more than 5% olivine phenocrysts plus basalts with olivine as the most abundant phenocryst mineral plus near-aphyric and microphyric basalts with visible phenocrysts of olivine only.

7) Rho roundness values (defined in the text), 2-3 = subangular class, 3-4 = subrounded class.

8) Based on the 25 largest fragments only.

9) 1 standard deviation.

phase (i.e. "olivine basalts") for all stations southwest and south of the Faeroes and for the station averages from the southeast slope and southeast shelf. It is unlikely that the "olivine basalts" (olivine tholeiites) from the southwestern shelf were derived from the exposed western areas of the Faeroe Islands since these mainly consists of Lower Basalts and Middle Basalts. It seems more likely that they were eroded from the outer southwestern shelf which is probably formed mainly of late Middle Basalts and Upper Basalts (section 2.2.4.). Many of the "olivine basalts" have an ophitic texture which suggest that they are depleted in LIL-elements (sections 3.3.2. and 3.3.3.) and they thus resemble the basalts from the Eide group in the Middle Basalts.

Stations 80 and 81 on the Suduroy Ridge are considered to have yielded some nearly _in situ_ rock fragments. Most of these are pebble-sized and were recovered with the tube sampler. The basalts from station 80 are nearly all slightly plagioclase-phyric and contain a few per cent olivine in the groundmass. Several of the basaltic pebbles from station 81 show ophitic texture and as this type of basalt is infrequent on the islands, they are also supposed to be of local origin.

Noe-Nygaard (1949) has described a dredge sample from the northern Faeroe slope (330 metres depth; $62^{\circ}44'$ N, $6^{\circ}06'$ W). Numerous small basalt fragments make up about 92 per cent of the sample and suggest a local origin of much of the sample whether derived from the bed rock or a lodgement till. Thin section descriptions of three basalt fragments might suggest an Upper Basaltic origin of the fragments (one is ophitic with 15 per cent olivine). Two fragments dredged further upslope were chemical analysed (Noe-Nygaard 1949). The one is an andesite, the other a LIL-element rich olivine tholeiite, but as they are the only fragments recovered from this place they may be ice-rafted erratics.

3.5.   Petrography of the sedimentary shelf

Subordinate tuff-carbonate sediments have been recovered together with the basaltic erratics from the sedimentary shelf areas southeast and southwest of the Faeroes and also in the deep dredge hauls on the southeastern slope. At one of the dredge stations on the southeastern shelf edge, station 5 with the greatest number of erratic samples, 11 of the erratics are varied tuff-carbonate sediments and 29 are basalts. Stations 65 and 88 recovered two tuff-carbonate concretions which show no signs of glacial transport indicating a local origin for this rock type. The tuff-carbonate sediments are absent from the dredge hauls from the southeastern flank of the Faeroe-Shetland Channel and from the southwestern banks.

The tuff-carbonate sediments often show signs of bioturbation. A single sample exhibits graded bedding from sand to silt size over a few millimetres above a sharp sedimentary contact, and may have formed by direct deposition from a volcanic eruption. Another sample which is nearly a pure carbonate rock is cut by a basalt vein up to a few millimetres thick.

Within the tuff-carbonate rock type, the proportion of tuff varies almost from 0 to 100%. The carbonate matrix is fine-grained and recrystallized. A few samples show indeterminable microfossils.

The tuff component is nearly always completely altered. It is mainly silt- and sand-sized and consists of irregularly shaped fragments. Several samples range up to coarse sands containing grains up to 2 mm in size. The grains, in this case, are well rounded with occasional vesicles. These samples often show a crude layering on a centimetre scale. The grains are dominantly converted to finely crystalline or amorphous alteration products

with colours in the range of green, yellow and brown, and was almost certainly originally volcanic glass judged on the presence of a few phenocrysts. Occasionally, fresher microcrystalline ash grains are seen and contain recognizable plagioclase and ore suggesting an originally basaltic composition for the grains. Phenocrysts of plagioclase, more rarely ore, occur in both the "glassy" and microcrystalline grains and are also probably the source of scattered crystals of these minerals in the carbonate matrix.

It is concluded that the coarse-grained tuffaceous sediments have undergone reworking. The same may also apply to most of the fine-grained sediments but in their case more prolonged reworking would be required to produce a noticeable rounding of the grains. A basaltic composition is suggested for most of the tuff fragments.

3.6.   Petrology of the Faeroe Bank, Bill Bailey Bank and Lousy Bank

3.6.1.   Petrography

Textures of basalts from the southwestern banks give no indication of submarine eruption and are very similar to the textures of basalts from the Faeroe Islands. Ophitic texture, which is occasionally seen in olivine-rich basalts on the Faeroes has only been observed in a single sample, possibly an erratic. The basalts from the banks range from olivine tholeiites with up to 10% olivine to quartz tholeiites which are olivine-free.

Two of the 48 chemically analysed basalts contain more than 30% plagioclase phenocrysts which are subequant and millimetre--sized; these samples are considered to be partial cumulates. The remaining basalts carry up to 15% plagioclase phenocrysts, most of them less than 5%. Only a few are completely aphyric. No basalts have olivine as the major phenocrysts phase. About 10 of the plagioclase-phyric basalts contain subordinate phenocrysts of both olivine and clinopyroxene, 6 carry phenocrysts of plagioclase and olivine but microphenocrysts of clinopyroxene, while 9 carry phenocrysts of plagioclase and microphenocrysts of olivine and clinopyroxene (Table 18). It thus appears that all these three phases are on or slightly below the liquids of these basalts, but sometimes plagioclase starts to crystallize before olivine, and olivine before clinopyroxene. Seven basalts carry phenocrysts of plagioclase and olivine but lack phenocrysts or microphenocrysts of clinopyroxene, but this group shows no clear chemical signs of being more primitive (Mg-rich).

Plagioclase phenocrysts occasionally show signs of resorption. Samples 28-4 and 28-24 exhibit two generations of plagioclase phenocrysts one of which is strongly resorbed and shows a more albitic composition than the groundmass plagioclase.

3.6.2. Low-temperature alterations

Chemical variations arising from the low-temperature alteration of the dredged basalts can be studied in a number of ways.

Table 13 compares the modal and normative compositions of nine dredged fragments. Contents of modal and normative ore in all the fragments are in close agreement suggesting that the techniques of point counting and norm calculation, summarized as a footnote to Table 13, are essentially correct. The small differences observed generally lie within the imprecision of the modal analyses. Significant differences in modal and normative olivine, however, do occur and can be related to the mechanics of rock alteration.

Only the first sample (37-4) contains high proportions of fresh olivine and fresh glass. It shows 1.0% modal olivine but 1.4% normative quartz. Modal olivine resides in the basaltic component of the sample whereas the normative quartz arises from the contribution of SiO_2-rich interstitial glass to the whole-rock composition. Thus fresh tholeiitic basalts can be expected to show a few per cent more of modal olivine than of normative olivine.

Most of the other samples have a worse state of preservation judged on the proportion of fresh olivine and glass; they also contain less modal olivine than normative olivine. In these samples, it is likely that SiO_2 has been released during the alteration of the mesostasis and lost from the rock. As a consequence, levels of normative olivine are increased over their true value.

The variable alteration of dredged basalt "pairs" has also been studied. As might be expected, dredging often recovers samples which are virtually identical in petrographic features and contents of immobile elements; such "pairs" or matching samples, are probably fragments of a single lava flow. Percentage differences in

TABLE 13. MODAL COMPOSITION OF BASALTS FROM FAEROE BANK, BILL BAILEY BANK AND LOUSY BANK AND COMPARISON WITH NORMATIVE PERCENTAGES OF OLIVINE AND ORE

Sample No.	37-4	57-4	57-14	57-3	60-6	28-1	28-26	28-24	34-7
Whole rock modal composition (%)									
Olivine	0.8	8.8	5.1	4.2	6.0	8.3	9.2	3.7	5.4
Plagioclase	40.5	38.5	45.9	41.5	44.6	42.9	44.9	42.9	} 86.9
Clinopyroxene	41.2	46.5	42.3	32.3	29.6	34.6	37.8	39.1	
Ore	6.7	3.4	3.7	6.8	6.2	6.0	6.8	9.8	2.0
Mesostasis	10.0	2.8	3.0	14.8	13.6	7.6	1.3	4.0	} 5.7
Amygdales	0.8				0.4		0.6		0.5	
Total	100.0	100.0	100.0	100.0	100.0	100.0	100.0	100.0	100.0
Modal % phenocrysts and microphenocrysts									
Olivine	0.7	< 1	0.3	0.6	4.1	3.8	1.4	1.0	1.5
Plagioclase	2.7	0.8	2.4	3.7	10.8	9.8	6.6	15.3	12.2
Clinopyroxene	1.1	< 1	0.2			0.8	2.1	0.1	3.0
State of preservation									
Fresh olivine	0.7	0.3			+	1.1	0.9		+
Fresh glass	3.1				+			+	
Zeolites	0.2					0.1	1.1		5.4
Estimated medium size of groundmass minerals (mm)									
Olivine		0.09	0.11	0.11	0.14	0.15	0.07	0.06	0.08
Ore	0.09	0.06	0.09	0.12	0.12	0.08	0.07	0.06	0.10
Normative and corrected modal percentages compared									
Modal olivine	1.0	9.5	5.6	4.6	6.3	10.1	10.0	3.7	6.1
Normative olivine		9.1	8.0	9.8	12.4	10.9	14.2	4.8	14.3
Normative quartz	1.4								
Modal ore	8.1	3.4	4.5	8.8	8.1	6.8	7.4	10.1	5.4
Normative ore	6.7	4.4	5.1	8.5	7.5	5.9	5.4	9.3	4.8

Comments on next page

TiO_2 contents between any dredged sample and all the other samples analysed from the same dredge (Fig. 23a) reveal a large number of pairs, i.e. samples whose TiO_2 values vary by less than 7 per cent relative.[1] A second population of samples cannot be matched closely with any other samples and these samples almost certainly derive from independent flows.

Those samples judged to be pairs have been studied for chemical variations arising from sea-floor alteration (Figs. 23b and c). Differences in contents of volatile components determined as loss on ignition (LOI) and other components between the paired samples have been plotted against each other. The LOI - SiO_2 plot reveals that many samples with higher LOI contents have lower SiO_2 contents. (A similar result was discussed in section 3.3.4.). Dredged pairs with similar SiO_2 contents may have undergone similar losses in SiO_2; this situation commonly prevails when two very wet samples are compared. Other elements show an erratic behaviour with either lower or higher values in H_2O^+-richer samples (K_2O, Rb). Significantly, TiO_2, P_2O_5, La, Nb and Zr show little or no variation among variably altered samples.

The observed variation of element contents between the members of a pair can be compared with variations arising from analytical imprecision. Analytical imprecision for most major elements is within a few per cent and for trace elements it is within about 5-10 per cent. Unfortunately, the analysts have not always been able to quantify exactly the level of imprecision when the present analyses were performed. Clear examples of excellent precision for fresh pairs of basalts, however, can be seen in Table 19 (samples 48-1 and 48-2, samples 28-6, 28-11 and 28-12).

The observed variations for Cu, Rb and K (Table 14, column 1) are distinctly higher than the analytical imprecision. These elements were also found to show wide variations in a single lava

---

[1] These samples are underlined in Table 19, except 48-5 and 33-10 which have 54-88 % more Cr than their counterparts similar in TiO_2.

No. of sample pairs
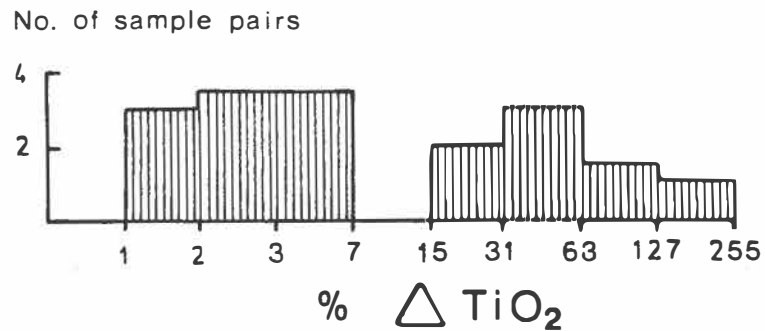
FIGURE 23a. Semilogaritmic histogram of per cent relative increase of TiO_2 from one basalt to the next when arranged in rising order of TiO_2 content in each dredge haul
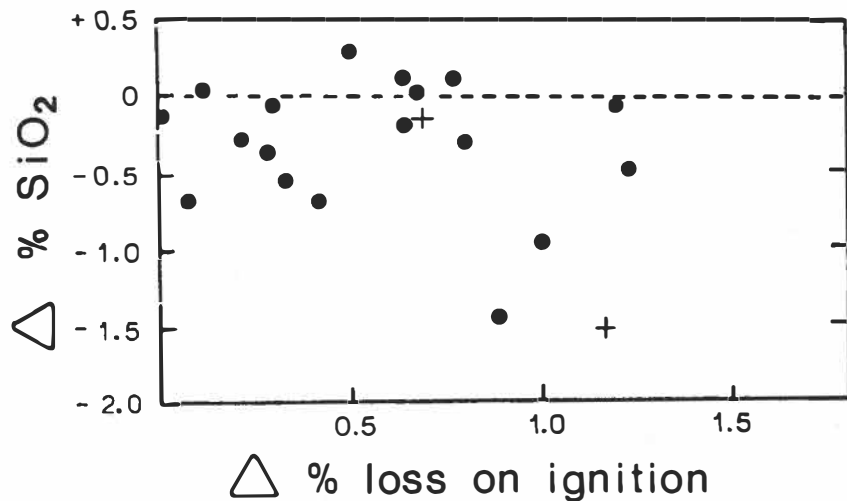
FIGURE 23b. Variation of SiO_2 with loss on ignition inside pairs of chemical similar samples; + = weathering crust
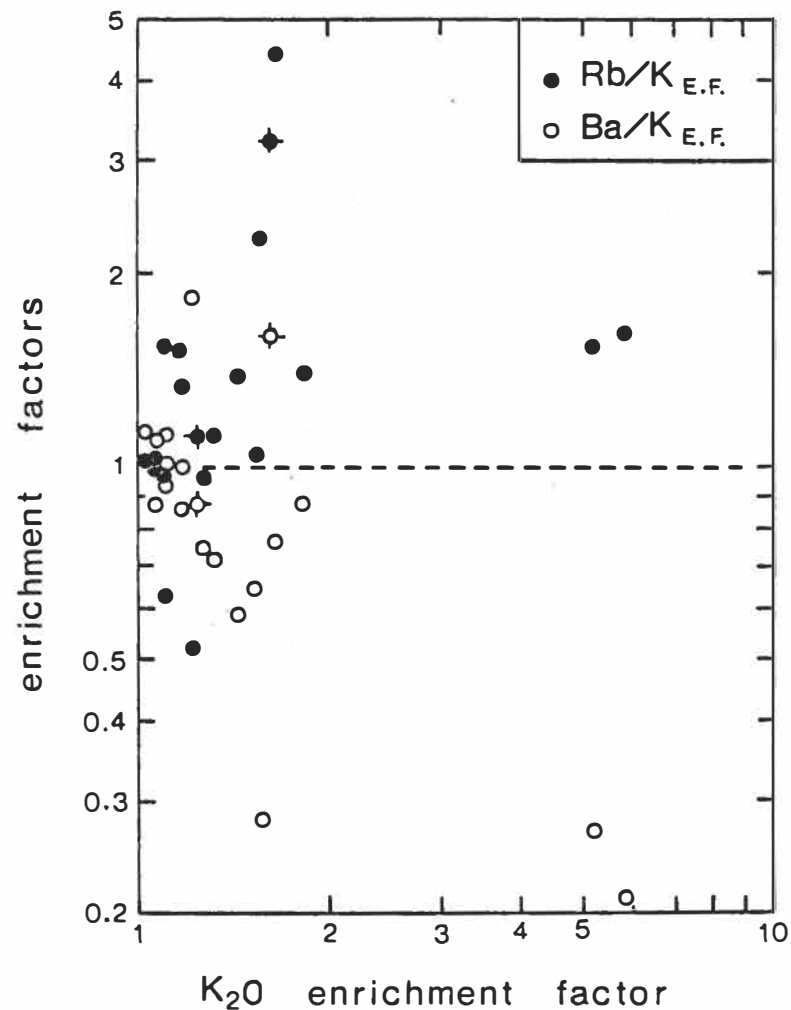
FIGURE 23c. Rb/K and Ba/K enrichment factors versus relative enrichment of K_2O as displayed by pairs of basalts of otherwise very similar composition. ● = Rb/K enrichment factor; O = Ba/K enrichment factor; ✦ and ◇ enrichment of weathering crust relative to the interior of the same boulder

TABLE 14. VARIATION IN COMPOSITION OF PAIRS OF SIMILAR SAMPLES FROM THE SOUTHWESTERN BANKS AND COMPOSITION OF EARTHY AMYGDALES AND BASALT FROM CORES AND WEATHERING CRUSTS OF THE SAME FRAGMENTS

	Intra-set CV(%)	60-7 amygdales from		37-1 amygdales from		28-24 amygdales, core	34-5 whole rock		37-7 whole rock	
		core	crust	core	crust		core	crust	core	crust
SiO_2	0.7	41.00	38.44	49.49	44.13	43.61	50.22	47.83	47.16	47.24
TiO_2	2.5	0.34	0.42	0.18	0.38	0.34	2.58	2.71	2.47	2.46
Al_2O_3	1.4	10.96	10.52	4.63	5.22	2.86	13.30	13.79	13.82	14.12
Fe_2O_3	22	13.19	18.56	10.02	17.25[1]	20.61	3.21	5.65	5.76	7.06
FeO		6.36	2.48	6.99		2.52	11.33	8.87	8.80	7.65
MnO	7.2	0.12	0.20	0.13	0.26	0.26	0.25	0.20	0.29	0.28
MgO	2.6	10.66	11.17	18.05	15.00	8.53	5.75	5.48	6.11	6.07
CaO	1.4	2.17	1.72	0.69	1.57	1.31	9.97	10.06	10.08	9.85
Na_2O	3.0	3.09	2.44			1.61	2.57	2.73	2.48	2.57
K_2O	29	0.29	1.36	0.56	0.63	0.32	0.28	0.34	0.21	0.35
P_2O_5	4.5	0.11	0.14	0.07	0.08	0.10	0.29	0.31	0.27	0.27
LOI^+	}34	6.84	7.87	5.37	5.46[2]	7.17	}0.56	}1.73	}1.81	}2.50
H_2O^-		4.99	3.95	2.73	6.70	10.24				
Total		100.12	99.27	(98.91)	(96.68)	99.48	100.31	99.70	99.26	100.42
FeO^*	2.0	18.23	19.18	16.01	15.53	21.07	14.22	13.96	13.98	14.00
FeO^*/MgO		1.71	1.72	0.89	1.04	2.47	2.47	2.55	2.29	2.31

Trace elements (ppm)

	Intra-set CV(%)	core	crust	core	crust	core	core	crust	core	crust
Rb	51	3.1	183	4.2	4.6	4.1	3.6	4.9	3.4	17.9
Ba	18	n.d.	n.d.	n.d.	n.d.		126	108	37	50
La	11						16	17	14	14
Nb	11						12.2	13.3	14.8	14.8
Zr	3.6	66	76	37	70		182	193	170	170
Sr	2.0	71	89	20	64	7.8	182	199	159	163
Y	3.4						41	42	34	35
Ga	12	21	22	17	16		23	25	21	28
Cu	22	620	860	320	205		280	250	180	100
V	6.3	63	82	55	87		380	400	440	400
Co	4.6	59	64	74	73		45	42	53	55
Ni	5.4	133	160	69	66		46	46	53	59
Cr	7.0	10	20	< 10	< 10		55	65	82	81

Note: LOI^+ = loss on ignition above 110^OC; n.d. = not detected (detection limit < 5 ppm Ba). 1) Total Fe as Fe_2O_3; 2) not corrected for oxidation of FeO.

flow from East Iceland (Watkins and others 1970; Hart and others 1971). These authors present evidence that the variation in this flow was largely due to the internal differentiation of the flow. Residual patches, for example, which crystallized potash feldspar, had notably higher levels of K and Rb than the bulk of the flow (see section 3.3.4.). In the present study, with very little geological control, the large variations of Cu, Rb and K are simply assigned to sampling variability.

Variations in Rb/K and Ba/K ratios against changes in K contents of dredged pairs are shown in Fig. 23c. When K levels increase, then Rb/K ratios are also raised; this implies that Rb is even more sensitive to the process or processes which caused an increase in K levels. The reverse applies to the Ba/K ratio implying that Ba is less responsive than K to these processes.

A number of earthy amygdales, from the cores and weathered margins of dredged basalt fragments, have been analysed for major and trace elements (Table 14). Amygdales from the fresher cores contain higher levels of Cu, Mg and Fe than in the host basalt suggesting mobility of these elements, perhaps as a result of diagenesis (burial metamorphism). Lower contents of Ba, Sr, CaO, TiO_2 and Zr, however, point to the immobility of this group of elements, though Ba, Sr and Cao may be concentrated in rare zeolite-bearing basalts (cf. Wood and others 1976). Samples 47-1 and 34-7 are distinctly high in Ba and Sr, respectively. In the former plagioclase is strongly zeolitized while the latter has a mesostasis of zeolites (mode in Table 13). Levels of K and Rb in the earthy amygdales are similar to those in the enclosing basalt suggesting only limited mobility.

Earthy amygdales from weathered margins, i.e. from basalts which have suffered low-temperature sea-floor weathering, show

more violent differences in chemistry. Contents of Cu, Fe_2O_3, MgO, Rb and K_2O can be distinctly high indicating either an increased mobility for this elemental group, or their introduction, under these conditions of alteration. The continued immobility of Ba, Sr, Zr, TiO_2 and CaO is reflected in their low levels of concentration. These variations are of limited relevance to the present study as "fresh" samples were always taken for investigation.

These various chemical studies on the alteration of dredged tholeiites reveal a variety of mechanisms within the general title of alteration. The main purpose of the studies was to locate the more stable and immobile elements which will be suitable for correlation purposes and the discussion of primary petrologic features.

3.6.3. Chemistry

Forty-eight samples which were recovered from thirteen stations on the banks have been analysed for major and trace elements (Table 19).

Seven stations were studied from the Faeroe Bank, four from Bill Bailey Bank and two from Lousy Bank.

These samples represent at least thirty different flows, some of the samples almost certainly being replicates of individual lava flows (see section 3.6.2.).

All samples from the banks are tholeiitic basalts and include both olivine tholeiites and tholeiites. On the histogram of FeO^*/MgO ratios (Fig. 14b), a bimodal distribution is suggested and is reminiscent of the distribution on the Faeroe Islands. The tholeiitic status of nearly all the lavas from the banks is confirmed on the alkalis versus SiO_2 diagram (Fig. 18a) where they fall in the field of Hawaiian tholeiitc basalts. Chemical coherence for tholeiites on the banks is suggested by colinear plots between the high valency incompatible elements (Ti, P, Sm, Hf, Zr, La, Nb) (Figs. 21 and 22). Normalized La/Sm ratios, on a few selelcted samples, range from 0.4-1.1 at Lousy Bank, 0.7-1.6 at Faeroe Bank, and 0.9-1.7 at Bill Bailey Bank (Table 15, Fig. 20).

The basalts from the southwestern banks range in composition from olivine tholeiites to tholeiites. They range from 4.8-8.7% in MgO, from 9.6-14.4% in FeO^* excluding two plagioclase-rich cumulates 47-1 and 28-25), and from 0.97-2.99 in the FeO^*/MgO ratio (Table 19 and Fig. 19).

Attention should be drawn to three samples, almost certainly from a single flow at station 28 on Bill Bailey Bank, which possess high total alkalis (Fig. 18a), TiO_2, P_2O_5 and incompatible

FIGURE 18
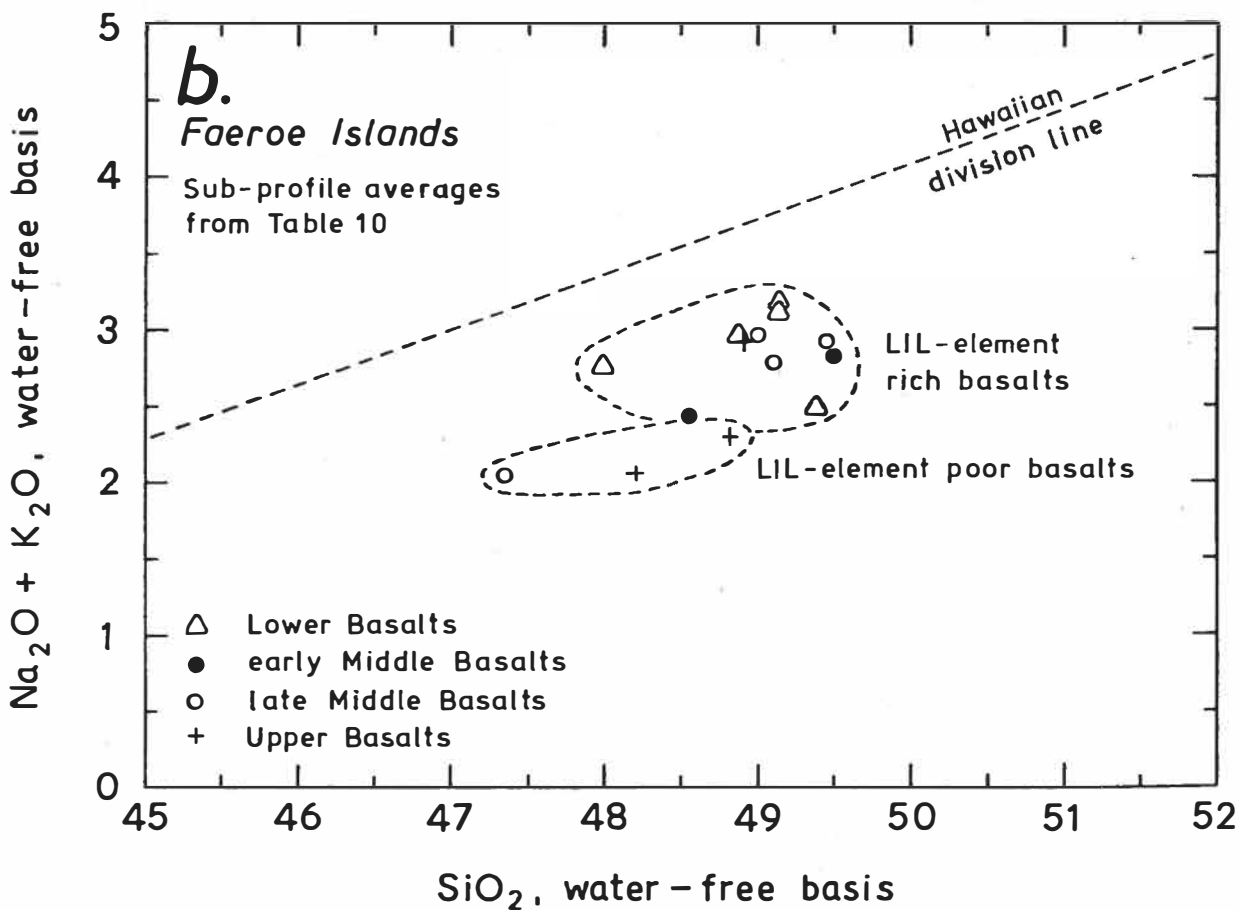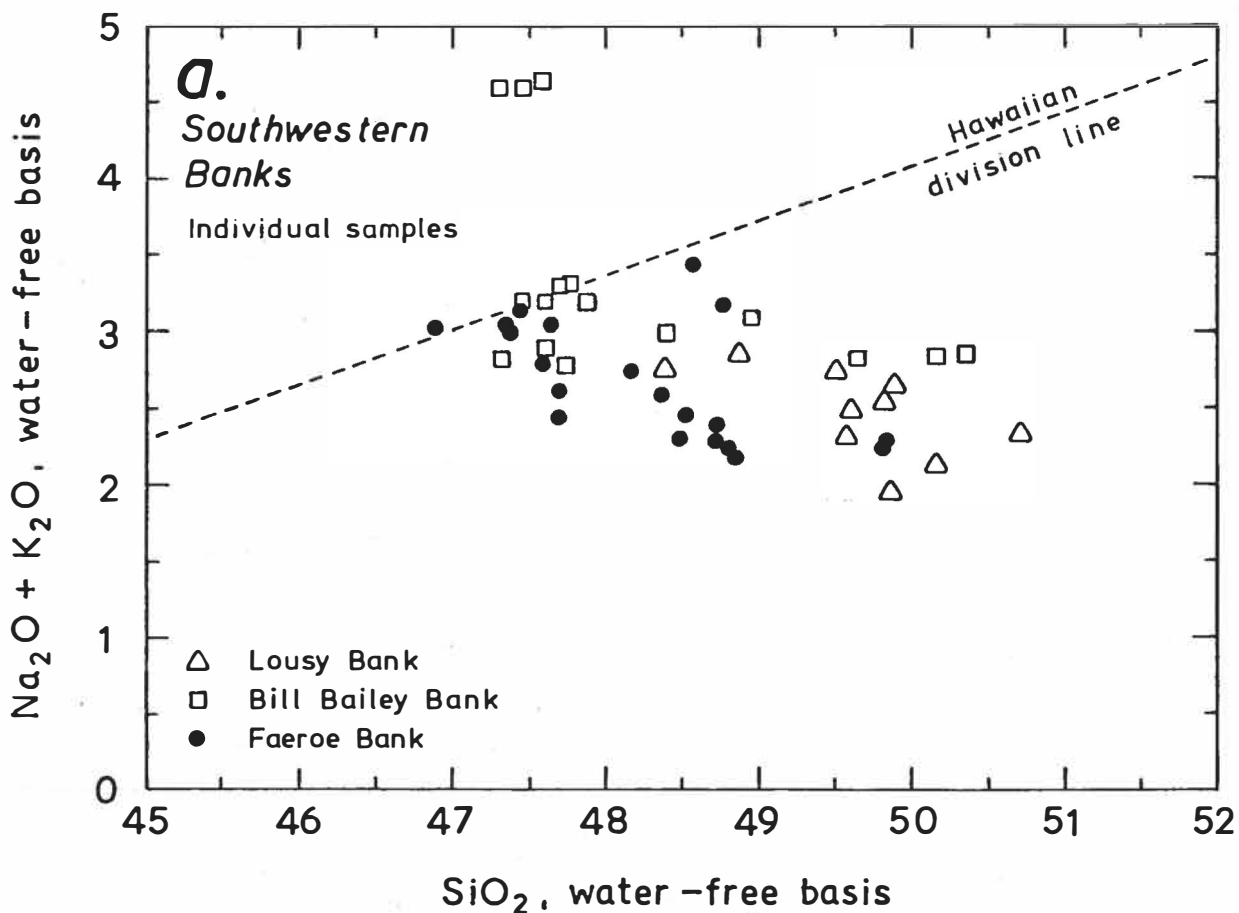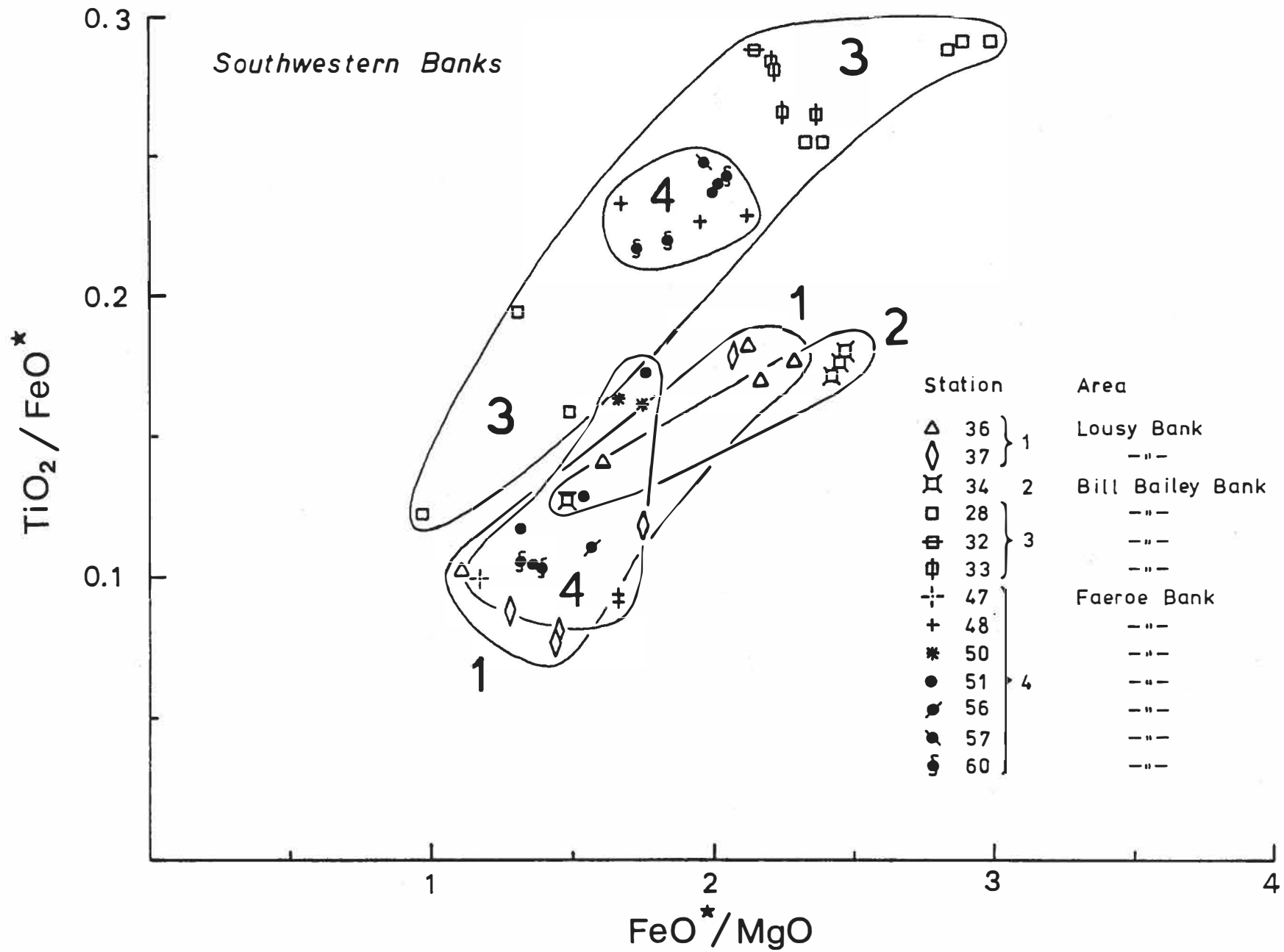
FIGURE 19. TiO_2/FeO^* versus FeO^*/MgO diagram for basalts from the southwestern banks

Table 15.   Neutron activation analyses of basalts from the banks SW of the Faeroe Islands

Area	Lousy Bank				Faeroe Bank			Bill Bailey Bank		
Sample No.	36-5	37-6	37-1	37-4	57-4	57-1	57-3	28-26	28-4	28-6
La, ppm	1.2	2.7	8.3	10.2	2.9	6.2	17.5	6.2	15.6	32.7
Ce	-	-	17.5	20.8	-	13.5	33.7	11.6	34.1	76.5
Sm	1.8	2.0	3.7	5.3	2.5	4.1	6.2	3.8	7.2	11.1
Eu	0.76	0.70	1.3	1.7	1.1	1.5	2.2	1.3	2.2	3.2
Yb	2.7	1.9	3.0	3.6	2.2	2.7	3.2	1.9	3.5	3.5
Lu	0.44	0.32	0.40	0.53	0.34	-	0.48	0.36	0.64	0.55
La/Sm$_{E.F.}$	0.4	0.8	1.3	1.1	0.7	0.9	1.6	0.9	1.2	1.7
Sc	51.9	46.8	46.2	42.6	44.9	40.6	35.9	37.7	37.9	25.4
Cr	79	213	31	64	225	162	146	256	129	23
Co	56.4	54.9	55.7	57.4	53.2	50.5	51.2	52.3	50.3	49.5
Hf	1.5	1.5	2.3	4.1	1.8	3.2	5.0	2.8	5.6	8.3
Ta	-	-	0.5	1.2	-	0.4	1.4	0.4	1.1	2.6
Th	-	-	0.6	0.8	-	0.4	1.5	0.6	1.5	2.7

Additional results: 0.81 ppm Tb in 28-26; 54.9 ppm Nd, 8.7 ppm Gd, and 1.1 ppm Tb in 28-6.

FIGURE 20
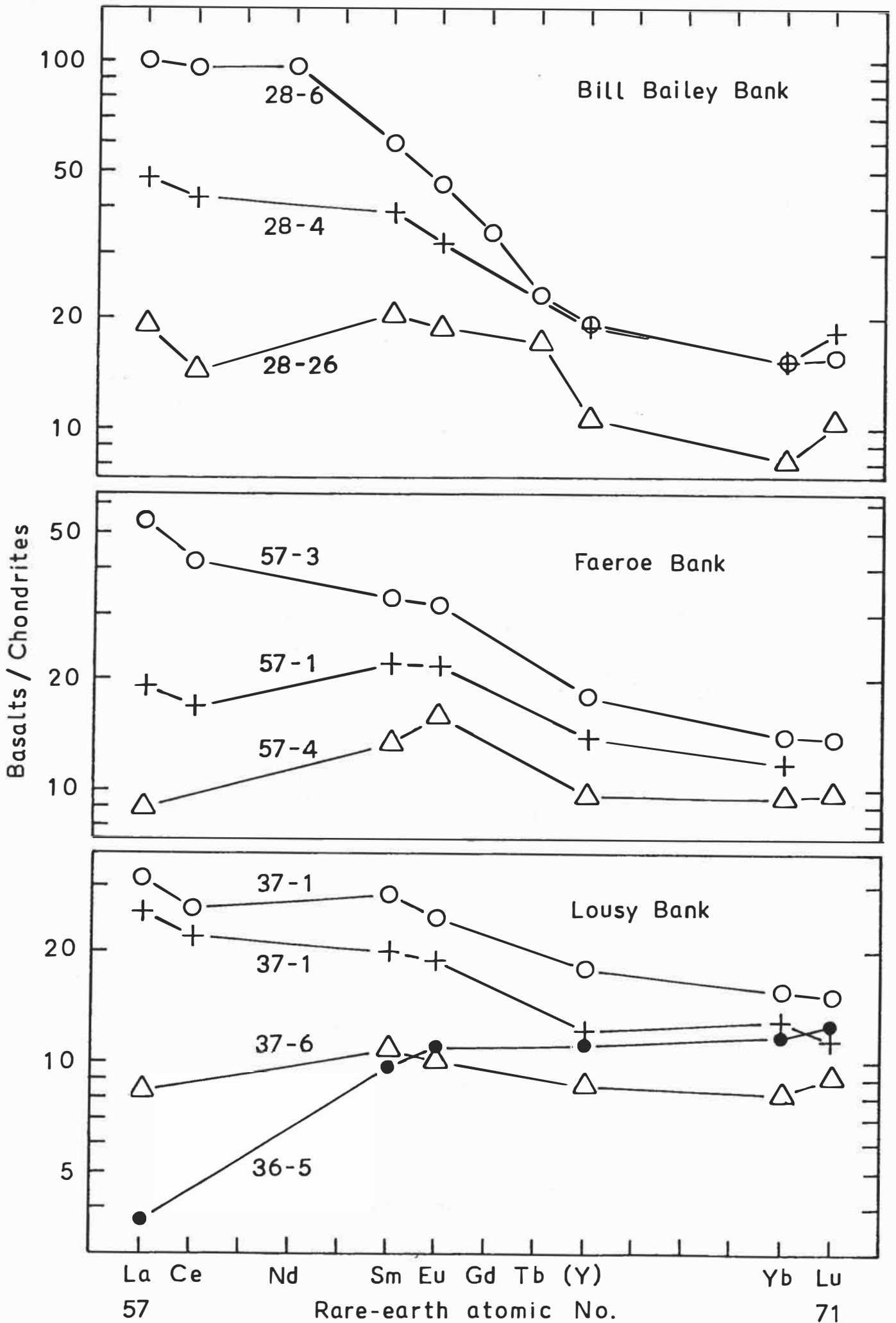
FIGURE 21. TiO_2, P_2O_5, Sm and Hf versus Zr in basalts from the banks southwest of the Faeroe Islands

△ Lousy Bank
□ Bill Bailey Bank
● Faeroe Bank
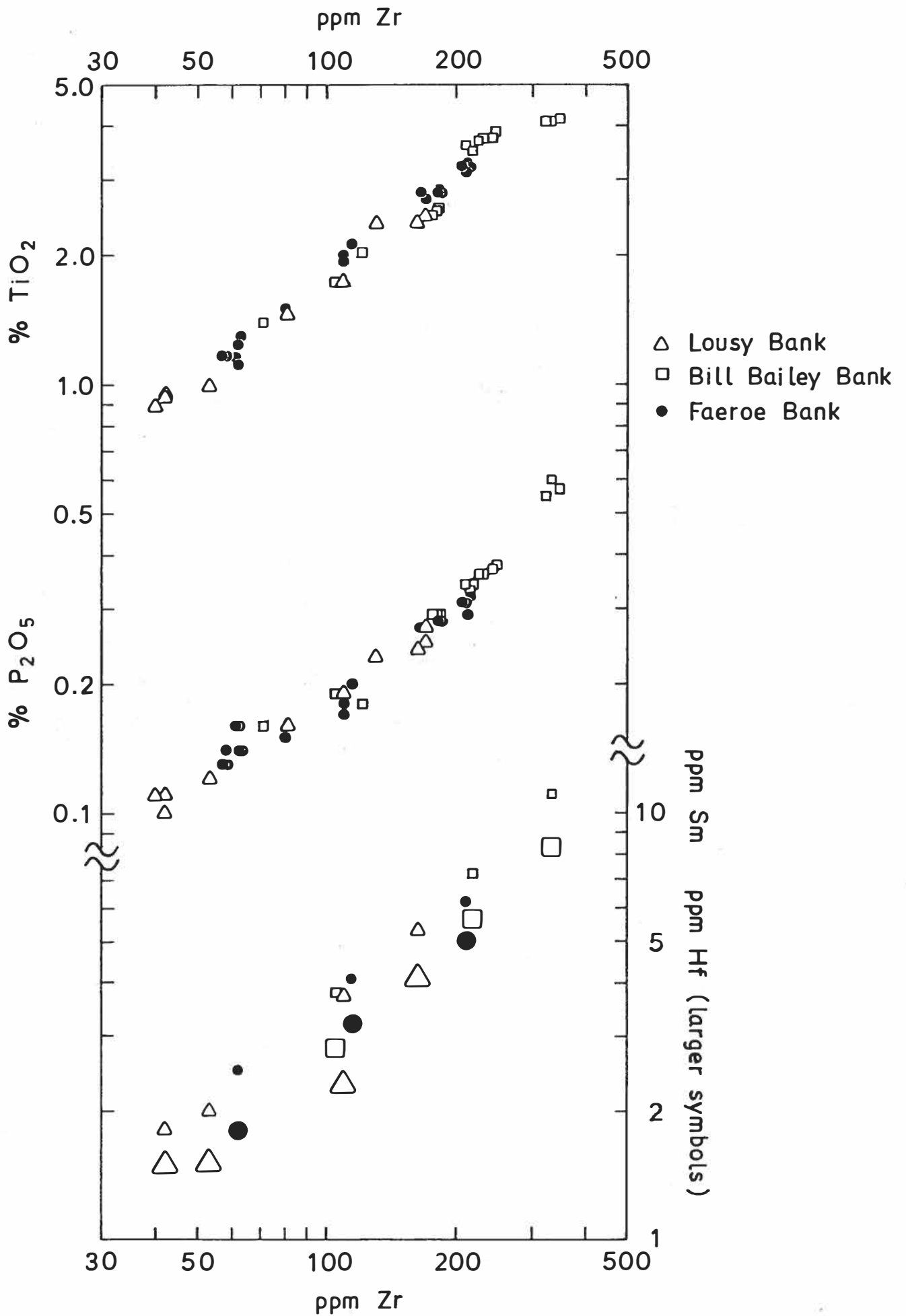
FIGURE 22. La and Nb versus Zr for basalts from the southwestern banks
Same symbols as in Fig. 19
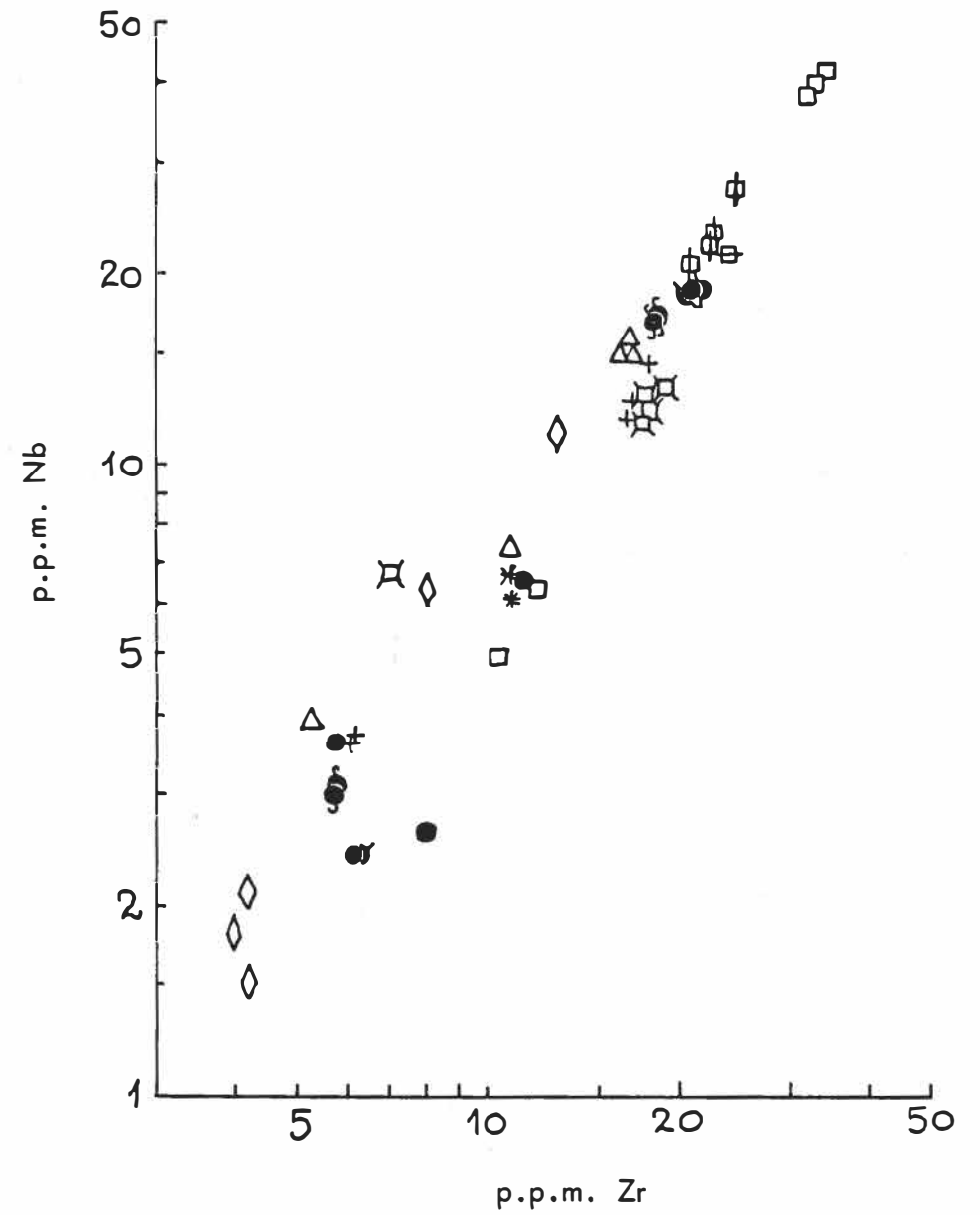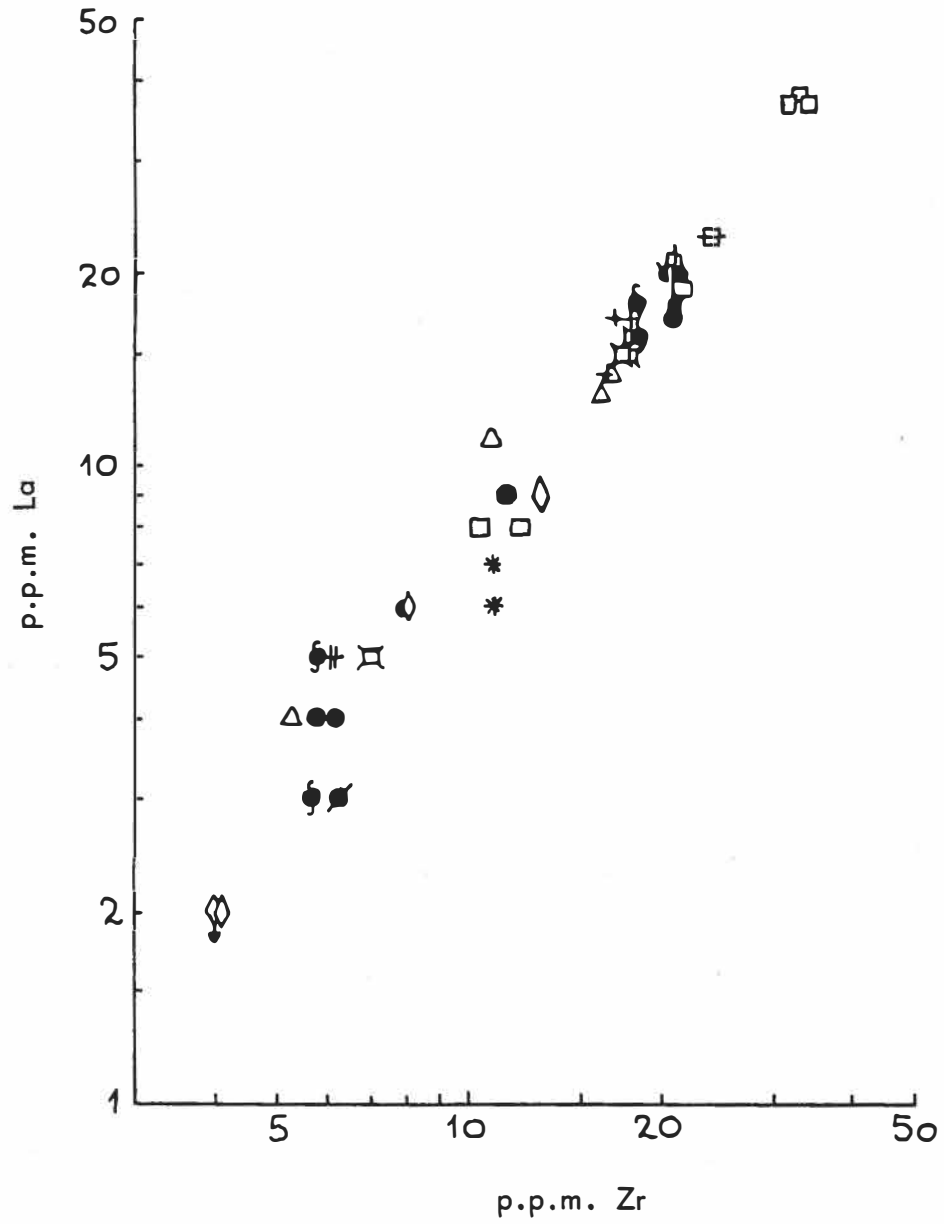
trace elements (Table 19) but low normative hypersthene. They can be matched with transitional basalts from the Icelandic eastern neovolcanic zone (Jakobsson 1972).

The plot of total alkalis versus SiO_2 for the banks (Fig. 18a) reveals an unexpected feature. Contents of Na_2O plus K_2O increase, as expected, along with basalt differentiation but this is accompanied by a fall in SiO_2 levels. This trend can be discerned for individual banks, as well as for all the banks together. According to the petrographic classification, this trend corresponds to a change from olivine tholeiites to tholeiites.

The reasons for the unexpected fall in SiO_2 contents almost certainly lie in the differing alteration histories of these basalts. Tholeiites, which are more evolved, develop a greater proportion of interstitial rhyolitic material and, as already postulated, this material is subject to SiO_2 loss during the widespread alteration.

Fig. 18a also reveals that at a fixed value of SiO_2, total alkali values tend to increase from the Faeroe Bank basalts through the Lousy Bank basalts and into the Bill Bailey Bank basalts. In the MgO versus SiO_2 diagram (not presented), the basalts from Lousy Bank are generally about 1% higher in SiO_2 than the basalts from Faeroe Bank while the basalts from Bill Bailey Bank show a large scatter in their SiO_2 values.

The incompatible elements can be divided into different groups according to their range in concentration through all the basalts analysed from the banks. La varies from less than 2 ppm to about 38 ppm, a factor of over 19 and likewise Nb varies from 1.5 ppm to about 42 ppm, a factor of roughly 28. Ba varies from 6 to 349 ppm, a factor of 58. Although Ta and Th could not be detected below about 0.4 ppm, the remaining values indicate a wide varia-

tion following the variations of La and Nb (Table 15). Zr only varies by a factor of nearly 9, passing from 40 to 346 ppm. Again, ignoring cumulate rocks, TiO_2 only ranges from 0.9 to 4.2%, a factor of 4.7. P_2O_5 ranges from 0.10 to 0.60%, a factor of 6. Sm ranges from 1.8 to 11.1 ppm, i.e. by 6.2, and Hf varies from 1.5 to 8.3 ppm, i.e. by about 5.5. Thus Ba, Nb and La show a much greater variation than the other incompatible elements. It appears that those incompatible elements with the largest ionic radii in each valency group exhibit the greatest range in concentration.

Considerable variations in the contents of incompatible elements are also visible even when the results from the individual banks are compared. However, there is a general shift in the absolute contents of these elements, the contents increasing in the sequence Lousy Bank, Faeroe Bank, Bill Bailey Bank (Figs. 21 and 22).

MgO variation diagrams reveal that groups of basalts with different levels of some incompatible elements (Zr, Nb and La) exist on a single bank (e.g. the two stations on Lousy Bank) or even at a single dredge station (e.g. station 57 on Faeroe Bank)(Fig. 24). In addition, different groups can be distinguished on Lousy Bank and the Faeroe Bank. On the MgO variation diagrams, a group of samples from Faeroe Bank consistently plot at intermediate levels for Zr, Nb and La between the two groups recognized on Lousy Bank.

The basalt groups outlined above may in fact be members of different tholeiitic magma series though this possibility cannot be substantiated using the few samples available at present. These supposed series are unlikely to be generated by a simple mechanism of fractional crystallization because different incompatible elements vary by different factors along the series. For example,

FIGURE 24. MgO variation diagrams for Zr, Nb and La for
selected stations from Lousy Bank and Faeroe Bank.
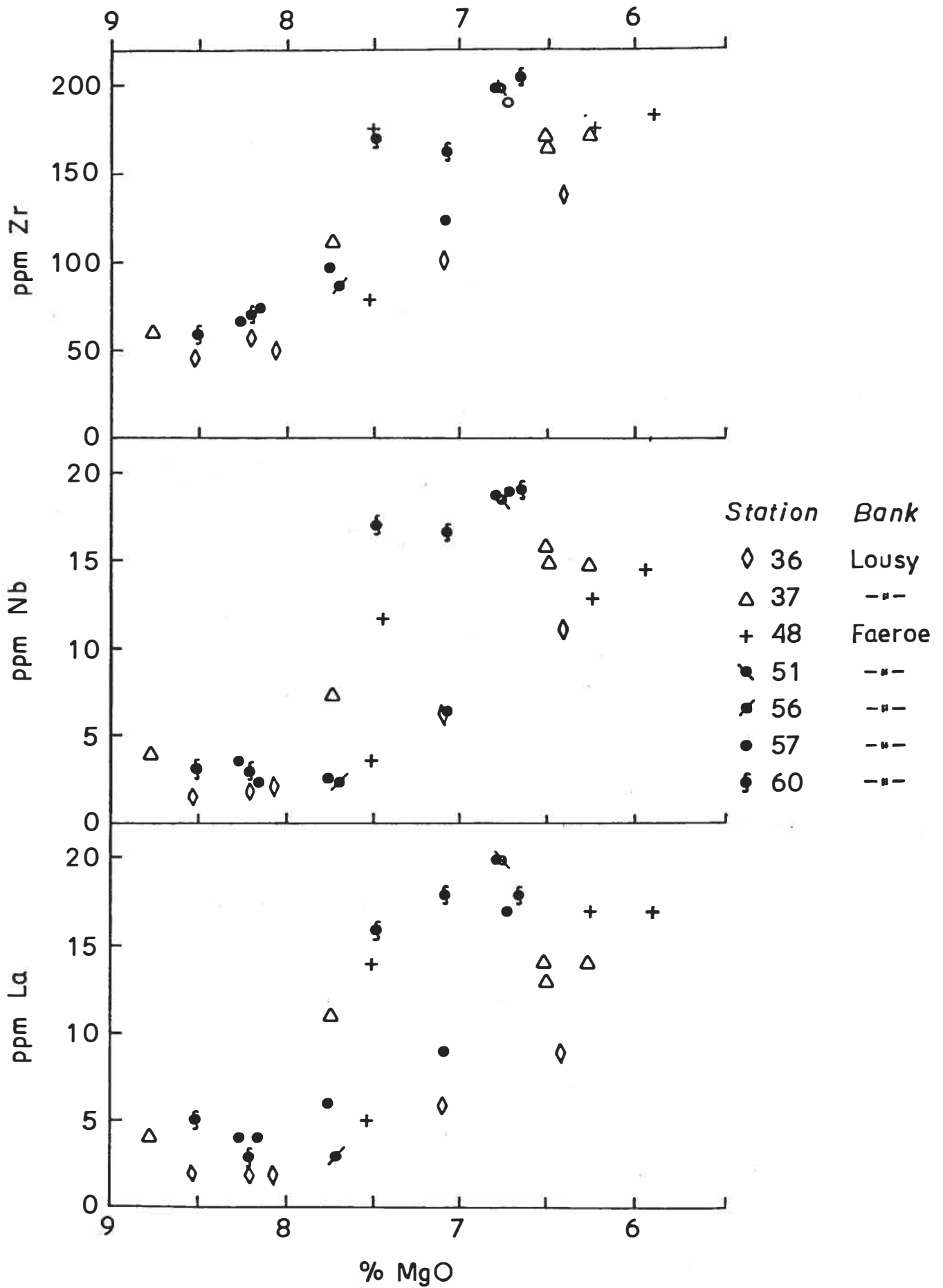
Nb varies by a factor of 8 in the "series" from station 36 on Lousy Bank whereas TiO_2 only varies by a factor of 2.5. The wide variations in Nb and La are also inconsistent with the small changes in contents of major elements within this "series".

3.7. Chemical comparison between the Faeroe Islands and the southwestern banks

In general, the major element contents of the basalts from the southwestern banks show similar ranges and levels to those from the Faeroe Islands. An important exception is the absence of olivine-rich (picritic) basalts from the dredged materials though further dredging may possibly remove this difference. In addition, the three samples with high total alkalis at station 28 on Bill Bailey Bank cannot be matched with any known lavas on the Faeroe Islands.

On the TiO_2/FeO^* versus FeO^*/MgO grid (Fig. 19), the olivine tholeiites from Lousy Bank lie in the same area as the Upper Basalts from the Faeroes (Fig. 15). The tholeiites from Lousy Bank lie on the extension of the field for the Faeroese Upper Basalts towards higher FeO^*/MgO ratios. Some overlap also occurs with the Faeroese Lower Basalts. Lousy Bank tholeiites are similar to the Lower Basalts in contents of most elements (Table 16), except for their lower Ba, Sr and Zr contents which are more comparable to tholeiites from the Upper Basalts.

The westernmost station on Bill Bailey Bank (station 34) is similar to the Lousy Bank samples in most respects (Table 16, Fig. 19). They are higher in Ba, and one of the samples is higher in Sr also, than Lousy Bank basalts with similar FeO^*/MgO ratios and cannot be distinguished from the Faeroese Lower Basalts. The basalts from the remaining stations on Bill Bailey Bank all fall together with the LIL-element enriched flows from the Middle Basalts (Table 16, Fig. 19).

Faeroe Bank yielded basalts which exhibit a bimodal distribution. Some of them are very similar to the LIL-element depleted olivine tholeiites from the Middle and Upper Basalts. The other

TABLE 16.   COMPARISON OF CHEMICAL COMPOSITION OF BASALTS FROM THE FAEROE ISLANDS AND THE SOUTHWESTERN BANKS

Sample No.	Lousy Bank 36-6	Lousy Bank 37-5	Bill Bailey 34-2	Lower Bas. III[1]	Bill Bailey 34-7	Lower Bas. III.7[2]	Bill Bailey Bank 28-26	Bill Bailey Bank 28-1	Middle Bas. VIII-1[2]
SiO_2	49.08	47.79	48.86	47.71	47.28	47.81	46.95	47.92	48.06
TiO_2	2.36	2.46	2.47	2.25	1.40	1.38	1.74	2.03	2.29
Al_2O_3	13.82	14.05	12.83	13.99	15.46	15.35	15.53	14.86	15.39
Fe_2O_3	3.71	5.11	7.37	5.80	3.23	5.53	5.45	4.32	4.06
FeO	9.82	8.92	7.71	7.68	8.02	6.50	6.03	6.51	6.70
MnO	0.23	0.23	0.27		0.19		0.18	0.16	0.16
MgO	6.37	6.38	5.92	6.37	7.37	6.46	7.34	7.93	6.72
CaO	10.82	9.84	9.88	11.21	11.67	12.38	12.23	11.00	11.26
Na_2O	2.58	2.64	2.56	2.20	2.54	2.02	2.51	2.73	2.52
K_2O	0.14	0.15	0.22	0.36	0.38	0.25	0.22	0.28	0.28
P_2O_5	0.23	0.25	0.29		0.16		0.19	0.18	
H_2O	1.02	1.92	0.98		2.42		1.67	2.37	
Total	100.18	99.74	99.36	(97.57)	100.12	(97.68)	100.04	100.29	(97.44)
FeO^*	13.16	13.52	14.34	12.90	10.93	11.48	10.94	10.40	10.35
FeO^*/MgO	2.07	2.12	2.42	2.03	1.48	1.78	1.49	1.31	1.54
TiO_2/FeO^*	0.179	0.182	0.172	0.174	0.128	0.120	0.159	0.195	0.221
Ba	48	46	91	95	78	52	49	79	85
La	9	14	15	12.2	5	5.8	6.2	8	
Nb	11.2	15.8	11.6		6.7		4.9	6.3	
Zr	130	169	176	150	71	96	105	121	190
Sr	166	165	177	205	394	150	215	306	240
Cu	190	210	215	160	157	128	135	122	200
V	380	460	420	320	270	280	320	250	255
Sc	40	37[4]	40[4]	38	37	38	31		
Co	57	53	51	48	51	45	47	45	44
Ni	75	56	46	72	88	72	88	120	160
Cr	99	82	65	134	175	128	250	320	275
$La/Sm_{E.F.}$		1.1[4]		1.5		1.4	0.9		

TABLE 16.   (Continued)

	Faeroe Bank		Middle Bas.	Bill Bailey	Middle Bas.	Bill Bailey	Middle Bas.
	60-9	48-5	X.5[2]	28-4	66[3]	33-4	69[3]
SiO_2	46.72	46.35	47.77	46.75	47.42	46.62	46.96
TiO_2	2.82	2.81	2.96	3.50	3.49	3.90	3.99
Al_2O_3	14.38	14.07	14.42	14.31	13.78	13.18	12.89
Fe_2O_3	4.71	4.26	4.26	4.98	5.77	4.17	5.89
FeO	8.57	8.25	8.55	9.26	8.51	10.11	9.35
MnO	0.20	0.22	0.21	0.25	0.21	0.21	0.22
MgO	6.95	7.23	6.33	5.91	6.00	6.24	5.91
CaO	10.83	10.16	11.01	10.75	10.35	10.35	9.98
Na_2O	2.56	2.48	2.34	2.59	2.24	2.71	2.32
K_2O	0.18	0.15	0.19	0.19	0.27	0.43	0.28
P_2O_5	0.28	0.27	0.24	0.34	0.39	0.38	0.39
H_2O	2.11	3.20		1.10	1.30	1.50	1.15
Total	100.31	99.45	(98.28)	99.93	99.73	99.80	99.33
FeO^*	12.81	12.08	12.38	13.74	13.70	13.86	14.65
FeO^*/MgO	1.84	1.67	1.96	2.33	2.28	2.22	2.48
TiO_2/FeO^*	0.220	0.233	0.239	0.255	0.255	0.281	0.272
Ba	56	44	60	59	46	102	61
La	18	14	14.1	19		21[4]	
Nb	16.7	11.8		18.5		27.4	
Zr	184	166	165	218	220	247	250
Sr	270	234	300	244	230	274	230
Cu	210	245	150	280	220	250	270
V	320	305	300	370	360	370	380
Sc	30[4]	38		31	33	29[4]	33
Co	47	50	40	45	47	47	47
Ni	103	105	100	78	78	82	82
Cr	188	225	150	130	125	102	125
$La/Sm_{E.F.}$			1.3				

TABLE 16. (Continued)

	Lousy Bank		Bill Bailey	Faeroe Bank			Upper Bas.
	36-5	37-6	28-25	57-4	47-1	48-1	C-horizon[3]
SiO_2	49.15	49.28	44.81	48.03	46.80	49.23	47.63
TiO_2	0.94	0.99	1.11	1.25	0.78	1.12	1.05
Al_2O_3	14.08	14.94	17.17	14.67	19.93	13.85	15.05
Fe_2O_3	3.39	2.62	4.04	3.23	2.89	4.22	4.73
FeO	7.69	7.27	5.38	7.69	5.22	8.54	6.15
MnO	0.16	0.16	0.15	0.20	0.12	0.21	0.20
MgO	8.36	8.66	9.32	8.03	6.68	7.45	8.30
CaO	12.01	12.81	10.73	12.98	13.19	11.76	12.71
Na_2O	2.04	1.87	2.30	2.09	1.77	2.13	1.80
K_2O	0.05	0.07	0.54	0.13	0.12	0.13	0.31
P_2O_5	0.11	0.12	0.13	0.14	0.10	0.16	0.08
H_2O	2.00	1.61	4.95	1.44	1.93	0.94	1.16
Total	99.98	100.40	100.63	99.88	99.53	99.74	99.17
FeO*	10.74	9.63	9.02	10.60	7.82	12.34	10.41
FeO*/MgO	1.28	1.11	0.97	1.32	1.17	1.66	1.25
TiO_2/FeO*	0.087	0.103	0.23	0.118	0.100	0.091	0.101
Ba	7	20	38	30	190	40	< 10
La	1.2	2.7	3	2.9	3	5	2.2
Nb	1.5	3.9	3.2	2.4	0.8	3.7	
Zr	42	53	65	62	43	62	70
Sr	75	110	456	166	165	111	105
Cu	130	127	63	127	97	190	125
V	260	260	205	290	200	330	240
Sc	38	36		36		42[4]	40
Co	48	47	49	47	42	55	50
Ni	69	85	205	99	103	72	135
Cr	92	220	500	225	225	76	310
La/Sm$_{E.F.}$	0.4	0.8		0.7			0.6

COMMENTS TO TABLE 16

The rare-earth element data for Faeroese basalts are from Schilling and Noe-Nygaard (1974); Ba, La, Nb, Zr and Sr in the basalts from the banks are XRF analyses; all other trace element results are emission spectrography analyses. 1) Average of all ten basalts in profile III (see Table 10); 2) revised analysis from the Faeroese main profile; 3) analysis from the Sneis profile (Table 17); 4) La, Sm and/or Sc results are from another, but similar, sample from the same dredge haul.

group of basalts is similar to the LIL-element enriched tholeiites from the Middle and Upper Basalts. These two types occur together at three out of the seven dredge stations (Table 16, Fig. 19).

Tholeiitic basalts from the banks and from the Faeroe Islands show similar ranges and contents of La and TiO_2 (Fig. 27) whereas Na_2O contents in basalts from the banks are generally higher (Fig. 25) and Zr contents are generally lower (Fig. 26) than in basalts from the Faeroe Islands.

Allowing for the differences in Na_2O and Zr, some long-distance lithostratigraphic correlations can be suggested between the banks and the Faeroe Islands. Faeroe Bank samples correlate with the upper part of the Middle Basalts or the Upper Basalts. Bill Bailey Bank samples are very similar to the early and late Middle Basalts excluding station 34 which perhaps correlates with the uppermost part of the Lower Basalts. Lousy Bank tholeiites show similarities with the tholeiites from the Lower Basalts but also show some similarities with tholeiites from the Upper Basalts. It should be noticed that the geographic distribution of the LIL--element depleted flows seems partly controlled by proximity to the ocean floor (section 3.3.). They are thus less suitable for long distance correlations, and their presence on Lousy Bank together with samples like the Lower Basalts may simply reflect their earlier appearance in the volcanic sequence due to the closeness of this bank to the ocean floor.

FIGURE 25

● Faeroe Islands
○ Southwestern Banks

% Na₂O

% TiO₂

FIGURE 26

- ● Faeroe Islands
- ○ Southwestern Banks

Y-axis: ppm Zr (emission spectrography)

X-axis: % TiO$_2$
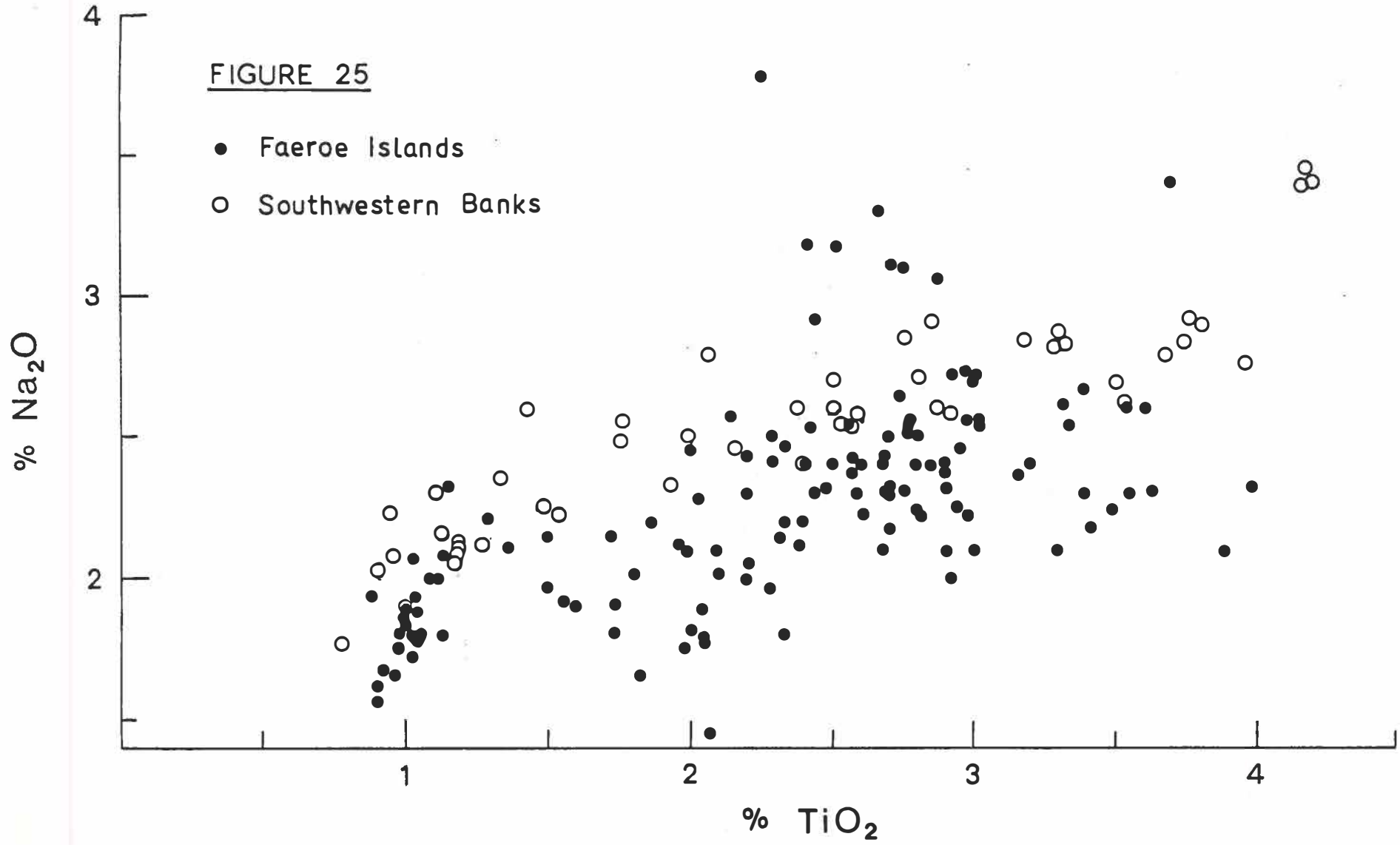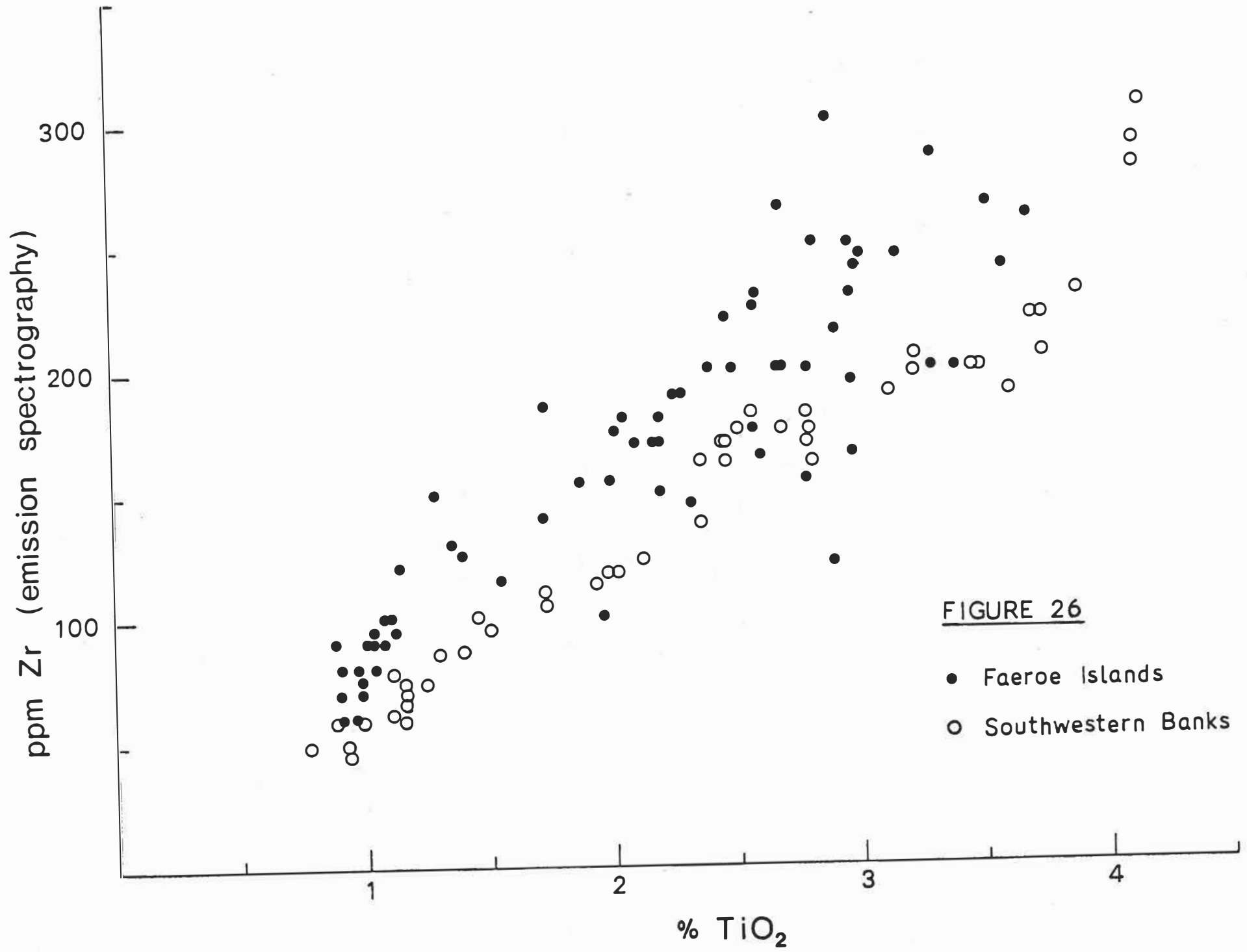
FIGURE 27 La versus TiO$_2$ for the southwestern banks and the Faeroe Islands.
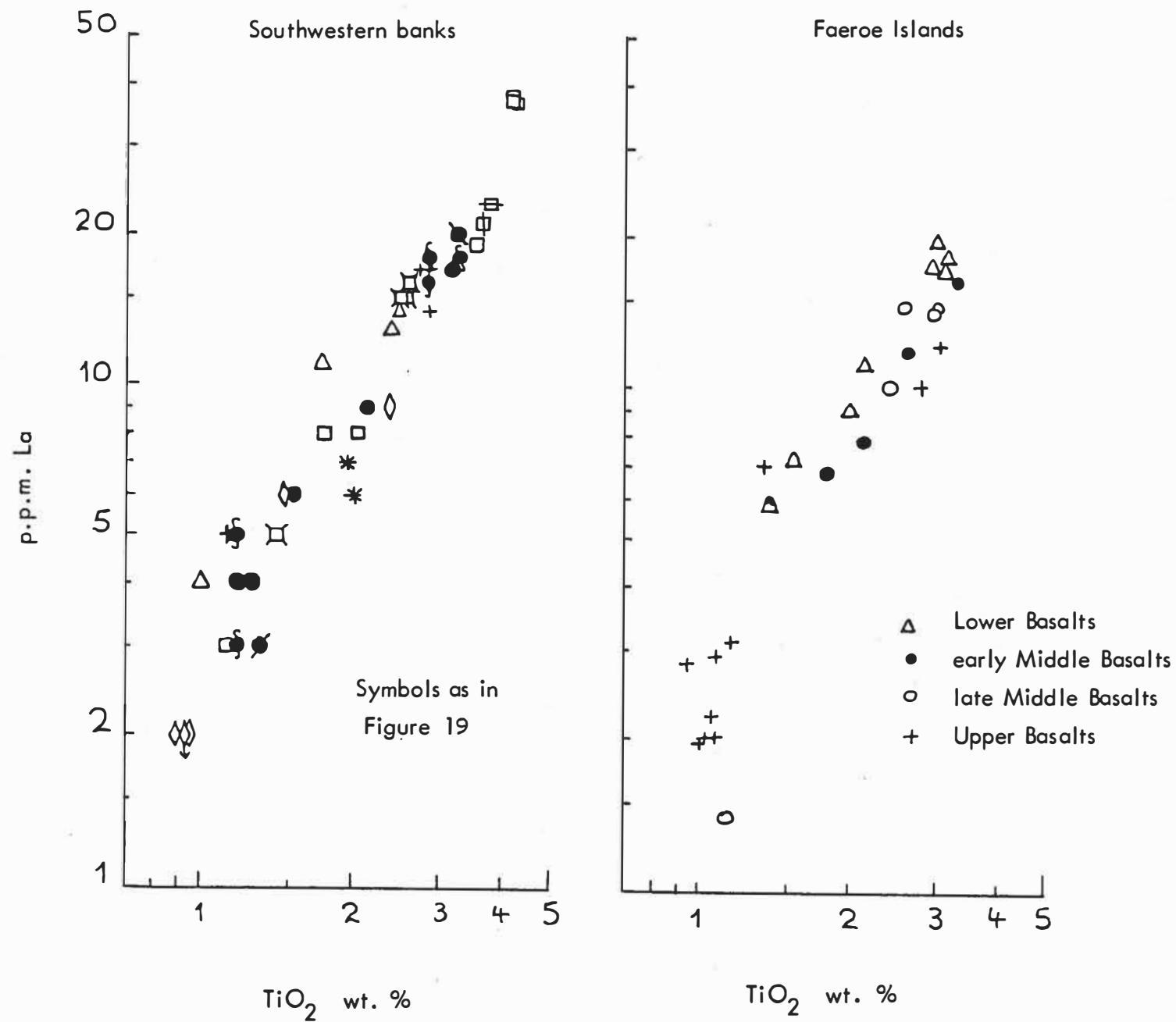
CHAPTER 4

DISCUSSION AND CONCLUSIONS

The Faeroe Islands and the southwestern banks form the north-
ern part of the Faeroe Rise which, from geophysical evidence, is
considered to constitute a largely submerged micro-continent,
partly or completely separated from the Northwestern European
shelf (see Introduction). The islands and the banks are composed
of basalts which form part of the Lower Tertiary North Atlantic
igneous province whose formation has been linked with the opening
of the N.E. Atlantic.

According to K-Ar dating by Tarling and Gale (1968), the Fae-
roese lavas yield ages between 50 and 60 m.y. B.P. and the dif-
ferent ages show no correlation with stratigraphic level. Due
to the rather high degree of alteration of the Faeroese thole-
iites some of the samples have probably suffered loss of argon and
will therefore give ages which are too young. The older values
of 60 m.y. B.P. are therefore thought to be closer to the true
age. The appearance of ocean floor in the N.E. Atlantic has been
estimated to date from about 53 m.y. B.P. (Soper and others 1976 b).
Thus the Faeroese basalts appear to slightly pre-date the actual
opening of the N.E. Atlantic.

The exposed thickness of the basalts on the Faeroes is about
3500 metres and seismic refraction work by Pálmason (1965) sug-
gests a further 2-3 kilometres of hidden basalts. Pálmason di-
vided the lava sequence into an upper part equivalent to the
Upper Basalts with V_p equal to 3.9 km/sec and a lower part equi-
valent to the Middle Basalts plus Lower Basalts with V_p equal to
4.9 km/sec. Time term analysis suggests a maximum thickness of
roughly 5 km for the 4.9 km/sec layer (Bott and others 1974).
The exposed thickness of the Upper Basalts on the Faeroes is

about 900 metres and the interpretation of bathymetric profiles suggests that their thickness on the southeastern shelf is roughly 1300 metres. As discussed below, the final flows in the Upper Basalts may still be preserved at the southeastern limit of the basalt plateau. The maximum total thickness of the Faeroese basalt plateau is therefore about 6 kilometres.

There is no evidence of appreciable thinning of the basalt plateau or lateral transition into tuff-breccias consequent on the arrival of the lava flows into water (see sections 2.1.2. and 3.5.). Given the great thickness of the Faeroese, it is most likely that a similar thickness of lavas will occur over most of the Faeroe block. According to the limited evidence for an increase in the dip of the lavas near the outer limit of the basaltic shelf (section 2.2.4.), the basalt plateau underlies the sedimentary parts of the shelf. It may possibly continue beneath the Faeroe Bank Channel (where a magnetic basement has been recognized at fairly shallow depths (Bott and Stacey 1967)) and pass into the area of the southwestern banks. Dredging of in situ material from these banks recovered only basalts which are very similar in petrographic and chemical features to the Faeroese basalts and this confirms the extension of the basalt plateau to the area of the banks.

Detailed comparisons of the basalts from the banks and the islands suggest that: Faeroe Bank basalts correlate with the upper part of the Middle Basalts or the Upper Basalts, the Bill Bailey Bank basalts correlate with the Middle Basalts and uppermost part of the Lower Basalts, and Lousy Bank basalts may possibly be correlated with the Lower Basalts.

This last suggestion assumes that the presence of LIL-element depleted flows on Lousy Bank together with samples like the Lower

Basalts may be due to their early appearance in the volcanic sequence which in turn is related to the closeness of this bank to the ocean floor (see section 3.7.). The possibility of lateral variations in the proportions of different basalt types receives some support from the distribution of erratics and exposed Faeroese basalts which, in conjunction, show that the LIL-depleted basalts increase rapidly in abundance towards the outer oceanic edge of the basalt plateau. Based on geophysical interpretation of the East Greenland continental margin, Featherstone and others (1977) found evidence for the former presence of oceanic crust in the area immediately west of the Faeroe Islands and immediately north of the banks.

Soper and others (1976) have noted the occurrence of marine horizons at the base and near the top of the thick East Greenland lava pile and concluded that subsidence roughly kept pace with the build-up of most of the pile. In the Faeroes, the occurrence of laterally extensive and uniform groups of flows (e.g. the B- and C-horizons) and the coal-bearing A-horizon, together with the lack of major erosional topographic features, point to an extremely flat, possibly low-lying, topography throughout the extensive period of formation of the pile. Thus build-up and contemporaneous subsidence may also have characterized the development of the Faeroese lava sequence.

The tuff-carbonate sediments (section 3.5.) are likely to have been widespread in the sedimentary parts of the Faeroese shelf because the prograding beds expose most of the sedimentary sequence and tuff-carbonate sediments, despite their friability, are the only type of sediments found.

The abundance of reworked basaltic tuffs suggests that the primary ashes were produced by submarine volcanism as subaerial ba-

saltic eruptions from the present-day North Atlantic basalt province (e.g. on Iceland) normally produce only minor ashes. These ashes were probably erupted in the final stages of Faeroese volcanism and suggest that the basalt plateau was submerged. Because of this submergeance, and by analogy to the Móberg formation of Iceland, large volumes of ashes could have been produced. It is possible that local uplift followed by erosion contributed reworked tuffaceous materials to the sedimentary shelf.

The youngest fine-grained tuff horizons in the northern part of the North Sea, a few hundred kilometres to the southeast of the Faeroe Islands, have been shown to be about 53 m.y. in age (Jacqué and Thouvenin 1975). These horizons could not be related to any nearby volcanic activity. If they represent the distant deposition of Faeroese ashes, they then suggest an upper date of 53 m.y. for this activity.

The doming which post-dates the lava eruption on the Faeroe Islands may well have been synchronous with the formation of sedimentary basins on the surrounding shelf which contain tuff--carbonate sediments overlying Upper Basalts (Fig. 9). It is possible that the highest flows of the Upper Basalts are still preserved at the margin of the sedimentary basins. The doming took place before the completion of intrusive activity (section 2.1.7) which, on chemical grounds, seems to be a continuation of the Upper Basalt magmatic activity (section 3.3.5.).

The monotonous levels of mountain summits on the Faeroe Islands appear to define a relict, somewhat deformed, peneplain. The formation of this peneplain took place after the episode of doming and basin formation. The renewed pulse of erosion which dissected this peneplain may possibly be correlated with the development of a thick sedimentary wedge on the outer part of the sedi-

mentary shelf southeast of the Faeroe Islands which overlies an unconformity within the sedimentary sequence there (section 2.3.). Korsakov (1964) suggests that the continuation of this unconformity in the central part of the Faeroe-Shetland Trough may be Middle Tertiary in age. The peneplain is found at higher levels in the northern Faeroes indicating greater uplift in that area.

REFERENCES

Avery, C.E., Burton, G.D., and Heirtzler, J.R., 1968, An aeromagnetic survey of the Norwegian Sea: Jour. Geophys. Research, v. 73, p. 4583-4600.

Badgley, P.C., 1965, Structural and tectonic principles: New York, Harper and Row, 521 p.

Bailey, E.B., Clough, T.C., Wright, W.B., Richey, J.E., and Wilson, G.V., 1924, The Tertiary and post-Tertiary geology of Mull, Loch Aline and Oban: Scotland Geol. Survey Mem.

Baker, I., and Haggerty, S.E., 1967, The alteration of olivine in basaltic and associated lavas, pt. 2. Intermediate and low temperature alteration: Contr. Mineralogy and Petrology, v. 16, p. 258-273.

Belderson, R.H., Kenyon, N.H., and Stride, A.H., 1971, Holocene sediments on the continental shelf west of the British Isles, in Delany, F.M., ed., ICSU/SCOR Symposium on East Atlantic continental margins 1970: Inst. Geol. Sci. Rept. 70/14, p. 157-170.

Belderson, R.H., Kenyon, N.H., and Wilson, J.B., 1973, Iceberg plough marks in the North East Atlantic: Palaeogeog. Palaeoclim. Palaeoecol., v. 13, p. 215-224.

Berthois, L., 1969, Bathymetrie de l'Atlantique nord entre les Faeroe et les Hebrides et lithologie des blocs epars sur le fond: L. Ass. Fr. et Grandes Profondeurs Ocean, No. 6, p. 1-28.

Berthois, L., and Du Buit, M.-H., 1971, Contribution à l'étude de la sedimentation en Atlantique nord: Bull. Inst. Géol. Basin Aquitaine, v. 11, p. 365-374.

Bollingberg, H., Brooks, C.K., and Noe-Nygaard, A., 1975, Trace element variations in Faeroese basalts and their possible relationship to ocean floor spreading history: Geol. Soc. Denmark Bull., v. 24, p. 55-60.

Bott, M.H.P., 1973, The evolution of the Atlantic north of the Faeroe Islands, in Tarling, D.H., and Runcorn, S.K., eds., Implications of continental drift to earth sciences, Vol. 1: New York, Academic Press, p. 175-189.

— 1975a, Structure and evolution of the north Scottish shelf, the Faeroe block and the intervening region, in Petroleum geology and geology of the North Sea and N.E. Atlantic continental margin: Norges Geol. Undersøgelse, No. 316, p. 105-116.

Bott, M.H.P., 1975b, Structure and evolution of the North Scottish Shelf, the Faeroe Block and the intervening region, in Woodland, A.W., ed., Petroleum and the continental shelf of North West Europe, Vol. 1, Geology: Barking, Applied Science Publishers LTD, p. 105-113.

Bott, M.H.P., Browitt, C.W.A., and Stacey, A.P., 1971, The deep structure of the Iceland-Faeroe ridge: Marine Geophys Research, v. 1, p. 328-351.

Bott, M.H.P., Nielsen, P.H., and Sunderland, J., 1976, Converted P-waves originating at the continental margin between the Iceland-Faeroe Ridge and the Faeroe Block: Royal Astron..Soc. Geophys. Jour., v. 44, p. 229-238.

Bott, M.H.P., and Stacey, A.P., 1967, Geophysical evidence on the origin of the Faeroe Bank Channel, pt. 2. A gravity and magnetic profile: Deep-Sea Research, v. 14, p. 7-12.

Bott, M.H.P., Sunderland, J.,Smith, P.J., Casten, U., and Saxov, S., 1974, Evidence for continental crust beneath the Faeroe Islands: Nature, v. 248, p. 202-204.

Bott, M.H.P., and Tuson, J., 1973, Deep structure beneath the Tertiary volcanic regions of Skye, Mull and Ardnamurchan, north-west Scotland: Nature Phys. Sci., v. 242, p. 114-116.

Bott, M.H.P., and Watts, A.B., 1970, Deep sedimentary basins proven in the Shetland-Hebridean continental shelf and margin: Nature, v. 225, p. 265-268.

— 1971, Deep structure of the continental margin adjacent to the British Isles, in Delany, F.M., ed., ICSU/SCOR Symposium on East Atlantic continental margins 1970: Inst. Geol. Sci. Rept. 70/14, p. 89-109.

Bullard, E.C., Everett, J.E., and Smith, A.G., 1965, The fit of the continents around the Atlantic: Royal Soc. London Philos. Trans., ser. A, v. 258, p. 41-51.

Carmichael, I.S.E., 1964, The petrology of Thingmuli, a Tertiary volcano in Eastern Iceland: Jour. Petrology, v. 5, p. 435-460.

Casten, U., 1971, Seismic measurements on the Faeroe Islands: Fródskaparrit, v. 19, p. 105-116.

— 1973, The crust beneath the Faeroe Islands: Nature Phys. Sci., v. 241, p. 83-84.

— 1974, Eine Analyse seismischer Registrierungen von den Färöer Inseln. Hamburger Geophysikalische Einzelschriften No. 21 (Geophysikalische Institut der Universität Hamburg), 109 p.

Casten, U., and Nielsen, P.H., 1975, Faeroe Islands - a micro-continental fragment?: Jour. Geophys., v. 41, p. 357-366.

Chayes, J., 1956, Petrographic modal analysis: Wiley & Sons, Inc., 133 p.

Crease, J., 1965, The flow of Norwegian sea water through the Faeroe Bank Channel: Deep-Sea Research, v. 12, p. 143-150.

Deer, W.A., Howie, R.A., and Zussmann, J., 1962, Rock forming minerals, Vol. 3: London, Longmans, Green and Co. LTD.

Dobinson, A., 1970, I - The development of a marine seismic recording system, II - A magnetic survey of the Faeroe Bank (Ph. D. thesis): Durham, University of Durham, 55 + 72 p.

Donaldson, C.H., 1976, An experimental investigation of olivine morphology: Contr. Mineralogy and Petrology, v. 57, p. 187-213.

Ellett, D.J., and Roberts, D.G., 1973, The overflow of Norwegian Sea Deep Water across the Wyville-Thomson Ridge: Deep-Sea Research, v. 20, p. 819-835.

Erlank, A.J., and Kable, E.J.D., 1976, The significance of incompatible elements in Mid-Atlantic Ridge basalts from 45° N with particular reference to Zr/Nb: Contr. Mineralogy and Petrology, v. 54, p. 281-291.

Ewing, J., and Ewing, M., 1959, Seismic-refraction measurements in the Atlantic ocean basins, in the Mediterranean Sea, on the the mid-Atlantic Ridge, and in the Norwegian Sea: Geol. Soc. America Bull., v. 70, p. 291-318.

Featherstone, P.S., Bott, M.H.P., and Peacock, J.H., 1977, Structure of the continental margin of South-eastern Greenland: Royal Astr. Soc. Geophys. Jour., v. 48, p. 15-27.

Flanagan, F.J., 1973, 1972 values for international reference samples: Geochim. et Cosmochem. Acta, v. 37, p. 1189-1200.

Fleischer, U., 1971, Gravity surveys over the Reykjanes Ridge and between Iceland and the Faeroe Islands: Marine Geophys. Research, v. 1, p. 314-327.

Fleischer, U., Holzkamm, F., Vollbrecht, K., and Voppel, D., 1974, Die Struktur des Island-Färöer Rückens aus geophysikalishen Messungen: Deutschen Hydrographischen Zeitschrift, v. 27, p. 97-113.

Flinn, D., 1973, The topography of the seafloor around Orkney and Shetland and the northern North Sea: Geol. Soc. London Jour., v. 129, p. 39-59.

Flinn, R.F., 1971, Glacial and Quaternary geology: New York, Wiley & Sons, Inc., 892 p.

Folk, R.L., 1955, Student operator error in determination of roundness, sphericity, and grain size: Jour. Sedimentary Petrology, v. 25, p. 297-301.

Geikie, J., 1880, On the geology of the Færöe Islands: Royal Soc. Edinburgh Trans., v. 30, p. 217-269.

Hald, N., Noe-Nygaard, A., and Waagstein, R., 1969, On extrusion forms in plateau basalts, pt. 2. The Klakksvík flow, Faeroe Islands: Geol. Soc. Denmark Bull., v. 19, p. 2-7.

Hart, S.R., Gunn, B.M., and Watkins, N.D., 1971, Intralava variation of alkali elements in Icelandic basalt: Am. Jour. Sci., v. 270, p. 315-318.

Harvey, J., 1965, The topography of the South-Western Faeroe Channel: Deep-Sea Research, v. 12, p. 121-127.

Heinrich, K.F.J., 1966, in McKinley, T.D., Heinrich, K.F.J., and Wittry, D.B., eds., The electron microprobe: New York, Wiley & Sons, Inc., p. 296-377.

Himsworth, E.M., 1973, Marine geophysical studies between northwest Scotland and the Faeroe Plateau (Ph. D. thesis): Durham, University of Durham, 125 p.

Holtedahl, O., 1970, On the morphology of the West Greenland shelf with general remarks on the "marginal channel" problem: Marine Geol., v. 8, p. 155-172.

Inman, D.L., 1963, Sediments: physical properties and mechanics of sedimentation, in Shepard, F.P., ed., Submarine geology, 2nd ed.: New York, Harper and Row, p. 101-151.

Jacqué, M., and Thouvenin, J., 1975, Lower Tertiary tuffs and volcanic activity in the North Sea, in Woodland, A.W., ed., Petroleum and the continental shelf of North West Europe, Vol. 1, Geology: Barking, Applied Science Publishers, p. 455-466.

Jakobsson, S.P., 1972, The chemistry and distribution pattern of recent basaltic rocks in Iceland: Lithos, v. 5, p. 365-386.

Johnson, G.L., and Schneider, E.D., 1969, Depositional ridges in the North Atlantic: Earth and Planetary Sci. Letters, v. 6, p. 416-422.

Jones, E.J.W., Ewing, M., Ewing, J.I., and Eittreim, S., 1970, Influences of Norwegian Sea overflow water on sedimentation

in the northern North Atlantic and Labrador Sea: Jour. Geophys. Research, v. 75, p. 1655-1680.

Kent, P.E., 1975, The tectonic development of Great Britain and the surrounding seas, in Woodland, A.W., ed., Petroleum and the continental shelf of North West Europe, Vol. 1, Geology: Barking, Applied Science Publishers, p. 3-28.

Kenyon, N.H., and Stride, A.H., 1970, The tide-swept continental shelf between the Shetland Isles and France: Sedimentology, v. 14, p. 159-173.

Korsakov, O.D., 1974, O tektonike Farero-Shetlandskogo Zheloba (Tectonics of the Faeroe-Shetland trench): Akad. Nauk Doklady SSSR, v. 214, no. 3, p. 647-650.

Krumbein, W.C., 1941, Measurement and geologic significance of shape end roundness of sedimentary particles: Jour. Sedimentary Petrology, v. 11, p. 64-72.

Laughton, A.S., 1975, Tectonic evolution of the Northeast Atlantic Ocean; a review, in Petroleum geology and geology of the North Sea and N.E. Atlantic continental margin: Norges Geol. Undersøgelse, no. 316, p. 169-193.

Laughton, A.S., Berggren, W.A., and others, 1972, Initial reports of the Deep Sea Drilling Project, Vol. 12: Washington D.C., U.S. Govt. Printing Office, 1243 p.

Macdonald, G.A., 1967, Forms and structures of extrusive basaltic rocks, in Hess, H.H., and Poldervaart, A., eds., Basalts: The Poldervaart treatise on rocks of basaltic composition, Vol. 1: New York, Interscience, p. 1-61.

Macdonald, G.A., and Katsura, T., 1964, Chemical composition of Hawaiian lavas: Jour. Petrology, v. 5, p. 82-133.

Montadert, L., Roberts, D.G., and others, 1976, Glomar Challenger sails on Leg 48 from Brest to Aberdeen: Geotimes, v. 21, no. 12, p. 19-23.

— 1977, Rifting and subsidence on passive continental margins in the North East Atlantic: Nature, v. 268, p. 305-309.

Moore, J.G., and Evans, B.W., 1967, The role of olivine in the crystallization of the prehistoric Makaopuhi tholeiitic lava lake: Contr. Mineralogy and Petrology, v. 15, p. 202-223.

Morgan, W.J., 1971, Convection plumes in the mantle: Nature, v. 230, p. 42-43.

Muir, I.D., and Tilley, C.E., 1964, Basalts from the northern part of the rift zone of the MidAtlantic Ridge: Jour. Petrology, v. 5, p. 409-434.

Murray, J., and Philippi, E., 1925, Die Grundproben der "Deutschen Tiefsee-Expedition", in Chun, C., Brauer, A, Vanhöffen, E., and Apstein, C., eds., Wissenschaftliche Ergebnisse der Deutschen Tiefsee-Expedition auf dem Dampfer "Valdivia" 1898-1899, Vol. 10, pt. 4: Jena, Verlag von Gustav Fischer, p. 77-206, plates 16-22, and 2 maps.

Nielsen, P.H., 1976, Seismic refraction measurements around the Faeroe Islands: Fródskaparrit, v. 24, p. 9-45.

Noe-Nygaard, A., 1949, Samples of volcanic rocks from the sea bottom between the Faroes and Iceland, in Glaciers and Climate: Geografiska Annaler 1949, p. 348-356.

— 1966, Chemical composition of tholeiitic basalts from the Wyville-Thompson Ridge belt: Nature, v. 212, p. 272-273.

— 1967, Variation in titania and alumina content through a three kilometres thick basaltic lava pile in the Faeroes: Geol. Soc. Denmark Bull., v. 17, p. 125-128.

— 1968, On extrusion forms in plateau basalts, shield volcanoes of "scutulum" type: Science in Iceland, v. 1 (Reykjavík, Vísindafélag Íslendinga), p. 10-13.

— 1974, Cenozoic to recent volcanism in and around the North Atlantic basin, in Nairn, A.E.M., and Stehli, F.G., eds., The ocean basins and margins, Vol. 2. The North Atlantic: New York, Plenum, p. 391-443.

Noe-Nygaard, A., and Pedersen, A.K., 1974, Progressive chemical variation in a tholeiitic lava sequence at Kap Stosch, northern East Greenland: Geol. Soc. Denmark Bull., v. 23, p. 175-190.

Noe-Nygaard, A., and Rasmussen, J., 1968, Petrology of a 3000 metre sequence of basaltic lavas in the Faeroe Islands: Lithos, v. 1, p. 286-304.

Padfield, T., and Gray, A., 1971, Major element analysis by X-ray fluorescence - a simple fusion method: Philips Bulletin Analytical Equipment, FS 35, 4 p.

Pálmason, G., 1965, Seismic refraction measurements of the basalt lavas of the Faeroe Islands: Tectonophys., v. 2, p. 475-482.

Peterson, W.H., and Rooth, C.G.H., 1976, Formation and exchange of deep water in the Greenland and Norwegian seas: Deep-Sea Research, v. 23, p. 273-284.

Powers, M.C., 1953, A new roundness scale for sedimentary particles: Jour. Sedimentary Petrology, v. 23, p. 117-119.

Rasmussen, J., 1962, Um goshálsar í Føroyum (about vents in the Faeroe Islands): Fródskaparrit, v. 11.

   — 1973, Fyribils frásøgn um botnkanningar á sjóøkinum uttan um Føroyar (Preliminary report about sea floor studies in the sea territory around the Faeroe Islands): Fródskaparrit, v. 21, p. 86-93.

   — 1974, Botnkort sum ískoyti til greinina "Fyribils frásøgn um botnkanningar á sjóøkinum uttan um Føroyar" (Bathymetric map as supplement to "Preliminary report about sea floor studies in the sea territory around the Faeroe Islands"): Fródskaparrit, v. 22, p. 141-143, and 1 map.

Rasmussen, J., and Noe-Nygaard, A., 1969, Beskrivelse til geologisk kort over Færøerne i målestok 1:50.000 (Description to geological map of the Faeroe Islands, scale 1:50,000): Danmarks Geologiske Undersøgelse, 1. række (Geological Survey of Denmark, I. Series), no. 24, 370 p., and 6 map sheets.

   — 1970, Geology of the Faeroe Islands (Pre-Quaternary): Danmarks Geologiske Undersøgelse, I. række (Geological Survey of Denmark, I. Series), no. 25, 142 p., and 1 map, scale 1:200,000.

Roberts, D.G., 1975a, Marine geology of the Rockall Plateau and Trough: Royal Soc. London Philos. Trans., ser. A, v. 278, p.447-509.

   — 1975b, Tectonic and stratigraphic evolution of the Rockall Plateau and Trough, in Woodland, A.W., ed., Petroleum and the continental shelf of North West Europe, Vol. 1. Geology: Barking, Applied Science Publisher, p. 77-92.

Roberts, D.G., Bishop, D.G., Laughton, A.S., Ziolkowski, A.M., Scrutton, R.A., and Matthews, D.H., 1970, New sedimentary basin on Rockall Plateau: Nature, v. 225, p. 170-172.

Roberts, D.G., Matthews, D.H., and Eden, R.A., 1972, Metamorphic rocks from the southern end of the Rockall Bank: Geol. Soc. London Jour., v. 128, p. 501-506.

Ruddiman, W.F., 1972, Sediment redistribution on the Reykjanes Ridge: seismic evidence: Geol. Soc. America Bull., v. 83, p. 2039-2062.

Ruddiman, W.F., and McIntyre, A., 1973, Time-transgressive deglacial retreat of polar waters from the North Atlantic: Quaternary Research, v. 3, p. 117-130.

Sahu, B.K., and Patro, B.C., 1970, Treatment of sphericity and roundness data of quartz grains of clastic sediments: Sedimentology, v. 14, p. 51-66.

Saxov, S., 1969, Gravimetry in the Faroe Islands: Geodætisk Institut (Copenhagen), Meddelelse no. 43, 24 p.

― 1971, Additional gravity observations in the Faeroe Islands. Fródskaparrit, v. 19, p. 9-19.

Saxov, S., and Abrahamsen, N., 1964, A note on some gravity and density measurings in the Faeroe Islands: Boll. di Geofisica Teorica ed Applicata, v. 6, p. 249-259.

― 1966, Some geophysical investigations in the Faroe Islands, a preliminary report: Zeitschrift für Geophysik, Sonderheft 32, p. 455-471.

Schilling, J.-G., 1973, Iceland mantle plume: geochemical evidence along Reykjanes Ridge: Nature, v. 242, p. 565-571.

― in press, Rare earth, Sc, Cr, Fe, Co, and Na abundances in DSDP Leg 38 basement basalts: some additional evidence on the evolution of the Thulean volcanic province, in Initial reports of the Deep Sea Drilling Project, Vol. 38: Washington D.C., U.S. Govt. Printing Office.

Schilling, J.-G., and Noe-Nygaard, A., 1974, Faeroe-Iceland plume: rare-earth evidence: Earth and Planetary Sci. Letters, v. 24, p. 1-14.

Schroeder, N.F., 1971, Magnetic anomalies around the Faeroe Islands: Fródskaparrit, v. 19, p. 20-29.

Soper, N.J., Downie, C., Higgins, A.C., and Costa, L.I., 1976b, Biostratigraphic ages of Tertiary basalts on the East Greenland continental margin and their relationship to plate separation in the Northeast Atlantic: Earth and Planetary Sci. Letters, v. 32, 149-157.

Soper, N.J., Higgins, A.C., Downie, C., Matthews, D.W., and Brown, P.E., 1976a, Late Cretaceous - early Tertiary stratigraphy of the Kangerdlugssuaq area, east Greenland, and the opening of the northeast Atlantic: Geol. Soc. London Jour., v. 132, p. 85-102.

Stride, A.H., Belderson, R.H., Curray, J.R., and Moore, D.G., 1967, Geophysical evidence on the origin of the Faeroe Bank Channel, pt. 1. Continuous reflection profiles: Deep-Sea Research, v. 14, p. 1-6.

Stride, A.H., Curray, J.R., Moore, D.G., and Belderson, R.H., 1969, Marine geology of the Atlantic continental margin of Europe: Royal Soc. London Philos. Trans., ser. A, v. 264, p. 31-75.

Talwani, M., and Eldholm, O., 1972, Continental margin off Norway: a geophysical study: Geol. Soc. America Bull., v. 83, p. 3575-3606.

— 1977, Evolution of the Norwegian-Greenland Sea: Geol. Soc. America Bull., v. 88, p. 969-999.

Talwani, M., Udintsev, G., and others, 1975, Leg 38: Geotimes, v. 20, no. 2, p. 24-26.

Tarling, D.H., and Gale, N.H., 1968, Isotopic dating and paleo-magnetic polarity in the Faeroe Islands: Nature, v. 218, p. 1043-1044.

Turner, F.J., and Verhoogen, J., 1960, Igneous and metamorphic petrology: New York, McGraw-Hill, 694 p.

Vance, J.A., 1969, On synneusis: Contr. Mineralogy and Petrology, v. 24, p. 7-29.

Vogt, P.R., 1972, The Faeroe-Iceland-Greenland aseismic ridge and the Western Boundary Undercurrent: Nature, v. 239, p. 79-81.

Waagstein, R., and Rasmussen, J., 1975, Glacial erratics from the sea floor south-east of the Faeroe Islands and the limit of glaciation: Fródskaparrit, v. 23, p. 101-119.

Wadell, H., 1933, Sphericity and roundness of rock particles: Jour. Geology, v. 41, p. 310-331.

Wager, L.R., 1947, Geological investigations in east Greenland, pt. 4. The stratigraphy and tectonics of Knud Rasmussen Land and the Kangerdlugssuaq region: Meddr. Grønland, v. 134, pt. 5, p. 1-64.

Walker, F., and Davidson, C.F., 1936, A contribution to the geo-logy of the Faeroes: Royal Soc. Edinburgh Trans., v. 58, p. 869-897.

Watkins, N.D., Gunn, B.M., and Coy-yll, R., 1970, Major and trace element variations during the initial cooling of an Icelandic lava: Am. Jour. Sci., v. 268, p. 24-49.

Watts, A.B., 1971, Geophysical investigations on the continental shelf and slope north of Scotland: Scottish Jour. Geology, v. 7, p. 189-217.

Whitbread, D.R., 1975, Geology and petroleum possibilities west of the United Kingdom, in Woodland, A.W., ed., Petroleum and the continental shelf of North West Europe, Vol. 1. Geology: Barking, Applied Science Publishers, p. 45-57.

Wilkinson, J.F.G., 1967, The petrography of basaltic rocks, in Hess, H.H., and Poldervaart, A., eds., Basalts: the Poldervaart treatise on rocks of basaltic composition, Vol. 1: New York, Interscience, p. 163-214.

Wilkinson, J.F.G., and Duggan, N.T., 1973, Some tholeiites from the Inverell area, New South Wales, and their bearing on low pressure tholeiite fractionation: Jour. Petrology, v. 14, p. 339-348.

Wood, D.A., Gibson, I.L., and Thompson, R.N., 1976, Elemental mobility during zeolite facies metamorphism of the Tertiary basalts of eastern Iceland: Contr. Mineralogy and Petrology, v. 55, p. 241-254.

Worthington, L.V., 1970, The Norwegian Sea as a Mediterranean basin: Deep-Sea Research, v. 17, p. 77-84.

Yoder, H.S., Jr., and Tilley, C.E., 1962, Origin of basalt magmas - an experimental study of natural and synthetic rock systems: Jour. Petrology, v. 3, p. 342-532.

TABLE 17. CHEMICAL ANALYSES AND PHENOCRYST CONTENTS OF BASALT FLOWS FROM THE SNEIS PROFILE, FAEROE ISLANDS

Sample No.	86	87	88	89	90	2	3	4	6	7	9	10	11
	B-horizon flows								Picrite flows				
Height, m	+ 2	+ 8	+ 16	+ 26	+ 29	+ 55	+ 61	+ 76	197	200	205	209	216
SiO_2	46.51	46.83	47.66	47.79	47.58	48.51	48.23	46.13	45.13	44.63	47.77	47.60	48.92
TiO_2	0.93	1.02	2.58	2.52	2.62	2.55	2.52	2.93	1.03	1.03	2.75	2.67	2.78
Al_2O_3	15.80	15.52	16.14	13.76	15.30	15.11	17.15	16.55	12.50	12.47	15.24	15.41	14.40
Fe_2O_3	1.68	3.03	4.13	4.51	4.50	3.71	3.53	5.55	1.61	1.76	4.02	3.79	4.31
FeO	7.75	6.92	7.58	8.22	7.42	7.40	6.40	5.70	9.49	9.27	7.72	7.74	8.49
MnO	0.18	0.19	0.21	0.22	0.21	0.19	0.14	0.17	0.21	0.20	0.18	0.19	0.21
MgO	9.30	9.15	5.30	7.00	6.30	6.35	4.50	4.80	14.48	14.36	6.05	5.80	5.55
CaO	12.73	12.38	11.52	10.76	11.60	10.92	9.86	10.10	10.22	10.27	10.61	10.43	10.83
Na_2O	1.68	1.72	2.39	2.60	2.23	2.61	3.18	2.72	1.80	1.93	3.10	3.30	2.56
K_2O	0.14	0.28	0.16	0.18	0.18	0.21	0.48	0.32	0.19	0.13	0.18	0.19	0.36
P_2O_5	0.07	0.08	0.28	0.23	0.32	0.32	0.28	0.31	0.07	0.07	0.28	0.28	0.32
H_2O^+	2.69	2.59	1.78	2.04	1.50	1.52	3.64	4.33	2.54	3.10	2.14	2.36	0.98
Total	99.46	99.71	99.73	99.83	99.76	99.40	99.91	99.61	99.27	99.22	100.04	99.76	99.71
FeO^*	9.26	9.65	11.30	12.28	11.47	10.74	9.58	10.70	10.94	10.85	11.34	11.15	12.37
FeO^*/MgO	1.00	1.05	2.13	1.75	1.82	1.69	2.13	2.23	0.76	0.76	1.87	1.92	2.23
TiO_2/FeO^*	0.100	0.106	0.228	0.205	0.228	0.237	0.263	0.274	0.094	0.095	0.243	0.239	0.225

Modal % plagioclase phenocrysts

	86	87	88	89	90	2	3	4	6	7	9	10	11
	0	0	20	0	10	10	20	25	0	0	15	15	10

Maximum size of phenocrysts or microphenocrysts (mm)

	86	87	88	89	90	2	3	4	6	7	9	10	11
Plagioclase	1.2	1.1	2.4	0.4	2.5	3.5	10	16	0.6	0.4	3	2.3	3
Olivine	1.0	0.8	(1.0)	0.5	(0.3)	(1.1)	(1.2)	0.3	2.2	2.8	(1.3)	(1.5)	(1.2)
Pyroxene			0.7	0.4	0.5	0.6	0.4	0.3			0.5	0.6	1.8

TABLE 17. (Continued)

Sample No.	13	14	16 P	17	19 SV	20 SV	22	24	26	27 SV	29	30	33
Height, m	219 ?	226	244	248	257	262	275	288	306	306	323	326	332
SiO_2	48.66	48.16	48.00	47.93	46.38	46.69	48.78	48.46	47.79	46.75	47.71	48.84	47.50
TiO_2	2.77	2.68	2.85	2.95	3.88	4.17	2.74	3.34	3.02	3.49	2.87	2.71	2.41
Al_2O_3	14.90	15.37	15.05	14.90	13.16	12.58	16.37	14.55	15.80	13.22	15.41	16.29	15.57
Fe_2O_3	4.24	4.20	4.68	6.27	4.63	7.48	3.22	3.74	4.33	7.71	4.23	4.09	3.98
FeO	8.48	8.09	7.74	6.55	10.15	8.91	8.30	9.46	8.58	6.13	7.93	7.21	7.23
MnO	0.21	0.19	0.19	0.19	0.30	0.25	0.19	0.21	0.20	0.25	0.19	0.19	0.17
MgO	5.30	5.70	5.90	5.50	6.50	5.70	5.35	5.20	5.00	5.70	5.60	5.10	5.40
CaO	10.96	11.22	11.04	10.82	9.45	10.18	10.75	10.40	10.83	9.86	10.03	9.95	10.19
Na_2O	2.54	2.40	2.40	2.46	1.99	2.24	2.65	2.54	2.54	1.75	3.06	3.11	3.18
K_2O	0.38	0.17	0.34	0.32	0.64	0.24	0.28	0.45	0.29	0.66	0.24	0.47	0.40
P_2O_5	0.30	0.34	0.38	0.35	0.41	0.50	0.29	0.43	0.36	0.33	0.32	0.28	0.29
H_2O^+	0.94	1.50	1.52	1.19	2.65	1.49	0.79	0.82	1.07	4.05	2.35	2.02	3.55
Total	99.68	100.02	100.09	99.43	100.14	100.43	99.71	99.60	99.81	99.90	99.94	100.26	99.87
FeO^*	12.30	11.87	11.95	12.19	14.32	15.64	11.20	12.83	12.48	13.07	11.74	10.89	10.81
FeO^*/MgO	2.32	2.08	2.03	2.22	2.20	2.74	2.09	2.47	2.50	2.29	2.10	2.14	2.00
TiO_2/FeO^*	0.225	0.226	0.238	0.242	0.271	0.267	0.245	0.260	0.242	0.267	0.244	0.249	0.223

Modal % plagioclase phenocrysts

	10	15	15	15	3	2	20	15	15	7	15	<1;20	15

Maximum size of phenocrysts or microphenocrysts (mm)

	13	14	16	17	19	20	22	24	26	27	29	30	33
Plagioclase	2	4	5	7	6	5	10	12	13	8	11	14;6	2.2
Olivine	1	(1)	(1.5)	(0.7)		(0.8)	1.3	(2)	2	(1.3)	(1)	(1.7)	(1.5)
Pyroxene	0.4	0.5	0.6	0.6	0.3	0.3	0.5	0.7	1.3	0.4	0.4	0.4	0.8

TABLE 17. (Continued)

Sample No.	34	35 SP	37	38	39	42	43.A P	44	46	48	50	51
Height, m	342	350	359	360	368	396	402	409	415	434	449	458
SiO_2	49.06	48.85	48.15	48.16	48.73	50.57	47.98	48.84	50.01	48.32	49.20	50.22
TiO_2	2.44	2.83	2.42	2.80	2.82	2.14	3.41	2.41	2.57	2.69	2.94	3.01
Al_2O_3	15.62	14.62	15.50	14.94	14.49	16.05	13.57	16.33	14.36	15.43	13.99	14.43
Fe_2O_3	4.21	6.45	2.89	5.23	4.01	3.75	4.54	7.48	4.10	3.79	3.70	3.49
FeO	7.03	6.41	8.40	7.01	9.00	7.12	9.77	4.34	7.70	8.36	9.26	9.07
MnO	0.19	0.18	0.20	0.21	0.24	0.16	0.25	0.17	0.19	0.20	0.20	0.18
MgO	5.70	4.70	6.10	5.75	5.65	5.25	5.90	5.05	6.20	5.70	6.10	5.20
CaO	10.77	9.78	10.67	10.77	10.68	10.55	10.43	10.43	10.52	11.01	10.40	9.97
Na_2O	2.30	1.48	2.54	2.24	2.22	2.57	2.18	2.29	2.42	2.30	2.25	2.72
K_2O	0.70	1.77	0.22	0.48	0.33	0.30	0.22	0.74	0.31	0.16	0.21	0.53
P_2O_5	0.27	0.27	0.27	0.29	0.36	0.25	0.34	0.23	0.28	0.31	0.30	0.30
H_2O^+	1.72	2.11	2.48	1.73	1.33	0.99	1.06	1.51	0.84	1.80	1.09	1.04
Total	100.01	99.45	99.84	99.61	99.86	99.70	99.65	99.82	99.50	100.07	99.64	100.16
FeO^*	10.82	12.22	11.00	11.72	12.61	10.50	13.86	11.07	11.39	11.77	12.59	12.21
FeO^*/MgO	1.90	2.60	1.80	2.04	2.23	2.00	2.35	2.19	1.84	2.07	2.06	2.35
TiO_2/FeO^*	0.226	0.232	0.220	0.239	0.224	0.204	0.246	0.218	0.226	0.229	0.234	0.247

Modal % plagioclase phenocrysts

	< 1;25	< 1;10	< 1;25	10	10	10	1	20	3	< 1;15	5	< 1;10

Maximum size of phenocrysts or microphenocrysts (mm)

	34	35	37	38	39	42	43.A	44	46	48	50	51
Plagioclase	4.5;0.8	3;1.6	3;1.3	6	4	10	13	12	10	9.5;4	12	15:2.8
Olivine	(2;0.3)		(1.2)	1.7	(0.9)	(1.7)	(2)	(1)	1.8	(1.3)	(0.8)	(2;1.3)
Clinopyroxene	0.3	0.3	0.25	0.5	0.5	0.5	0.5	0.3	0.15	0.7	0.5	0.9

TABLE 17. (Continued)

Sample No.	54	55	58	59	60	62	63	65	66 P	67 P	68	69.B
						Hypersthene-phyric flows						
Height, m	481	486	506	516	522	531	535	543	547	549	554	563
SiO_2	48.48	49.09	48.71	49.16	49.24	53.61	53.84	53.65	47.42	48.07	47.95	46.96
TiO_2	3.00	2.97	2.90	2.75	2.46	1.49	1.54	1.50	3.49	3.55	3.16	3.99
Al_2O_3	13.60	13.65	13.74	13.99	14.75	13.01	13.09	12.84	13.78	13.47	14.85	12.89
Fe_2O_3	4.12	3.27	3.20	3.63	4.77	2.57	2.08	2.45	5.77	4.80	5.75	5.89
FeO	8.89	9.49	9.61	9.22	7.31	7.30	7.80	7.37	8.51	9.72	7.70	9.35
MnO	0.21	0.22	0.22	0.20	0.17	0.17	0.18	0.17	0.21	0.21	0.17	0.22
MgO	6.60	6.48	6.70	6.00	6.08	7.80	7.05	7.65	6.00	6.07	5.49	5.91
CaO	10.30	10.38	10.70	10.71	10.71	8.90	9.04	9.18	10.35	10.36	10.63	9.98
Na_2O	2.10	2.22	2.37	2.30	2.34	2.38	2.55	2.42	2.24	2.30	2.37	2.32
K_2O	0.22	0.29	0.26	0.35	0.49	0.91	0.75	0.74	0.27	0.22	0.20	0.28
P_2O_5	0.30	0.29	0.30	0.30	0.26	0.15	0.14	0.14	0.39	0.38	0.35	0.39
H_2O^+	1.68	2.25	0.86	0.66	1.28	1.32	1.08	1.00	1.30	1.10	1.37	1.15
Total	99.50	100.60	99.57	99.27	99.86	99.61	99.14	99.11	99.73	100.25	99.99	99.33
FeO*	12.60	12.43	12.49	12.49	11.60	9.61	9.67	9.58	13.70	14.04	12.88	14.65
FeO*/MgO	1.91	1.92	1.86	2.08	1.91	1.23	1.37	1.25	2.28	2.31	2.35	2.48
TiO_2/FeO*	0.238	0.239	0.232	0.220	0.212	0.155	0.159	0.157	0.255	0.253	0.245	0.272

Modal % plagioclase phenocrysts

	2	<1;1	<1;2	<1	1;15	0	<1	<1	<1;10	<1;10	<1;15	3

Maximum size of phenocrysts or microphenocrysts (mm)

	54	55	58	59	60	62	63	65	66	67	68	69.B
Plagioclase	5	9;2.7	8;3.5	3	8;2.6	0.6	0.7	0.8	30;4.3	18;1.9	18;2.5	14
Olivine	(0.6)	(0.5)	(0.6)	(1.4)	(0.9)	1.2	1	1.5	(0.5)	(0.6)	(0.9)	(0.6)
Clinopyroxene	0.5	0.4	0.6	1.6	1.3	?	3	1.8	0.3	0.25	0.25	0.1
Orthopyroxene						2.3	3.5	3				

TABLE 17. (Continued)

Sample No.	70	72	73 SP	74	75.A SV	76	77	78	80 SV	82	83	84
						Composite flow				C-horizon flows		
Height, m	567	576	582	585	590	591	592	593	602	609	628	647
SiO_2	46.94	49.33	50.63	51.07	50.76	48.95	49.38	48.54	49.54	47.63	47.64	48.82
TiO_2	3.89	2.57	2.44	2.98	3.44	3.39	3.10	3.63	3.28	1.05	1.14	3.55
Al_2O_3	12.69	16.05	17.30	14.36	13.09	13.37	14.92	12.82	13.42	15.05	14.87	12.73
Fe_2O_3	5.31	4.25	6.42	4.63	5.31	6.06	4.54	6.59	6.88	4.73	3.16	6.09
FeO	9.75	7.08	4.17	7.70	7.79	7.97	8.30	7.69	6.78	6.15	7.85	9.22
MnO	0.25	0.17	0.17	0.21	0.25	0.21	0.19	0.19	0.19	0.20	0.20	0.24
MgO	6.35	5.25	4.05	4.45	4.80	5.40	4.95	5.65	5.05	8.30	8.55	5.25
CaO	10.10	10.55	9.82	9.18	8.90	9.45	9.63	9.34	9.24	12.71	12.74	9.82
Na_2O	2.10	2.54	2.92	2.80	2.69	2.67	2.65	2.30	2.67	1.80	1.80	2.54
K_2O	0.26	0.30	0.53	1.01	1.08	0.41	0.42	0.42	1.08	0.31	0.08	0.35
P_2O_5	0.44	0.35	0.26	0.46	0.33	0.47	0.41	0.42	0.35	0.08	0.10	0.34
H_2O^+	1.64	1.11	0.66	0.99	1.45	1.75	1.31	2.28	1.65	1.16	1.36	0.78
Total	99.72	99.55	99.37	99.84	99.89	100.10	99.80	99.87	100.13	99.17	99.49	99.73
FeO^*	14.53	10.91	9.95	11.87	12.57	13.42	12.39	13.62	12.97	10.41	10.69	14.70
FeO^*/MgO	2.29	2.08	2.46	2.67	2.62	2.49	2.50	2.41	2.57	1.25	1.25	2.80
TiO_2/FeO^*	0.268	0.236	0.245	0.251	0.274	0.253	0.250	0.267	0.253	0.101	0.107	0.241

Modal % plagioclase phenocrysts

	70	72	73	74	75.A	76	77	78	80	82	83	84
	< 1	20	15	10	0	3	10	0	1	0	0	2

Maximum size of phenocrysts or microphenocrysts (mm)

	70	72	73	74	75.A	76	77	78	80	82	83	84
Plagioclase	10	12	9	7	4	6.5	7	0.8	6	1	0.9	3.5
Olivine	(0.6)	1.6	0.8	(0.8)		(0.6)	(0.5)	(0.7)	(0.8)	4.3	0.6	(0.3)
Clinopyroxene	0.5	0.3	0.6	0.4	0.4	0.6	0.5	0.5	0.5			> 0.4

COMMENTS TO TABLE 17

The samples are identified by the last two digits of the field numbers (MM 15501-15590, Geologisk Museum, Copenhagen). Samples from the same flow-unit are identified by a connecting line below the sample numbers. The height of the sampling site along the Sneis profile (= profile X of Rasmussen and Noe-Nygaard 1969, 1970) is the stratigraphic height (identified by a plus sign) above the base of the B-horizon flows corrected for the dip of strata in the lowermost part of the profile but as height above sea level higher up.

SV = segregation vein; SP = sample from an indistinct segregation patch; P = basalt with small segregation patches.

Modal % plagioclase phenocrysts is estimated in hand specimens. The maximum size of large phenocrysts is measured in hand specimen while the maximum size of small phenocrysts is mostly measured in thin section. Some basalts contain two sizes of phenocrysts of plagioclase and sometimes also of olivine. The maximum size of olivine is given in brackets when the olivine is completely altered.

TABLE 18.   ABUNDANCE AND SIZE OF PHENOCRYSTS AND MICROPHENOCRYSTS IN BASALTS FROM FAEROE BANK, BILL BAILEY BANK AND LOUSY BANK

Sample No.		36-5	36-24	36-2	36-13	36-6	37-6	37-1	37-5	37-4	37-7	37-7B
Modal % phenocrysts and microphenocrysts												
OLIVINE	phen.					}0	0.2	}0	}0	0.7	}0	
	mph.	< 1	+	< 1	+					0		
PLAG.	phen.	< 1	< 1	< 1		< 1	3.5		1.6	1.8		+
	mph.	3-5	+	3-5	+			+	2.0	0.7		+
CLINOPX.	phen.						0.5		0.6	0.5		+
	mph.	3-5	+	5-7	+	< 1	+	+	1.5	0.6		+
Maximum crystal size (mm)												
OLIVINE		0.7	0.6	0.6	0.5	–	1.8	–	–	2.1^f	–	
PLAG.		0.7	1.1	0.7	0.6	1.0	4.4	0.8	1.6^r	2.0^r	1.6^r	
CLINOPX.		0.6	0.5	0.5	0.5	0.5	2.8	0.6	1.7	2.1	0.8	

Sample No.		47-1	48-1	48-2	48-5	48-10	48-8	50-1	50-2	51-1	56-1
Modal % phenocrysts and microphenocrysts											
OLIVINE	phen.	}0.9				}2.1		< 0.1	< 0.1	}0	< 1
	mph.		+	+							
PLAG.	phen.	}36.1	< 1	1	}4.2	6.0	}14.1	9.3		2.2	0.7
	mph.		+	+		5.5		0.4			
CLINOPX.	phen.						}1.3	< 0.1		}0	
	mph.	+	+	+		0.2		1.0			0.2
Maximum crystal size (mm)											
OLIVINE		1.0^f	0.5	0.4	–	1.6^{f}_{R}	0.8^{f}_{R}	0.2	0.4	–	0.2
PLAG.		5.5	1.0	1.3	2.5	2.2^R	2.4^R	2.6	2.0	8	1.8
CLINOPX.		0.6	0.5	0.5	–	1.0	1.0	0.6	0.6	–	0.5

TABLE 18.(Continued)

Sample No.		57-4	57-26	57-14	57-1	57-3	57-16	60-1	60-3	60-6	60-9	60-7
		\}< 1	< 1	\}0.4	\}1.0	\}0.6	\}0.9	\}0	< 1	\}4.1	\}~ 1	\}0.3
Modal % phenocrysts and microphenocrysts												
OLIVINE	phen. / mph.	\}< 1	< 1	\}0.4	\}1.0	\}0.6	\}0.9	\}0	< 1	\}4.1	\}~ 1	\}0.3
PLAG.	phen. / mph.	0.8	2.0	\}2.4	\}9.4	\}3.7	\}3.0	1.4	3.0	6.7 / 4.1	\}~15	2.0 / 1.0
CLINOPX.	phen. / mph.	< 1	< 1	\}0.2	2.7	\}0	\}0	< 0.1	< 0.1	\}0		< 0.1
Maximum crystal size (mm)												
OLIVINE		0.7^f	0.6	1.3	0.7	0.8	0.8	–	0.4	2.7^f	7.5^f	0.7
PLAG.		1.2^r	2.6^r	1.8^r	2.0^r	5.0^r	3.2^r	1.7	4.7	7.5^r	3.8^r	4.0
CLINOPX.		0.5	0.5	0.9	0.6	–	–	0.3	0.4	–	–	0.3

Sample No.		28-25	28-1	28-26	28-4	28-24	28-11	28-6	28-12
Modal % phenocrysts and microphenocrysts									
OLIVINE	phen. / mph.		\}3.8	0.6 / 0.8	1 ?	\} 1.0	+	+	+
PLAG.	phen. / mph.		\}9.8	4.6 / 2.0	5-10	\}15.3	+	+	0.1 / +
CLINOPX.	phen. / mph.		\}0.8	2.1	+	\} 0.1	+	+	+
Maximum crystal size (mm)									
OLIVINE		1.4^f	2.0^f	1.4^f	1.7	1.0	0.7	0.8	1.2^f
PLAG.		4.5	1.4	1.7	4.7^R	5.5^R	1.4	2.0	1.4
CLINOPX.		–	1.2	0.9	0.5	0.5	1.0	1.0	1.3

TABLE 18.(Continued)

Modal % phenocrysts and microphenocrysts

Sample No.		32-1	33-10	33-4	33-5	33-2	34-7	34-2	34-4	34-5	34-5B
OLIVINE	phen.	}0			~1	<1	0.7		<1 ?	<1 ?	
	mph.						0.8				
PLAG.	phen.	<1	<1	3-5	5-7	~10	11.1	~1	<1	<1	
	mph.						1.1				
CLINOPX.	phen.	<1			<1		1.5	~1	<1	<1	
	mph.		+ ?			<1 ?	1.5				

Maximum crystal size (mm)

	32-1	33-10	33-4	33-5	33-2	34-7	34-2	34-4	34-5	34-5B
OLIVINE	—	0.9^f	0.8	0.9^f	0.8	1^f	—	—	—	
PLAG.	1.2	2.9	3.0	3.8	3.8	2.4	1.5	1.4	1.0	
CLINOPX.	1.2	—	0.3	1.1	0.5	1.5	1.6	1.0	2.4	

Comments. The phenocrysts and microphenocrysts are distinguished from each other not only by size but also by appearance and relationships with other minerals as explained in the text.

+ denotes that phenocrysts or microphenocrysts are present; f denotes that the olivine is more or less fresh; r denotes that the outline of some of the plagioclase phenocrysts are slightly rounded or embayed; R denotes that some of the plagioclase phenocrysts are strongly resorbed. Samples which are very similar in chemistry and possibly derived from the same lava flow are listed next to each other and are identified by a connecting line below the sample numbers.

Table 19. Chemical analyses of basalts from Lousy Bank

Sample No.	36-5	36-24	36-2	36-13	36-6	37-6	37-1	37-5	37-4	37-7	37-7B
SiO_2, Wt %	49.15	48.40	48.56	49.77	49.08	49.28	48.80	47.79	49.14	47.16	47.24
TiO_2	0.94	0.89	0.93	1.46	2.36	0.99	1.73	2.46	2.37	2.47	2.46
Al_2O_3	14.08	13.76	14.10	13.84	13.82	14.94	13.74	14.05	13.37	13.82	14.12
Fe_2O_3	3.39	3.96	4.52	3.14	3.71	2.62	4.41	5.11	4.01	5.76	7.06
FeO	7.69	8.01	7.40	9.39	9.82	7.27	8.26	8.92	10.33	8.80	7.65
MnO	0.16	0.19	0.17	0.20	0.23	0.16	0.19	0.23	0.22	0.29	0.28
MgO	8.36	8.01	7.90	6.97	6.37	8.66	7.61	6.38	6.41	6.11	6.07
CaO	12.01	12.03	11.76	10.92	10.82	12.81	10.76	9.84	10.02	10.08	9.85
Na_2O	2.04	1.98	2.18	2.21	2.58	1.87	2.44	2.64	2.37	2.48	2.57
K_2O	0.05	0.28	0.25	0.09	0.14	0.07	0.15	0.15	0.14	0.21	0.35
P_2O_5	0.11	0.11	0.10	0.16	0.23	0.12	0.19	0.25	0.24	0.27	0.27
LOI	2.00	2.08	2.33	1.69	1.02	1.61	1.71	1.92	0.92	1.81	2.50
Total	99.98	99.70	100.20	99.84	100.18	100.40	99.99	99.74	99.54	99.26	100.42
Σ FeO	10.74	11.57	11.47	12.22	13.16	9.63	12.23	13.52	13.94	13.98	14.00
Σ FeO/MgO	1.28	1.44	1.45	1.75	2.07	1.11	1.61	2.12	2.17	2.29	2.31
Rb, ppm	0.7	5.7	4.9	0.5	1.4	0.4	0.7	1.1	1.0	3.4	17.9
Ba	7	6	10	40	48	20	38	46	55	37	50
La	2	2	< 2	6	9	4	11	14	13	14	14
Nb	1.5	1.8	2.1	6.3	11.2	3.9	7.3	15.8	14.9	14.8	14.8
Zr	42	40	42	81	130	53	109	169	163	170	170
Sr	75	70	72	121	166	110	155	165	159	159	163
Y	22	21	22	24	34	17	24	31	35	34	35
Ga	11	14	12	18	20	15	17	25	23	21	28
Cu	130	82	46	185	190	127	180	210	215	180	100
V	260	290	270	360	380	260	360	460	380	440	400
Sc	38	n.d.	n.d.	44	40	36	36	n.d.	37	n.d.	n.d.
Co	48	53	51	60	57	47	48	53	51	53	55
Ni	69	77	75	69	75	85	53	56	53	53	59
Cr	92	101	95	73	99	220	36	82	73	82	81

Table 19 (Continued). <u>Chemical analyses of basalts from Faeroe Bank</u>

Sample No.	47-1	48-1	48-2	48-5	48-10	48-8	50-1	50-2	51-1	56-1
SiO_2, Wt %	46.80	49.23	49.22	46.35	47.52	47.56	47.03	47.26	46.31	47.21
TiO_2	0.78	1.12	1.16	2.81	2.70	2.80	1.94	1.99	3.23	1.30
Al_2O_3	19.93	13.85	13.90	14.07	14.70	14.80	15.68	15.25	13.89	14.45
Fe_2O_3	2.89	4.22	3.95	4.26	4.67	5.04	5.19	5.54	5.67	5.20
FeO	5.22	8.54	8.80	8.25	7.71	7.71	7.17	7.27	7.95	7.05
MnO	0.12	0.21	0.21	0.22	0.19	0.19	0.20	0.19	0.20	0.23
MgO	6.68	7.45	7.45	7.23	6.10	5.78	7.10	6.99	6.61	7.49
CaO	13.19	11.76	11.77	10.16	10.71	10.45	11.71	11.90	10.40	11.84
Na_2O	1.77	2.13	2.11	2.48	2.78	2.84	2.33	2.50	2.80	2.29
K_2O	0.12	0.13	0.09	0.15	0.31	0.52	0.09	0.10	0.25	0.11
P_2O_5	0.10	0.16	0.16	0.27	0.27	0.28	0.17	0.18	0.31	0.14
LOI	1.93	0.94	0.26	3.20	2.15	1.38	1.52	1.40	2.24	2.39
Total	99.53	99.74	99.08	99.45	99.81	99.35	100.13	100.57	99.86	99.70
Σ FeO	7.82	12.34	12.36	12.08	11.91	12.25	11.84	12.26	13.05	11.73
Σ FeO/MgO	1.17	1.66	1.66	1.67	1.95	2.12	1.67	1.75	1.97	1.57
Rb, ppm	2.7	1.2	0.6	0.9	2.0	14.7	0.7	1.3	2.0	1.1
Ba	190	40	42	44	135	154	33	30	85	41
La	3	5	5	14	17	17	7	6	20	3
Nb	0.8	3.7	3.6	11.8	12.6	14.5	6.7	6.1	18.6	2.4
Zr	43	62	61	166	170	181	109	109	206	63
Sr	165	111	110	234	377	366	182	186	276	136
Y	15	24	26	29	25	26	27	27	31	22
Ga	16	15	19	36	25	26	20	21	25	18
Cu	97	190	97	245	145	160	175	200	86	135
V	200	330	330	305	370	340	330	370	360	320
Sc	n.d.	n.d.	42	38	n.d.	31	n.d.	n.d.	n.d.	n.d.
Co	42	55	54	50	47	47	48	53	48	53
Ni	103	72	72	105	75	69	85	88	99	82
Cr	225	76	81	225	125	120	188	195	210	195

Table 19 (Continued). <u>Chemical analyses of basalts from Faeroe Bank</u>

Sample No.	<u>57-4</u>	<u>57-26</u>	57-14	57-1	<u>57-3</u>	<u>57-16</u>	60-1	60-3	60-6	60-9	60-7
SiO_2, Wt %	48.03	48.08	47.93	47.77	46.59	46.00	47.96	47.57	47.38	46.72	46.12
TiO_2	1.25	1.17	1.51	2.13	3.13	3.23	1.16	1.17	2.80	2.82	3.24
Al_2O_3	14.67	14.69	14.28	14.72	14.10	13.95	14.57	14.67	14.36	14.38	13.92
Fe_2O_3	3.23	4.40	3.95	5.07	5.88	9.80	3.62	3.15	4.13	4.71	5.95
FeO	7.69	7.17	8.18	7.76	7.94	4.65	7.73	8.37	9.16	8.57	7.95
MnO	0.20	0.20	0.21	0.19	0.21	0.22	0.19	0.18	0.20	0.20	0.21
MgO	8.03	8.16	7.63	7.00	6.62	6.67	8.35	8.05	7.45	6.95	6.49
CaO	12.98	12.43	12.16	11.39	10.62	10.30	12.31	12.54	10.68	10.83	10.30
Na_2O	2.09	2.10	2.19	2.43	2.79	2.77	2.01	2.07	2.70	2.56	2.76
K_2O	0.13	0.16	0.16	0.13	0.18	0.21	0.13	0.20	0.33	0.18	0.20
P_2O_5	0.14	0.13	0.15	0.20	0.31	0.32	0.14	0.13	0.28	0.28	0.29
LOI	1.44	1.74	0.71	1.73	1.66	2.89	1.11	1.40	0.91	2.11	2.63
Total	99.88	100.43	99.06	100.52	100.03	101.01	99.28	99.50	100.38	100.31	100.06
Σ FeO	10.60	11.13	11.74	12.32	13.23	13.47	10.99	11.21	12.88	12.81	13.31
Σ FeO/MgO	1.32	1.36	1.54	1.76	2.00	2.02	1.32	1.39	1.73	1.84	2.05
Rb, ppm	1.5	1.0	1.1	0.9	1.0	1.7	1.3	2.2	6.3	2.4	1.2
Ba	30	43	37	40	73	80	44	50	88	56	77
La	4	4	6	9	17	20	5	3	16	18	18
Nb	2.4	3.6	2.6	6.5	19.0	18.9	3.1	3.0	17.2	16.7	19.1
Zr	62	58	80	115	211	216	58	57	186	184	213
Sr	166	151	171	202	256	249	149	158	265	270	249
Y	19	20	22	27	35	34	20	20	31	30	35
Ga	17	17	17	23	25	21	11	17	21	20	26
Cu	127	118	103	42	97	94	81	170	210	210	107
V	290	280	330	360	330	370	260	310	320	320	380
Sc	36	n.d.	n.d.	36	30	n.d.	34	n.d.	30	n.d.	n.d.
Co	47	47	48	48	45	45	42	48	48	47	48
Ni	99	82	85	85	78	75	75	85	107	103	82
Cr	225	218	150	180	144	144	202	210	188	188	170

Table 19 (Continued). **Chemical analyses of basalts from Bill Bailey Bank**

Sample No.	28-25	28-1	28-26	28-4	28-24	28-11	28-6	28-12
SiO_2, Wt %	44.81	47.92	46.95	46.75	47.30	46.78	46.96	47.17
TiO_2	1.11	2.03	1.74	3.50	3.49	4.13	4.13	4.16
Al_2O_3	17.17	14.86	15.53	14.31	14.47	13.48	13.58	13.46
Fe_2O_3	4.04	4.32	5.45	4.98	4.76	5.27	5.30	5.87
FeO	5.38	6.51	6.03	9.26	9.43	9.62	9.44	9.01
MnO	0.15	0.16	0.18	0.25	0.22	0.22	0.21	0.22
MgO	9.32	7.93	7.34	5.91	5.74	5.08	4.92	4.78
CaO	10.73	11.00	12.23	10.75	10.75	9.18	9.29	9.28
Na_2O	2.30	2.73	2.51	2.59	2.67	3.41	3.35	3.37
K_2O	0.54	0.28	0.22	0.19	0.21	1.15	1.18	1.23
P_2O_5	0.13	0.18	0.19	0.34	0.33	0.55	0.60	0.57
LOI	4.95	2.37	1.67	1.10	1.60	1.59	1.38	1.37
Total	100.63	100.29	100.04	99.93	100.97	100.46	100.34	100.49
Σ FeO	9.02	10.40	10.94	13.74	13.71	14.36	14.21	14.29
Σ FeO/MgO	0.97	1.31	1.49	2.33	2.39	2.83	2.89	2.99
Rb, ppm	4.1	1.5	2.7	2.8	1.9	20.9	22.0	21.7
Ba	38	79	49	59	82	326	320	349
La	3	8	8	19	19	37	38	37
Nb	3.2	6.3	4.9	18.5	19.1	38.3	39.8	41.7
Zr	65	121	105	218	216	322	333	346
Sr	456	306	215	244	244	444	445	445
Y	15	20	21	37	37	38	38	40
Ga	18	23	18	25	30	28	32	30
Cu	63	122	135	280	270	270	225	210
V	205	250	320	370	370	370	380	370
Sc	n.d.	n.d.	31	31	n.d.	n.d.	28	n.d.
Co	49	45	47	45	45	45	47	45
Ni	205	120	88	78	82	44	48	44
Cr	500	320	250	130	130	25	29	25

Table 19 (Continued). <u>Chemical analyses of basalts from Bill Bailey Bank</u>

Sample No.	32-1	33-10	33-4	33-5	33-2	34-7	34-2	34-4	34-5	34-5B
SiO_2, Wt %	46.99	46.80	46.62	47.12	47.73	47.28	48.86	49.38	50.22	47.83
TiO_2	3.76	3.71	3.90	3.62	3.75	1.40	2.47	2.52	2.58	2.71
Al_2O_3	13.72	13.82	13.18	13.59	13.52	15.46	12.83	13.05	13.30	13.79
Fe_2O_3	4.84	6.04	4.17	3.55	5.49	3.23	7.37	3.93	3.21	5.65
FeO	8.70	7.61	10.11	10.43	9.21	8.02	7.71	10.66	11.33	8.87
MnO	0.18	0.19	0.21	0.21	0.23	0.19	0.27	0.27	0.25	0.20
MgO	6.08	5.90	6.24	6.06	5.96	7.37	5.92	5.79	5.75	5.48
CaO	10.66	10.80	10.35	10.39	10.42	11.67	9.88	9.78	9.97	10.06
Na_2O	2.86	2.87	2.71	2.75	2.84	2.54	2.56	2.50	2.57	2.73
K_2O	0.40	0.27	0.43	0.39	0.47	0.38	0.22	0.29	0.28	0.34
P_2O_5	0.37	0.36	0.38	0.34	0.36	0.16	0.29	0.29	0.29	0.31
LOI	1.20	1.69	1.50	1.34	0.70	2.42	0.98	1.21	0.56	1.73
Total	99.76	100.06	99.80	99.79	100.68	100.12	99.36	99.67	100.31	99.70
Σ FeO	13.06	13.05	13.86	13.63	14.15	10.93	14.34	14.20	14.22	13.96
Σ FeO/MgO	2.15	2.21	2.22	2.25	2.37	1.48	2.42	2.45	2.47	2.55
Rb, ppm	2.8	2.3	6.4	6.1	9.8	2.9	2.9	4.3	3.6	4.9
Ba	151	83	102	91	99	78	91	87	126	108
La	23	n.d.	n.d.	21	n.d.	5	15	15	16	17
Nb	21.5	22.3	27.4	20.7	23.3	6.7	11.6	12.8	12.2	13.3
Zr	243	226	247	210	229	71	176	179	182	192
Sr	436	280	274	269	275	394	177	180	182	199
Y	29	33	34	33	35	21	39	41	41	42
Ga	25	28	25	23		16	20	18	23	25
Cu	135	185	250	230	320	157	215	270	280	250
V	370	400	370	340	380	270	420	420	380	400
Sc	n.d.	n.d.	n.d.	29	n.d.	37	n.d.	40	n.d.	n.d.
Co	47	49	47	42	47	51	51	47	45	42
Ni	66	103	82	78	88	88	46	46	46	46
Cr	73	200	102	124	130	175	65	68	55	65

Note: Samples which are very similar in chemistry and possibly derived from the same lava flow are listed next to each other and are identified by a conneting line below the sample numbers.

TABLE 20. LOCATIONS AND CONTENTS OF DREDGE HAULS

Station number New	Old	Date	Lati-tude North	Longi-tude West	Depth Meters	Dredge type 1)	No. of rock fragments >64 mm Bas	Tuf	Sed	Met	Other frag-ments	Tube sample 2)
The western Faeroe shelf
13	XIII	73-05-28	61°51.9, 61°52.0	7°07.1, 7°07.4	82	Small +	2	..	..	..	..	..
14	XIV	73-05-28	61°51.8, 61°52.5	7°09.2, 7°09.6	ca. 70	Small	..	..	..	..	..	..
15	XV	73-05-28	61°47.0, 61°48.5	7°22.8, 7°25.3	130 128	Small +	..	..	..	..	..	..
16	XVI	73-05-28	61°39.7, 61°39.7	7°35.6, 7°34.2	214 190	Small	..	..	..	..	..	..
17	XVII	73-05-28	61°39.5, 61°38.4	7°39.6, 7°41.4	262 154	Small	..	..	3	..	..	..
18	XVIII	73-05-29	61°31.2, 61°30.9	7°50.8, 7°51.6	174 187	Small	..	..	..	..	..	..
19	XIX	73-05-29	61°29.5, 61°29.7	8°00.2, 8°00.5	194 201	Small +	13	..	..	1	..	..
20	XX	73-05-29	61°30.6, 61°32.1	8°08.5, 8°10.4	263 260	Small	128	3	5	4	1 basalt pebble	..
21	XXI	73-05-29	61°28.6, 61°29.1	8°07.1, 8°07.1	307 232	Small	49	2	1	..	1 basalt pebble	..
27A	26	74-04-29	61°24.6, 61°25.1	7°36.6, 7°37.7	199 208	Small	4	..	..	..	..	2 pebbles, shell sand
27B	27	74-04-29	61°25.0, 61°25.3	7°38.6, 7°38.5	225 210	Small	2	..	1	..	..	pebbles, shell sand

TABLE 20. LOCATIONS AND CONTENTS OF DREDGE HAULS

Station number New Old	Date	Lati- tude North	Longi- tude West	Depth Meters	Dredge type 1)	No. of rock fragments >64 mm Bas	Tuf	Sed	Met	Other frag- ments	Tube sample 2)
					The Suduroy Ridge						
79	74-06-28	60°54.7' 60°54.6'	6°10.2' 6°11.2'	190 190	Small	..	..	..	..	..	shell sand, pebbles
80	74-06-28	60°45.4' 60°45.9'	6°15.8' 6°15.2'	172 180	Small	3	..	..	..	..	shell sand, pebbles
81	74-06-28	60°48.7' 60°48.4'	6°20.9' 6°22.2'	180 180	Small	..	..	..	..	..	shell sand, pebbles
82	74-06-28	60°53.5' 60°53.0'	6°29.9' 6°30.2'	160 156	Small +	..	..	..	..	..	shell sand
83	74-06-28	60°50.0' 60°50.4'	6°49.6' 6°50.6'	212 214	Small	..	..	..	..	..	shell sand
					The eastern Faeroe shelf						
1 I	72-08-01	61°39.7' 61°38.7'	5°17.4' 5°18.1'	229	Small	5	..	..	1	..	..
2 II	72-08-01	61°38.9' 61°37.9'	4°54.4' 4°53.0'	234-238	Small	7	..	..	..	..	..
5 V	72-08-02	61°43.8' 61°43.6'	4°43.9' 4°43.3'	219-258	Small	29	11	1	..	..	..
6 VI	72-08-02	61°46.1' 61°45.7'	5°13.3' 5°12.1'	201-210	Small	2	..	..	..	..	..
63	74-06-26	61°46.1' 61°46.9'	5°59.9' 5°59.3'	250 250	Small	14	..	1	..	..	sand
64	74-06-26	61°47.5' 61°47.9'	5°48.0' 5°46.8'	248 246	Small	1	..	..	..	..	sand

TABLE 20. LOCATIONS AND CONTENTS OF DREDGE HAULS

Station number New Old	Date	Lati-tude North	Longi-tude West	Depth Meters	Dredge type 1)	No. of rock fragments >64 mm Bas	Tuf	Sed	Met	Other frag-ments	Tube sample 2)
				The eastern Faeroe shelf							
65	74-06-26	61°40.6' 61°41.2'	5°35.8' 5°35.2'	255	Small	5	2	o o	..	..	mud
66	74-06-26	61°47.6' 61°47.3'	4°59.2' 4°58.2'	ca. 220	Small	1	..	..	1	..	sand
67	74-06-26	61°50.6' 61°50.4'	4°44.2' 4°43.4'	230	Small	8	..	..	o o	..	empty
72	74-06-27	61°24.8' 61°25.3'	4°53.4' 4°54.1'	290 270	Small	5	..	..	..	21 pebbles	sandy mud
73	74-06-27	61°28.2' 61°28.4'	5°06.5' 5°05.5'	250 250	Small	7	o o	..	..	1 basalt pebble	mud
74	74-06-27	61°19.6' 61°18.9'	5°28.6' 5°27.7'	200 200	Small	..	..	..	o o		shell sand, 1 pebble
75	74-06-27	61°13.5' 61°12.8'	5°11.1' 5°12.6'	400 400	Small	2	..	..	..	..	sand
78	74-06-28	60°54.0' 60°54.4'	5°50.9' 5°52.2'	353 350	Small	..	..	..	..	..	sand
85	74-06-29	61°30.2' 61°32.5'	5°59.9' 6°03.1'	170 170	Small	..	o o	..	..	..	shell sand
86	74-06-29	61°32.8' 61°33.3'	6°13.9' 6°14.9'	264 270	Small	..	..	o o	..	..	sand
87 F1615	71-06-16	61°50'	5°18'	182-201	Large	..	1	o o	o o	..	..
88 "Vónin"	71-08	62°15.5' 62°18.9'	5°56.7' 5°54.6'		Trawl	1	..	o o	..	..	..